WESTERN RESOURCES PROJECT FINAL REPORT— PRODUCED GROUNDWATER ASSOCIATED WITH COALBED NATURAL GAS PRODUCTION IN THE POWDER RIVER BASIN

Mark D. Zoback
Editor



Report of Investigations No. 55
2005

Laramie, Wyoming

Wyoming State Geological Survey

Ronald C. Surdam, Director/State Geologist

Geological Survey Board

Ex Officio

Dave Freudenthal, *Governor*
Ronald C. Surdam, *Director/State Geologist*
Randi S. Martinsen, *University of Wyoming*
Don J. Likwartz, *Oil and Gas Supervisor*

Appointed

Gordon G. Marlatt, *Laramie*
Christopher E. Mullen, *Casper*
John P. Simons, *Cheyenne*
John E. Trummel, *Gillette*
Wallace L. Ulrich, *Moose*

Geological Survey Staff

Applied Geology Division

Alan J. Ver Ploeg, *Manager*
GIS Section
Allory P. Deiss, *Manager*
Phyllis A. Ranz, *GIS Specialist*
David W. Lucke, *GIS Specialist*
Geophysical Section
Yuri V. Ganshin, *Senior Geophysicist*
Mapping Section
Alan J. Ver Ploeg, *Senior Geologist*
J. Fred McLaughlin, *Geologist*
Process Modeling Section
Zunsheng (John) Jiao, *Senior Geologist*
Surficial Processes Section
Seth J. Wittke, *Geologist*

Natural Resources Division

Rodney H. De Bruin, *Manager*
Coal Section
Vacant, *Senior Geologist*
Nicholas R. Jones, *Geologist*
Industrial Minerals Section
Ray E. Harris, *Senior Geologist*
Metals and Precious Stones Section
W. Dan Hausel, *Senior Economic Geologist*
Wayne M. Sutherland, *Geologist*
Robert W. Gregory, *Geologic Analyst*
Oil and Gas Section
Rodney H. De Bruin, *Senior Geologist*
Ramsey D. Bentley, *Geologist*
Geohydrology Section
Keith E. Clarey, *Senior Geohydrologist*
James E. Stafford, *Geohydrologist*

Support Division

Director's Section
Joan E. Binder, *Executive Assistant*
Human Resources/Financial Section
Susanne G. Bruhnke, *Manager*
Information Technology Section
Jesse T. Bowen, *Manager*
Brett E. Bates, *IT Specialist*
Editorial Section
Richard W. Jones, *Editor in Chief*
Kathy L. Walker, *Associate Editor*
Megan L. Ewald, *Associate Editor*
Publication Sales Section
Chad P. Hartwick, *Manager*

This and other publications available from:

Wyoming State Geological Survey
P.O. Box 1347
Laramie, WY 82073-1347

Phone: (307) 766-2286
Fax: (307) 766-2605
Email: sales-wsgs@uwyo.edu

Web Page: http://www.wsgs.uwyo.edu



Individuals with disabilities who require an alternative form of communication in order to use this publication should contact the Editor, Wyoming State Geological Survey at (307) 766-2286. TTY Relay operator 1-800-877-9975.

NOTICE TO USERS OF WYOMING STATE GEOLOGICAL SURVEY INFORMATION

Although most information produced by the Wyoming State Geological Survey (WSGS) is in the public domain and not copyrighted, and may be used without restriction, as a coutesy we ask that users credit the WSGS when using this information in whole or in part. This applies to published and unpublished materials in printed or electronic. Contact the WSGS if you have questions on citing materials or preparing acknowledgements. Your cooperation is appreciated.

Any use of trade, product, or firm names in this publication is for descriptive purposes only and does not imply endorsement or approval by the State of Wyoming or the Wyoming State Geological Survey.

First printing of 1000 copies by Pioneer Printing and Stationery Company, Cheyenne, Wyoming, March 2006.

Western Resources Project Final Report—Produced groundwater associated with coalbed natural gas production in the Powder River Basin, Mark D. Zoback, Editor. Wyoming State Geological Survey Report of Investigations No. 55, 2005.
ISBN 1-884589-37-5

Front cover: A produced water retention pond from a coalbed natural gas field south of Gillette, Wyoming has transformed this part of the Powder River Basin.

WYOMING STATE GEOLOGICAL SURVEY
Ronald C. Surdam, State Geologist

Report of Investigations No. 55

Western Resources Project Final Report—Produced Groundwater Associated with Coalbed Natural Gas Production in the Powder River Basin

Mark D. Zoback
Editor

Prepared in cooperation with the Western Resources Project (sponsored by Apache Corporation, Conoco Phillips, and Marathon), the Ucross Foundation, Stanford University, the University of Wyoming, Montana Bureau of Mines and Geology, and Western Research Institute

Printed from funds provided by the Western Resources Project and the Office of Research and Economic Development, University of Wyoming

Laramie, Wyoming
2005

Table of contents

Preface 1
Raymond Plank
Foreword 3
Mark D. Zoback

Chapter 1

Surface water hydrology and shallow groundwater effects of coalbed natural gas development, upper Beaver Creek drainage, Powder River Basin, Wyoming 5
Aaron A. Payne and Demian M. Saffer
Table of contents 6
List of photographs 6
List of figures 7
List of tables 7

Chapter 2

Predicting changes in groundwater quality associated with coalbed natural gas infiltration ponds 45
John Wheaton and Terry H. Brown
Table of contents 46
List of figures 46
List of appendices 46

Chapter 3

Assessment of the environmental impacts of coalbed natural gas development in the Powder River Basin – Use of coalbed natural gas-produced water for cropland irrigation 71
Terry H. Brown and Chris Johnston
Table of contents 72
List of figures 72
List of tables 72
List of appendices 72

Chapter 4

Strontium isotopic tracing of the effects of coal bed natural gas (CBNG) development on shallow and deep groundwater systems in the Powder River Basin, Wyoming 93
Carol D. Frost and Elizabeth Brinck
Table of contents 94
List of figures 94
List of tables 94

Chapter 5

Time-lapse seismic monitoring of coalbed natural gas production: A case study from the Powder River Basin 109
Jerry M. Harris and Martins Akintunde
Table of contents 110
List of figures 110

Chapter 6

Geomechanics and the effectiveness of wellbore completion methods of coalbed natural gas (CBNG) wells in the Powder River Basin: Implications for water and gas production 127
Lourdes Colmenares and Mark D. Zoback
Table of contents 128
List of figures 128
List of tables 129

Preface

During Apache's fifty year history in the oil and gas exploration business, there have been many precedents for undertaking the Western Resources Project (WRP). As the founder of Apache Corporation and throughout my five-decade association with the company, the word "values" carries strong meaning for us, and is central to our successes and collegial learning, personal growth, and happiness along the way with like-minded men and women. Since the roots of these values predate Apache, I comment on two of their earlier sources as guide posts.

My father, equipped with a seventh-grade education, migrated west to Minneapolis in 1882, carrying with him a single suitcase, $2,500 (his worldly savings), the tears of his parents and siblings, and the memory of three bouts with pneumonia from Pennsylvania coal mines (he survived until he was 93). I think of my dad as a gentleman and his teachings as golden. "Try," he once said, "to leave the world a little better place than you found it." Secondly, he believed in and practiced integrity. He said, "Never tell me a lie and we'll get along just fine."

As a combat bomber pilot, I was fortunate to survive and escape injury from 40 missions in the South Pacific and over Japan. This was in 1944 and 1945, when the Army Air Corps was losing more men in a day over Germany than perished in two lightning-like Iraq wars. So many friends lost their lives in a cause bigger than any of us, that I felt and deeply believe that the healthy survivors might best honor the sacrifice of those killed in duty by accepting responsibility that Americans have not died in vain. Accordingly, ethics, coupled with life-long learning, has been central to outreach, both corporate and individual.

An immensely stimulative and happy life has marked my path over the decades. It was with that background that Apache and I became intrigued with what the Ucross Foundation, Apache Corporation, and dedicated and knowledgeable scientists and humanitarians might contribute through formation of a research group (WRP) for baseline studies of coalbed natural gas (CBNG) and potable water in Wyoming.

When an Apache group, two renowned professors, and a Boeing scientist met together in Houston on September 3, 2000, a near frenzy of CBNG gold-rush-type mentality was sweeping Wyoming as well as the global media. Claims and countercharges seemed focused more on conflicting self-interest than the assembly and analysis of data to provide understanding of essentially longer-term trade-offs for short-term fortune-seeking.

By the time Dr. Mark Zoback of Stanford University and Dr. Roger Anderson of Columbia University convened the formative session of WRP at the Ucross Foundation's 22,000-acre spread on October 3, 2000, our group had expanded to bring aboard additional perspectives from participants in the CBNG play.

Jack Ellbogen, now deceased, a successful oil operator, wonderful supporter of the University of Wyoming and the Ucross Foundation, and a close friend, arranged for five associates within the CBNG business unit of Huber Oil and Gas to make a presentation at the session and conduct a field visit to the development in full swing. They participated at Ucross as well. We were further joined by Wyoming State Senator John Schiffer, who in numerous ways exceeds my expectations, and by Mark Gordon of Merlin Ranch, who runs Ucross Foundation lands as a developing model and demonstration that commercial ranching, conservation, and open space values can successfully coexist through responsible holistic land management.

Among those present from Apache were CEO Steve Farris; Mike Bahorich, Executive V.P. – Exploration and Production Technology; and Craig Jarchow, a Stanford Ph.D. and MIT MBA, who was then reporting to Mike Bahorich.

Steve Farris and I believed then—and we have since had our views reinforced—that CBNG development, properly planned for and conducted, can make a meaningful contribution to energy supplies and the economic well-being of Wyoming and the world.

We remain concerned that because all CBNG was not created equal, there are significant risks to the quality and quantity of water produced as well as to aquifer replenishment in arid regions. Many areas in the coal fields are widely underlain by coal, but unfortunately, much of it is in beds too thin to be economically viable as either coal resources or CBNG sources.

We believe that the costs associated with responsible practices—the social costs—should be borne by the operator extracting the resource. If operators are unwilling or unable to bear these costs of restoration and remediation, then permits to conduct activity should be withheld. Secondly, to assure long term preservation of the land and potable water, the State of Wyoming should set aside funds from CBNG-generated revenues in order to preserve and reclaim the land.

Apache and Ucross Foundation, as well as the able scientists involved in WRP, are grateful to ConocoPhillips, and Marathon for joining Apache in funding the start-up of the $700,000 project and quality staff professionals—including Britt Dearman of Apache, David Searle of Marathon, and Steve de Albuquerque of ConocoPhillips—have done outstanding work. We are pleased that the U.S. Department of Energy, through Dr. Dag Nummedal of the Colorado Energy Research Institute at the Colorado School of Mines, has granted additional funding to the WRP scientists.

At the October 3, 2000 meetings, the organizers, presenters, and participants comprised the right people at the right place and time to lead to accomplishment. Although he was absent at the meeting, Mark Zoback was selected to be Science Director by unanimous vote of others present, including Stanford University's Sandy Robertson. I can understand why: brilliant and outgoing, he is recognized as a leading earth scientist. When a Stanford man or woman shows up at Apache having studied under Mark Zoback, ears, eyes, and even pay may perk up.

Mark was soon to be joined by a diverse and talented group of scientists. Eight of the ten serving on the board, participating in project management or the Science Advisory board, hold Ph.D.s and have made outstanding contributions. After a review of the presentations, the industry founders of the project concluded that those presentations by the following authors were outstanding: Aaron Payne and Demian Saffer of the University of Wyoming; John Wheaton of the Montana Bureau of Mines and Geology and Terry Brown of the Western Research Institute (now at Poudre Valley Environmental); Chris Johnston of the Western Research Institute; Carol Frost and Elizabeth Brinck of the University of Wyoming; Jerry Harris and Martins Akintunde of Stanford University; and Lourdes Colmenares and Mark Zoback, also of Stanford University. I'm pleased that these six WRP research papers are being published in a special Report of Investigations of the Wyoming State Geological Survey.

How is this writer (who majored in Latin American Relations) going to handle all this erudition? I have every confidence that the work product of this project may, can, and will make a difference.

Raymond Plank

March 16, 2004

Foreword

The papers in this special publication describe the accomplishments of the Western Resources Project science team in its first year of activity. The objective of these studies was to better understand a variety of issues related to water produced during production of coalbed natural gas.

In the first paper, Aaron Payne and Demian Saffer of the University of Wyoming describe their study of the water budget in the upper Beaver Creek drainage. Beaver Creek is a site where a number of shallow wells were drilled and studies carried out to investigate an area of in-channel CBNG water disposal. This study was carried out in cooperation with ConocoPhillips, the operator in the area. The study addresses a number of questions about the fate of surface discharged waters in terms of evaporation, runoff, and infiltration.

In the second paper, John Wheaton of Montana Bureau of Mines and Geology and Terry Brown, formerly of the Wyoming Research Institute, present water quality data from the Beaver Creek and Coal Creek areas and elsewhere. Coal Creek is another site of concentrated WRP investigations where CBNG water is pumped into out-of-channel ponds. Wolverine Energy is the local operator in the area and we thank them for their cooperation.

The next paper, by Terry Brown and Chris Johnston, investigates the effects of using CBNG water for cropland irrigation. CBNG water is used in various concentrations and with different surface treatments. This study was carried out in the Piney Creek/Clear Creek area also in cooperation with Wolverine Energy.

The fourth paper, presented by Carol Frost and Elizabeth Brinck of the University of Wyoming, is a generic study related to using strontium isotopes as a tracer for CBNG waters in various parts of Powder River Basin. Such a technique could have widespread applicability throughout the basin as the fate of CBNG waters in the regional hydrologic system is tracked and could also help identify the origin of waters produced from a single well.

The fifth paper, by Jerry Harris and Martins Akintunde of Stanford University, uses cross-well tomography in wells drilled on the Ucross Ranch (operated by the Apache Foundation) in an attempt to demonstrate how one could observe the effect of water production and free-phase methane on the seismic properties of coal. This work has the potential for revealing how dewatering and CBNG production are related at the reservoir scale.

In the final paper presented, Lourdes Colmenares and Mark Zoback, also of Stanford University, investigate how the rates of CBNG water production (and gas production) are related to wellbore completion methods. After investigating water and gas production from about 550 wells, they offer an explanation of how wellbore completion techniques result in approximately 70% of CBNG waters coming from around 30% of the wells and suggest methods for modifying wellbore completion techniques to reduce the number of high-water-producing wells.

These research projects were selected following a scientific review of proposals by the WRP Science Advisory Board that included Dr. John Bredehoeft (USGS emeritus), Dr. Bill Gern (Vice President at the University of Wyoming), Dr. Frank Sanders (CBNG consultant), and Lance Cook (then Wyoming State Geologist). We thank them for their advice and contributions to this work.

We wish to thank the sponsors of WRP (Apache Corporation, Marathon, and ConocoPhillips) for making this research possible. None of this would have been possible without the inspiration and leadership of Raymond Plank and Steve Farris of Apache and the efforts of Mike Bahorich and Britt Dearman at Apache, Steve de Albuquerque at ConocoPhillips, and Dave Searle at Marathon. Terry Brown served ably as WRP Project Director and contributed much to the overall success of the research program. We would also like to recognize the U.S. Bureau of Land Management and the many companies who cooperated in the studies presented here.

Finally, we wish to thank Ron Surdam, Wyoming State Geologist, and the Wyoming State Geological Survey for publishing these papers. Jamie R. Stine, former Assistant Editor at the WSGS, deserves special recognition and credit for organization. additional editing and formatting, reference checking and compilation, design, and layout of the publication. Megan L. Ewald and Richard W. Jones of WSGS made additional corrections and revisions to the final manuscript and layout.

Mark D. Zoback

August 3, 2005

CHAPTER 1

Surface water hydrology and shallow groundwater effects of coalbed natural gas development, upper Beaver Creek drainage, Powder River Basin, Wyoming

Aaron A. Payne and Demian M. Saffer
Department of Geology and Geophysics
University of Wyoming
Laramie, Wyoming

Table of contents

Page

List of photographs 6
List of figures 7
List of tables 7
Abstract 9
Introduction 9
Setting and field area 10
Geology of the Powder River Basin 11
Hydrogeology of the Powder River Basin 11
Methods 14
Field methods 14
Monitoring wells 14
V-notch weir installation 16
Evaporation pans 17
Rain gauge 21
Surface area of the stream and ponds 21
Direct aquifer property measurements 21
Water budget analysis 22
Results 22
Field results: Water budget and shallow aquifer response 22
Precipitation 22
Evaporation pan results 22
Water budget results 24
Shallow aquifer response 30
Slug testing 33
Discussion 34
Water budget 34
Spatial variations 34
Temporal variations 35
Additional considerations 38
Stream channel infiltration rates per unit stream length 40
Shallow aquifer response 40
Conclusions 41
References cited 42

List of photographs

1. Upper monitoring wells 17
2. Middle monitoring wells 17
3. Lower monitoring wells, looking to the northwest 18
4. Tributary monitoring wells 18
5. Weir leveling instrument 18
6. Upper weir 19
7. Middle weir 19
8. Lower pond weir 19
9. Lower weir 20
10. Upper pond showing placement of evaporation equipment 20
11. Lower stream section vegetation change 36
12. Upper pond outfall area vegetation change 36
13. Ice around the middle weir, February 2004 39
14. Ice at the lower weir, February 2004 39

List of figures

Page

1. Open-hole completion technique for a typical coalbed natural gas well 9
2. Map of Wyoming showing Beaver Creek site location 10
3. Beaver Creek study area and regional topography 11
4. Geologic map of the Powder River Basin 12
5. Generalized stratigraphic column of the Wasatch Formation, Fort Union Formation, and Upper Cretaceous Lance Formation in the Powder River Basin 13
6. Beaver Creek study area site map 15
7. Sample evaporation calculation from ground evaporation pan, August 13-21, 2003 21
8. Precipitation data from August 6 to November 1, 2003 23
9. Precipitation data from March 25 to September 18, 2004 23
10. Surface water flow through weirs and CBNG water input, July 23 to November 1, 2003 26
11. Water budget conveyance losses as a percentage of total CBNG input, 2003 season 27
12. Three week-long water budget intervals detailing conveyance losses by block, CBNG water input, and surface flow, 2003 27
13. Average manual water level readings at four monitoring well locations, December 17, 2002 to July 23, 2003 31
14. Water level change for logger instrumented wells, July 23, 2003 to September 18, 2004 32
15. Synthesis of manual and logger water level data at all monitoring well sites, December 17, 2002 to September 18, 2004 32
16. Synthesis of manual and logger water level data, middle and lower instrumented wells, adjusted to control site, December 17, 2002 to September 18, 2004 33
17. Time-drawdown data for two slug tests 34
18. Schematic of seepage beneath a ponded surface 35
19. Infiltration rate through time, 2003 water budget 37

List of tables

1. Monitoring wells 16
2. Area of infiltration blocks 21
3. Ground evaporation pan data, August 13 to October 16, 2003 24
4. Floating evaporation pan data, August 21 to October 28, 2003 24
5. Floating evaporation pan data, May 25 to September 18, 2004 24
6. Daily evaporation rates from reservoirs for each month in the Gillette area assuming an annual lake evaporation of 47 inches 24
7. Evaporation rates for 2003 water budget 24
8. Evaporation rates for 2004 water budget 25
9. CBNG water volumes, conveyance losses, and surface runoff, 2003 budget 26
10. CBNG water input, surface flow, and conveyance losses for infiltration blocks, 2003 budget 28
11. Infiltration in each conveyance loss block and calculated infiltration rates, 2003 budget 28
12. CBNG water input, surface flow, and conveyance losses for infiltration blocks, 2004 budget 29
13. Infiltration in each conveyance loss block and calculated infiltration rates, 2004 budget 30
14. Summary of slug test results 34
15. May through September evapotranspiration distribution 35

Abstract

A water budget was determined from July through November 2003, and from March through September 2004, to quantify the fate of coalbed natural gas (CBNG) co-produced water at a study site in the Upper Beaver Creek drainage, within the Powder River watershed. Production of CBNG water initiated in November 2002, and was discharged into two in-channel infiltration ponds. Four v-notch weirs were installed at locations between and downstream of the ponds to quantify surface flow throughout the system. Infiltration was specifically examined in the water budget to determine the spatial and temporal variations associated with this aspect of conveyance loss. Calculated infiltration averaged 46.1% of the conveyance loss for 2003 within the study site. Calculated infiltration rates in the streams were significantly higher than in the ponds, and calculated infiltration rates seem to increase in the summer months and decline in the fall, likely due to the omission of transpiration in the water budget analysis. Average calculated infiltration rates for 2003 were 0.037 cubic feet per second per mile (cfs/mi) in a 0.8 m average width stream channel, and 0.063 cfs/mi in a 1.4 m average width stream channel. Water level data from the shallow aquifer indicated a approximate 2 to 3 foot annual rise in the local water table due to CBNG water infiltration.

Introduction

Coalbed natural gas (CBNG) is natural gas found at depth in coal beds. In the past 15 years, the Powder River Basin (PRB) has become one of the nation's leading producing areas of coalbed natural gas. According to the Wyoming Oil and Gas Conservation Commission (WOGCC), coalbed natural gas development began in the PRB in 1989 with only 18 producing wells. By 1998, the number of wells in the PRB grew to over 350 and production of CBNG reached over 30 billion cubic feet (BCF). Coalbed natural gas production reported by the WOGCC for the state of Wyoming in 2003 was 348.2 BCF, with 346.0 BCF produced in the PRB alone. Coalbed natural gas accounted for 19.0% of the total natural gas production for Wyoming in 2003. At the end of 2003, the WOGCC reported 12,196 producing wells across the state, with the vast majority in the PRB (De Bruin and others, 2004). The U.S. Bureau of Land Management (BLM) projects 40,000 new wells will be developed in the next decade.

Coalbed natural gas wells in the Powder River Basin coal beds are completed open-hole and casing is set to the top of the target coal bed. The underlying coal zone is under-reamed and cleaned out with a fresh-water flush. CBNG extraction requires pumping water from the coalbed aquifers to de-pressurize the system and allow the methane to desorb from the surface of the coal. A downhole submersible pump moves the water up the casing while the gas separates from the water and travels up through the annulus (**Figure 1**).

In the production of coalbed natural gas, large volumes of fresh water from these coal seams are produced. In the Powder River Basin, after the initial dewatering of the coal seams (usually several months) an average of almost 16,800 gallons of water are produced each day and primarily discharged to the surface (De Bruin and others, 2001). Thus, a single well is expected to produce about 18.8 acre-feet of water annually. The majority of this water is released into storage impoundment ponds that are designed to promote evaporation and infiltration into the shallow aquifer.

There are a multitude of concerns related to the development of coalbed natural gas in the Powder River Basin. In the final environmental impact statement (FEIS) for the Powder River Oil and Gas Project (U.S. Bureau of Land Management, 2003), the BLM estimates that a single CBNG well can lower the water table by 34 feet in a 10-foot-radius of the well. The FEIS predicts a maximum drawdown in the PRB of more than 700 feet in Fort Union Formation coal beds, which could impact between 2500 to 6500 groundwater wells. In the Wasatch Formation, groundwater models indicate a much lower regional drawdown of only

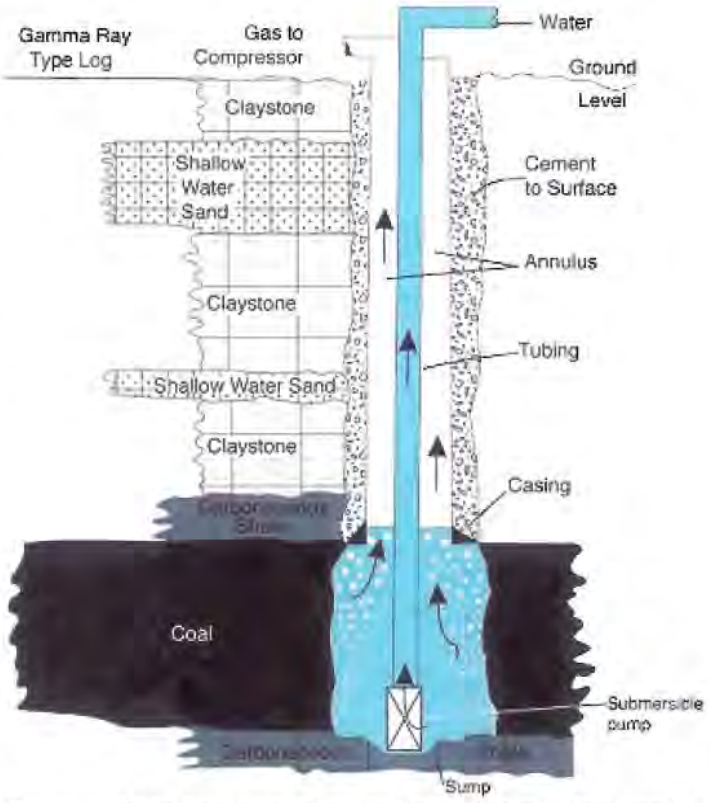


Figure 1. Open-hole completion technique for a typical coalbed natural gas well. Adapted from De Bruin and Lyman, 1999.

40 to 70 feet from CBNG production, which may impact the 3300 to 7000 production water wells in this formation and lead to decreased yields.

There is also a water quality problem associated with the disposal of CBNG co-produced water. Much of this water has a high sodium-adsorption ratio (SAR), and/or high specific electrical conductivity (EC). A common ion-exchange reaction is the replacement of calcium in soil with sodium. If the CBNG water that reaches the soil is high in sodium and low in calcium, the cation-exchange complex can become saturated with sodium, which can destroy soil structure by dispersion of clay particles (Fetter, 2001). The SAR value is an indicator of the hazards associated with this reaction. The SAR ratio of CBNG water from the Powder River Basin in Wyoming varies from 5.7 to 32, with an average value of 12 (Rice and others, 2000). Generally, a value from 7 to 18 indicates medium hazards from sodium, high hazards between 11 and 26, and very high hazards above that (Fetter, 2001). Impacted soil can accumulate these salts, which will not only destroy soil structure, but inhibit water absorption by plants (Warrance and others, 2001).

Little is known about the effects that this co-produced water will have on the shallow aquifers and water budget in areas of CBNG development. The discharge of these large volumes of water create new wetland environments in a semi-arid basin and often transform historically ephemeral stream drainages into streams that support perennial flow (De Bruin and Lyman, 1999). As CBNG development is a very recent technique in energy production, few physical studies concentrating on conveyance loss of CBNG water and the effects of the shallow aquifer have yet been completed to the author's knowledge. Two consulting firm studies commonly reported in CBNG permitting documents suggest that conveyance loss in ephemeral stream channels will occur at a rate of 0.1 cfs/mile (approximately 45 gallons per minute) (Western Land Services, 2001; Hydrologic Consultants, Inc., 2001).

Assumptions by the BLM in the FEIS include that 20% of the CBNG co-produced water would be lost to conveyance. They also assume that 15% of the infiltrating water will reappear as base flow to local streams. The BLM estimates are not based on any specific scientific or empirical data. Quantifying the amount of CBNG water that is actually lost to conveyance (evapotranspiration and infiltration) will be an important aspect to monitor over the course of CBNG development.

In this study, we quantify the fate of CBNG water in a low-order tributary watershed in the Powder River Basin by determining water budgets for the period of July 23 through November 1, 2003, and from March 25 through September 18, 2004. Infiltration rates have been calculated in four discrete blocks in the study area, and they are analyzed to determine spatial and/or temporal variations in infiltration. Monitoring wells have been installed at several locations to observe the changes in the local water table from CBNG infiltration.

Setting and field area

The Beaver Creek study area is in the southern portion of the Powder River Basin, in Campbell County, Wyoming (**Figure 2**). The site is located in the upper reaches of the Beaver Creek drainage, which empties into the Powder River to the west (**Figure 3**). Two in-channel storage impoundment ponds have been excavated to hold CBNG co-produced water from five producing wells. Initial production of CBNG water began in November 2002. Both ponds feature an in-line water level control structure, which maintains a constant pond level as input from CBNG water fluctuates. Water flows out of the ponds and down the previously ephemeral stream channel and intersects with Beaver Creek about 3/4-mile downstream from the study area boundary.

This region of Wyoming is a major area of activity for coalbed natural gas wells. In township 47N, range 75W, where the Beaver Creek site lies, there are 105 CBNG wells permitted by the WOGCC. In the eight surrounding township and range one square-mile sections, there are over 1500 permitted wells (Wyoming State Engineers Office, 2004).

Geology of the Powder River Basin

The Powder River Basin is an asymmetric intermontane basin with a basin axis on the western margin of the basin,



Figure 2. Index map of Wyoming showing Beaver Creek site location.

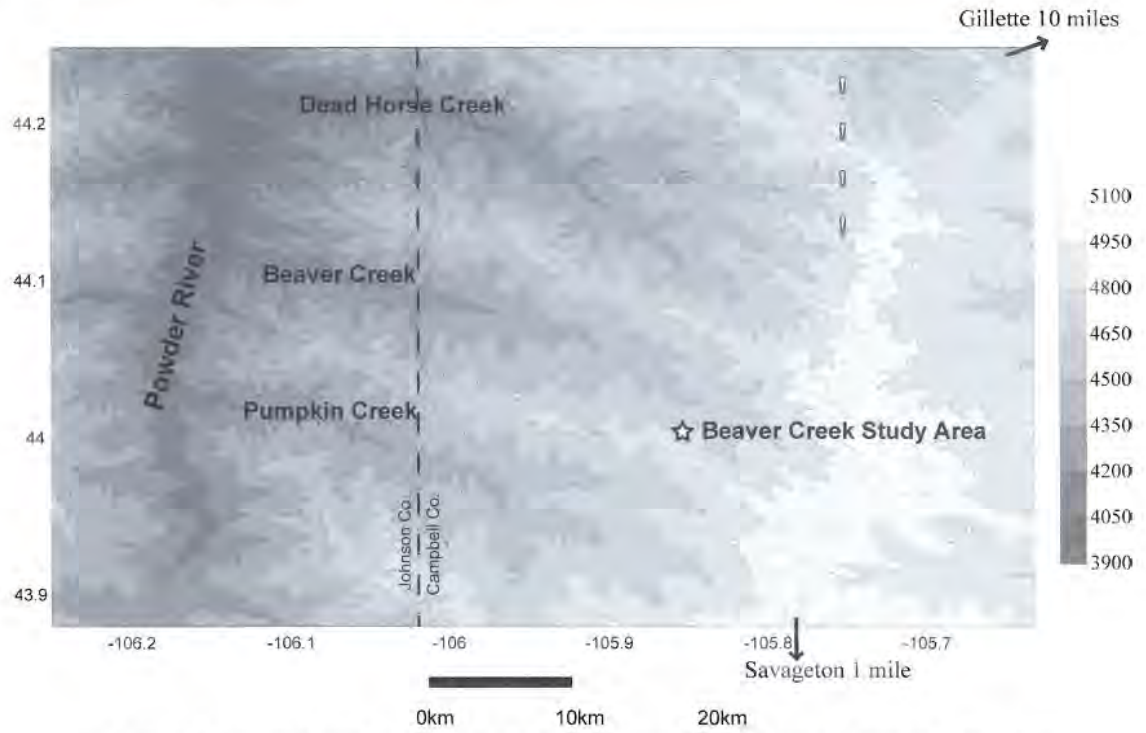


Figure 3. Beaver Creek study area and regional topography. Contour interval is 150 feet.

adjacent to the Bighorn Mountains. The area of the basin is approximately 22,000 square miles, 75% of which lies in Wyoming (**Figure 4**). Phanerozoic rocks range in thickness from 3000 feet on the basin margins to 17,000 feet near the basin axis (Crockett, 1999). Thick sequences of laterally extensive coal beds are found in much of the Powder River Basin in both Wyoming and Montana. According to the BLM, Wyoming is the leading coal producer in the nation, producing over 380 million tons in 2003, 97% of which was mined from the PRB.

Basin fill consists mainly of Cretaceous and Tertiary rocks representing marine and fluvial-deltaic deposits up to 15,000 feet thick. Uppermost Cretaceous and lower Tertiary formations include the siliciclastic, coal-bearing Lance, Fort Union, and Wasatch formations (**Figure 5**) (Montgomery, 1999). The Lance Formation is overlain by the Paleocene Fort Union Formation, which is composed of the Tullock, Lebo Shale, and Tongue River Member. The Eocene Wasatch Formation overlays the Fort Union in much of Wyoming (**Figures 4** and **5**). The Oligocene White River Formation outcrops in only a few upland areas, most notably in the Pumpkin Buttes (Flores, 1999).

The major coal deposit in the Powder River Basin in Wyoming and Montana is the Wyodak-Anderson coal zone of the Fort Union Formation (**Figure 5**). Thick coal seams are most abundant in the upper Tongue River Member, where they are interbedded with mudstones and thick sandstones (Ayers, 1986). The Wyodak-Anderson coal seam is a major target for CBNG production, but other coal zones in the Tongue River Member, as many as 32 different coal beds according to Ayers (1986), are also drilled for CBNG. Most of these coal beds can be found within 2500 feet of the surface. The coals of the Wyodak-Anderson are mainly subbituminous and can reach thicknesses of 202 feet (Ayers, 1986). Natural gas produced from these coal seams is interpreted as biogenic methane, which is generated as a byproduct of bacterial respiration (Flores, 1999).

Hydrogeology of the Powder River Basin

The Powder River Basin is classified as semi-arid and receives 12 to 16 inches of average annual precipitation in the central portion of the basin (Rankl and Lowry, 1990). Groundwater is the primary water source for rural-domestic, municipal, industrial, and agricultural usage in the PRB. The Lower Tertiary Wasatch/Fort Union aquifer is a primary water source in the central PRB (Lindner-Lunsford and Wilson, 1991). The city of Gillette, which is the largest city in the area of coalbed natural gas development, relies on groundwater from wells completed in the Fort Union and Lance/Fox Hills aquifers, and in the Mississipian age Madison Formation located 60 miles to the east of Gillette, in an area unaffected by CBNG development. The city has experienced considerable drawdown and reduced production from the wells in the Fort Union and Lance/Fox Hills aquifers, but it is unclear how much is due to population growth, coalbed natural gas development, or dewatering

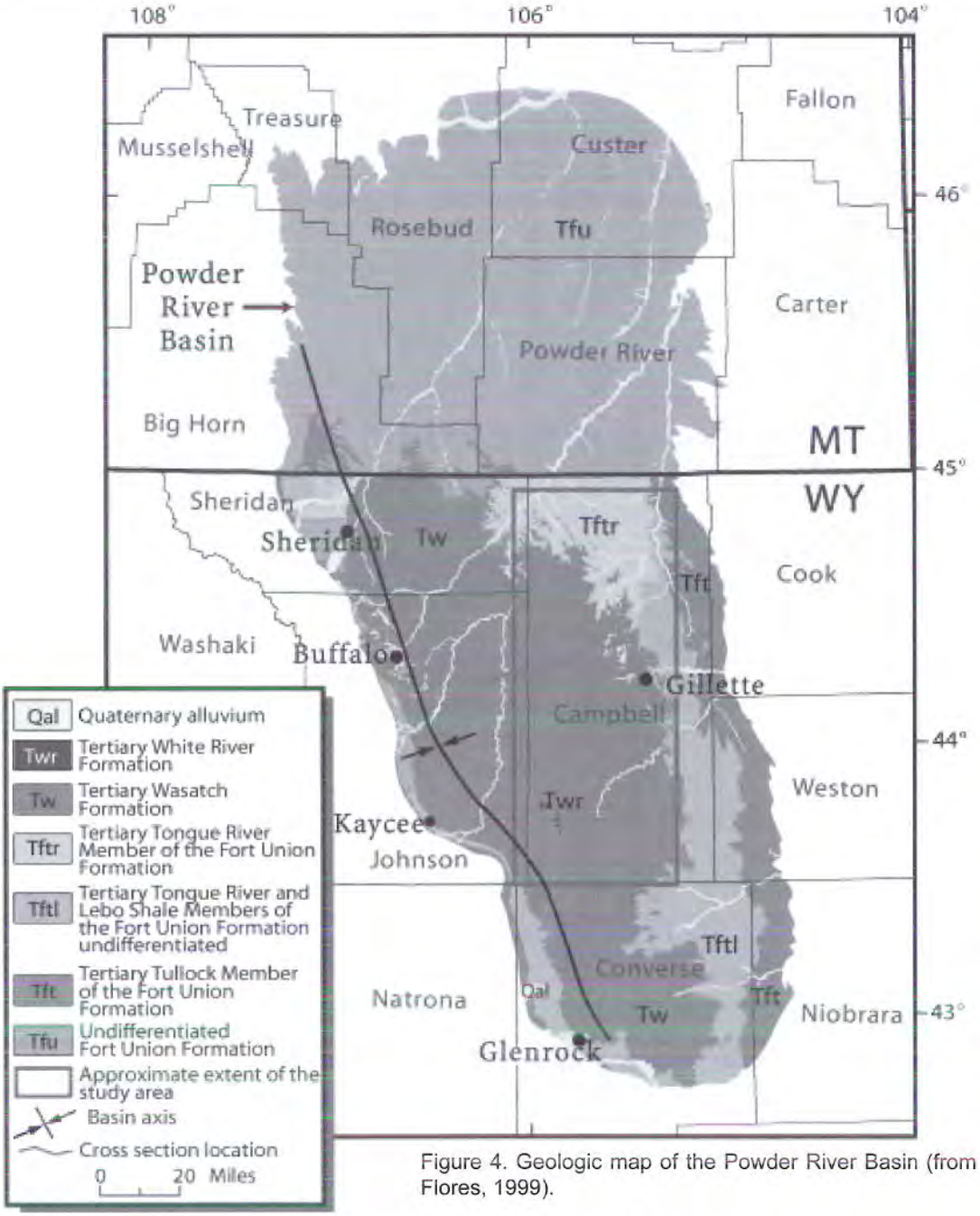


Figure 4. Geologic map of the Powder River Basin (from Flores, 1999).

of coal seams from surface mines (U.S. Environmental Protection Agency, 2004).

Two systems of regional groundwater flow were identified by Rankl and Lowry (1990) in the Powder River Basin: 1) generally northward flow that is stratigraphically controlled, and 2) baseflow into major streams deduced from analysis of flow-duration curves and average daily discharge hydrographs. Groundwater flow in local flow regimes appears to dominate over the regional system. Local flow systems identified by Rankl and Lowry (1990) through streamflow data are bedrock, alluvial, and clinker. Most of the groundwater discharge from bedrock aquifers is above stream level as a result of heterogeneity of the formations. This water tends to evaporate or transpire during the growing season and does not contribute to stream baseflow. Local systems in the alluvium and clinker have a more pronounced effect on streamflow than the regional flow system (Rankl and Lowry, 1990)

Easterly groundwater movement toward the Cheyenne River is observed in the southern portion of the Powder River Basin, and northerly groundwater flow toward the Tongue, Powder, and Little Powder River is seen in the northern portion of the basin. Also, water levels indicate easterly flow to the Belle Fourche River on the eastern side of the basin

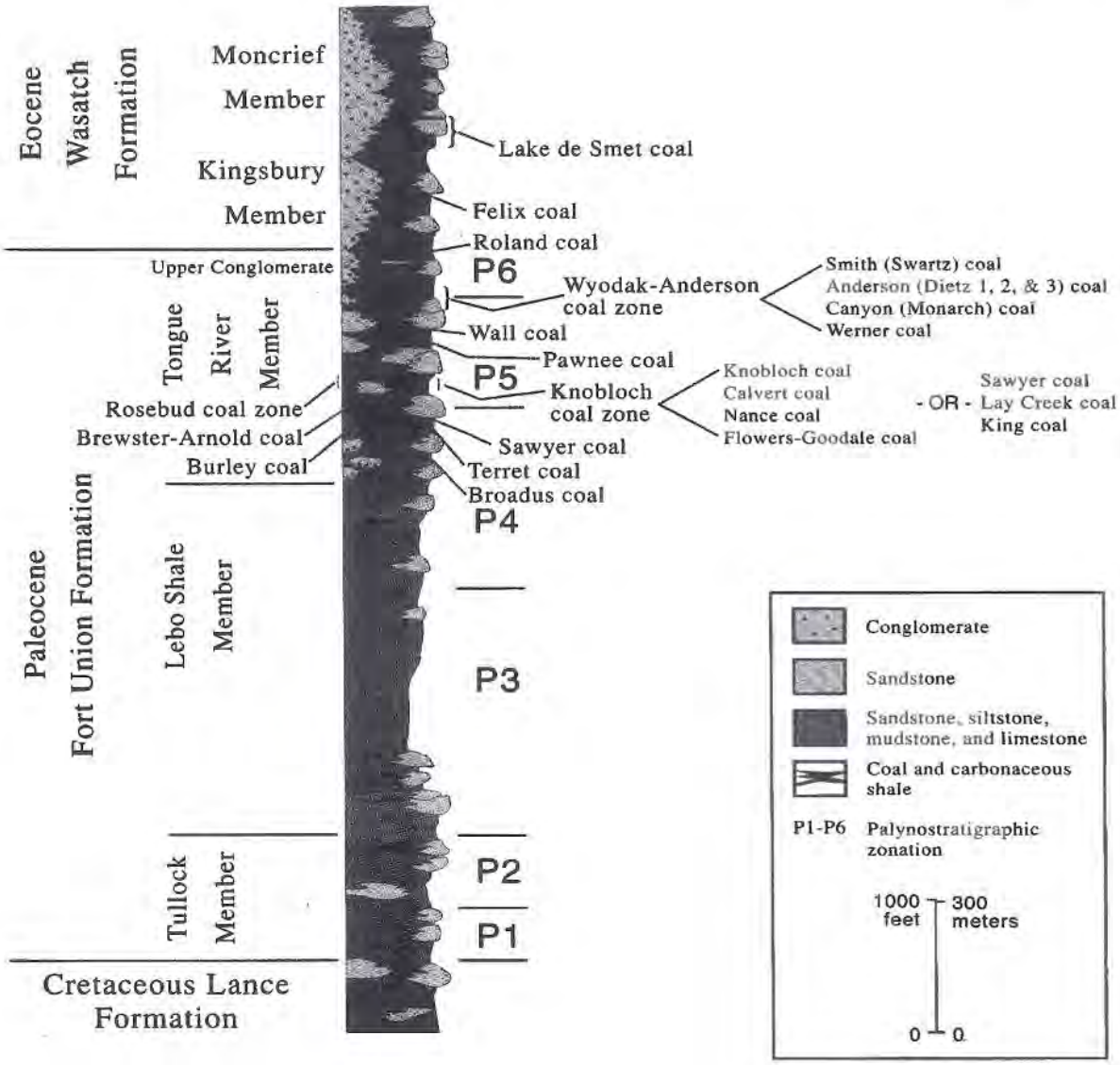


Figure 5. Generalized stratigraphic column of the Wasatch Formation, Fort Union Formation, and Upper Cretaceous Lance Formation in the Powder River Basin (from Flores, 1999).

(Fogg and others, 1991). Local flow systems are affected by topography and the presence of almost impermeable shale layers that impede downward movement of water. Water enters the local flow systems by surface infiltration and moves from areas of higher hydraulic head to areas of lower hydraulic head. In recharge areas, which generally correspond to topographically high areas, hydraulic head decreases with depth, indicating a downward component of groundwater flow. Where this downward flowing water intersects the relatively impermeable shale layers, vertical water movement is retarded and water tends to move laterally and discharge at the surface as contact springs. If the water does not encounter these aquitard layers, water will continue to move downward (Fogg and others, 1991).

The most productive aquifers in the shallow groundwater of the Powder River Basin are the alluvial deposits, sandstone beds, and fractured coal beds (Fogg and others, 1991). The limited thickness and areal extent of alluvial deposits precludes the widespread use of these layers as a major source of water. Sandstone beds tend to be lenticular and do not extend for more than a few miles, while coal aquifers are more laterally extensive. These coal aquifers are recharged at coal outcrops around the basin and where highly fractured clinker deposits cap the coal beds (Fogg and others, 1991).

Well yields in the shallow aquifers are highly variable in the PRB. Yields sufficient for livestock watering and domestic supply can generally be obtained from shallow wells (<500 feet) completed in the Wasatch Formation and the Tongue River Member of the Fort Union Formation. Wells in the northern part of the basin completed in the Wasatch

Formation and Tongue River Member may produce 10 to 50 gal/min; wells completed in these formations in the southern part of the basin may yield as much as 500 gal/min. Yields sufficient for municipal and industrial uses are generally obtained from the Tullock Member of the Fort Union Formation or some deeper aquifer. Wells completed in the Tullock Member typically yield 15 to 40 gal/min, but yields of 150 gal/min or more have been observed. Most alluvium in the basin contains too much fine-grained material to yield much water, but clean, coarse-grained deposits along rivers may yield as much as 1000 gal/min (Fogg and others, 1991).

The chemical quality of water from shallow bedrock aquifers in the basin is highly variable. Chemical analyses of water from the Fort Union Formation indicated TDS levels ranging from about 250 to 5600 mg/L. Water is mostly a sodium bicarbonate type, and to a lesser extent, a sodium sulfate type. Water from the Wasatch Formation exhibits TDS levels ranging from about 150 to 8200 mg/L, also of a sodium bicarbonate or sodium sulfate type. In both of these formations, the levels of TDS tend to increase in the northern part of the basin when compared to the southern portion. The large range in water quality in the Wasatch and Fort Union aquifers is caused by chemical changes as water moves down through the formations, as the chemical type is altered by cation exchange and sulfate reduction. Water from wells less than 200 feet deep is generally hard (calcium magnesium sulfate type), whereas water from deeper wells is generally soft (sodium bicarbonate type) (Fogg and others, 1991).

The quality of water in the alluvial aquifer is also highly variable with TDS levels ranging from about 250 mg/L to about 6600 mg/L. Water in the alluvium in the southwest part of the basin and in the Powder River valley is generally more mineralized than alluvial water in other parts of the basin. Water near the recharge areas of the Black Hills and Bighorn Mountains is generally lower in TDS than water elsewhere in the basin. The alluvial aquifer water is chemically similar to that in the upper part of the bedrock aquifer, but may contain a larger concentration of dissolved solids because of concentration by evapotranspiration (Fogg and others, 1991).

Studies of recharge in the central portion of the PRB suggest that recharge to the overburden (all rocks above the Wyodak-Anderson coal, including the Wasatch Formation and alluvium) occurs over most of the land surface by infiltration from precipitation and streamflow. Brown (1980) estimated recharge to the overburden to be 1 to 5% of annual precipitation (0.15 to 0.75 inch per year), and postulated that recharge to the underlying coal was through downward leakage through the overburden. Jordan and others (1984) estimated the average annual recharge from infiltration to the overlying layers to be 0.2 inch per year, and assumed principal recharge to the Wyodak-Anderson coal occurs at outcrop areas. Recharge to the underburden (Lebo Shale Member of the Fort Union Formation) is believed to originate from an unidentified source in the southern part of the basin (Jordan and others, 1984).

Methods

Field methods

The purpose of the field instrumentation at the Beaver Creek site is to establish a water budget and determine the fate of the CBNG co-produced water, with emphasis on quantifying infiltration. Within the scope of this study, water conveyance loss is categorized as evaporation and/or infiltration. Four v-notch weirs were installed at locations between and downstream of the infiltration ponds. A floating evaporation pans was installed in the upper pond, and a ground evaporation pan was installed next to the upper pond. A rain gauge was placed in the approximate center of the study site. Monitoring wells were installed at four locations to determine the response of the shallow aquifer to this infiltrating water.

Knowledge of the input of CBNG co-produced water (provided by the producers) at each pond, and the placement of four weirs which quantify surface flow, allow us to analyze four discrete blocks for conveyance loss (**Figure 6**). A complete water budget from July 23 to November 1, 2003, was established for the Beaver Creek site. Possible instrumental error precluded full completion of a water budget for the interval from March 25 (after spring thaw) to the September 18, 2004 (end of study interval). Incomplete temporal data from 2004 for the four blocks are presented when we have reasonable confidence in the available data. Considering data from the 2003 field season, and a subset of data from 2004, we were able to analyze the spatial and temporal variations in infiltration throughout the study site.

Monitoring wells

Monitoring wells were installed at four separate locations; up-gradient of the two CBNG ponds, between the two ponds, downstream of the lower pond, and up an ephemeral drainage southwest of the lower pond (see **Figure 6**, and **Photographs 1** through **4**). The monitoring wells at the upper site serve as a control on the regional water level in the shallow aquifer. Since the wells are higher topographically and up-gradient of regional groundwater flow (generally downstream to the north), we assume that the water levels in these wells act independently of the CBNG

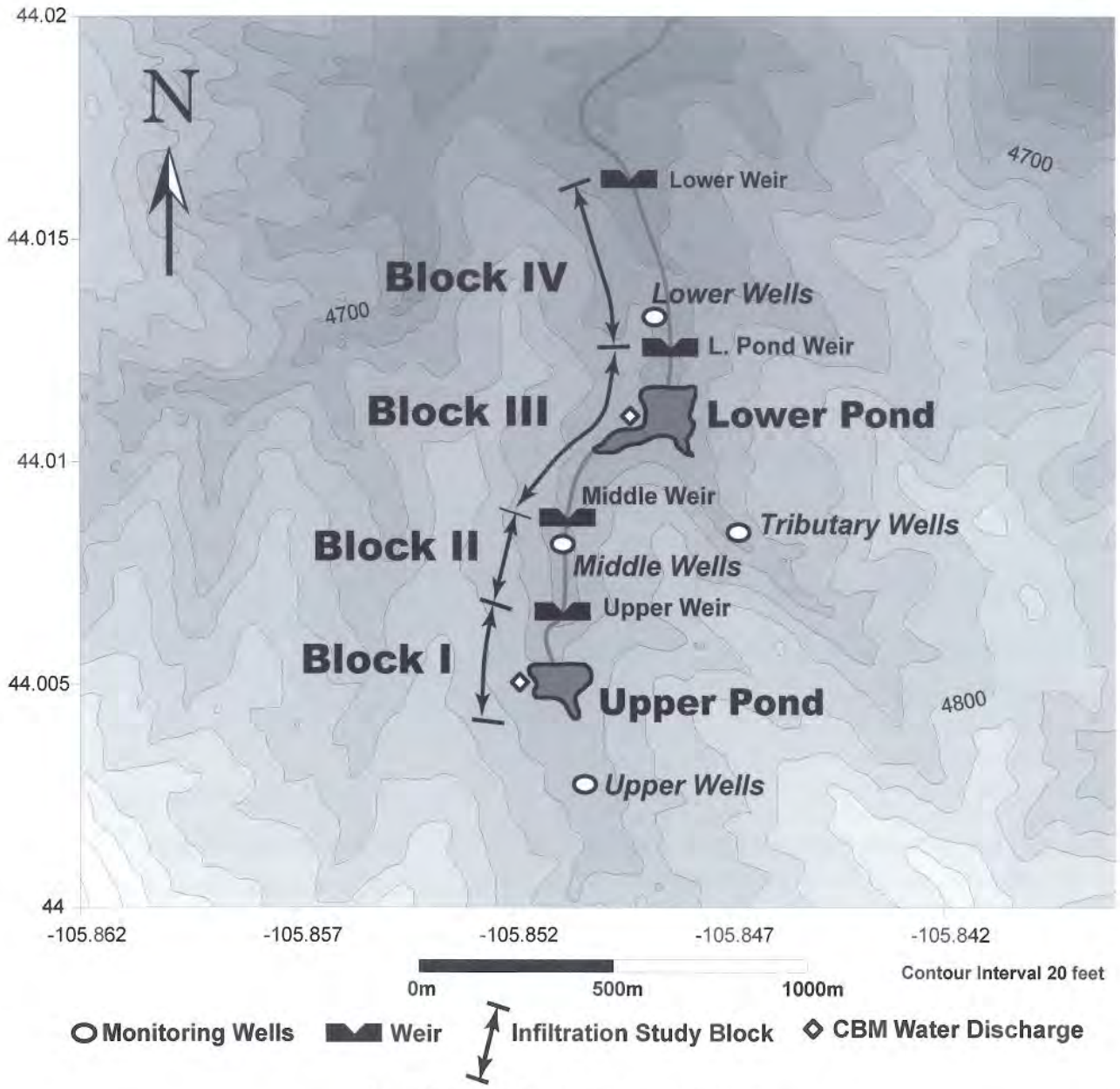


Figure 6. Beaver Creek study area site map.

co-produced water which begins infiltrating in the upper pond. The wells at the middle and lower sites serve to gauge the shallow aquifer response to this introduction of CBNG water at two proximal locations within the site. Monitoring wells at the tributary site provide off-axis resolution of the changes in water level with distance from the main stream channel.

Monitoring wells were drilled using a hollow-stem auger on December 17, 2002. Wells were completed into the alluvium layer, and one well at each site was completed into the top of the weathered bedrock of the Wasatch Formation (**Table 1**). The wells were completed with 2-inch and 4-inch schedule 40 PVC, and screened at various intervals using 0.015-inch slot screen PVC. A filter sand pack was placed between the borehole from just above the screened interval to the bottom of the borehole, and a bentonite slurry was used to seal the well from the sand pack to the surface. Wells were developed through the use of a hand bailer and submersible pump and pumped until the water was clear. This development process helps to move finer sediments back and forth through the screened interval and greatly improves the reliability of water-level and water-quality data (Weight and Sonderegger, 2001).

It is important to note the relations between monitoring wells and surface water at the middle site versus the lower site (**Photographs 2** and **3**). The wells in the middle site lie in a relatively broad and flat plain, in close proximity and at about the same elevation as the stream channel. **Photograph 2** is

Table 1. Monitoring wells. Non-alluvium wells are completed into the weathered part of the Wasatch Formation.

Site	Well Name	Formation	Total Depth (feet)	Casing Dia. (in)	Screen Top (feet)	Screen Bottom (feet)	Screen Length (feet)
Upper	BC-1	Alluvium	18	4	13	18	5
Upper	BC-2	Alluvium	18	2	13	18	5
Upper	BC-3	Alluvium	18	2	13	18	5
Upper	BC-4	Wasatch	31.5	2	24	31.5	7.5
Middle	BC-5	Wasatch	38	2	33	38	5
Middle	BC-6	Alluvium	25.8	2	15.8	25.8	10
Middle	BC-7	Alluvium	25	2	15	25	10
Middle	BC-8	Alluvium	23.5	4	14	23.5	9.5
Middle	BC-15	Alluvium	7	2	5	7	2
Lower	BC-11	Wasatch	38	2	24	32	8
Lower	BC-12	Alluvium	15	2	10	15	5
Lower	BC-13	Alluvium	15	4	10	15	5
Lower	BC-14	Alluvium	15	2	10	15	5
Tributary	BC-9	Wasatch	28	2	18	28	10
Tributary	BC-16	Alluvium	12	2	8.5	12	3.5

from the spring of 2003, when flow spreads out and follows livestock trails. The main channel of flow is just to the west (left) of the wells. During and after the summer of 2003, surface water flows almost exclusively in this main channel, possibly due to an increase of vegetation. The monitoring wells at the lower site are perched on a terrace, several feet higher in elevation than the level of the stream channel. These wells are in off-channel locations, about 18 to 45 feet west of the stream channel.

Manual water level measurements were taken using an electrical tape at periodic intervals up until July 23, 2003. On July 23, 2003, barometrically compensated water level loggers (Global Water WL-15 Loggers, range 0 to 15 feet) were installed in one well at each of the three main well sites: BC-3 at the upper site, BC-6 at the middle site, and BC-12 at the lower site. These loggers provide a submersible pressure transducer that measures water depth. Knowing the initial water level before emplacement of the loggers provides a continuous record of water level in a monitoring well. For the duration of the study, these loggers gathered hourly data. Manual water level measurements were also gathered at the remaining non-instrumented wells during each field visit, and as a periodic check on data logger levels.

V-notch weir installation

Four weirs were emplaced on July 8-10, 2003, below the upper pond, above the lower pond, below the lower pond, and at the extreme downstream end of the site (see **Figure 6**, and **Photographs 6** through **9**) to quantify surface flow through the system. Ninety-degree, 1-foot v-notch weirs were constructed of three overlapping 10 feet by 10 feet steel plates, emplaced deep enough in the ground to inhibit underflow beneath the weir, and wide enough to contain the pond so that no flow is allowed to skirt around the edges of the weir. Barbed wire fencing was constructed around the weir ponds to prohibit entry of roaming livestock.

Four- and six-inch screen-slotted stilling wells (**Photograph 5**) were emplaced on July 22, 2003 to house shaft encoders with data loggers (Thalimedes logger produced by Ott Hydrometrie, vertical resolution of 1 mm) to measure the water level in the ponds behind each weir. Changes in water level are transferred via a float-cable-counterweight-system to a pulley on the encoder, and any rotation in this pulley is converted to an electrical signal, which is transferred to the data logger and saved as a measured value. The stillwells were placed slightly off-center of the thalweg, and far enough behind the v-notch (about 5 feet) so that the loggers are not recording water levels that slope toward the notch of the weir. Following Buchanan and Somers (1969), the level of the water in the pond behind the weir is calibrated to discharge by:

$$Q_{cfs} = 2.47*h^{2.5} \qquad \text{(Eqn. 3.1)}$$

where

Q_{cfs} = discharge in cubic feet per second

h = height of water level (feet)

Discharge was also calibrated by bucket measurements through the v-notch, using a leveling instrument to measure the water level above the notch (**Photograph 5**). Bucket calibrations were performed during each download of the data as a check on automated measurements.

The placement of the v-notch weirs and knowledge of daily CBNG input into each impoundment pond allows the analysis of conveyance losses in four separate blocks (see **Figure 6**). Block I is a pond dominated section including the upper pond and the stream reach above the upper weir. Block II is a stream channel section between the upper weir and the middle weir. Block III is a pond-dominated section composed of the stream section between the middle weir and the lower pond, the lower pond, and the stream section above the lower pond weir. Finally, block IV is a stream channel between the lower pond weir and the lower weir.

Evaporation pans

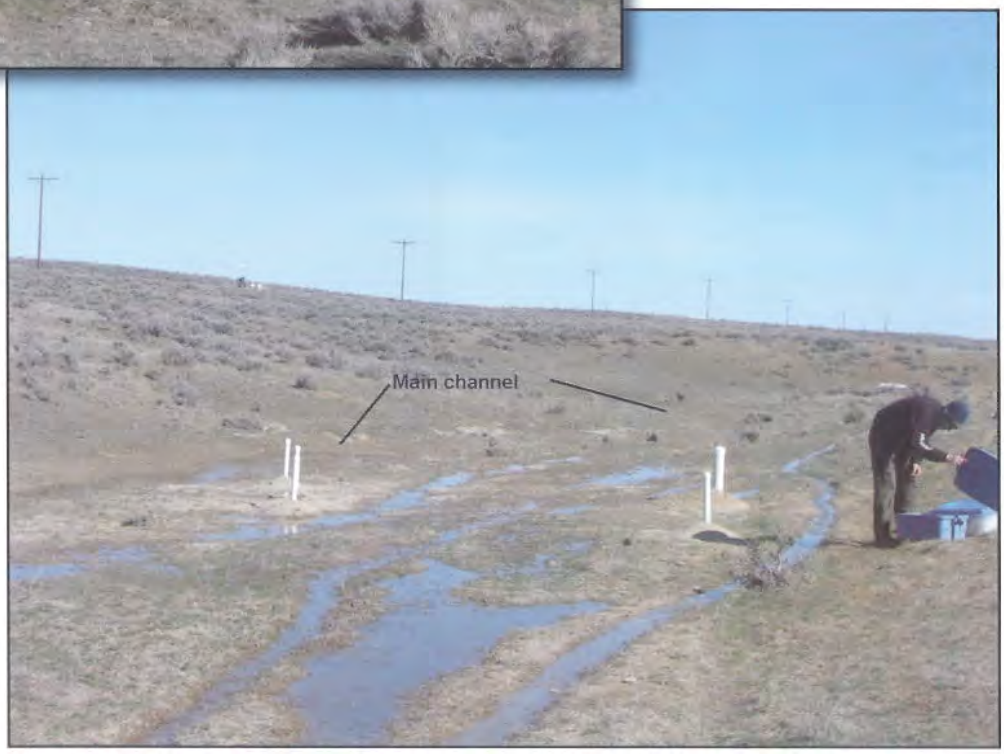
Two evaporation pans were installed in the upper pond area (see **Photograph 10**). A 4-foot by 1-foot circular pan was placed on the ground, set atop 6-inch blocks, on the south bank of the upper pond. A barometrically

compensated water level logger (Global Water, WL-15, 0 to 3 foot range) recorded the drop in water level over time. A floating evaporation pan of the same size was suspended in the middle of the upper pond. A float is perched on top of the pan water level and attached to a release valve, which is connected by a hose to a re-fillable reservoir tank on the south bank of the upper pond. When the float in the pan drops due to evaporation, water in the reservoir tank flows by gravity to refill the pan to its original level. A Stephens recorder logs the drop in the reservoir tank, which is converted to an evaporative loss in the pan. Data from the two pans proved similar during the summer and fall of 2003, thus only the floating evaporation pan was utilized during the 2004 field season.

Due to the fact that evaporation from smaller water bodies is greater than that of larger water bodies, it is necessary to include a reduction coefficient to convert



Photograph 1. Upper monitoring wells. View to the north (downstream).



Photograph 2. Middle monitoring wells. View to the north (downstream).



Photograph 3. Lower monitoring wells, looking to the northwest. Stream is behind photographer to the east.



Photograph 4. Tributary monitoring wells. View to the southeast.



Photograph 5. Weir leveling instrument. Picture from lower weir.



Photograph 6. Upper weir.



Photograph 7. Middle weir.



Photograph 8. Lower pond weir.



Photograph 9. Lower weir.



Photograph 10. Upper pond showing placement of evaporation equipment.

pan evaporation data to lake or reservoir evaporation (Lewis, 1978). Upon review of previous work done on pan evaporation, Lewis (1978) concluded that a coefficient of 0.7 is applicable to reservoir evaporation. This coefficient was used to convert all gathered evaporation pan data to values for evaporation in the CBNG ponds and stream sections.

Figure 7 shows the method of calculation for an average evaporation rate in the ground pan for a weekly interval. Had there been precipitation during this interval, the rainfall amount would be summed with the total drop in water level. The logger used to measure water level in the stillwell is advertised as barometrically compensated, but inspection of the graph representing water level drop over time suggests that atmospheric pressure does affect water level in the pan. There appears to be a regular trend of higher atmospheric pressure (depressed water levels) early in the day, and a subsequent drop in atmospheric pressure and rise in water level in the afternoon. Upon inspection of atmospheric pressure data (not shown in **Figure 7**)

from the Gillette-Campbell County Airport (about 30 miles away), this trend is in fact normal for daily pressure changes. As a result, a best-fit line is utilized to connect data points reflecting higher atmospheric pressure conditions.

The floating evaporation pan utilizes a Stephens recorder which recorders the water level drop in a water reservoir situated on the bank above pond level. This drop in water level is converted to a corresponding drop in the evaporation pan by the following formula:

$$(\text{Evaporation Pan})_{\text{Loss}} = (\text{Reservoir})_{\text{Loss}} * (\pi R_{res}^{2})/(\pi R_{pan}^{2}) \quad \text{(Eqn. 3.2)}$$

where

R_{res} = radius of reservoir tank

R_{pan} = radius of evaporation pan

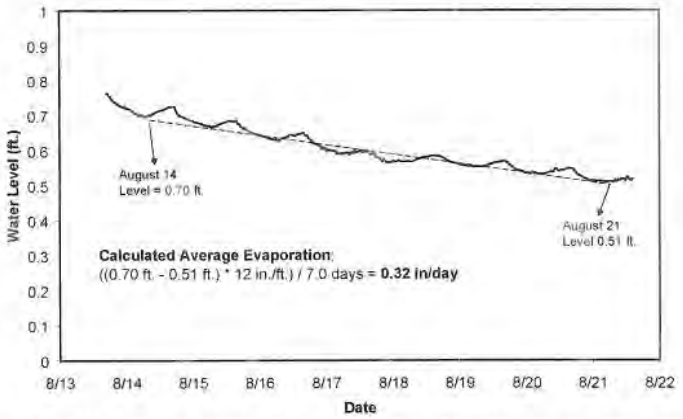


Figure 7. Sample evaporation calculation for ground evaporation pan, August 13 through 21, 2003. Dashed line connects inferred periods of highest atmospheric pressure.

Rain gauge

A tipping-bucket rain gauge with an event logger (Onset RG-2 gauge, with HOBO event logger, data resolution of 0.01" of rainfall) was installed on August 6, 2003, within the fenced-in area of the middle weir (**Picture 7**). We placed the rain gauge in the middle of the site to best estimate rainfall over the entire study area. The gauge was removed in November 2003, for the duration of the winter, and re-deployed on March 25, 2004.

Precipitation data was primarily employed to compensate evaporation pan data. It was also used to qualitatively analyze surface flow through the weirs. Periods of intense rainfall produced spikes in surface flow throughout the system. These periods were omitted in the water budget because of the addition of overland flow to the system.

Surface area of the stream and ponds

For the purpose of calculating infiltration rates per unit area and total evaporative loss, it was necessary to measure the surface area of surface water bodies. We used a measuring wheel and a compass to encircle the perimeter of the two ponds to establish surface area. The measuring wheel was used to measure length along the stream bank and a measuring tape utilized to estimate stream width. Stream widths were noted at irregular intervals when there was a noticeable change in width. Average stream width along the upper stream section (block II) was 0.8 meters (2.6 feet). The average stream width in the lower stream section (block IV) was 1.4 meters (4.6 feet). **Table 2** summarizes the results of this survey.

Direct aquifer property measurements

Slug tests were conducted in August and September 2004, using a falling head slug test method. A PVC-pipe section with a known amount of water and a valve attached at the bottom was used to introduce water into the formation. Introduced water volume ranged from 2.16 to 2.36 L. The valve fits on top of the monitoring well casing, with a water level logger in place to measure the recovery of water level to its original level. The valve is opened and introduces an instantaneous slug of water into the monitoring well. Water level recovery was monitored for 5 minutes, at 10-second intervals, which was sufficient time for the water levels to recover to within approximately 0.1 to 0.2 feet of initial static water level.

Table 2. Area of infiltration blocks.

Infiltration Block	Area of Surface Water Bodies (ft²)
Block I (Pond)	36,950
Block II (Stream)	2,350
Block III (Pond)	114,000
Block IV (Stream)	8,170

Because these wells were only partially penetrating into an unconfined aquifer, hydraulic conductivity was determined from the Hvorslev (1951) method by:

$$K = r^2 \ln(L_e/R) / 2 L_e t_{37} \quad \text{(Eqn. 3.3)}$$

where

K = Hydraulic conductivity (m/s)
r = Radius of the well casing (m)
R = Radius of the well screen (m)
L_e = Length of the well screen (m)

t_{37} = Time it takes for water level to fall to 37% of the initial change (s)

If the length of the screen is eight times more than the radius of the well screen (which it is for all of the monitoring wells), the Hvorslev method is valid. The initial height to which the water rises in the well is defined as h_0. The height of the water in the well after some time, t, is h. This head ratio, h/h_0, is plotted versus time on semilogarithmic paper, and the time-drawdown data should plot as a straight line. A best-fit line is applied to the time-drawdown data, and t_{37} is determined from this best-fit line.

Water budget analysis

The method for calculating the water budget is based upon the following formula:

$$Q_{in} = Q_{out} \pm \Delta\text{Storage} \quad \text{(Eqn. 3.4)}$$

Because pond levels are maintained at a constant height by a water level control structure, changes in storage in the surface water system are approximately 0. Expanding the terms of the water budget formula, the water budget is described by:

$$(\text{CBNG water} + \text{Precipitation} + \text{Runoff}_{in}) - (\text{Runoff}_{out} + \text{Evapotranspiration} + \text{Infiltration}) = 0 \quad \text{(Eqn. 3.5)}$$

Barring a major storm event, runoff_{in} is equal to zero, and no non-CBNG water drains into the system. In the absence of significant vegetation, transpiration (T) is assumed to be zero in this analysis. Recorded rainfall events at the study site tend to be of short duration, and weir surface flow peaks related to stormflow dissipate relatively quickly. Because rainfall quickly moves out of the system, we ignored these time intervals in the water budget and do not need to account for the volumetric input of precipitation. Equation 3.5 can be rearranged to solve for infiltration within the entire system:

$$\text{Infiltration} = \text{CBNG water} - (\text{Runoff}_{out} + \text{Evaporation}) \quad \text{(Eqn. 3.6)}$$

Infiltration is reported in standard units of gallons per minute (gpm). For calculation of infiltration within the four infiltration blocks, a slight modification needs to be made to account for surface flow entering each infiltration block in the upstream direction. In blocks II, III, & IV, surface water enters each of these blocks through the upper weir, middle weir, and lower pond weir, respectively. Considering this source term, Runoff_{in}, block infiltration is determined by:

$$\text{Infiltration} = (\text{CBNG water} + \text{Runoff}_{in}) - (\text{Runoff}_{out} + \text{Evaporation}) \quad \text{(Eqn. 3.7)}$$

Infiltration rate is determined through infiltration and surface areas from **Table 3** and reported as inches per day (in/day) by:

$$\text{Infiltration Rate (in/day)} = \text{Infiltration/Area} \quad \text{(Eqn. 3.8)}$$

and converting:

Infiltration = gpm * (231 in^3/gal) * (1440 min/day) = in^3/day

Area = ft^2 * (12 in/ft)^2 = in^2

Results

Field results: Water budget and shallow aquifer response

Precipitation

Precipitation data was gathered from August 6 to November 1, 2003, and from March 25 to September 18, 2004. The 2004 field season had more total precipitation and many more precipitation events than 2003. Overall, the summer of 2003 was a relatively dry interval in the PRB, while the months during the 2004 study interval were generally wetter than normal in this region (Wyoming State Climate Office). **Figures 8** and **9** provide a graphical representation of precipitation in 2003 and 2004, respectively. On July 22 through23, 2004, there were three large storm events that generated 1.36 inches of rain in two days. On July 22, two storms brought 0.36 inches of precipitation. The next day, an unusually long storm lasting about 10 hours dropped 1.00 inches of rainfall. During a field visit on August 26, 2004, stream debris was observed around the edges of the lower pond weir, indicating the stream channel had breached the capacity of the weir.

Evaporation pan results

Evaporation pan data were gathered for the period from August 13 through October 28, 2003, and from May 25 through September 18, 2004. Two evaporation pans were utilized for most of the 2003 budget season. A floating evaporation pan was anchored in the middle of the upper pond, and a ground evaporation pan was placed in the grass near the upper pond (see **Picture 10**). Only the floating evaporation pan was utilized for the 2004 season, owing to the similarity of results from both pans in 2003.

Tables 3 and **4** compare the data for the 2003 budget season for both evaporation pans. Note that the time intervals do not necessarily overlap, but data agreement is good. Corrected evaporation rates (multiplication by a 0.7 reduction coefficient) for the ground evaporation pan ranged from 0.10 to 0.22 in/day (**Table 3**). In the floating

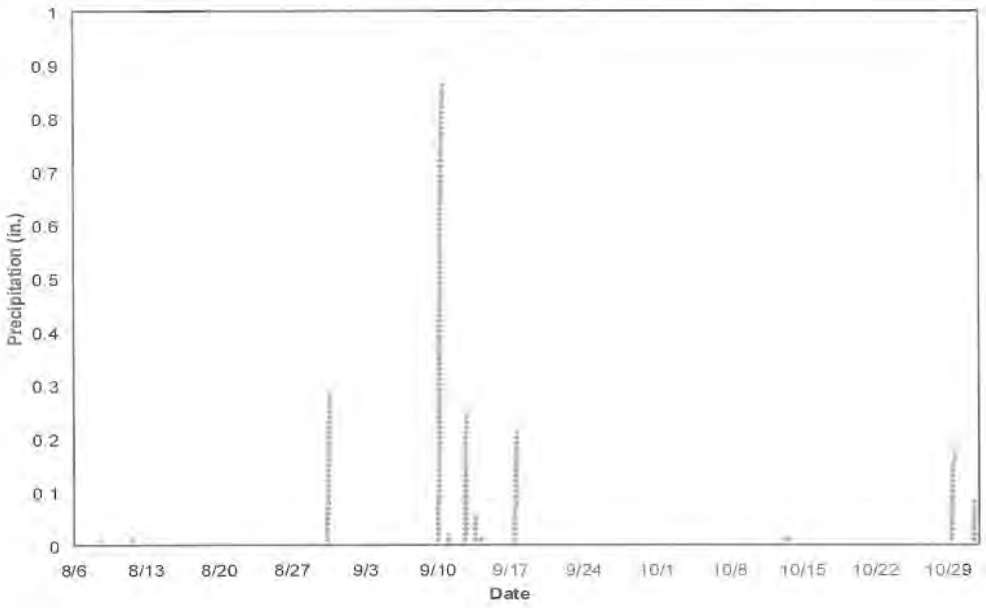


Figure 8. Precipitation data from August 6 to November 1, 2003.

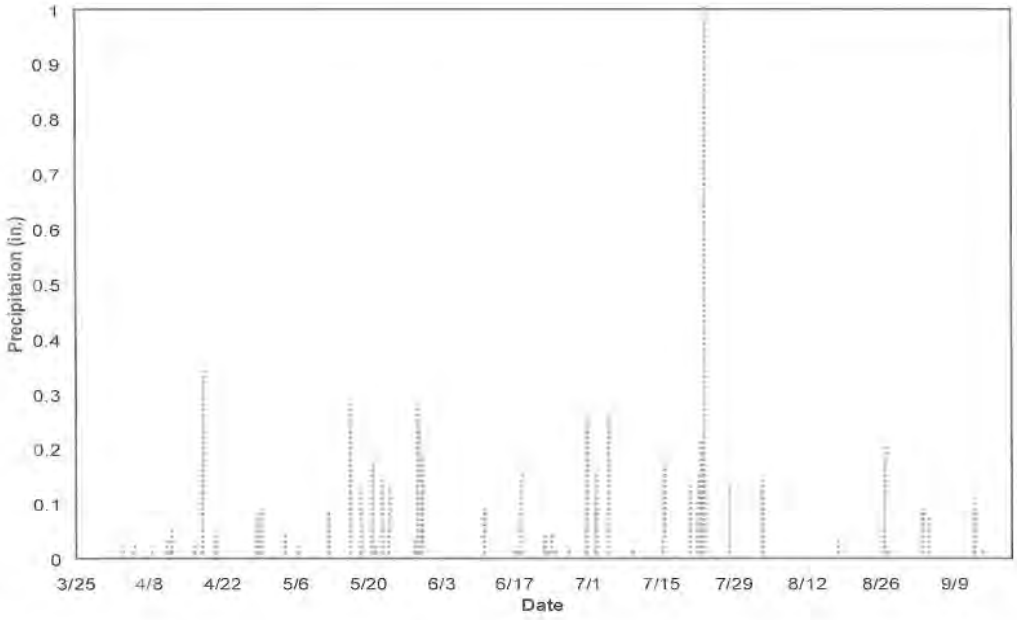


Figure 9. Precipitation data from March 25 to September 18, 2004.

pan, corrected evaporation rates varied from 0.11 to 0.20 in/day (**Table 4**). For the intervals of August 22 through September 7, and September 8 through 20, 2003, results for the ground pan and floating pan agree to within 0.01 inches/day. **Table 5** shows the data for the floating evaporation pan from May 25 through September 18, 2004, in two-week intervals. Corrected evaporation rates ranged from 0.11 to 0.24 in/day. There was a data loss from August 9-26 because the water in the reservoir tank ran out before a return visit to the field site could be made. The hose that connects the reservoir tank to the floating evaporation pan was cleaned out on August 27 for the first time since installation. It was discovered that a large amount of algae growth was flushed out of the hose. No determination could be made about the effect that this had on calculated evaporation results.

Table 6 shows evaporation studies from several authors for reservoir evaporation. Lahoti (1968), Brown (1970), and Lewis (1978) are master's thesis research that focused on evaporation in the state of Wyoming. Assuming an annual reservoir evaporation of 47 inches for the Gillette area (Lewis, 1978), the four authors calculated percentage of annual evaporation by month. An average daily evaporation rate is calculated from these monthly percentage values, and an average value is calculated from the results of all authors.

Table 3. Ground evaporation pan data, August 13 to October 16, 2003.

GROUND EVAPORATION PAN		
Time Interval	Calculated Evaporation	Corrected Evaporation (*0.7)
August 13-21, 2003	0.32 in/day	0.22 in/day
August 22-September 7, 2003	0.27 in/day	0.19 in/day
September 8-20, 2003	0.17 in/day	0.12 in/day
September 21-27, 2003	0.18 in/day	0.13 in/day
September 28-October 16, 2003	0.14 in/day	0.10 in/day

Table 4. Floating evaporation pan data, August 22 to October 28, 2003.

FLOATING EVAPORATION PAN		
Time Interval	Calculated Evaporation	Corrected Evaporation (*0.7)
August 22-September 7, 2003	0.29 in/day	0.20 in/day
September 8-20, 2003	0.19 in/day	0.13 in/day
September 21-October 16, 2003	0.16 in/day	0.11 in/day
October 16-28, 2003	0.20 in/day	0.14 in/day

Table 5. Floating evaporation pan data, May 25 to September 18, 2004.

FLOATING EVAPORATION PAN		
Time Interval	Calculated Evaporation	Corrected Evaporation (*0.7)
May 25-June 9, 2004	0.26 in/day	0.18 in/day
June 10-24, 2004	0.15 in/day	0.11 in/day
June 25-July 8, 2004	0.26 in/day	0.18 in/day
July 9-23, 2004	0.34 in/day	0.24 in/day
July 24-August 9, 2004	0.25 in/day	0.18 in/day
August 9-26	No Data	No Data
August 27-September 10, 2004	0.22 in/day	0.15 in/day
September 11-18, 2004	0.25 in/day	0.18 in/day

For the ponds and streams at the Beaver Creek site, frozen conditions existed mid- to late-November until the end of March. For the purpose of the 2003 water budget, calculated evaporation rates, the average values from **Table 6**, and departure from normal temperatures were taken into account to determine an evaporation rate to apply to the entire study area. Both July and August 2003, experienced the second highest average temperature in Wyoming's 110-year record of climate history (Wyoming State Climate Office, 2004). Temperatures were normal in September 2003, and well above normal in October 2003. May and September 2004, were at or above normal average temperature, and the summer months of June through August experienced cooler than normal average temperatures. **Table 7** shows the evaporation rates that were used for each of the intervals

Table 6. Daily evaporation rates in inches per day from reservoirs for each month in the Gillette area assuming an annual lake evaporation of 47 inches, various authors.

Month	Meyer (1942)	Lahoti (1968)	Brown (1970)	Lewis (1978)	Average
January	0.024	0.041	0.073	0.041	0.04
February	0.030	0.057	0.052	0.042	0.05
March	0.055	0.096	0.039	0.059	0.06
April	0.097	0.146	0.118	0.125	0.12
May	0.129	0.182	0.197	0.174	0.17
June	0.200	0.224	0.204	0.205	0.21
July	0.284	0.235	0.223	0.259	0.25
August	0.284	0.205	0.211	0.237	0.23
September	0.200	0.163	0.165	0.180	0.18
October	0.129	0.102	0.139	0.115	0.12
November	0.067	0.053	0.061	0.061	0.06
December	0.029	0.038	0.049	0.039	0.04

in the 2003 water budget. **Table 8** shows the evaporation rates that were used for the 13 two-week-long budget intervals for the 2004 budget season. These rates were determined from the average of various authors from **Table 6** due to the uncertainty in the floating evaporation pan data from 2004.

Water budget results

A water budget was determined for July 23 through November 1, 2003, and divided into week-long intervals to examine any temporal changes. Due to periods of data loss of surface flow through the weirs and uncertainty in CBNG water input data, a partial water budget was determined from March 25 through September 18, 2004. Time was divided into two-week-long budget intervals for the 2004 water budget. Development of a water budget involves three variables: 1) CBNG water input into each pond, 2) surface

Table 7. Evaporation rates for 2003 water budget. Average daily temperatures (F°) and average high temperatures (F°) from Gillette-Campbell County Airport weather station.

Week	Dates	Average Temperature	Average High Temperature	Evaporation Rate
1	7/23-7/28	78.2	94.0	0.25 in/day
2	7/29-8/4	74.6	90.7	0.24 in/day
3	8/5-8/11	80.3	96.7	0.26 in/day
4	8/12-8/18	80	94.8	0.26 in/day
5	8/19-8/25	74.4	90.9	0.22 in/day
6	8/26-9/1	67.1	80.6	0.19 in/day
7	9/2-9/8	68.6	85.9	0.20 in/day
8	9/9-9/20	56.1	67.4	0.13 in/day
9	9/21-9/27	50.2	64.5	0.12 in/day
10	9/28-10/4	54.1	69.0	0.11 in/day
11	10/5-10/11	50.3	64.9	0.11 in/day
12	10/12-10/18	56.4	72.3	0.11 in/day
13	10/19-10/25	50.6	64.4	0.12 in/day
14	10/26-11/1	36.9	47.1	0.08 in/day

Table 8. Evaporation rates for 2004 water budget.

2-week interval #	Dates	Evaporation Rate
1	March 25 – April 7, 2004	0.07 in/day
2	April 8 – 21, 2004	0.12 in/day
3	April 22 – May 5, 2004	0.14 in/day
4	May 6 – 19, 2004	0.16 in/day
5	May 20 – June 2, 2004	0.19 in/day
6	June 3 – 16, 2004	0.20 in/day
7	June 17 – 30, 2004	0.21 in/day
8	July 1 – 14, 2004	0.22 in/day
9	July 15 – 28, 2004	0.23 in/day
10	July 29 – August 11, 2004	0.22 in/day
11	August 12 – 25, 2004	0.22 in/day
12	August 26 – September 8, 2004	0.20 in/day
13	September 9 – 18, 2004	0.17 in/day

flow through the four weirs, and 3) an evaporation rate. Coalbed natural gas co-produced water data were provided by the producing company reported in the form of barrels of water per day, which were converted to units of gallons per minute (1 barrel = 42 gallons) for consistency. Data from the weirs has a resolution of one reading per hour. Therefore, we used the average daily CBNG input value for all 24-hour time intervals for each day. Evaporation rates from **Tables 7** and **8** represent average values that are employed for each week-long or two-week-long budget interval.

Figure 10 shows the flow components of the entire system for the study interval in 2003. Notice that CBNG water represents a steadily declining input to the system. This is typical of CBNG production; water production is highest in the earlier stages of development and decreases as water levels in the coal aquifer are drawn down (De Bruin and Lyman, 1999). There are also prominent peaks in weir flow (notably on July 28 and September 11), which reflect large rainstorm events (**Figure 10**).

When determining a water budget for the system, it is ideal if the system is in equilibrium, such that the change in storage is zero (Equation 3.4). During periods of rainfall, there is an added element of overland flow and precipitation into the stream, which augments surface flow. In the middle stream section (between the upper weir and middle weir), during the two previously mentioned storm events, flow through the middle weir is greater at its peak than flow through the upper weir. When infiltration is calculated for this block using Equation 3.7 during this short time period, a negative value results. In addition, when CBNG water input drops for a short period, there is a delay in the surface water response, on the order of approximately 1-2 days. It is difficult to pinpoint this lag accurately because CBNG water input provided by the producing company represents an average value for each day. We did not consider these periods of transient behavior in analysis of the water budget.

Figure 11 shows the breakdown of conveyance loss from evaporation, calculated infiltration, and surface runoff out of the system as a percentage of total co-produced CBNG water for the 2003 water budget. Due to limits in data resolution for average daily CBNG water input, not all numbers add up to exactly 100%, but all numbers are within ± 1%. A budget for the week of September 2 through 8 was not calculated because of data loss at the lower weir resulting from a dead battery in the data logger.

Evaporation of CBNG water within the study site varied from 14.4% to 5.5% and generally decreased into the later months as air temperatures fell. Infiltration ranged from 39.5% to 55.7% of total CBNG input, with an average infiltration percentage of 46.1%. Surface runoff out of the study site ranged from 29.9% to 54.2%, with an average of 44.2%. It is important to note that "surface runoff" applies to surface water discharge that flows past the lower weir and out of the study site. This water most likely continues to infiltrate as it flows about 3/4-mile downstream to join Beaver Creek. (Inspection of this junction and upstream of the junction in the summer of 2004 revealed that Beaver Creek was flowing as a perennial stream, receiving an amount of water exceeding the input from the Beaver Creek study site. Presumably, this streamflow is due to upstream CBNG development in other areas of the Beaver Creek watershed). Excepting three budget intervals (August 12 through 18, September 9 through 20, and October 26 through November 1), percentage loss by infiltration and runoff remained consistently close to the average with no discernible trend in the 3+ month study interval.

In terms of water volume amounts, **Table 9** shows the total volume (in gpm) of CBNG water influx into the system, evaporative volume, surface runoff out of the study site, and calculated infiltration. CBNG water generally declines from week-to-week, decreasing from a high of 133.8 gpm in week 1, to 100.7 gpm in the final week. Evaporative losses also decrease from 17.9 gpm in week 3, to 5.6 gpm in the final week. Water flow out of the study site, defined as surface runoff, ranges from 60.2 gpm in week 2 to 35.9 gpm in week 4. Total infiltration ranges from 68.8 gpm in week 4, to 40.2 gpm in the final week. Surface runoff and calculated infiltration volumes generally declined through time over the study interval.

In addition to analyzing total conveyance loss through the system for the 2003 water budget, these losses were calculated for each discrete block in at the study site (see **Figure 6**). **Figure 12** is a schematic diagram of the study site detailing three selected week-long water budget intervals and displaying calculated conveyance losses in each infiltration block, average CBNG water input, and average

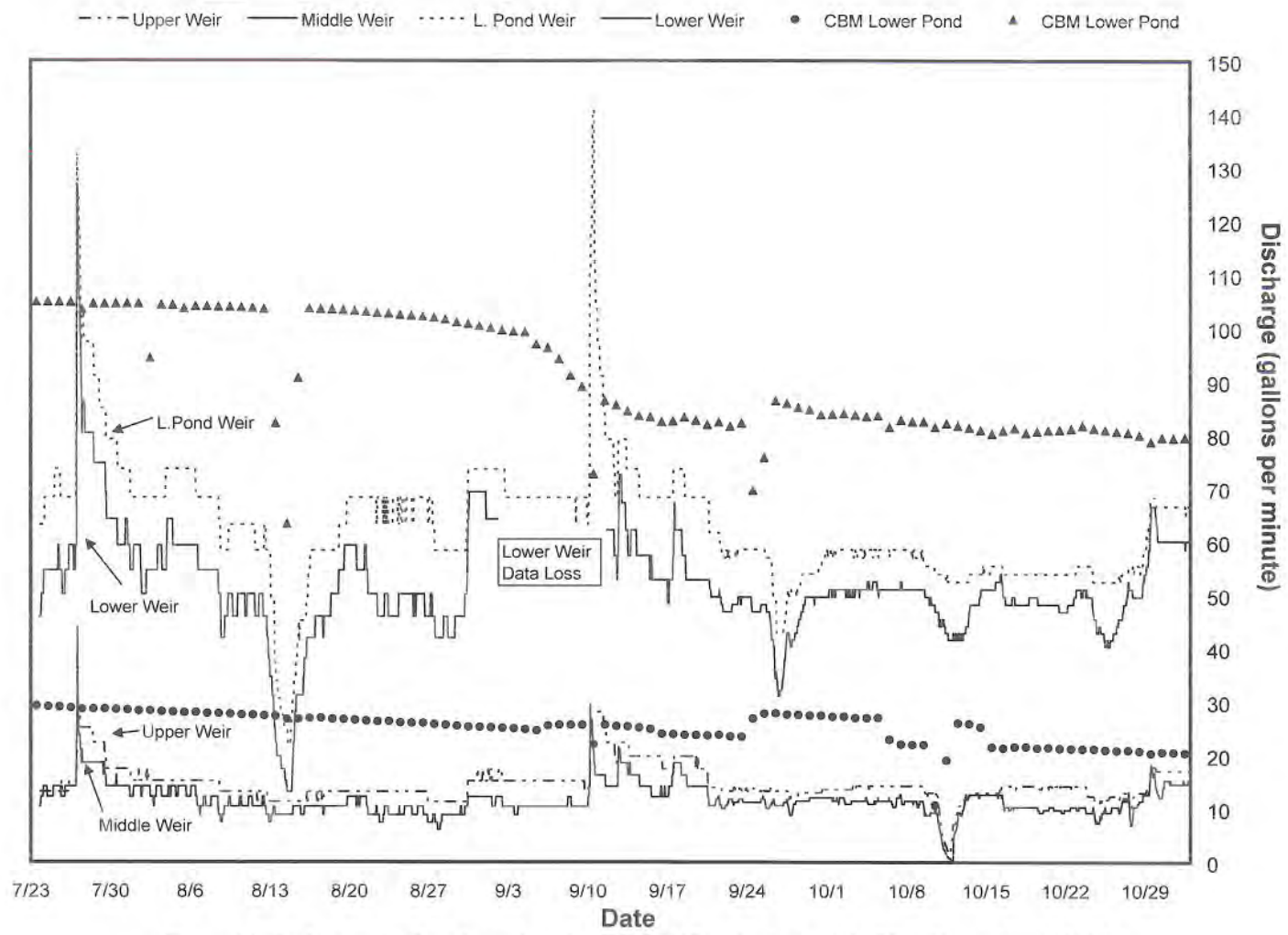


Figure 10. Surface water flow through weirs and CBNG water input, July 23 to November 1, 2003.

Table 9. CBNG water volumes, conveyance losses, and surface runoff in gallons per minute during 2003. ND = no data.

Week #	Dates	Total CBNG Water	Total Evaporation	Total Surface Runoff	Total Infiltration
1	7/23-7/28	133.8	17.2	57.1	59.7
2	7/29-8/4	131.4	16.6	60.2	54.8
3	8/5-8/11	131.7	17.9	52.5	61.3
4	8/12-8/18	119.9	17.2	35.9	68.8
5	8/19-8/25	129.2	15.2	51.7	62.4
6	8/26-9/1	126.8	13.2	53.6	60.0
7	9/2-9/8	122.0	13.9	ND	ND
8	9/9-9/20	107.7	9.0	56.9	42.2
9	9/21-9/27	106.4	8.3	45.5	52.6
10	9/28-10/4	111.4	7.6	49.5	54.5
11	10/5-10/11	105.6	7.6	49.4	47.0
12	10/12-10/18	104.0	7.6	48.1	48.2
13	10/19-10/25	102.4	8.3	47.5	46.6
14	10/26-11/1	100.7	5.6	54.5	40.5

surface flow through the weirs. The amount of infiltration and evaporation is greatest in block III, which represents the largest component of the system in terms of surface area (and thus infiltration area). The second largest component of evaporation predictably occurs in pond-dominated block containing the smaller upper pond, while evaporation is minimal from the stream channel blocks II and IV (only 1.0 gpm from August 5 through 11). Although the surface area of block I is about 4.5 times greater than the area of block IV (**Table 2**), the amount of infiltration is similar for each of the three budget weeks. **Table 10** shows the variables in the water budget equation (Equation 3.7) for all week-long intervals which were utilized to determine infiltration within each block.

An areal survey was conducted (September 27, 2003) for the express purpose of determining the area of surface water, and thus the approximate area of infiltration. Since the inputs to the system in the form of CBNG water are not constant, and generally decline through time, it is important

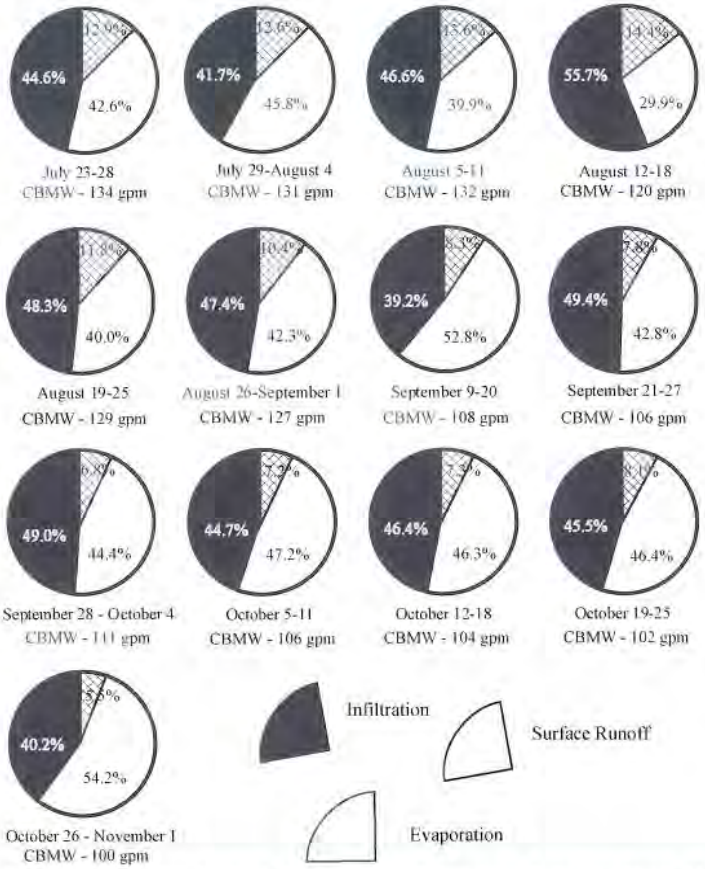


Figure 11. Water budget conveyance losses as a percentage of total CBNG input, 2003 season. Summation of percentage values are ± 1% of 100%.

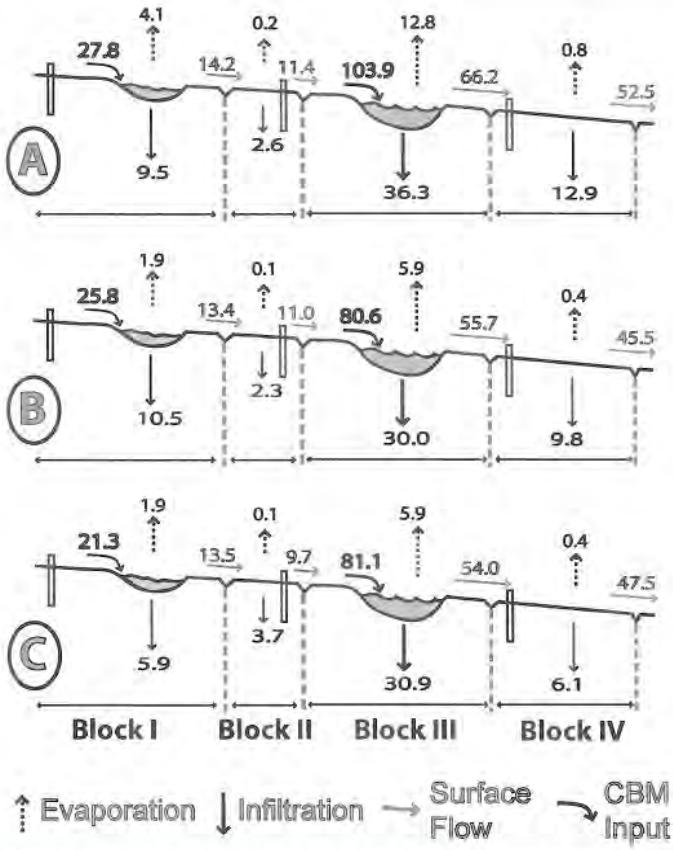


Figure 12. Three week-long water budget intervals detailing conveyance losses by block, CBNG water input, and surface flow in gallons per minute for 2003. A) August 5 through 11, B) September 21 through 27, and C) October 19 through 25.

to look at the infiltration as a rate (units of L/T) in each infiltration block. **Table 11** shows the conveyed water loss for each of the four discrete blocks, and a calculated infiltration rate for each budget interval by dividing a total volume of water over the infiltration area and converting to units of inches per day (Equation 3.8).

In general, the largest total amount of infiltration in terms of volume occurs in block III, a similar amount of infiltration occurs in block I and IV, and the least amount of infiltration occurs in block II (**Figure 12**; **Tables 10** and **11**). Calculated infiltration rates in the pond dominated blocks (blocks I and III) are similar and significantly less than the rates in the stream channel blocks (blocks II and III) (**Table 11**). Average infiltration rates throughout the 2003 water budget interval for the pond dominated blocks (I and III) are 0.53 and 0.65 inches/day, respectively. The average infiltration rates in the stream channel blocks (II and IV) are 2.68 and 2.82 in/day, respectively (**Table 11**).

It is difficult to discern any temporal trends in the infiltration data. In the pond-dominated block I, the lowest infiltration rate (week 8) is followed by the third-highest infiltration rate (**Table 11**). During the final two weeks (weeks 13 and 14) of the water budget, infiltration rates are low, but several weeks before in week 10, the infiltration rate is the highest of the budget season. In the other pond-dominated section (block III), infiltration rates vary little, excepting weeks 4 and 8, which exhibit the highest and lowest infiltration rates (0.86 and 0.43 in/day, respectively).

In the middle stream channel section (block II), calculated infiltration rates vary from 2.00 to 3.67 in/day, but there is no discernible trend from late July to the end of October (**Table 11**). In the lower stream channel section, block IV, there does appear to be a decrease in infiltration rates in the latter half of the 2003 water budget. In weeks 1 through 9, rates vary from 2.76 to 4.06 in/day, while in the final five weeks they range from only 1.61 to 1.99 in/day (**Table 11**).

For the 2004 season, water budget intervals were divided into two-week-long time periods to analyze temporal trends. Calculated infiltration for both budget years were similar in the two pond-dominated blocks (I and III), but calculated infiltration in the two stream channel blocks (I and IV) showed a significant difference from 2003 to 2004. **Table 12** summarizes CBNG input, surface flow, evaporative losses, and calculated infiltration for the 2004

Table 10. CBNG water input, surface flow, and conveyance losses for infiltration blocks, 2003 budget. ND = no data. All values in gallons per minute. Runoff$_{in}$ (R_{in}) is any water entering upstream, runoff$_{out}$ (R_{out}) is water leaving downstream, evaporation (E) is calculated for each block, and infiltration (I) = (CBNG Water + R_{in}) – (R_{out} + E). Uncertainty for CBNG water is ± 0.1 gpm, for R_{in} and R_{out}, the uncertainty is ± 0.1 gpm, and for E, the uncertainty is ± 0.05 gpm.

		BLOCK I: Upper pond to Upper Weir					BLOCK II: Upper Weir to Middle Weir					BLOCK III: Middle Weir to Lower Pond Weir					BLOCK IV: Lower Pond Weir to Lower Weir				
Week #	Dates	CBNG Water	R_{in}	R_{out}	E	I	CBNG Water	R_{in}	R_{out}	E	I	CBNG Water	R_{in}	R_{out}	E	I	CBNG Water	R_{in}	R_{out}	E	I
1	7/23-7/28	29.0	0	14.9	3.9	10.3	0	14.9	12.6	0.22	2.1	104.8	12.6	71.2	12.3	34.0	0	71.2	57.1	0.81	13.3
2	7/29-8/4	28.4	0	16.1	3.8	8.5	0	16.1	13.6	0.21	2.3	103.0	13.6	73.1	11.8	31.8	0	73.1	60.2	0.78	12.2
3	8/5-8/11	27.8	0	14.2	4.1	9.5	0	14.2	11.4	0.23	2.6	103.9	11.4	66.2	12.8	36.3	0	66.2	52.5	0.84	12.9
4	8/12-8/18	27.0	0	12.2	3.9	10.9	0	12.2	9.9	0.22	2.1	92.9	9.9	47.8	12.3	42.7	0	47.8	35.9	0.81	11.1
5	8/19-8/25	26.4	0	13.2	3.5	9.7	0	13.2	10.0	0.19	3.0	102.8	10.0	66.8	10.8	35.3	0	66.8	51.7	0.71	14.4
6	8/26-9/1	25.6	0	13.1	3.0	9.4	0	13.1	10.0	0.16	3.0	101.2	10.0	65.9	9.4	35.8	0	65.9	53.6	0.62	11.8
7	9/2-9/8	25.3	0	14.5	3.2	7.6	0	14.5	10.6	0.17	3.7	96.7	10.6	68.8	9.8	28.6	0	68.8	ND	0.65	ND
8	9/9-9/20	24.5	0	17.9	2.1	4.6	0	17.9	14.6	0.11	3.2	83.2	14.6	70.3	6.4	21.4	0	70.3	56.9	0.42	13.0
9	9/21-9/27	25.8	0	13.4	1.9	10.5	0	13.4	11.0	0.10	2.3	80.6	11.0	55.7	5.9	30.0	0	55.7	45.5	0.39	9.8
10	9/28-10/4	27.3	0	13.5	1.7	12.1	0	13.5	11.5	0.10	2.0	84.1	11.5	56.4	5.4	33.9	0	56.4	49.5	0.36	6.5
11	10/5-10/11	23.2	0	14.2	1.7	7.31	0	14.2	11.1	0.10	3.0	82.4	11.1	56.8	5.4	29.7	0	56.8	49.4	0.36	7.0
12	10/12-10/18	22.9	0	13.5	1.7	7.7	0	13.5	10.2	0.10	3.2	81.1	10.2	54.3	5.4	31.6	0	54.3	48.1	0.36	5.7
13	10/19-10/25	21.3	0	13.5	1.9	5.9	0	13.5	9.7	0.10	3.7	81.1	9.7	54.0	5.9	30.9	0	54.0	47.5	0.39	6.1
14	10/26-11/1	20.7	0	14.7	1.3	4.7	0	14.7	12.4	0.07	2.2	80.0	12.4	61.1	3.9	27.5	0	61.1	54.5	0.26	6.1

Table 11. Calculated infiltration in each conveyance loss block and calculated infiltration rates, 2003. ND = no data.

			BLOCK I Upper Pond to Upper Weir		BLOCK II Upper Weir to Middle Weir		BLOCK III Middle Weir to L. Pond Weir		BLOCK IV L. Pond Weir to Lower Weir	
Week #	Dates	Total CBNG Water (gpm)	Infil. Loss (gpm)	Infil. Rate (in/day)	Infil. Loss (gpm)	Infil. Rate (in/day)	Infil. Loss (gpm)	Infil. Rate (in/day)	Infil. Loss (gpm)	Infil. Rate (in/day)
1	7/23-7/28	133.8	10.3	0.64	2.11	2.08	34.05	0.69	13.31	3.76
2	7/29-8/4	131.4	8.54	0.53	2.30	2.26	31.80	0.64	12.17	3.44
3	8/5-8/11	131.7	9.50	0.59	2.59	2.54	36.26	0.73	12.92	3.65
4	8/12-8/18	119.9	10.89	0.68	2.10	2.07	42.69	0.86	11.12	3.14
5	8/19-8/25	129.2	9.71	0.61	2.96	2.91	35.30	0.71	14.37	4.06
6	8/26-9/1	126.8	9.44	0.59	3.02	2.97	35.84	0.73	11.75	3.32
7	9/2-9/8	122.0	7.61	0.48	3.72	3.64	28.59	0.58	ND	ND
8	9/9-9/20	107.7	4.57	0.29	3.18	3.12	21.46	0.43	13.04	3.67
9	9/21-9/27	106.4	10.46	0.65	2.33	2.29	29.96	0.61	9.76	2.76
10	9/28-10/4	111.4	12.09	0.76	2.04	2.00	33.94	0.69	6.50	1.84
11	10/5-10/11	104.7	7.31	0.46	2.80	2.75	29.67	0.60	7.04	1.99
12	10/12-10/18	104.0	7.70	0.49	3.15	3.10	31.60	0.64	5.69	1.61
13	10/19-10/25	102.4	5.89	0.37	3.74	3.67	30.86	0.62	6.10	1.73
14	10/26-11/1	100.7	4.74	0.30	2.22	2.18	27.52	0.56	6.11	1.73
Average Values			**8.48**	**0.53**	**2.73**	**2.68**	**32.11**	**0.65**	**10.00**	**2.82**

season, and **Table 13** details the calculated infiltration rates. There were several factors, which precluded full analysis for this budget season. On April 23, 2004, the CBNG water input changed drastically into the lower pond, resulting in dramatically higher flows in the lower stream section (see R_{in} and R_{out} for budget interval #3 in **Table 12**). Three new producing wells were partially diverted into the lower pond, with an unspecified portion flowing into the lower pond and the remaining water into another impoundment pond to the east, out of the study site. Thus, it was not possible to determine the amount of CBNG water flowing into the lower pond and conveyance losses in block III were not calculated after budget interval #2. From April 6 through 19 (#4), there was data loss in the lower weir logger resulting from a dead battery. From June 3 through 16 (#6), no flow was detected through the middle weir, and only a small amount of water discharged through the upper weir (about 1.2 gpm). Since most of the streambed was dry, no conveyance losses were calculated. In the next interval from June 17 through 30 (#7), there was substantial flow through the upper weir, but no flow reached the middle weir. Upon visual inspection of the streambed in block II on June 26, 2004, the stream had completely infiltrated downstream at about 2/3 of the distance between the upper and middle weirs. Therefore, the amount of infiltration calculated for block II in this interval is a conservative calculation. From July 1 through 14 (#8), the float in the upper weir appears to be stuck during this interval. There is flow downstream in the middle weir, but no flow indicated in the upper weir. A rainstorm on July 15 appears to dislodge the float, allowing conveyance losses to be calculated for succeeding two-week interval (#9). An intense two-day precipitation event (1.36 inches from July 22 through 23), again causes the float in the upper weir to lodge high in the stilling well, therefore the conveyance losses calculated in this interval represent data from July 15 through 22. Data collection at the upper weir is restored after a field visit on August 26, allowing calculation of conveyance losses in block I for the final two budget intervals, but flow into block II through the upper weir is too low to calculate conveyance losses in this section. Conveyance losses in block IV for the intervals between July 29 and August 25 (#10 and #11) were not calculated because the author lacked confidence in the streamflow data.

In the pond-dominated block I, infiltration is relatively high in the first budget interval, but declines in the next four intervals and ranges from 2.5 to 3.9 gpm (**Table 12**). From June 3 through 16, the amount of infiltration dramatically

Table 12. CBNG water input, surface flow, and conveyance losses for infiltration blocks, 2004 budget. Uncertainty for CBNG water is ± 0.1 gpm, for R_{in} and R_{out}, the uncertainty is ± 0.1 gpm, and for E, the uncertainty is ± 0.05 gpm. (-) indicates no calculation, for reasons discussed in the text.

		BLOCK I: Upper pond to Upper Weir					BLOCK II: Upper Weir to Middle Weir					BLOCK III: Middle Weir to Lower Pond Weir					BLOCK IV: Lower Pond Weir to Lower Weir				
2-Week #	Dates	CBNG Water	R_{in}	R_{out}	E	I	CBNG Water	R_{in}	R_{out}	E	I	CBNG Water	R_{in}	R_{out}	E	I	CBNG Water	R_{in}	R_{out}	E	I
1	3/25-4/7	21.0	0	14.1	1.1	5.8	0	14.1	1.9	0.06	12.2	51.1	1.9	14.1	3.5	35.5	0	14.1	8.8	0.23	5.1
2	4/8-4/21	19.4	0	13.5	1.9	3.9	0	13.5	4.7	0.10	8.7	48.6	4.7	19.7	5.9	27.6	0	19.7	13.0	0.39	6.3
3	4/22-5/5	21.1	0	16.4	2.2	2.5	0	16.4	7.0	0.12	9.3	-	-	-	-	-	0	75.1	69.0	0.45	5.7
4	5/6-5/19	16.0	0	9.8	2.5	3.7	0	9.8	4.1	0.14	5.5	-	-	-	-	-	0	-	-	-	-
5	5/20-6/2	21.1	0	6.4	3.0	2.6	0	6.4	3.1	0.16	3.2	-	-	-	-	-	0	94.7	86.5	0.62	7.6
6	6/3-6/16	11.4	0	1.2	3.2	7.1	0	-	-	-	-	-	-	-	-	-	0	77.0	64.7	0.65	11.7
7	6/17-6/30	12.9	0	4.9	3.3	4.8	0	4.9	0.0	0.18	4.9	-	-	-	-	-	0	74.1	52.6	0.68	20.9
8	7/1-7/14	14.3	-	-	-	-	0	-	-	-	-	-	-	-	-	-	0	79.2	65.3	0.71	13.1
9	7/15-7/28	18.9	0	7.4	3.6	7.9	0	7.4	2.5	0.20	4.1	-	-	-	-	-	0	66.7	47.9	0.75	18.1
10	7/29-8/11	14.4	-	-	-	-	0	-	-	-	-	-	-	-	-	-	0	-	-	-	-
11	8/12-8/25	10.9	-	-	-	-	0	-	-	-	-	-	-	-	-	-	0	-	-	-	-
12	8/26-9/8	11.8	0	0.9	3.2	7.7	0	-	-	-	-	-	-	-	-	-	0	37.9	32.1	0.65	5.1
13	9/9-9/18	11.0	0	0.6	2.7	7.7	0	-	-	-	-	-	-	-	-	-	0	39.7	33.7	0.55	5.5

Table 13. Calculated infiltration in each block and calculated infiltration rates, 2004. (-) indicates no calculation, for reasons discussed in the text.

			BLOCK I Upper Pond to Upper Weir		BLOCK II Upper Weir to Middle Weir		BLOCK III Middle Weir to L. Pond Weir		BLOCK IV L. Pond Weir to Lower Weir	
Week #	Dates	Total CBNG Water (gpm)	Infil. Loss (gpm)	Infil. Rate (in/day)	Infil. Loss (gpm)	Infil. Rate (in/day)	Infil. Loss (gpm)	Infil. Rate (in/day)	Infil. Loss (gpm)	Infil. Rate (in/day)
1	3/25-4/7	72.1	5.8	0.36	12.2	11.95	35.5	0.72	5.1	1.43
2	4/8-4/21	67.9	3.9	0.25	8.7	8.58	27.6	0.56	6.3	1.79
3	4/22-5/5	-	2.5	0.16	9.3	9.16	-	-	5.7	1.60
4	5/6-5/19	-	3.7	0.23	5.5	5.42	-	-	-	-
5	5/20-6/2	-	2.6	0.16	3.2	3.14	-	-	7.6	2.14
6	6/3-6/16	-	7.1	0.44	-	-	-	-	11.7	3.29
7	6/17-6/30	-	4.8	0.30	4.9	4.76	-	-	20.9	5.90
8	7/1-7/14	-	-	-	-	-	-	-	13.1	3.71
9	7/15-7/28	-	7.9	0.49	4.1	4.04	-	-	18.1	5.11
10	7/29-8/11	-	-	-	-	-	-	-	-	-
11	8/12-8/25	-	-	-	-	-	-	-	-	-
12	8/26-9/8	-	7.7	0.48	-	-	-	-	5.1	1.45
13	9/9-9/18	-	7.7	0.48	-	-	-	-	5.5	1.55

increases in budget interval #6 to 7.1 gpm, drops off slightly to 4.8 gpm in interval #7, and ranges from 7.7 to 7.9 gpm in the final three intervals where data are available (#9, #12, and #13). Infiltration rates until June in block I range from 0.16 to 0.36 in/day (**Table 13**), and except for the lower infiltration rate in interval #7 (0.30 in/day), infiltration rates vary from 0.44 to 0.49 in/day in the latter half of the 2004 water budget. In the stream channel block II, there is a decline in infiltration through the first five budget intervals, as infiltration reaches a maximum of 12.0 gpm in interval #1, and is only 3.1 gpm during interval #5. This corresponds to infiltration rates of 11.95 and 3.14 in/day, respectively (**Table 13**). In the remaining budget intervals where infiltration was determined (#7 and #9), the infiltration rate is slightly higher at 4.76 and 4.04 in/day, respectively. As mentioned previously, the calculated infiltration rate from interval #7 is a conservative estimate because flow did not reach the middle weir. In block III, infiltration could only be determined for the first two budget intervals. Infiltration rates were 0.72 and 0.56 in/day, which compares well with the average rate of 0.65 in/day calculated for 2003 (**Table 11**). In block IV, calculated infiltration is relatively low in the first four intervals, ranging from 5.1-7.6 gpm (**Table 12**). Infiltration is significantly higher from interval #6 to #10, ranging from 11.7 to 20.9 gpm, and is low in the final two intervals where infiltration ranges from 5.1 to 5.5 gpm. It is important to note that there is a dramatic change in surface flow for this infiltration block during the third interval. Additional wells begin to empty into the lower pond, thus causing streamflow to rise from 19.7 gpm through the lower pond weir in interval #2, to 75.1 gpm in interval #3. Total infiltration for intervals #3 and #5 remain similar to calculated infiltration in the first two budget intervals.

Shallow aquifer response

Discharge from CBNG co-produced water began in the lower pond on November 10, 2002, and initiated on November 20, 2002, for the upper pond. Initial water level readings began on December 17, 2002, with the installation of monitoring wells. Manual water level readings were taken periodically thereafter, until a data logger was emplaced at a single well in each of the upper, middle, and lower monitoring well clusters on July 23, 2003, which provided hourly water level data.

From the initial water level readings, water levels in the monitoring wells screened to the alluvium and those screened

to the weathered portion of the Wasatch Formation showed no discernible difference, thus these two lithology layers are in hydraulic pressure communication with each other. Water level changes for each of the four monitoring well locations (**Figure 13**) were determined by averaging water level change from the monitoring wells at each location. The tributary well set had only one well (BC-9) intersecting the water table. Water levels at the middle well location rose about 4 feet in the three weeks after the initial water level reading (**Figure 13**). Water levels continued to rise to almost 6 feet at the beginning of April 2003, and they declined steadily after early April into June and July. A large snowstorm occurred during the middle of March 2003, accumulating about 1 foot of snow in the Powder River Basin, which up to that point had seen little snowfall over the previous several months. At the lower well locations, the water level rise due to infiltrating CBNG water and spring thaw moisture was more delayed. Water levels rose steadily through early April, followed by a dramatic rise of several feet to mid-May, after which water levels remained steady for the subsequent two-month interval. Water levels at the upper well location rose about 2 feet in the spring of 2003, and remained relatively steady until the end of July. The water level in the tributary well rose steadily in this eight-month interval, but only increased by about 1.5 feet.

A continuous record of water level response was achieved with the installation of level loggers at a single well at each of the upper, middle, and lower well-set locations. **Figure 14** shows the entire suite of level logger data for these three wells, until the end of the data collection period on September 18, 2004. **Figure 15** combines these data with the manual water level measurements to produce a complete record of water level change over a 21-month interval. From this complete record of water level data, the initial water level rise during the first four months of 2003 represents the greatest rise for the wells at the upper, middle, and lower sites. During the late summer and fall of 2003, there is a discernible steady rise in water level at the middle and lower wells from stream channel CBNG infiltration (ignoring the prominent peak in the middle well during the spring thaw). This is noted as the CBNG water "infiltrating CBNG water trend" in **Figure 15**. The water level from manual measurements in the tributary well shows a steady approximately 3 foot rise over the entire study interval, but without the temporal resolution of the logger data, the detailed timing of water level rise at this location cannot be constrained.

At the middle monitoring well, water levels increase steadily from November to the end of February 2004 (**Figure 14**). Thereafter, water levels at the middle well rise by approximately 3 feet into April, and then steadily decline into June. In the lower monitoring well (BC-12), the water level increases steadily from November 2003, through the end of May 2004 (**Figure 14**). There is a slight water level decline into the summer of 2004, with a pronounced peak at the end of July, after which levels recede and then remain steady until the end of the study period. Over the entire study interval, the lower well experiences a rapid increase in water level up until May 2003, declines slightly during the summer, then rises steadily through the spring of 2004, and falls slightly until the end of the study interval (**Figure 15**).

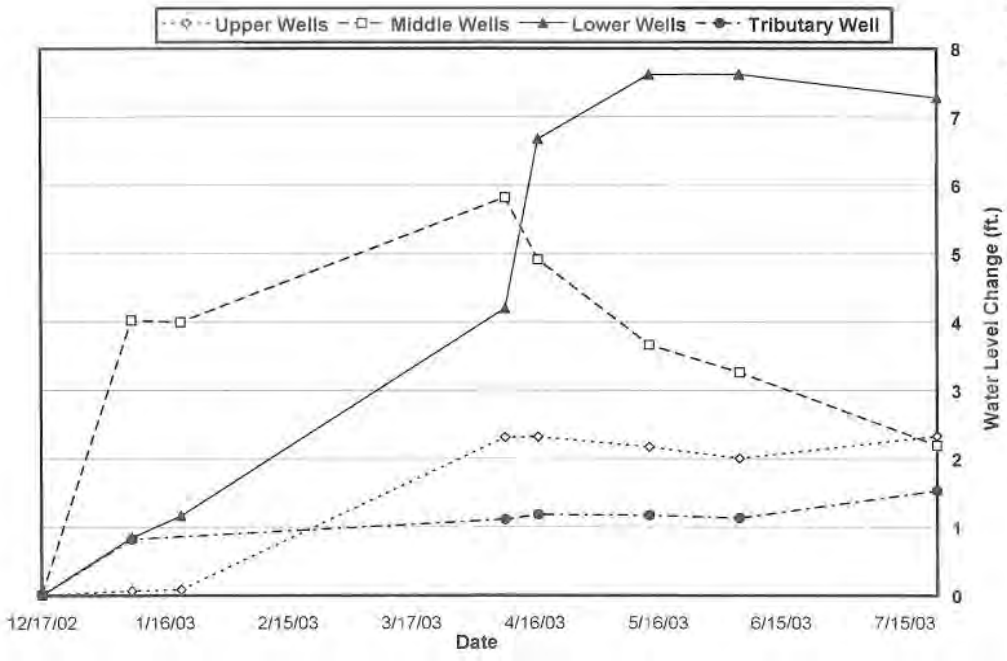


Figure 13. Average manual water level readings at four monitoring well locations, December 17, 2002 to July 23, 2003.

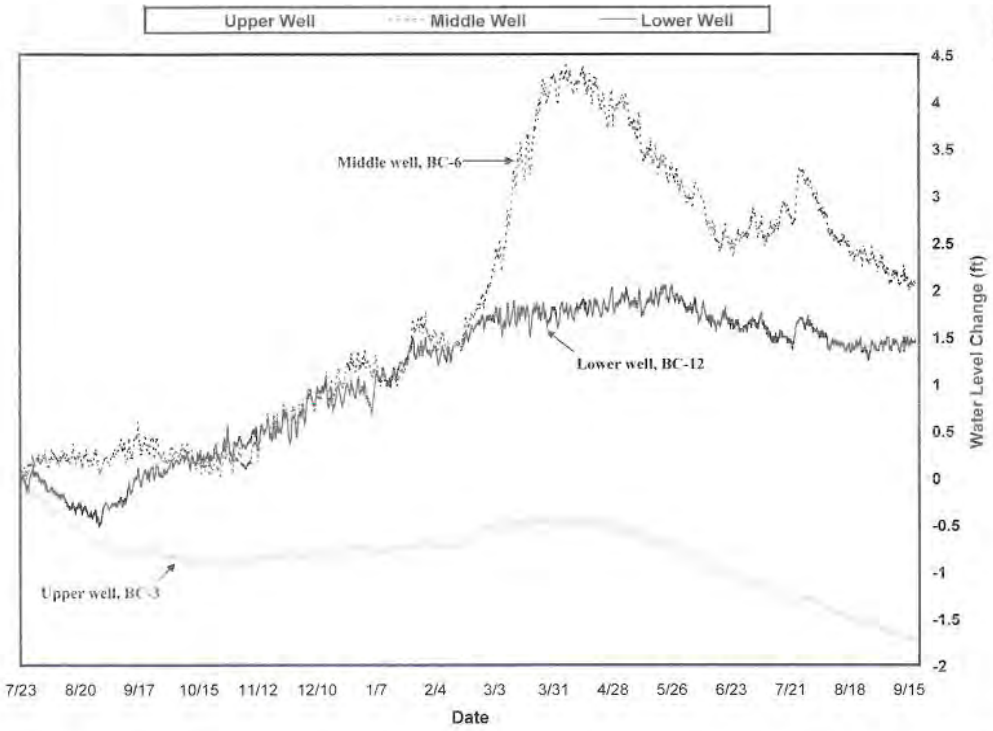


Figure 14. Water level change for logger instrumented wells, July 23, 2003 to September 18, 2004.

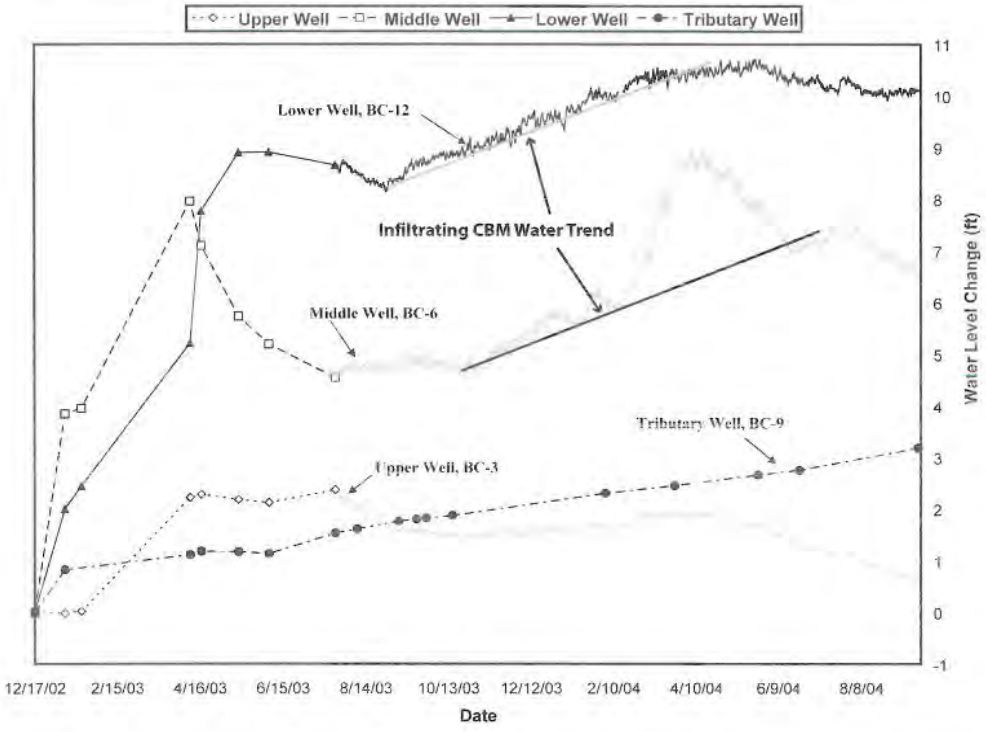


Figure 15. Synthesis of manual and logger water level data at all monitoring well sites, December 17, 2002 to September 18, 2004.

In the upper monitoring well (BC-3), water levels increased slightly from November 2003, until the spring of 2004 (**Figure 14**). In the middle of February, there was a slight rise in level, and then a steady decline from mid-May to the end of the study interval. Looking at the general response of the upper well over the entire study interval, water levels rose during the spring months of 2003 and 2004, but the decline in 2003 began at the end of July, while in 2004, this decline into the summer months began in mid-April (**Figure 15**).

The location and aquifer response in the upper monitoring wells is important in isolating the effect of infiltration of CBNG water on the shallow aquifer from effects of snowmelt and precipitation events. The upper monitoring wells are more than 500 feet upstream from

the upper reservoir pond and at a topographically higher location (**Figure 6**). Regional groundwater flow is generally to the north and downstream, so the water infiltrating at the upper pond does not affect the groundwater levels in the upper monitoring wells. These wells are designated as a control site for the regional shallow aquifer system, thus any change in the upper wells represents a change in the regional water table. For example, in early April 2003, there is a large rise in water levels at the upper monitoring wells. As mentioned previously, a large snowstorm occurred in mid-March and melted quickly thereafter, introducing a large amount of water into the shallow aquifer. It is likely that the rise in water level seen in the spring of 2003 at the upper monitoring wells (**Figure 15**) represents a regional recharge event. Removing the water level changes at the upper well location from the water level change in the middle and lower wells allows an estimate of aquifer response solely due to infiltrating CBNG water.

Figure 16 shows the synthesis of manual and logger level data for the middle and lower instrumented wells (BC-6 and BC-12), adjusted to the regional water level change observed in the instrumented well at the upper monitoring well location (BC-3). The overall trends seen at these two well locations remain the same, but the water level rises at the end of this 21 month period due to CBNG infiltration in the middle and lower well sites are approximately 4.2 and approximately 7.8 feet, respectively. This rise is about 2.5 feet less than the non-adjusted water level rise shown in **Figure 15**, which includes the regional rise in the shallow aquifer water table caused by snowmelt and precipitation. The steady water level rise from the late summer and fall of 2003 and into 2004 from CBNG infiltration is noted as the "infiltrating CBNG water trend" in **Figure 16**.

Slug testing

A total of six slug tests were performed in seven monitoring wells at the middle and lower sites to provide an estimate of intrinsic permeability as input for the alluvium/weathered bedrock layer in the SUTRA model. Five of these wells were screened to the alluvium layer, and two wells were screened into the top of the weathered portion of the Wasatch Formation. Results are summarized in **Table 14**. Permeabilities ranged from 7.76×10^{-13} m/s to 2.76×10^{-12} m^2, varying by a factor of less than four.

Figure 17 shows the time-drawdown data, screen length, well casing, and well screen radii from two slug tests. A best-fit line was used to determine t_{37}, which is the time it takes for water levels to fall to 37% of the initial water level change, by the Hvorslev (1951) method. Early time data (up to t_{37}) fits very well along the best-fit line for all slug tests. At later times in some of the slug tests, as seen in BC-14 from **Figure 17**, the head ratio tends to drift above the best-fit line, which does not affect the Hvorslev calculation. As head drops and time increases, it is common for these later data points to deviate from the curve fit (Fetter, 2001).

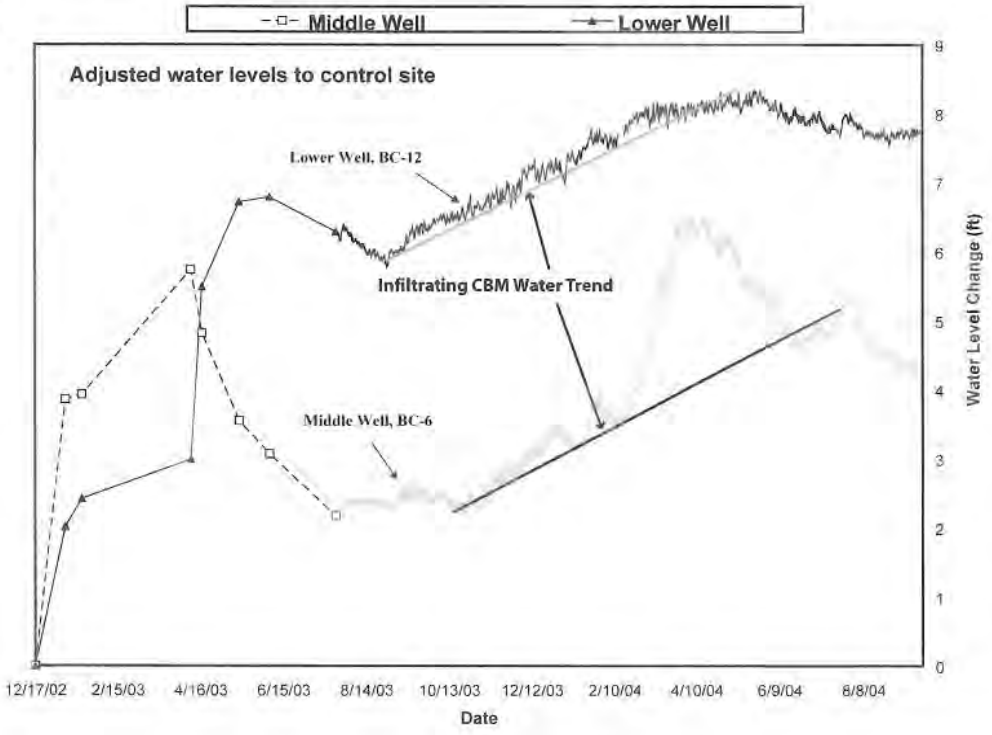


Figure 16. Synthesis of manual and logger water level data, middle, and lower instrumented wells, adjusted to control site, December 17, 2002 to September 18, 2004.

Table 14. Summary of slug test results.

Well Name	Location	Lithology	Hydraulic Conductivity (m/s)	Intrinsic Permeability (m^2)
BC – 5	Middle Site	Wasatch	2.16×10^{-5}	2.51×10^{-12}
BC – 7	Middle Site	Alluvium	2.37×10^{-5}	2.76×10^{-12}
BC – 8	Middle Site	Alluvium	9.70×10^{-6}	1.13×10^{-12}
BC – 11	Lower Site	Wasatch	2.01×10^{-5}	2.34×10^{-12}
BC – 12	Lower Site	Alluvium	6.67×10^{-6}	7.76×10^{-13}
BC – 14	Lower Site	Alluvium	9.96×10^{-6}	1.16×10^{-12}

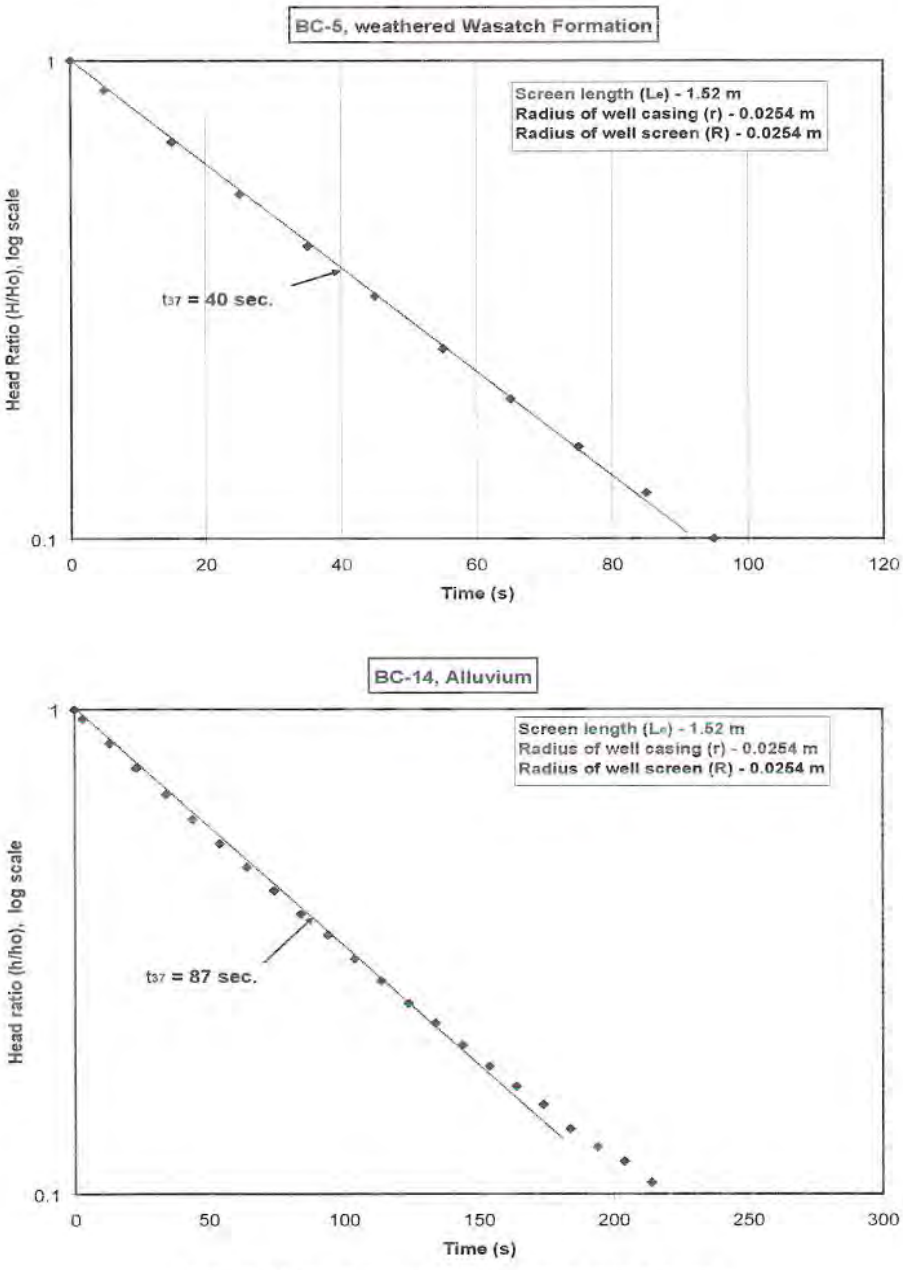


Figure 17. Time-drawdown data for two slug tests.

Discussion

Water budget

Within the two stream channel infiltration blocks, water budget data from 2003 and 2004 indicated infiltrative variability through time and between the two differing locations of block II (middle stream section) and block IV (lower stream section). Results for the two pond-dominated blocks (blocks I and III) for 2003 indicate slight temporal variation in infiltration, and the spatial variability in infiltration between these two blocks is minimal (at the lower pond, block III, infiltration rates are consistently slightly higher). Limitations in data collection for the 2004 budget preclude infiltration determinations for block III, but data from 2004 for block I indicates that infiltration increases through time in the latter half of the 2004 season. Overall, the calculated infiltration rates in the stream channel blocks for 2004 were greater than those calculated in 2003. In the pond-dominated blocks, calculated infiltration rates from both budget years were similar. Calculated infiltration rates in the stream channel blocks were significantly higher than infiltration rates for the two pond blocks.

Spatial variations

An important aspect of the water budget and calculated infiltration rates is the significant difference of calculated infiltration rates in the stream channel blocks compared to the calculated rates in the pond-dominated blocks. Average infiltration rates from the 2003 water budget (**Table 11**) in the stream channel blocks II and IV were 4 to 5 times greater than the rates in the two pond-dominated blocks I and III. There are five factors that might explain the lower infiltration rates of the pond-dominated sections: 1) compaction of soil in the ponds, 2) less vegetation in the pond infiltration areas, 3) a decrease in lateral flow beneath the soil in the ponds, 4) settling of fines in

the pond, and 5) the possibility that the bottom of the pond intersects a mounded water table.

First, the construction of ponds at Beaver Creek involved the excavation of storage impoundments in the channel. Heavy earth-moving machinery was utilized to dig out an area for the pond, which would have caused compaction of the upper soil layer. This compaction would have decreased the porosity of this soil and possibly closed off conduits of preferential flow. In the stream channel, the soil has been relatively undisturbed (except in the small construction areas of the weirs). Second, as noted earlier, vegetation growth in the ponds was primarily constricted to the banks and shallow shelf areas around the pond margins. In the stream channel, grass is present along the entire length of the channel, and at later stages of the budget interval (summer and fall of 2003, and most of 2004), tall grass was growing in most of the channel area. These grasses would increase the conveyance loss by uptake of soil moisture in the stream channel blocks, which would be calculated as infiltration under the author's water budget analysis. Third, the presence of a large block of infiltration area, like that seen in the ponds, would decrease the lateral flow component of water in the subsurface. In a large and concentrated infiltration area, the vertical flow component in the center of the area is channeling flow in a primarily downward direction. Only at the margins of the pond would one expect significant lateral flow out into the soil (**Figure 18**). In the stream channel, the infiltration area is long and sinuous, with much more of the infiltration area occurring along a margin where there is a higher lateral flow component. Fourth, the static nature of water in the ponds allows the settling of fine particles, either wind-blown, or from surface flow, onto the bottom of the pond. These fines would tend to decrease the permeability of the soil through which the water must infiltrate. Finally, there is the possibility that mounding beneath the ponds may intersect the bottom of the ponds (pond depth is estimated at about 15 feet). At the middle monitoring well locations where there is in-channel data on water levels, the water table was about 10 feet below the surface for most of 2004. If this is the case, the ponds could be receiving groundwater discharge from the shallow aquifer, thus reducing the total infiltration in the ponds.

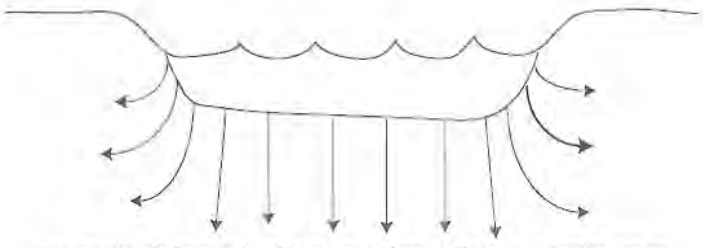


Figure 18. Schematic of seepage beneath a ponded surface.

A final point to consider in the spatial variability of infiltration is the minor difference in infiltration rate between the two pond-dominated sections. Both pond blocks contain a small amount of stream channel area outside of the excavated pond portion. In the upper pond (block I), the stream channel area between the pond outfall and above the upper weir represents about 10% of the total area of infiltration. In the lower pond (block III), stream channel areas compose approximately 8% of the total area. The average calculated infiltration rate for the 2003 budget in block III was 0.65 in/day, slightly more than the average calculated rate of 0.53 in/day in block I (**Table 11**). Assuming the infiltration rates in these stream channel areas are similar (calculated infiltration rates from **Table 12** in the two stream channel blocks were 2.68 in/day and 2.82 in/day), the fact that block III has a slightly higher calculated infiltration rate for 2003 and a smaller percentage of stream channel area suggests that the rate of infiltration in block III is larger than that observed in block I.

Temporal variations

A key assumption in the calculation of the water budget is that evapotranspiration (E-T) is assumed to equal evaporation (E). Thus, the calculated infiltration may be affected by transpiration (T). Two critical aspects of the study site to consider in analyzing infiltration are the temporal variability of vegetation and the spatial differences between the two stream channel blocks. Vegetative growth in Wyoming generally begins in late spring and tapers off during the fall season. Lewis (1978) considers seasonal evapotranspiration for the months of May through September (**Table 15**). Transpiration, or moisture uptake by plants, increases as grasses begin their growth cycle. A significant change in vegetation over time was observed at the Beaver Creek site, and the increase in conveyance loss from transpiration could have a profound effect on the infiltration through time. From **Table 15**, the amount of evapotranspiration (thus, including transpiration by plants) increases from May, reaching a peak in July, and declining sharply in September. Observations of plant growth at the Beaver Creek ponds showed that most of the plant growth in the ponds occurred along the banks of the ponds and in shallow water, thus affecting only a small portion of the

Table 15. May through September evapotranspiration distribution. From Lewis (1978).

Month	% of Evapotranspiration
May	16.6
June	19.0
July	24.9
August	24.2
September	15.3

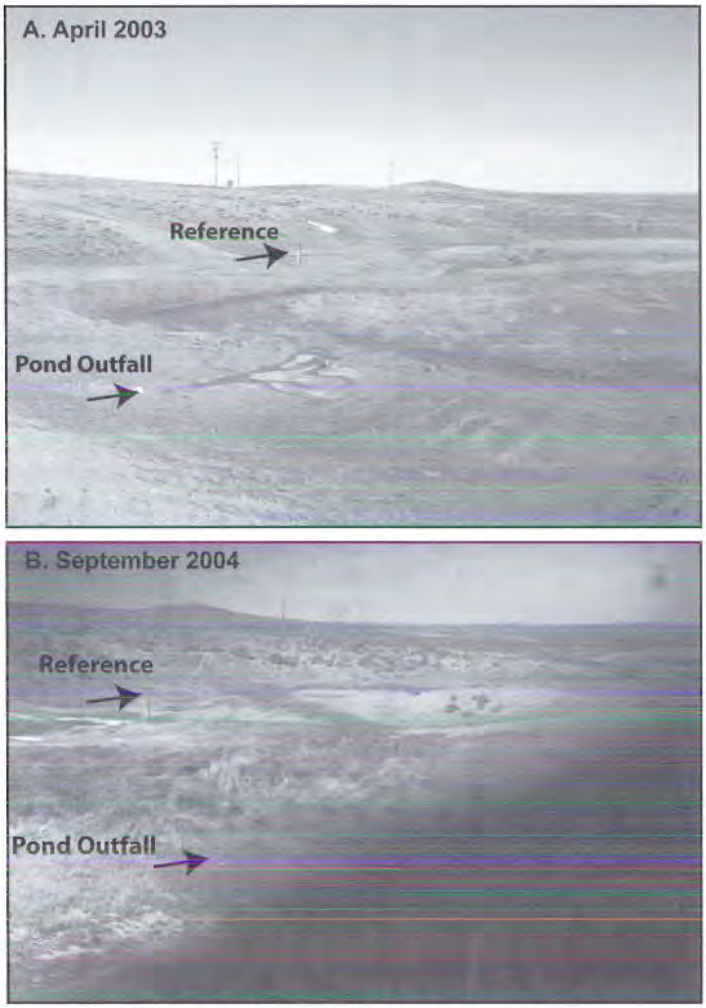
infiltration areas in the ponds. In the stream channel, the increase in vegetation occurred along the banks of the channel and within the narrower stretches of the channel, thus most of the stream infiltrating area was affected by grass growth. Thus, when considering the temporal character of infiltration within the stream channel, it is important to consider the effect that vegetation had within the stream channel. **Photographs 11** and **12** show the considerable increase in vegetation from April 2003, to September 2004, in a section of the lower stream and at the outfall area of the upper pond. In 2004, surface water is not even visible due to vegetation cover.

Considering the spatial differences between the two stream channel reaches, the middle stream section flows through a broader and less confined channel between the upper and lower pond (**Photograph 2**), while the channel from the lower pond weir to the lower weir is confined and is incised several feet below the surrounding topography (**Photograph 8**). The course of the stream channel within the lower stream section (block IV) was observed by the author to vary little, if any at all, because of the confined geometry of the drainage in this area. Within the middle stream section, especially in the broad and flat area from above the middle monitoring wells and downstream of the middle weir (seen in **Photograph 2**), the stream channel was observed to splay between a main channel and other channels where water can preferentially flow (mainly on livestock trails). This was especially evident during the spring months of 2003 (**Photograph 2** was taken during April 2003) when grass growth was limited, and during the spring of 2004 when there was visibly more grass, but much of it was brown. In the later months of 2003 the channel flow was observed to remain in a more confined channel as grass had grown and constricted flow from the lesser channels. Beginning in June 2004, flow in the middle stream section was intermittent with periods when no flow, or much less flow, was observed.

Calculated infiltration rates in the stream channel were observed to differ between the 2003 and 2004 budget



Photograph 11. Lower stream section vegetation change from April 2003 (A, top) to September 2004 (B, bottom). Both frames are looking downstream; frame B is slightly downstream from frame A.



Photograph 12. Upper pond outfall area vegetation change from April 2003 (A, top) to September 2004 (B, bottom). Both frames are looking downstream.

year. Calculated infiltration rates from the summer of 2004 were significantly larger than over the same time period in 2003. The water budget completed in 2003 does not allow an analysis of temporal change in infiltration during the spring season, but does allow an analysis of change up to November 1, several weeks before the initiation of the winter freeze. Analyzing the data from **Table 11** on infiltrative loss and calculated infiltration loss for each infiltration block, three of the four blocks show declining infiltration from the beginning of September to the end of the budget period for 2003. For the first six budget intervals up to September 1, the upper pond block (block I) has an average infiltration rate of 0.61 in/day, and in the following eight budget intervals, the average infiltration rate declines to 0.48 in/day (**Figure 19**). Over the same time period, the lower pond block (block III) has an average infiltration rate of 0.73 in/day for the first six intervals, and declines to an average of 0.59 in/day in the final eight intervals. In the lower stream block (block IV), the average infiltration rate over the first six intervals is 3.56 in/day, and declines dramatically to 2.19 in/day over the final eight intervals (considering the final five budget intervals, the average infiltration rate is even lower, at 1.78 in/day) (**Figure 19**). In the middle stream section (block II), the infiltration rates show no discernible trend, and the average infiltration rate actually increases slightly in the final eight intervals compared to the first six, 2.84 in/day and 2.47 in/day, respectively. For the three blocks that show a decline in infiltration in September and October, the decrease in moisture uptake by plants near the end of the growing season (**Table 15**) is a possible explanation of this behavior.

Partial data from the 2004 water budget allows an analysis of infiltration variability from the end of March to the middle of September. Insufficient data from block III (infiltration was determined for four weeks in March and April, thereafter the CBNG water input to the lower pond is uncertain) does not allow any conclusions to be drawn about temporal variability for infiltration during this year. One factor in the 2004 budget is the possibility of stream channel-course variability through time, since little change in vegetation was observed over the course of the 2003 budget. Observations from the spring of 2003 and 2004 indicate that during these time periods, the lower density of vegetation in the stream channel affected the channeling of surface flow, most prominently observed in the middle stream section. Prior to the increase in grass growth, channel flow was observed to splay and follow other pathways to flow (livestock trails) in the middle stream section (**Photograph 2**). After sufficient growth of grass, surface flow was more constricted in the main channel. This suggests that the area of infiltration during the spring months is greater than during the summer and fall months. Since the areal survey of stream dimension (**Table 3**) was conducted in September 2003, a calculation of infiltration rate in the spring months could represent an overestimation, thus explaining the high values of calculated infiltration rates in the spring of 2004 (**Table 13**). In the lower stream section, there is another aspect of uncertainty in the infiltration area used to calculate

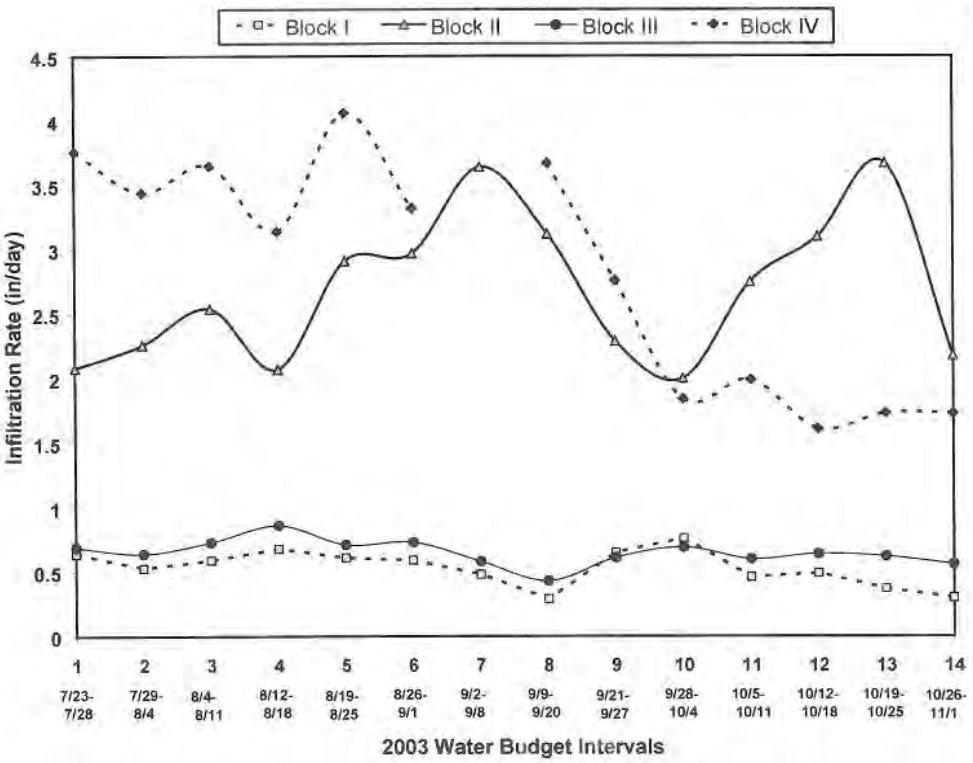


Figure 19. Infiltration rate through time, 2003 water budget.

the infiltration rate. Beginning on about April 23, there is a dramatic increase in surface flow seen through the stream channel as a result of an increase in CBNG water input to the lower pond (**Table 12**). From budget intervals #3 to #8, the flow through the lower pond weir ranges from 74.1 to 94.7 gpm, significantly higher than flows observed in the first four weeks of the 2004 budget and the 2003 budget. While the increased surface flow would presumably lead to an increase in infiltration area, the fact that the stream channel between the lower pond weir and lower weir is confined to a single incised channel leads the author to believe than any change in area would be minimal.

Due to the possible uncertainty for the infiltration rate calculation caused by changing areas, the temporal changes in the 2004 budget analysis are discussed in terms of total infiltration (gpm). In the upper pond block (block I), excepting the high infiltration (5.7 gpm) in budget interval #1, the infiltration ranges from 2.6 to 3.9 gpm in the next four intervals, until June 2 (**Table 12**). After June 2 and excepting the infiltration in interval #7 (4.8 gpm), the calculated infiltration for the remaining intervals where data is available ranges from 7.1 to 7.9 gpm. Considering the rise in evapotranspiration during the summer months (**Table 15**), an increase in vegetation density can explain this change. While the effect of vegetation density in the pond was previously assumed to be minimal on the pond infiltration area, the stream section below the upper pond and above the upper weir experienced a dramatic increase in grass growth in the 2004 season, compared with observations from 2003 (**Photograph 12**). In **Photograph 12B**, the density of vegetation in 2004 is such that it conceals much of the surface water. From the author's observations during August 2003, the density of vegetation was considerably less than in 2004 (**Photograph 12B**), and the small pond below the outfall (**Photograph 12A**) had not yet been overgrown by grasses. It is the author's belief that much of the water flowing out of the upper pond that does not infiltrate, is transpired by plants before reaching the upper weir.

During the 2004 budget, calculated infiltration from the middle stream section (block II) steadily declines through the first five budget intervals (**Table 13**), and then increases in the two determined intervals from the summer. In budget interval #1, infiltration loss is 12.2 gpm, or about 86% of the total surface flow into this block. In the next four intervals, infiltration declines from 8.7 gpm and 9.3 gpm in intervals #2 and #3, respectively, to 5.5 gpm and 3.2 gpm in intervals #4 and #5, respectively. In the two intervals during the summer (#7 and #9), infiltration loss is calculated at 4.9 gpm and 4.1 gpm, respectively. The steady decline in infiltration in budget intervals #1 through 5 may be due in part to the changing nature of the stream channel in this block, as discussed earlier. If surface flow is not constricted by vegetation and can flow over a larger area, then total infiltration would be expected to be larger during the earlier times because of the larger area where water can infiltrate. Though infiltration data are limited in the summer (only determined for the intervals #7 and #9 from June 17 through 30 and July 15 through 28), the infiltration increase may be related to rise in plant transpiration during the summer.

In the confined stream channel reach of block IV for the 2004 budget, infiltration values are relatively low in the first five budget intervals, ranging from 5.1 gpm to 7.6 gpm (**Table 13**). The observation that infiltration remains low in intervals #3 and #5 when there has been a dramatic increase in surface flow (during the first two intervals, average flow is about17 gpm; for intervals #3 and #5, average flow is about 85 gpm) seems to reinforce the assumption that the change in infiltration area for this confined channel reach is minimal. Corresponding to the expected increase in transpiration in June and increased vegetation density in the stream channel (**Photograph 11**), the four budget intervals from June 3 through July 28 have a dramatic increase in calculated infiltration, ranging from 11.7 gpm to 20.9 gpm. In the final two budget intervals from late August through September, the amount of infiltration declines to 5.1 gpm and 5.5 gpm, suggesting that transpiration uptake has decreased.

Additional considerations

A qualitative observation of surface water behavior was made during the winters of 2002-2003 and 2003-2004. During the winter freeze, CBNG water was stored in the form of ice in the stream channel. Both ponds froze on the surface during the winter months, but water continued to discharge through the outlet pipes (located at the base of the ponds) into the stream channel. The storage of CBNG water in ice was more evident during the winter of 2003-2004, which may be due to the presence of the weir structures in the stream channel. The calm water in the small ponds behind the weir was observed as the first water in the stream channels to freeze during a field visit in November 2003. The amount of ice behind and even covering the weir was dramatic from observations from February 2004. **Photographs 13** and **14** are photographs taken of the middle and lower weir and show the vast amount of ice that collected around the weirs.

The presence of ice was noted in the several field visits to the Beaver Creek site in the winter months of 2002-2003, but was much less voluminous than the amount of ice seen in the winter of 2003-2004. In 2003-2004 at the middle stream section, the ice froze in sheets 20 to 40 feet wide, and in the lower stream section, the ice in the incised channel was probably 1.5 to 2.5 feet above the base of the channel. At the



Photograph 13. Ice around the middle weir, February 2004. A (top) is looking downstream; B (bottom) is looking to the east.



Photograph 14. Ice at the lower weir, February 2004. View is looking downstream in both A (top) and B (bottom).

lower weir (**Photograph 14**), the channel widens slightly and the ice is about 30 feet wide, and probably several feet above the stream channel. At both stream locations, breaks in the ice were noticed where water broke through and froze on top of the existing ice. No determination could be made as to when those breaks occurred.

We conjecture that there may be three reasons why more ice accumulated in 2004 than in 2003. First, the winter of 2003-2004 was markedly colder than the winter of 2002-2003 (Wyoming State Climate Office, 2004). Secondly, CBNG infiltration only began in the stream channel at the beginning of December 2002. It is likely that the soil and alluvium above the existing water table was very low in soil moisture and high in infiltrative capacity since the summer and fall of 2002 were relatively dry. If that were the case, surface flow through the system would be less as more water was infiltrating, and less was available on the surface to freeze. The third possibility is that the presence of two weirs in each of the channel stretches changed the dynamic of surface water flow and freeze. Ponds dammed by the weirs containing tranquil water were observed to freeze first in the winter of 2004. The static nature of these ponds could have promulgated the freezing of surface water in the vicinity of the weirs, which would have spread throughout the stream channel. Many of the breaks in the ice and subsequent overflow of water occurred at or below the weirs, thus increasing the thickness and volume of ice downstream.

The presence of a significant volume of CBNG water stored in ice may have implications for the water budget. The ponding of ice would temporarily cause a larger area for infiltration to occur. Also, during the period of ice melt, a slug of runoff might be expected to flow down the stream channel, increasing the likelihood of transient loading of CBNG water in surface flow channels. If the spring thaw is relatively rapid and the ice melts quickly, much of the CBNG water would be expected to leave the Beaver Creek site as surface runoff. With the thawing of this ice, it is also expected that there will be a significant portion that can infiltrate into the shallow aquifer. Water level data in the middle stream section, where monitoring wells are located in the stream channel, shows a significant rise in water level after the 2004 thaw event. If the melting of the ice occurred

over a longer interval, or melted and then refroze, surface runoff would likely be less and the amount of stream infiltration would be greater. The timing of the ice melt in March 2004 could not be determined in this study due to limitations in the data logging equipment.

Stream channel infiltration rates per unit stream length

For the purpose of estimating stream channel infiltration over a larger scale (watershed), a more useful infiltration rate value is infiltrative loss per unit stream length. A common industry standard is cubic feet per second per mile (cfs/mi), which the authors also convert to units of gallons per minute per mile (gpm/mi). Budget calculations are converted for both stream sections, which have differing average widths. The middle stream section (block II) has an average width of 0.80 meters, and the lower stream section (block IV) has an average width of 1.4 meters.

For the 2003 budget season, the average infiltration rate in block II was 2.68 in/day. In terms of infiltrative loss per mile, this converts to 0.037 cfs/mi, or 16.5 gpm/mile. Converting the maximum and minimum values of infiltration rate for the 2003 budget (**Table 11**), infiltration per mile varied from 0.27 to 0.50 cfs/mi, or 12.1 to 22.2 gpm/mi. Over the 2004 budget interval (**Table 14**), infiltrative loss declined from 0.162 cfs/mi (72.4 gpm/mi) from the March 25 through April 7 interval, to 0.042 cfs/mi (19.0 gpm/mi) over the interval from May 20 through June 2. In the two summer months where data was available, the loss ranged from 0.055 to 0.064 cfs/mi (24.5 to 28.8 gpm/mi).

The average calculated infiltration rate in the lower stream block IV over the 2003 budget was 2.82 in/day (**Table 13**), or 0.063 cfs/mi (28.3 gpm/mi). The range of calculated infiltrative loss for 2003 ranged from 0.036 to 0.091 cfs/mi, or 16.1 to 40.7 gpm/mi. For the calculated infiltration rates from 2004 (**Table 13**), the infiltrative loss ranged from 0.032 cfs/mi (14.3 gpm/mi) over the first budget interval from March 25 through April 7, to a maximum of 0.132 cfs/mi (59.2 gpm/mi) over the summer interval from June 17 through 30 (**Table 13**).

A comparison of our field calculated results for infiltration with the 0.1-cfs/mi value from two industry quoted reports (Western Land Services, 2001; Hydrologic Consultants, Inc., 2001) suggest that the currently used value from these sources may be a slight overestimate for loss in the stream channel. We were unable to locate these reports or speak with the investigators to determine the details of these studies, including location of the stream channel investigated, average stream channel width, or at what time of year they were conducted.

Shallow aquifer response

Considering the response of the shallow alluvium aquifer, differences can be observed in water level changes at the two locations affected by CBNG water infiltration (the middle and lower well sites). The water levels at the in-channel location of the middle wells respond more rapidly and more dramatically to the spring thaw events and then steadily decline into the summer months. At the lower well location, the water level rise in the spring thaw period is more delayed and much less pronounced. As discussed earlier, the water levels at the upper well site reflect changes in the regional water table, presumably unaffected by CBNG infiltration. This change in regional water table is best seen in the early spring of 2003, where a large increase in water level (about 2 feet rise) in mid-April 2003, seen at the upper well is likely associated with a snowstorm followed by a rapid melting event. In the spring of 2004, the much less pronounced rise in the upper well may be due to the fact that there was less snowfall than in the previous year.

During the initial period of CBNG infiltration, the water level adjusted to the control site (upper well) at the middle well location (BC-6) rises about 4 feet after one month of observation (**Figure 16**). The rise at the lower well (BC-12) is only about 2 feet. Into April 2003, the comparative water level rise in the middle well to the lower well is much greater (5.7 feet in the middle well; about 3 feet in the lower well, **Figure 16**). After April 9, the adjusted water level in the middle well declines 3.5 feet until the end of July, and then remains steady into November. In the lower well, the water level after April 9 rises sharply by 3.7 feet on May 5, and then from June until the end of August declines only 1 foot (**Figure 16**).

At the middle and lower wells, a steady trend seems to indicate a 2 to 3 foot linear increase in water level due to CBNG infiltration over the course of 1 year (**Figures 15** and **16**). This increase begins near the end of the summer of 2003, after the system has equilibrated from the spring thaw of 2003. The increase continues into the early summer of 2004, when water levels in both well locations begin to decline slightly. At the middle well, a dramatic spike in water level is seen during the 2004 thaw, but after the water level declines, the water level rise seems to continue along this trend. This is an important trend to consider because it indicates that water from CBNG infiltration is augmenting the local water table at a relatively constant rate.

Figure 15 clearly illustrates the different aquifer response pattern during the spring thaw event of 2004 between the two downstream well locations. Water level changes in the middle and lower well track each other from October 2003, to February 2004. Near the end of

February 2004, the water level in the middle well begins to rise rapidly, eventually rising 2.5 feet by the middle of April (**Figure 15**). The water level rise in the lower well over this interval remains steady, rising at a similar rate as during the previous several months. After mid-April, the water level in the middle well declines almost as rapidly as it increased in the preceding two months, dropping by almost 2 feet at the end of June. The water level decline in the lower well is much less pronounced, and this decline begins much later, around the end of May (**Figure 15**).

To consider why the aquifer response in the middle wells is much more dynamic than the response seen at the lower wells, it is important to note the location of these well clusters. The middle well is located in the stream channel, while the lower wells are perched on a terrace, 18 to 45 feet off-channel. Infiltrating water at the middle wells only needs to travel about 10 to 12 feet vertically to reach the water table and impact the water levels seen in the monitoring wells. To affect levels at the lower wells, water must travel vertically downward to the water table, and then flow laterally outward. At the lower wells, the amount of mounding may be less due to a lower amount of infiltrating CBNG water (as demonstrated during the first three budget intervals of 2004, **Table 12**). It is also possible that mounding is dissipated by the regional groundwater flow (downstream, to the north), before the water can flow laterally and affect the levels in the lower wells.

This down-gradient dissipation of the groundwater mound may also explain the rapid decline in water levels seen at the middle well cluster. The response in the spring of 2004 at the middle well (**Figure 16**) best illustrates this behavior (a similar response is seen in 2003, but data resolution is much lower, and the system may not have reached an equilibrium during the first several months of CBNG infiltration). The large volume of ice in the stream channel observed during 2004 would dramatically affect the water table as it thaws and infiltrates. The mound developed over a period of 1.5 months, and then regional flow began to disperse the mound downstream over the next couple of months. A lag time for mound dispersal seems likely due to the fact that mounding is presumably occurring upstream of the monitoring wells.

Two other possible explanations for the differing aquifer response at the middle site are plant transpiration and an imperfect seal around the middle monitoring wells, producing a preferential conduit of flow down the PVC casing. Rankl and Lowry (1990) demonstrated that seasonal water level changes in alluvium wells in Sheridan County, Wyoming, correspond to seasonal changes in evapotranspiration. Vegetation density immediately above the wells at the middle site was observed to be greater than the density at the lower or upper well locations. The increased soil moisture uptake by plants at this site could also explain the more pronounced decline in levels at the middle site. Plant transpiration would likely be insignificant during the dramatic water level rise in the spring of 2004, but may contribute to the water level decline in May and June, at the beginning of the seasonal growth period (**Table 15**). Considering the possibility of an imperfect seal around the middle wells, preferential flow could have occurred during both spring thaw events as ice surrounding the wells melted. The fact that during 2004 the water level rise was sustained for several months leads the author to believe that this effect was minimal.

Conclusions

Determinations of water budgets for at the Beaver Creek site for 2003 and 2004 indicated that there are significant spatial and temporal variations in infiltration within the study site. Continuous monitoring of the shallow aquifer suggests that there is a steady rise in the local water table at those areas affected by CBNG infiltration.

1. Infiltration represents a significant portion of conveyed CBNG co-produced water loss, an average of 46.1% of the total CBNG water input for the 2003 water budget. Surface runoff out of the small study site (CBNG water – Evaporation – Infiltration) averaged 44.2% of total CBNG water input over the same interval. This surface runoff likely infiltrates at some point downstream.

2. Calculated infiltration rates are significantly higher in the stream channel areas than in the ponds. This is likely due to a combination of factors, including compaction of the soil in the ponds, lower vegetation density in the ponds compared to the streams, a lesser component of lateral flow beneath the ponds, settling of fine-grained material in the pond bottom, and the possibility that the pond intersects the water table at some point.

3. An analysis of temporal variations indicates that the author's assumption of transpiration as an insignificant element in the water budget may have been flawed. Calculated infiltration in the stream channel blocks was much larger in the summer months of 2004 than for the same period in 2003. Calculated infiltration appears to increase at the onset of the growing season in the late spring and then decline in late summer and fall, which likely corresponds to changes in soil moisture uptake by plants.

4. The storage of CBNG water in ice and subsequent spring thaw may result in large "slugs" of surface water which may exceed the "steady-state" discharge

into surface flow channels usually used to estimate the impact and loading to higher order stream channels.

5. Infiltrative loss per stream mile in the 0.8 m wide middle stream location varied from 0.027 to 0.050 cfs/mi over the 2003 budget, averaging 0.037 cfs/mi. This loss rate was much higher in the spring months of 2004, and the loss rate for two budget intervals during the summer months ranged from 0.055 to 0.064 cfs/mi. The loss rate in the 1.4 m wide lower stream section ranged from 0.036 cfs/mi to 0.091 cfs/mi over the 2003 budget, averaging 0.063 cfs/mi. The loss rate from 2004 ranged from a low of 0.032 cfs/mi in the spring, to a maximum rate of 0.132 cfs/mi during a summer interval.

6. The local water table in the shallow aquifer seems to rise 2 to 3 feet per year from CBNG infiltration. Different responses are seen in the in-channel well set location compared to the off-channel well set location. Both well locations respond dramatically in the first half of 2003 to a combination of initiation of CBNG infiltration and the spring thaw. The response in the middle well is more rapid, and the onset of water level decline occurs much earlier than in the lower well. In response to the spring thaw of 2004, the middle well exhibits a dramatic rise and subsequent decline, while the lower well response very small.

References cited

Ayers, W.B., Jr., 1986, Coal resources of the Tongue River Member, Fort Union Formation, Powder River Basin, Wyoming: Wyoming State Geological Survey Report of Investigations No. 35, 21 p.

Brown, D.J., 1970, Use of pans and model for evaporation role in water budgets of Laramie and Wyoming: M.S. thesis, University of Wyoming, Laramie, 133 p.

Brown, J.D., 1980, Regional hydrogeology of the Gillette, Wyoming area (with a discussion of cumulative regional impacts of surface coal mining and reclamation), *in* Proceedings, Second Wyoming Mining Hydrology Symposium: Wyoming Water Resources Research Institute, University of Wyoming, Laramie, p. 10-42.

Buchanan, T.J., and Somers, W.P., 1969, Discharge measurements at gauging stations, *in* Techniques of Water-Resources Investigations of the U.S. Geological Survey, Chapter A8.

Crockett, F.J., 1999, Summary of federal oil leasing in the Powder River Basin, Wyoming, 1990-1999, *in* Miller, W.R., editor, Coalbed methane and the Tertiary geology of the Powder River Basin, Wyoming and Montana: Wyoming Geological Association, 50th Annual Field Conference Guidebook, p. 73-82.

De Bruin, R.H., and Lyman, R.M, 1999, Coalbed methane in Wyoming, *in* Miller, W.R., editor, Coalbed methane and the Tertiary geology of the Powder River Basin, Wyoming and Montana: Wyoming Geological Association, 50th Annual Field Conference Guidebook, p. 61-72.

De Bruin, R.H., Lyman, R.M., Jones, R.W., and Cook, L., 2001, Coalbed methane in Wyoming: Wyoming State Geological Survey Information Pamphlet 7 (revised), 19 p.

De Bruin, R.H., Lyman, R.M., and Jones, N.R., 2004, Coalbed methane update, *in* Jones, R.W., editor, Wyoming Geo-notes: Wyoming State Geological Survey, No. 80, p. 21-22.

Fetter, C.W., 2001, Applied hydrogeology, 4th Edition: Prentice-Hall, Upper Saddle River, New Jersey, 598 p.

Flores, R.M., 1999, Wyodak-Anderson coal aone in the Powder River Basin, Wyoming and Montana: A tale of uncorrelatable coal beds, *in* Miller, W.R., editor, Coalbed methane and the Tertiary geology of the Powder River Basin, Wyoming and Montana: Wyoming Geological Association, 50th Annual Field Conference Guidebook, p. 1-24.

Fogg, J.L., Martin, M.W., and Daddow, P.B., 1991, Geohydrology and potential effects of coal mining in 12 coal-lease areas, Powder River structural basin, northeastern Wyoming: U.S. Geological Survey Water-Resources Investigations Report 87-4102, 49 p.

Hvorslev, M.J., 1951, Time lag and soil permeability in ground water observations: U.S. Army Corps of Engineers Waterway Experimentation Station, Bulletin 36, 50 p.

Hydrologic Consultants, Inc, 2001, Hydrologic and geochemical assessment, Wild Horse Creek, Campbell and Sheridan counties, Wyoming, unpublished report.

Jordan, P.R., Bloyd, R.M., and Daddow, P.B., 1984, As assessment of cumulative impacts of coal mining on hydrology in part of the Powder River structural basin, Wyoming—A progress report: U.S. Geological Survey Water-Resources Investigations Report 83-4235, 25 p.

Lahoti, R.B., 1968, Evaporation from water surfaces in Wyoming: M.S. thesis, University of Wyoming, Laramie, 46 p.

Lewis, L.E., 1978, Development of an evaporation map for the state of Wyoming for purposes of estimating evaporation and evapotranspiration: M.S. thesis, University of Wyoming, Laramie, 64 p.

Lindner-Lunsford, J.B., and Wilson, J.F., Jr., 1991, Shallow groundwater in the Powder River Basin, northeastern Wyoming—Description of selected publications, 1950-1991, and indications for further study: U.S. Geological Survey Water-Resources Investigations Report, 91-4067, 71 p.

Montgomery, S.L., 1999, Powder River Basin, Wyoming: An expanding coalbed methane (CBM) play: AAPG Bulletin, vol. 83, p. 1207-1222.

Rankl, J.G., and Lowry, M.E., 1990, Ground-water-flow systems in the Powder River structural basin, Wyoming and Montana: U.S. Geological Survey Water-Resources Investigations Report 85-4229, 39 p.

Rice, C.A., Ellis, M.S., and Bulluck, J.H., Jr., 2000, Water co-produced with coalbed natural gas in the Powder River Basin, Wyoming: Preliminary compositional data: U.S. Geological Survey Open-File Report 00-372, 20 p.

U.S. Bureau of Land Management, 2003, Powder River Basin Final Environmental Impact Statement, http://www.wy.blm.gov/nepa/prb-feis/, accessed November 12, 2004.

U.S. Environmental Protection Agency, 2004, Evaluation of impacts to underground sources of drinking water by hydraulic fracturing of coalbed methane reservoirs: U.S. Environmental Protection Agency Final Report 816-R-04-003.

Warrance, N. J., Bauder, J., and Pearson, K.E., 2001, Salinity, sodicity and flooding tolerance of selected plant species of the Northern Cheyenne Reservation: Department of Land Resources and Environmental Sciences, Montana State University, Bozeman, <http://waterquality.montana.edu/docs/methane/cheyenne.shtml>.

Weight, W.D., and Sonderegger, J.L., 2001, Manual of applied field hydrogeology: McGraw-Hill, New York, New York, 608 p.

Western Land Services, April 19, 2001, Sheridan, Wyoming.

Wyoming State Climate Office, <http://www.wrds.uwyo.edu>, accessed August 20, 2004.

Wyoming State Engineers Office, Water Rights Database, <http://seo.state.wy.us/wrdb/>, accessed September 10, 2004.

CHAPTER 2

Predicting changes in groundwater quality associated with coalbed natural gas infiltration ponds

John Wheaton
Montana Bureau of Mines and Geology
Billings, Montana
and
Terry H. Brown
Poudre Valley Environmental Sciences, Inc.
Fort Collins, Colorado

Table of contents

List of figures 46
List of appendices 46
Abstract 47
Introduction 47
Overview of water-quality evolution 48
Methods 49
Study sites and data collection 50
Water-quality changes near Decker 50
Water-quality changes at Coal Creek 50
Water-quality changes at Beaver Creek 54
Recommendations 56
Conclusions 56
References cited 57
Appendices 59

List of figures

1. Map showing study-site locations 48
2. Water quality evolution concepts 48
3. Changes in total dissolved solids in mine spoils near Decker, Montana 49
4. Map showing location of site near Decker, Montana 50
5. Mixing model for site near Decker, Montana 50
6. Map showing monitoring sites at Coal Creek, Wyoming 51
7. Typical gamma log for the Coal Creek site 51
8. Cross-section showing major ion chemistry for Coal Creek monitoring sites in July 2003 (Baseline) 52
9. Cross-section showing major ion chemistry for Coal Creek monitoring sites in December 2003 (6 Months after startup) 52
10. Cross-section showing major ion chemistry for Coal Creek monitoring sites in June 2004 (1 year after startup) 53
11. Graph of sulfate concentration and depth for saturated paste extract data from the Coal Creek site 53
12. Mixing model for the Coal Creek site 54
13. Map showing monitoring sites at Beaver Creek, Wyoming 54
14. Cross-section showing major ion chemistry for Beaver Creek monitoring sites in January 2003 (1 month after startup) 55
15. Cross-section showing major ion chemistry for Beaver Creek monitoring sites in December 2003 (1 year after startup) 55

List of appendices

A. Monitoring site information 60
B. Water-quality data from study sites 62
C. Saturated-paste-extract data 67

Abstract

Significant volumes of water are produced in association with coalbed natural gas (CBNG) production. This water must be disposed of economically to enhance gas development activities, yet in a manner that is sensitive to the semi-arid, agricultural area of southeastern Montana and northeastern Wyoming. Water produced with CBNG is high in bicarbonate, is low or devoid of sulfate, has low concentrations of calcium and magnesium, and has relatively high sodium concentrations (high sodium adsorption ratios or SARs). In southeastern Montana, where CBNG is being developed, coalbed water has higher salinity and higher SARs than in producing areas of the southern Powder River Basin in Wyoming, particularly those in the initial production areas near Gillette.

Infiltration basins have been in use in Wyoming and Montana for several years. These basins have several advantages in that they are an inexpensive means of disposing of production water and can help recharge the shallow groundwater system. The basins also have several potential disadvantages. The infiltrated water does not recharge the original deep aquifers but rather tends to stay fairly shallow and move laterally as well as vertically. As the sodium-bicarbonate discharge water moves through the shallow weathered bedrock, a series of chemical reactions (primarily dissolution and oxidation) may increase the salt load in the water. Depending on the site-specific hydrogeologic setting, production water will percolate downward from the ponds to the water table, possibly adding baseflow to streams, or could form sodic or saline seeps along hillsides.

Preliminary interpretations of data from three sites indicate that changes in groundwater quality will generally be reflected in increased total dissolved solids (TDS), Mg and SO_4. The maximum TDS increase at one off-channel site has reached 8.7 times the baseline concentration. At two on-channel sites, a combination of much smaller increases and decreases in TDS has occurred. The maximum concentrations have likely not been measured, and will be determined when decreasing values are documented. In on-channel sites where natural groundwater recharge and flow have flushed the salts from the alluvial aquifer, water quality may be diluted by CBNG discharge.

The duration of water-quality impacts is not yet known. Based on research in coal-mine-spoils aquifers, at least one pore volume of water must move along the flow path to flush the immediately available salts prior to any decrease in TDS. In some cases more than one pore volume will be necessary before improvement is seen.

Continued monitoring will improve the understanding of the groundwater systems and provide a foundation for permitting and production decisions. Much of the research on coalbed natural gas hydrogeology is based on research performed over the past three decades in coal strip mines. Those efforts have paid off several times in improved hydrogeologic understanding, and utilization and protection of resources. This current round of research will ultimately provide similar returns.

Introduction

In order to produce CBNG it is necessary to decrease the pressure in the coal seam, and create a pressure gradient in the reservoir. This is typically achieved by pumping groundwater out of the coal aquifer, which allows the natural gas to desorb from the coal surface and flow to the producing well. This production water must be disposed of in an economic manner to enhance gas development activities, yet in a manner that is sensitive to the semi-arid, agricultural area of southeastern Montana and northeastern Wyoming. During initial production from CBNG wells, the water discharge rate is high. Infiltration ponds can accept high discharge rates. However, improper design and siting may lead to impacts such as unacceptable changes in shallow groundwater quality. Design considerations that may affect impacts from ponds include the materials which make up the sides and bottom of the impoundment, duration of use, size, number of ponds in an area, depth of excavation, mineralogy of the soil profile and in the shallow subsurface, the hydrostratigraphy which underlies the impoundment, distance to outcrop, and reclamation.

During the early stages of production, water is discharged at fairly high rates, often exceeding 20 gallons per minute (gpm). During later stages of production discharge rates are expected to decrease, possibly to 5 gpm or less. Water production reported for existing CBNG wells in Montana is primarily early stage production and averages about 8.6 gpm. The productive life of individual wells is not yet known for the Powder River Basin (PRB), but estimates range from 5 to 20 years (U.S. Bureau of Land Management, 2003). The potential number of wells, the average water production, and the life of the wells demonstrate that carefully designed and implemented water-management plans are crucial to successful development of coalbed natural gas.

Water produced with CBNG is high in bicarbonate, low or devoid of sulfate (reduced conditions), has low concentrations of calcium and magnesium, and has relatively high sodium concentrations (high sodium adsorption ratios or SAR). In southeastern Montana where CBNG is being

developed, coalbed water has higher salinity and higher SAR than in producing areas of the southern PRB in Wyoming.

Infiltration basins have been in use in Wyoming and Montana for several years. These basins have several advantages. They are an inexpensive means of disposing of production water that comes from primary aquifers in the area, and they help recharge the shallow groundwater system. The basins also have several potential disadvantages. Flow directions and the ultimate destination of the infiltrating water are controlled by clay aquitards, discontinuous sandstone beds, and coal beds. The infiltrated water does not move into the original deep aquifers, but rather tends to move laterally as well as vertically, and in some situations may form sodic or saline seeps along hillsides or add sodic baseflow to streams. As the sodium-bicarbonate discharge water moves through the shallow weathered bedrock, a series of chemical reactions (primarily dissolution and oxidation) may increase the salt load in the water and detrimentally impact receiving waters.

The purpose of this study is to document short-term changes in the quality of shallow groundwater in response to CBNG infiltration ponds and to begin developing predictive tools. This report presents 1.5 years of data and interpretations of those data. Data collected near Decker, Montana during coal mine studies and the beginning of CBNG production provides some background on the anticipated issues. Detailed studies of two CBNG infiltration ponds in Wyoming were undertaken during this study (**Figure 1**). A network of monitoring sites was established that included monitoring wells (**Appendix A**) and surface-water sites. Data from these sites were collected and interpreted and include water quality (**Appendix B**), and drill cuttings for saturated paste extract analyses (**Appendix C**).



Figure 1. The two study sites are located in the Wyoming part of the Powder River Basin. A reference site is located in Montana.

Overview of water-quality evolution

The quality of groundwater in the Fort Union Formation changes through a well-known series of chemical reactions (Van Voast and Reiten, 1988). This evolution of water quality is generalized in **Figure 2**. In recharge areas, calcium and magnesium carbonates are dissolved resulting in groundwater that is dominated by the cations Ca and Mg, the HCO_3 anion, and having a moderate concentration of total dissolved solids (TDS) (**1** on **Figure 2**). Dissolution of gypsum and other SO_4 containing minerals will add SO_4 to the water. Slightly further along the flow path, oxidation of pyrite significantly increases both the SO_4 and TDS concentrations (**2** on **Figure 2**). Where groundwater contacts sodic shales, Ca and Mg ions are exchanged for Na ions, further increasing TDS as the ionic valence requires desorption of two Na ions for each Ca or Mg ion (**3** on **Figure 2**). Under anaerobic conditions in deeper parts of the flow systems, SO_4 reducing bacteria force precipitation of sulfide, which in turn causes Ca and Mg carbonate precipitation to maintain the cation/anion balance. The result of reactions in these deep anaerobic settings is groundwater that is dominated by Na and HCO_3 ions, and has a moderate TDS concentration (**4** on **Figure 2**).

Studies of coal mine hydrogeology in the PRB over the past three decades provide an important understanding of

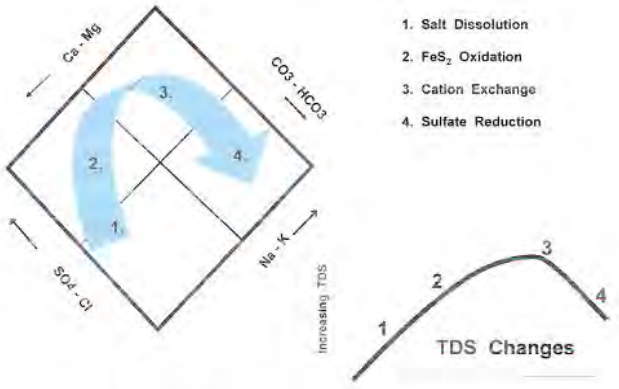


Figure 2. Changes in water quality along groundwater flow paths proceed in a predictable fashion, dominated by ions of calcium-bicarbonate near recharge areas and dominated by ions of sodium-bicarbonate in deep aquifers. Total dissolved solids concentrations increase along the flow path until reducing conditions are encountered in deep coal beds (Van Voast and Reiten, 1988).

the groundwater systems, and have produced methods of predicting groundwater impacts. Predicting the water quality of coal mine spoils in the PRB is required for permitting and is necessary for proper reclamation. Saturated paste extract (SPE) data are a primary tool for predicting water quality in coal-mine-spoils aquifers.

Methods

Saturated paste extracts are used to evaluate soluble salts that are available for reaction with water within lithologic zones such as soils or overburden. The method was primarily developed for use in soils studies (U.S. Salinity Laboratory Staff, 1954). For this study, saturated pastes were prepared using the method described in Page (1982). A lithologic sample of 200 to 400 grams of air dry material is saturated by adding distilled water until the sample just flows but has no standing water. The sample is allowed to sit for 8 hours, then the water is collected using a vacuum filter. The amount of water added is used to calculate the saturation water percentage. The water sample is analyzed using standard laboratory procedures. The results are reported in meq/L, and are used to describe the relative percentages of ions in the water.

Saturated-paste-extract data from lithologic material collected from overburden drill holes are used to predict the ratios of cation species in groundwater in coal-mine-spoils aquifers. Dissolution reactions in the paste-extraction simulate those that occur in mine spoils and are expected to occur during saturation beneath infiltration ponds. Saturated-paste-extract data, therefore, provide a simple model of changes in water quality. Concentrations of ions within spoils aquifers vary both locally and regionally, but are generally expected to increase rapidly as the spoils re-saturate, then decrease as the groundwater flow system is established, which flushes the available salts. The flushing process must be dynamic enough to transport the salts to the surface-water system or to other aquifers. As the salts are flushed from the spoils, the TDS is expected to return to near background levels, possibly after as little as one pore volume of water has moved through the system. The increase in TDS concentrations followed by the eventual decrease is demonstrated very well by data from a mine-spoils monitoring well in the Decker Coal Mine (**Figure 3**).

The quality of shallow groundwater beneath CBNG infiltration ponds is expected to change in a manner that reflects the above processes. Concentrations of Ca, Mg, Na, SO_4, and TDS will increase due to dissolution by the infiltrating production waters. Ionic concentrations of elements such as Ca, Mg, and in some cases SO_4^{-2}, will be controlled by mineralogy. Preliminary computer modeling indicates control by calcite, magnesite, and gypsum. Elements such as Na, and in some cases SO_4, will move through

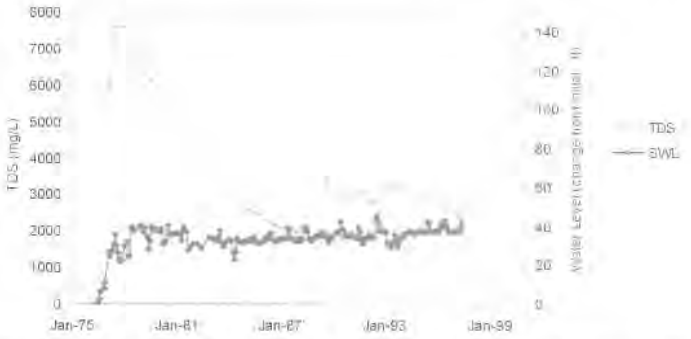


Figure 3. Total dissolved solids concentrations in coal-mine-spoils aquifers eventually decrease as the available salts are flushed from the system, as demonstrated at monitory well DS-03.

the system without the control of mineral dissolution/precipitation reactions and will result in high TDS levels. As the available salts are flushed the concentrations will decrease. Only rarely will infiltrated water reach anaerobic regions of flow systems, allowing SO_4 reduction to occur. However, significant reductions in TDS will occur if infiltration water does reach these anaerobic regions.

It should be noted that the presence of magnesite as a mineral at equilibrium in this near surface environment is supported by research conducted by Kittrick and Peryea (1986) and Sadiq and Lindsay (1979). However, other researchers have suggested that magnesite does not form under these conditions. As noted above, the modeling results of our data show that magnesite is likely controlling solution Mg levels. Thus at this time, this study will assume that magnesite is present and will form under the near surface environments. The magnesite question will be addressed as this research effort continues.

It is important to note that rising water levels do not directly relate to the arrival of infiltrated water. Water-pressure increases can be transmitted ahead of the physical migration of water. Only in a water table aquifer does the rise in water level directly correspond with the arrival of infiltration water, and water-quality data are interpreted accordingly.

This study of CBNG infiltration ponds is based on the hypothesis that the quality of water infiltrating from CBNG ponds will change along known reaction paths, and that saturated paste extract data from drilled holes adjacent to infiltration pond sites can successfully predict those changes.

Study sites and data collection

Water-quality changes near Decker

Groundwater monitoring has been conducted near Decker, Montana for more than 30 years due to planned and existing coal mines. The surficial geologic unit is the Tongue River Member of the Paleocene Fort Union Formation. Coalbed natural gas is currently being produced from the Anderson (D1), Upper Dietz (D2), Lower Dietz (D3), Canyon (Monarch), and Carney coal beds of the Tongue River Member. In addition, proposals have been made to test CBNG potential from the Wall and Flowers-Goodale coal seams in Montana.

During 2000, a CBNG infiltration pond was constructed approximately 200 feet north of a pre-existing, overburden monitoring well (WR-17A) that is 88 feet deep, and 1/4 mile south of saturated paste extract data point CX-50 (**Figure 4**). As a result of water infiltrating from the pond, groundwater levels at WR-17A rose 25 feet (MBMG file data). Water-quality data indicate the SO_4 concentration increased from 419 mg/L to 1,890 mg/L, TDS increased from 2566 to 3548 mg/L, SAR decreased from 43 to 14, and Fe increased from 0.13 to 0.85 mg/L (**Appendix B**). The infiltrating CBNG water had very little SO_4, lower TDS, and higher SAR than the overburden water. Therefore, these changes in shallow groundwater quality cannot be explained by simple mixing, and are best explained by dissolution of minerals from overburden material along the flow path of the infiltrating water.

Saturated paste extract data from bore hole CX-50 was used to model water quality in the shallow sandstone aquifer at WR-17A, and then compared to analytical data for that site (**Figure 5**). Values for SAR are particularly appropriate to predict using SPE data. Averaging the SPE data from CX-50 over the saturated interval of WR-17A during baseline conditions (54 to 88 feet below ground surface) produced SAR values that are nearly identical with those measured before CBNG development. To investigate changes in water quality, CBNG water-quality data were mathematically mixed with the SPE data (available for 5-foot depth intervals and listed in **Appendix C**). Mixing results from each depth interval were progressively mixed with the next deeper SPE data. These data are plotted on **Figure 5**. Above the original water table, downward moving water was mixed at a ratio of 50% to 50% SPE data, as there would be very little other water in the system at this point. Below this level, the ratio was adjusted to 10% to 90% to allow for assumed heterogeneity and aquifer through flow. Averaging the results over the saturated interval after the impact of infiltration water (29 to 88 feet below ground surface) produces a good approximation of the measured SAR at WR-17A (**Figure 5**).

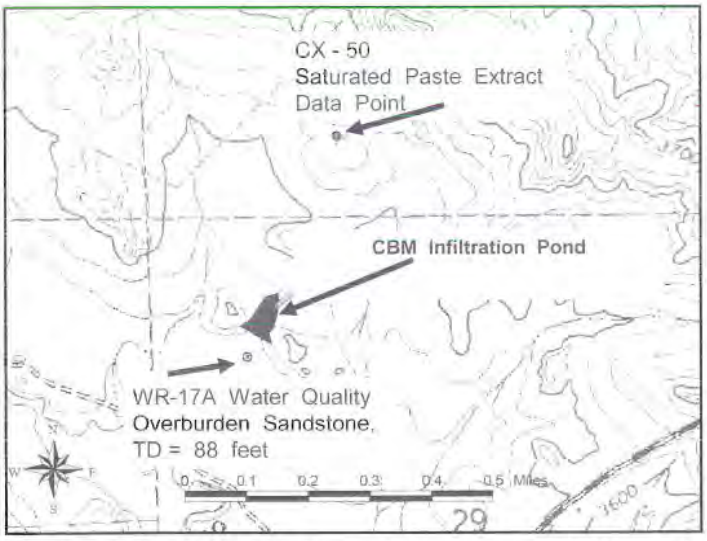


Figure 4. Saturated paste extract data, and groundwater quality data are available near a CBNG infiltration pond in southern Montana.

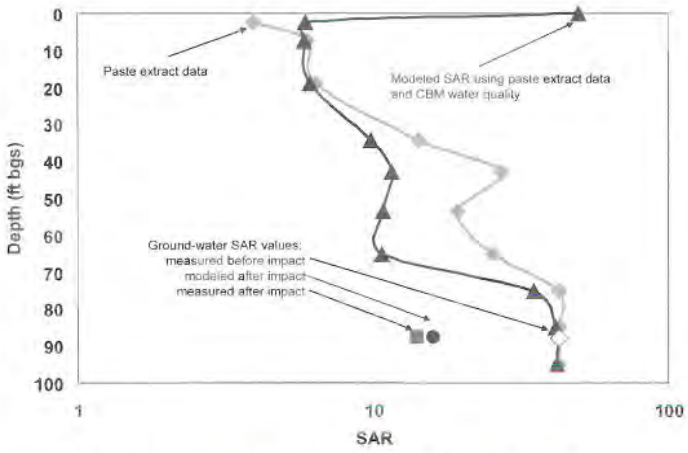


Figure 5. Mathematically mixing paste extract data and CBNG data successfully predicts the change in SAR values measured at monitoring well WR-17A in southern Montana near a CBNG infiltration pond.

The resultant water quality is likely the product of dissolution of a number of minerals of varying dissolution capacities. The system appears to be in equilibrium with calcite and magnesite. Gypsum may be associated with increased SO_4 concentrations. Pyrite oxidation may also contribute to the SO_4 and Fe concentrations (**Appendix B**).

Water-quality changes at Coal Creek

The primary study sites for this research project were established at two locations in Wyoming; the Coal Creek and Beaver Creek study sites (**Figure 1**). At Coal Creek,

monitoring wells were installed prior to the discharge of CBNG-production water and during construction of the infiltration pond (**Figure 6**). Monitoring site information, monitoring well completion records, and lithologic logs are listed in Appendix A. Additional discussions of the hydrogeology of this site are presented in this volume by Frost and Brinck (2005) and Payne and Saffer (2005).

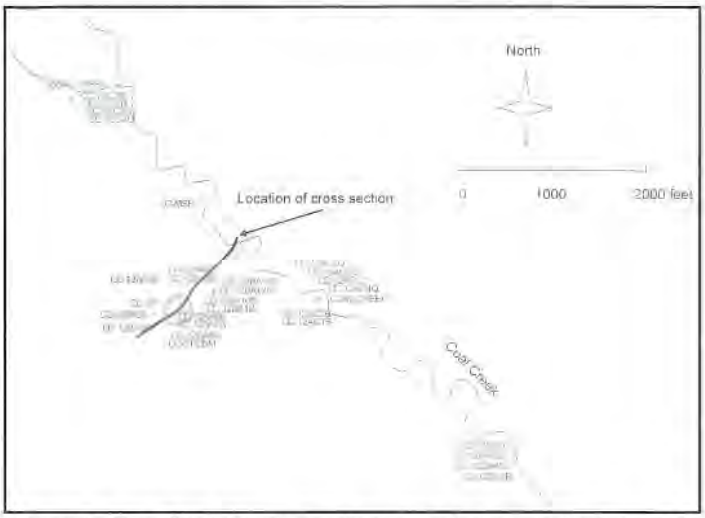


Figure 6. The Coal Creek study site includes monitoring wells, stream gauging stations, and a CBNG infiltration pond.

The Eocence Wasatch Formation is exposed at ground surface at the Coal Creek site. Underlying the infiltration pond are interbedded sandstone, clay and coal (**Figure 7**). Coalbed natural gas is produced from the Roland coal (Wasatch Fm.) and to a lesser extent from the Anderson coal (Fort Union Fm.). During November 2003 CBNG water began to be discharged to the infiltration pond used in this study.

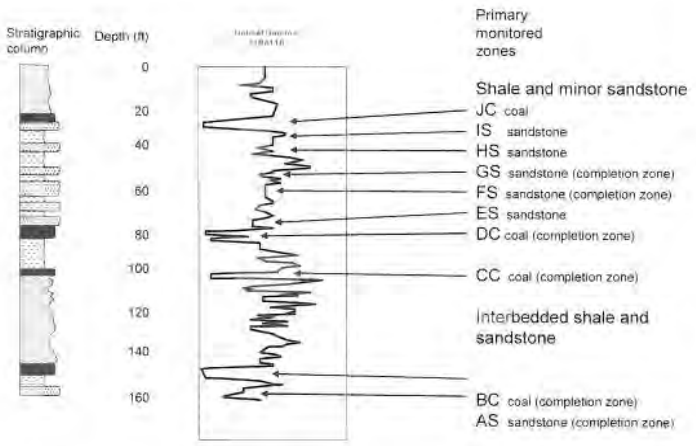


Figure 7. A typical gamma geophysical log for the Coal Creek study area shows the interbedded nature of the coal, sandstone, and clay units in the Wasatch Formation. Completion zones of monitoring wells are indicated.

The infiltration pond at Coal Creek is off-channel, constructed in a gently sloping uplands area, south of Coal Creek. Colluvial material was scraped away to expose weathered bedrock at the bottom of the pond. The bedrock material is silty clay (46% clay, 43% silt, 11% sand; **Appendix C**). Saturated paste extract data from drill cuttings that were collected at a well drilled in the pond are listed in **Appendix C**.

Based on the expected chemical reactions for water in the PRB, baseline data indicate water quality at this site is both intermediate and near the normal end point of **Figure 2**. Shallow groundwater is dominated by near-equal concentrations of the cations Ca, Mg, and Na with moderate levels of TDS. Slightly deeper water in a thin coal is dominated by Na and HCO_3 ions and has a lower TDS concentration (**Figure 8**). Apparently, the SO_4 is removed from the system by means of sulfate reduction mechanisms shown in **Figure 2**. Sulfate-reducing bacteria are common in PRB aquifers (Dockins and others, 1980). The presence of SO_4 reducing bacteria in a shallow flow system is unusual, but may (with continued monitoring) afford an opportunity to observe the effects of this process on infiltrated CBNG water.

Water quality in the pond is essentially the same as that measured at the CBNG discharge point, indicating that reactions are not occurring in the pond. The water table directly beneath the pond responded to CBNG-production-water discharges to the pond in less than one month, rising from 17.1 to 9.4 feet below the floor of the pond. Water quality data from samples collected during December 2003 (1 month after the first discharge to the pond) show increases in concentrations of all cations and in SO_4 (**Figure 9** and **Appendix B**). Beneath the pond, at well CC12BA7B, the TDS concentration increased from 1433 to 6795 mg/L. After 7 months of use, saturation beneath the pond had risen to the floor of the pond, and changes in water quality were migrating laterally (**Figure 10**). Directly beneath the pond, the water quality in the previously unsaturated material is dominated by ions of Na and SO_4. Coalbed natural gas production water is dominated by anions of HCO_3, and depleted of SO_4. The SO_4 in the monitoring well is, therefore, a product of reactions along the flow path rather than ions in the CBNG-production water. At the depth of the baseline water table, Na, Mg, and SO_4 concentrations increased and TDS increased from 6795 to 12,411 mg/L (**Figure 10** and **Appendix B**). Northeast of the pond, about 100 feet, concentrations of Mg and SO_4 increased as the TDS rose from 1337 to 3293 mg/L. Increasing TDS is primarily controlled by Mg, Na, and SO_4 ions. The maximum change will not be confirmed until decreases in TDS are documented. The increase in TDS is

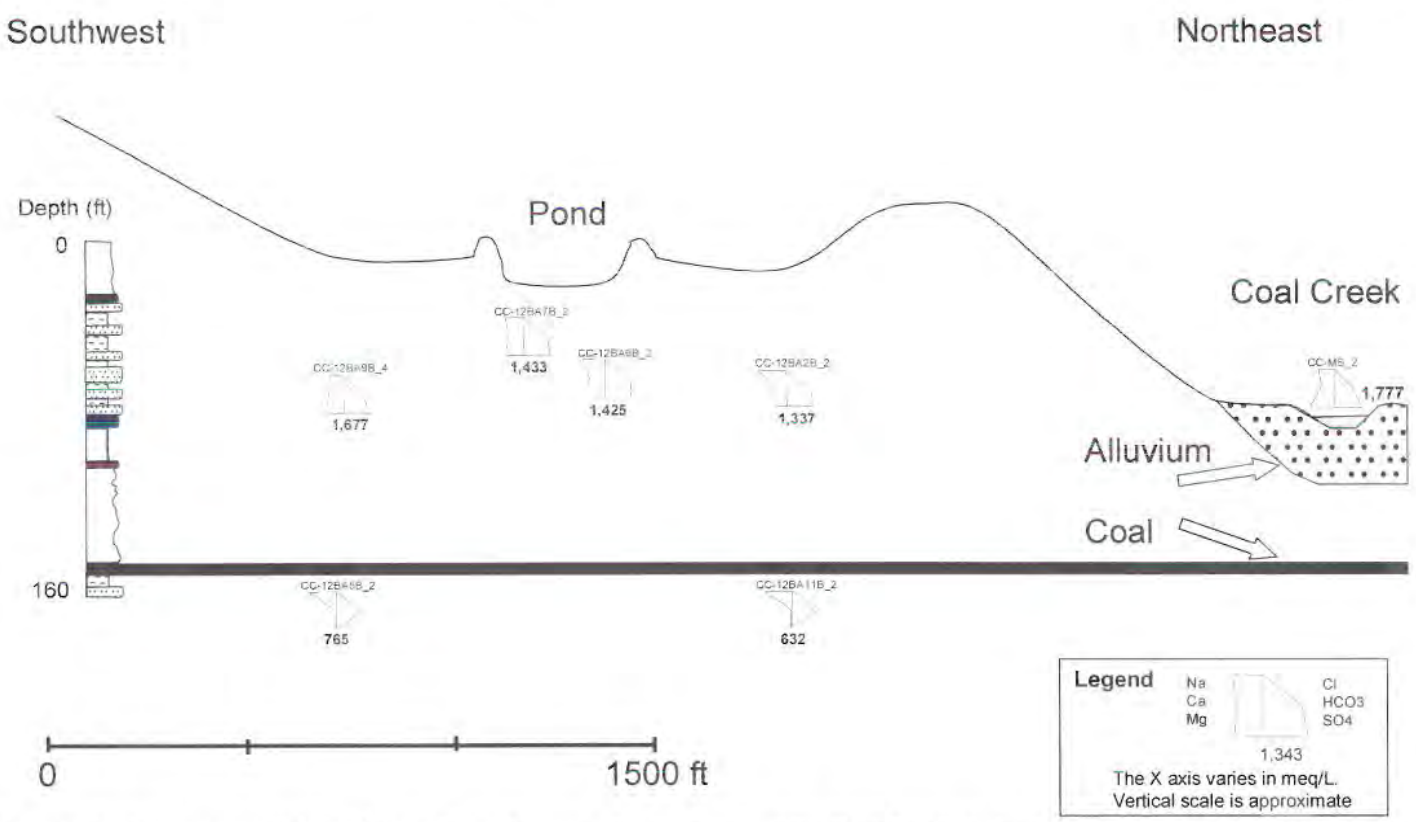


Figure 8. During baseline (July 2003) conditions the groundwater quality at the Coal Creek study site shows natural evolution. The location of cross section is shown on Figure 6.

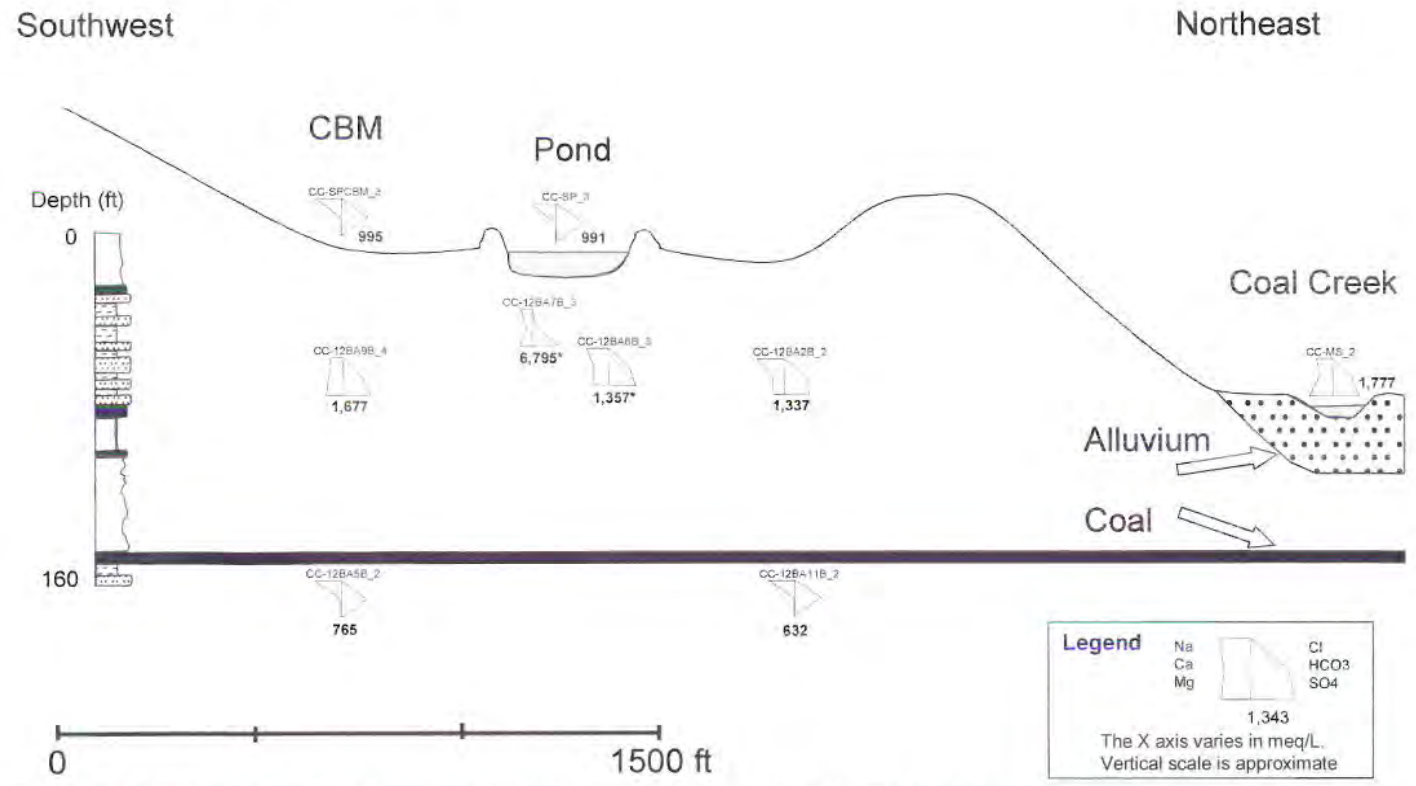


Figure 9. After about 1 month of discharge to the CBNG pond (December 2003) the total dissolved solids in the shallow groundwater at the Coal Creek study site has increased (CC-12BA6B_3, CC-12BA7B_3). The location of cross section is shown on Figure 6. *Total dissolved solid values have changed.

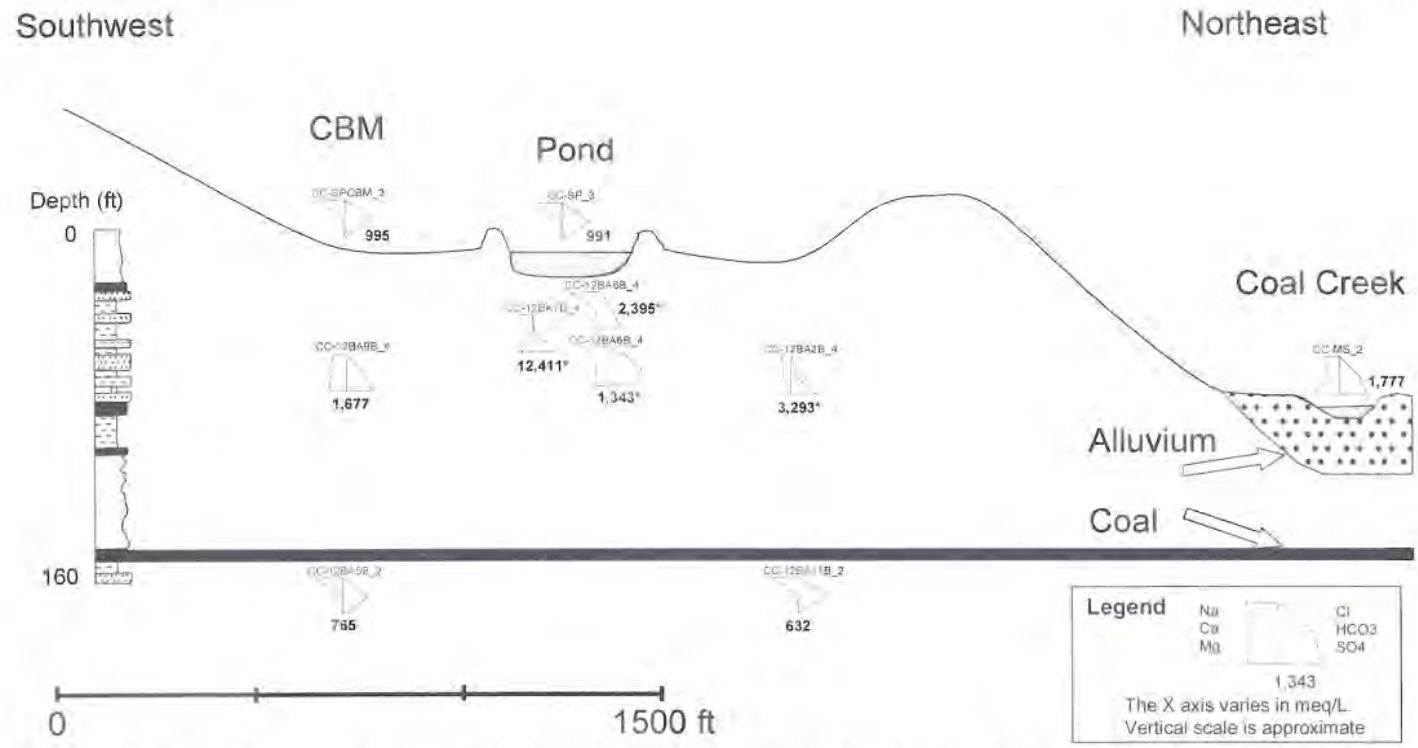


Figure 10. After about 7 months of discharge to the CBNG pond (June 2004) the total dissolved solids in the groundwater beneath and to the northeast of the pond at the Coal Creek study site has increased (CC-BA6B_4, CC-BA7B_4, CC-BA8B_4, CC-BA2B_4). Groundwater is flowing downward from the pond, and will eventually flow toward Coal Creek. The location of cross section is shown on Figure 6. *Total dissolved solid values have changed.

likely associated with the dissolution of minerals present in the overburden material and is not directly associated with the CBNG production water. In fact, similar TDS levels would be expected if a surface water source, or rainwater, had been pumped into the pond. Much of the increased concentrations of cations and anions in the baseline water-table aquifer are associated with the dissolution of minerals and fossil salts present in the overburden materials.

Saturated paste extract data indicate the increase in SO_4 from about 627 mg/L to 8604 mg/L, directly beneath the pond, likely is occurring in the uppermost 10 feet of material, and is being carried vertically by groundwater flow (**Figure 11** and **Appendix B**). These data support the previous conclusion that the dissolution of soluble minerals, rather than infiltrating water quality, appears to control ultimate water quality in the receiving aquifer. The fact that Na concentration, the primary concern with CBNG water, does not increase more than other cations supports this conclusion.

Using the same procedure that was used with data from WR-17A, SPE values were mathematically mixed with CBNG water at the Coal Creek site (**Figure 12**). The SPE values are very close to the baseline water quality, and the mixing model results are close to the measured SAR in the groundwater beneath the pond. Therefore, changes in water quality at this site are probably controlled by dissolution reactions and possibly ion exchange.

The Sr ratio data presented by Frost and Brinck (2005) can be used to estimate the approximate impact that the constituents of the CBNG production water and the dissolution of minerals have on resultant water quality. Well CC-12BA8B is completed at a depth of 5.8 feet and is located in the infiltration pond. Using the Sr ratio data in a direct relationship without consideration for mineral precipitation and cation exchange, the water quality at this

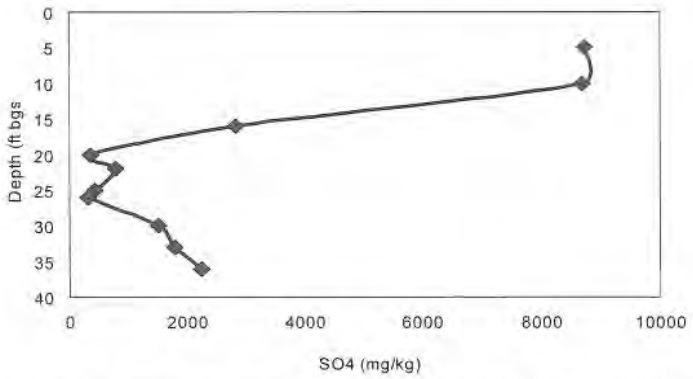


Figure 11. Based on saturated paste extract data from monitoring well CC-12BA6B, most of the increases in SO_4 beneath the CBNG pond occurs in the upper most 10 feet of the groundwater flow path.

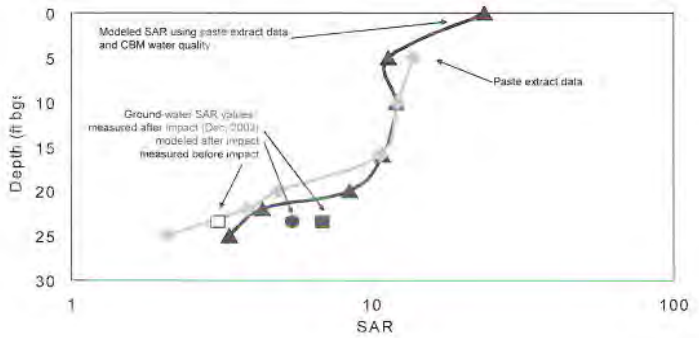


Figure 12. Mathematically mixing saturated paste extract data from well CC-12BA6B with CBNG data successfully predicts the change in SAR values measured in the Coal Creek, Wyoming CBNG infiltration pond.

well reflects a mixture of 30% CBNG-production water and 70% dissolution products. If the relationship between depth and influence of dissolution reactions is approximately linear, then the change in dissolved constituents in the CBNG-production water was negligible at depths greater than about 7.7 feet when the June 2004 sample was collected. This agrees well with SPE data presented in Figure 12. Additional monitoring will document whether CBNG-production water quality influences shallow groundwater quality as available salts are flushed by the infiltrating water.

Water-quality changes at Beaver Creek

The location of the Beaver Creek research site is shown on **Figure 1**. The locations of monitoring wells at the site are shown on **Figure 13** and site details and well completion records are in **Appendix A**. Physical hydrogeology is presented in Payne (2004) and Payne and Saffer (2005, this volume) and discussions of isotopic chemistry are presented in Frost and Brinck (2005, this volume).

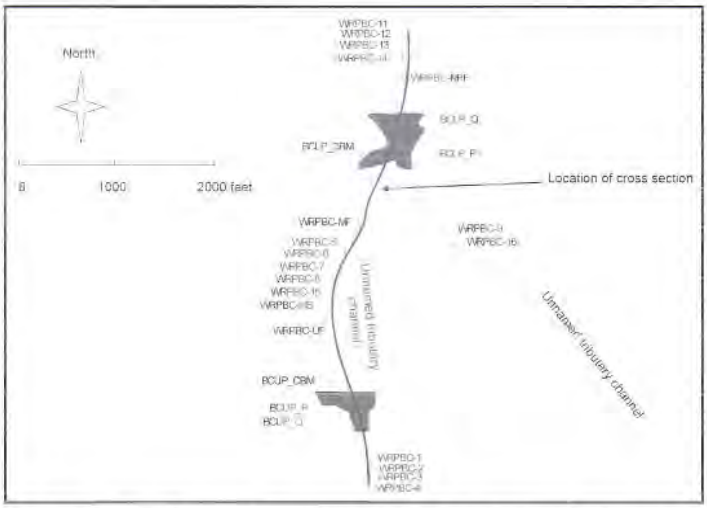


Figure 13. The Beaver Creek study site includes monitoring wells, stream gauging stations and two CBNG infiltration ponds.

The Eocene Wasatch Formation is exposed at ground surface. Coalbed natural gas production is from the Big George coal (Fort Union Formation) and production water was first discharged to the infiltration ponds in November 2002.

Two CBNG infiltration ponds are in use at the Beaver Creek site. Both ponds are on-channel, constructed by building dams across the channel of an ephemeral tributary to Beaver Creek. Due to CBNG-production water discharge, this tributary is now perennial, and infiltration to the groundwater systems occurs both from the ponds and from the stream through the alluvial material. Monitoring wells were drilled and completed in the alluvium and in the shallow, weathered bedrock directly underlying the alluvium. The alluvium consists of fine sand, silt, and gravel overlying weathered sandstone of the Wasatch Formation. Monitoring well completion records and lithologic logs are presented in **Appendix A**. The Wasatch Formation is exposed on the land surface where it is not covered by alluvial or colluvial deposits.

Baseline data from the Beaver Creek site indicate the groundwater quality is dominated by ions of Ca, SO_4, and HCO_3 (**Figure 14**). Total dissolved solids concentrations generally increase and HCO_3 decreases downgradient along the flow paths. Prior to CBNG development, recharge to these shallow groundwater systems only occurred in response to precipitation events. Coalbed natural gas production water is dominated by ions of Na and HCO_3, with TDS concentrations ranging from 1267 mg/L to 1390 mg/L. The influence of CBNG production water is expected to increase TDS and other constituents in the shallow aquifers due to dissolution of minerals and fossil salts.

The alluvial water table and the shallow bedrock water level rose in response to infiltration from the ponds and along the stream. Water samples collected during December 2003 (after 1 year of CBNG-water discharge) indicate a mixture of decreasing and increasing concentrations. In the middle reach of the study site, SO_4 and TDS concentrations decreased in the alluvial aquifer from 807 to 320 mg/L and 1345 to 960 mg/L, respectively (**Figure 15**). In the bedrock aquifer, SO_4 and TDS concentrations decreased from 1602 to 379 mg/L and 2502 to 926 mg/L respectively. At this site, Na concentrations decreased to below the CBNG discharge concentration. An evaluation of the solution chemistry indicates that the system remains saturated with respect to calcite. The reduction in TDS seems to show that minerals such as gypsum, dolomite, and magnesite are being depleted and much of the resulting constituents are being leached from the system. This preliminary interpretation indicates that the maximum concentrations of constituents

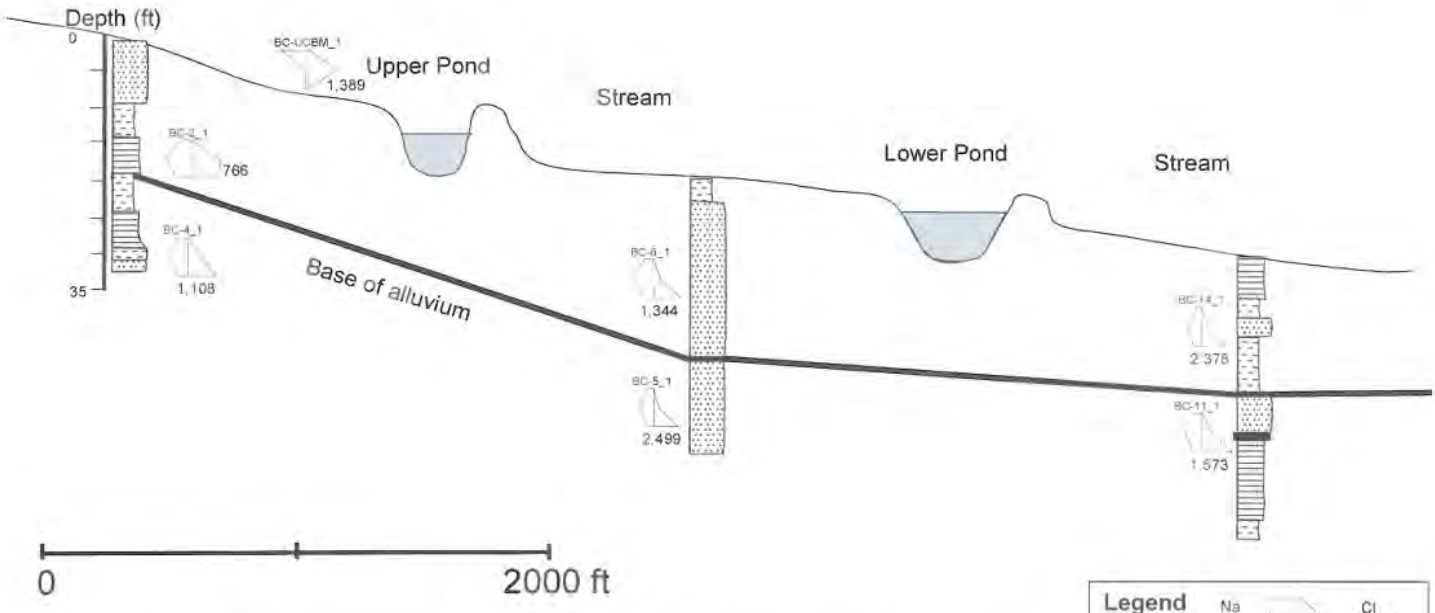


Figure 14. Shortly after CBNG production began (January 2003) groundwater quality at the Beaver Creek study site reflects normal alluvial conditions. The location of cross section is shown on Figure 13.

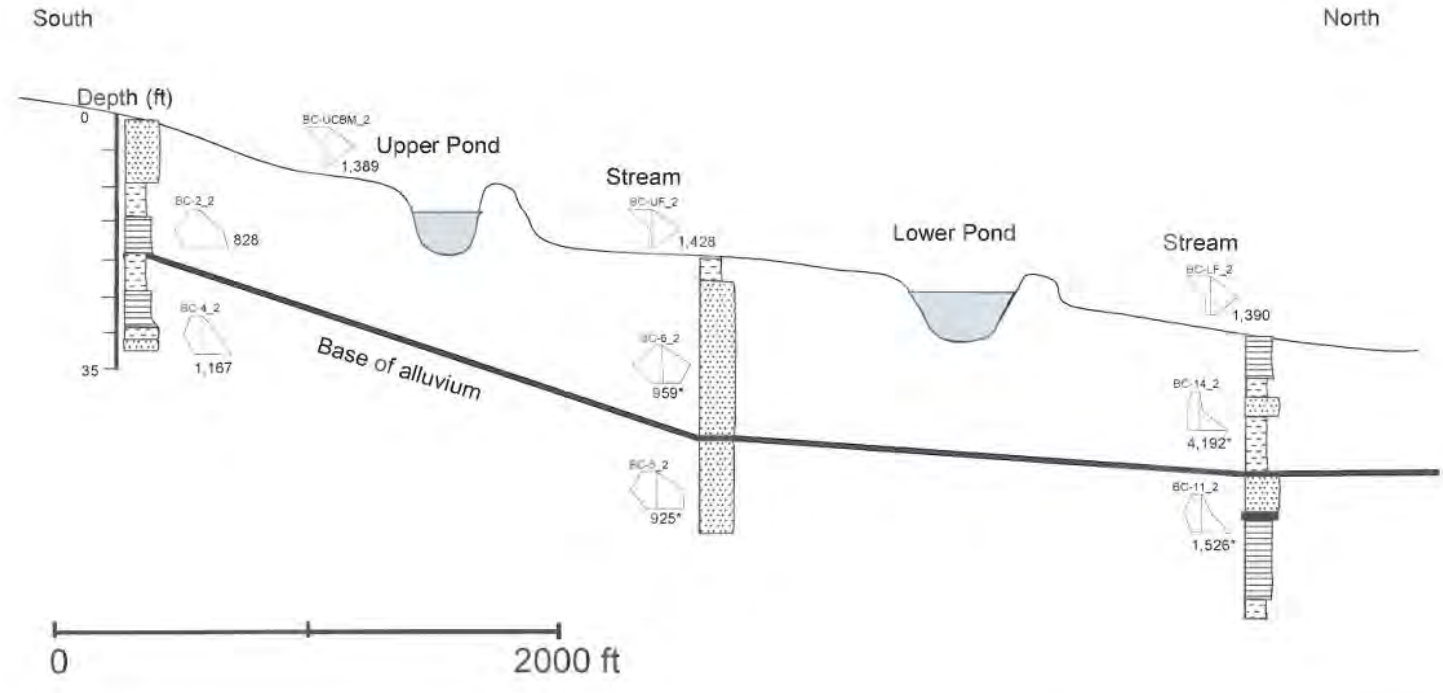


Figure 15. After about 1 year of discharge to the CBNG ponds (December 2003) the total dissolved solids have decreased in the groundwater in the alluvium in the center of the Beaver Creek study site (BC-5_2, BC-6_2) and has increased in the lower reaches (BC-11_2, BC-14_2). Location of cross section is shown on Figure 13. *Total dissolved solid values have changed.

were reached and not documented by monitoring data. The geochemical model used in this evaluation does not show the depletion of SO_4 due to the precipitation of gypsum or other minerals. Additional study must be conducted to develop a better understanding of the solution chemistry observed at this site.

In the alluvial aquifer in the lower reach of the site, SO_4 increased from 1514 to 2848 mg/L and Fe concentrations nearly doubled from 0.051 to 0.098 mg/L. Total dissolved solids concentration increased from 2383 to 4202 mg/L. The shallow bedrock aquifer at the lower site showed no change. The dissolution of minerals such as gypsum, dolomite, and magnesite likely contribute to the increased levels of TDS and SO_4. The oxidation of pyritic materials may also contribute to the increased SO_4 levels as evidenced by the increase in Fe (magnetite or similar mineral may be the contributor).

It is important to note that the upper CBNG pond was constructed where a stock pond had previously existed. The stock pond may have enhanced local recharge and flushed salts from the system. This may explain why concentrations of ions in the groundwater at the middle site did not increase. However, concentrations decreased to below that of the CBNG water, indicating that precipitation and/or leaching had occurred. In the lower reach of the site, salts may not have been flushed prior to CBNG development,

As discussed previously in this report, the Sr ratio data presented by Frost and Brinck (2005) can be used to estimate the approximate impact that the constituents of the CBNG production water and the dissolution of minerals have on resultant water quality. Using this approach, the water quality below the infiltration ponds reflect a mixture of ambient groundwater and infiltrated CBNG-production water. At the middle site (BC-6) the shallow alluvial water quality is approximately 50% CBNG-production water and 50% ambient groundwater. The Wasatch Formation water quality at this site (BC-5) indicates a mixture of about 40% CBNG-production water and 60% ambient groundwater. At the lower site (BC-14), Sr ratio data show greater variability, but seem to indicate a mixture of about 20% CBNG-production water and 80% ambient groundwater. Neither the groundwater chemistry nor the groundwater levels in the bedrock aquifers of the Wasatch Formation have been influenced by infiltrating CBNG-production water.

Recommendations

A usable understanding of the magnitude, duration, and geographic extent of impacts to groundwater systems from infiltration ponds must include modeling, which is calibrated with monitoring data. Documentation of changes through monitoring at selected sites is critical to provide calibration for models and a foundation for permitting and development decisions. Approaches to decision making must be adjusted as better understandings of the systems are developed. Monitoring of key sites in support of decision-making is best maintained for the duration of CBNG production and reclamation. Monitoring data should be stored in a public database, which allows access for all interested parties.

Continued research should include the use of coal-mine-spoils data and publications on mine-spoils aquifers as a basis for understanding the influences of CBNG production on surface and groundwater issues. Water quality in mine-spoils aquifers reflects saturation of geologic material that has not previously been saturated. Dissolution of salts and eventual flushing of those salts are processes that parallel the processes near CBNG infiltration ponds.

Based on data available after 1.5 years of research at four pond sites, simple mixing models provide a reasonable estimate of changes in cationic concentrations as water moves from ponds to receiving aquifers. Saturated paste extract data, lithology, and strontium data provide input data for mixing models. Saturated paste extract data also provide site-specific data that can identify zones or locations that should be avoided in pond design in order to minimize increases in TDS.

A decision matrix can be developed that uses infiltration rates, SPE data, and groundwater data to determine the suitability of specific locations for siting CBNG infiltration ponds. Regulators should work together with researchers to develop such a decision matrix.

Conclusions

Infiltration ponds provide an economical means of storing CBNG production water. Water infiltrating from these ponds may recharge shallow aquifers, potentially enhancing groundwater resources. However, as the infiltrating water moves through the previously unsaturated material, a series of reactions occurs that increases TDS and other constituents. Predicting these changes is an important step in successfully designing and siting infiltration ponds.

Data and preliminary interpretations from three sites indicate changes in water quality that will occur as CBNG-production water infiltrates into the shallow aquifers. Findings include sites that experience either increased or decreased levels of TDS and other constituents. At one off-channel site, significant increases in TDS, Mg, and SO_4 occurred. The maximum increase in SO_4 has reached 13 times the baseline concentrations and the maximum TDS increase has reached 8.7 times the baseline concentration. At two on-channel sites, a combination of increases and

decreases in TDS has occurred. Increases of SO_4 and TDS are nearly double the baseline concentrations. Where decreasing concentrations occurred, concentrations of SO_4 and TDS have dropped by as much as 75% and 67%, respectively. The maximum concentrations have likely not been measured at all sites, and will only be determined when decreasing values are documented.

The changes in water quality are controlled by available soluble minerals in the shallow soil and bedrock profile. Calcite, dolomite, and gypsum are common minerals in the Powder River Basin. Dissolution of these minerals increases Ca, Mg, and SO_4 ion concentrations. Pyrite may be involved in the reactions in some settings, further increasing SO_4 and Fe concentrations. However, increases in Fe are rare in the data collected during this study indicating that pyrite may not be a significant source of SO_4.

At off-channel ponds, the quality of the infiltrating water has little effect on the ultimate water quality, within the time frames currently researched. Mineralogy controls the reactions and resultant concentrations, which so far exceed any CBNG-production-water ionic concentrations. For this reason, the Na concentration in the CBNG water is less of a concern than is the mobilization of salts which have accumulated in the unsaturated zone over thousands of years. In on-channel sites where natural groundwater recharge and flow have flushed the salts from the alluvial aquifer, water quality may be diluted by CBNG discharge.

The duration and geographic extent of water-quality impacts is not yet known. Based on research in coal-mine-spoils aquifers, at least one pore volume of water must move along the flow path to flush the immediately available salts prior to any decrease in TDS. In some cases, more than one pore volume will be necessary before improvement is seen. The improvement is likely to be local, however, because the salt-laden groundwater will continue migration, ultimately to surface discharge or to other aquifers.

The results of decades of mine spoils research provides appropriate methods for assessing CBNG infiltration ponds. The mineralogy and reactions are very similar and the SPE data can be used to successfully predict water quality trends. Both sites and specific depths with generally high levels of available salts can be identified and avoided during the pond-design phase. Relative concentrations of cations are particularly appropriate for SPE assessment, giving reliable estimates of SAR values.

Coal mine spoils studies have shown the value of long-term studies, and similar continued research is vital to successfully evaluating CBNG ponds. The study sites chosen for this research have been well established with monitoring wells and stream gauging stations. The research now underway should be maintained until recovery of water quality in underlying aquifers is documented.

References cited

Dockins, W.S., Olson, G.J., McFeters, G.A., Turbak, S.C., and Lee, R.W., 1980, Sulfate reduction in groundwater of southeastern Montana: U.S. Geological Survey Water-Resources Investigation 80-9, 132 p.

Frost, C.D., and Brinck, E., 2005, Strontium isotopic tracing of the effects of coalbed natural gas (CBNG) development on shallow and deep groundwater systems in the Powder River Basin, Wyoming, *in* Zoback, M.D., editor, Western Resources Project Final Report—Produced groundwater associated with coalbed natural gas production in the Powder River Basin: Wyoming State Geological Survey Report of Investigations No. 55, p. 93-108.

Kittrick, J.A., and Peryea, F.J., 1986, Determination of the Gibbs free energy of formation of magnesite by solubility methods, Soil Science Society of America Journal v. 50, p. 243-247.

Page, A.L., editor, 1982, Methods of soil analysis part 2—Chemical and microbiological procedures: American Society of Agronomy, Inc., Soil Science Society of America, Inc., Madison, Wisconsin, 1159 p.

Payne, A., 2004, Surface water hydrology and shallow groundwater effects of coalbed methane development, upper Beaver Creek drainage, Powder River Basin, Wyoming: M.S. thesis, University of Wyoming, Laramie, 116 p.

Payne, A.A., and Saffer, D.M., 2005, Surface water hydrology and shallow groundwater effects of coalbed natural gas development, upper Beaver Creek drainage, Powder River Basin, Wyoming, *in* Zoback, M.D., editor, Western Resources Project Final Report—Produced groundwater associated with coalbed natural gas production in the Powder River Basin: Wyoming State Geological Survey Report of Investigations No. 55, p. 5-44.

Sadiq, M, and Lindsay, W.L., 1979, Selection of standard free energies of formation for use in soil chemistry, Colorado State University Experimental Station Technical Bulletin 134, 1069 p.

U.S. Bureau of Land Management, 2003, Montana final statewide oil and gas environmental impact statement and proposed amendment of the Powder River and

Billings resource management plans: U.S. Bureau of Land Management, BLM/MT/PL-03/005, 2 vol.

U.S. Salinity Laboratory Staff, 1954, Diagnosis and improvement of saline and alkali soils: U.S. Department of Agriculture Handbook No. 60, U.S. Government Printing Office, Washington, D.C., 160 p.

Van Voast, W.A., and Reiten, J.C., 1988, Hydrogeologic responses: Twenty years of surface coal mining in southeastern Montana: Montana Bureau of Mines and Geology Memoir 62, 30 p.

Appendices

Appendix A. Monitoring site information including location, aquifer formation, lithology, static water level, and date completed.

Site Name	GWIC ID	Type	* Latitude	* Longitude	Total Depth	Altitude	Town.	Range	Sec.	Tract	County
BCLP_P	209043	Pond	44.0133	-105.8490		4710	47N	75W	34	BBBC	Campbell
BCUP_P	209050	Pond	44.0026	-105.8508		4740	47N	75W	34	DAAB	Campbell
BC-MF	209046	Stream	44.0088	-105.8508		4720	47N	75W	34	ADAC	Campbell
BC-UF	209051	Stream	44.0065	-105.8509		4725	47N	75W	34	ADDD	Campbell
BCLP_CBM	209042	CBM well	44.0133	-105.8490		4710	47N	75W	34	AADA	Campbell
BC-15	207122	Well	44.0082	-105.8514	7.00	4720	47N	75W	34	ADAC	Campbell
BC-5	207123	Well	44.0082	-105.8514	38.00	4720	47N	75W	34	ADAC	Campbell
BC-6	207124	Well	44.0082	-105.8514	25.80	4720	47N	75W	34	ADAC	Campbell
BC-7	207125	Well	44.0082	-105.8514	25.00	4720	47N	75W	34	ADAC	Campbell
BC-8	207126	Well	44.0082	-105.8514	23.50	4720	47N	75W	34	ADAC	Campbell
BC-MS	209045	Stream	44.0082	-105.8514		4720	47N	75W	34	ADAC	Campbell
BCUP_Q	209049	Pond Discharge	44.0026	-105.8508		4730	47N	75W	34	ADDC	Campbell
BCUP_CBM	209047	CBM well	44.0026	-105.8508		4740	47N	75W	34	DAAB	Campbell
BC-1	207129	Well	44.0026	-105.8508	18.00	4755	47N	75W	34	DAAC	Campbell
BC-2	207130	Well	44.0026	-105.8508	18.00	4755	47N	75W	34	DAAC	Campbell
BC-3	207131	Well	44.0026	-105.8508	18.00	4755	47N	75W	34	DAAC	Campbell
BC-4	207132	Well	44.0026	-105.8508	31.50	4755	47N	75W	34	DAAC	Campbell
BC-LF	208571	Stream	44.0165	-105.8492		4670	47N	75W	35	BBBB	Campbell
BC-NPF	208572	Stream	44.0128	-105.8484		4700	47N	75W	35	BBBC	Campbell
BC-11	207118	Well	44.0133	-105.8490	38.00	4700	47N	75W	35	BBBC	Campbell
BC-12	207119	Well	44.0132	-105.8490	15.00	4700	47N	75W	35	BBBC	Campbell
BC-13	207120	Well	44.0132	-105.8490	15.00	4700	47N	75W	35	BBBC	Campbell
BC-14	207121	Well	44.0132	-105.8490	15.00	4700	47N	75W	35	BBBC	Campbell
BCLP_Q	209044	Pond Discharge	44.0166	-105.8490		4700	47N	75W	35	BBBC	Campbell
BC-16	207127	Well	44.0082	-105.8474	12.00	4725	47N	75W	35	BCAC	Campbell
BC-9	207128	Well	44.0082	-105.8474	28.00	4725	47N	75W	35	BCAC	Campbell
CC-1CC1B	207109	Well	44.5879	-106.5665	27.00	4180	53N	81W	1	CCAC	Sheridan
CC-1CC2Q	207110	Well	44.5879	-106.5665	17.00	4180	53N	81W	1	CCAC	Sheridan
CC-1CC3Q	207111	Well	44.5879	-106.5664	19.00	4180	53N	81W	1	CCAC	Sheridan
CC-1CC4Q	207112	Well	44.5878	-106.5663	19.50	4180	53N	81W	1	CCAC	Sheridan
CC-UW	202187	Stream	44.5880	-106.5664		4170	53N	81W	1	CCAC	Sheridan
CC-UTW	202185	Stream	44.5822	-106.5569		4170	53N	81W	1	CDBA	Sheridan
CC-SP	209363	Pond	44.5817	-106.5625		4225	53N	81W	12	CCDD	Sheridan
CC-SPCBM	209364	CBM Well	44.5817	-106.5625		4240	53N	81W	12	CCCC	Sheridan
CC-12AC3Q	207115	Well	44.5823	-106.5570	14.00	4150	53N	81W	12	ACAD	Sheridan
CC-12AC4Q	207116	Well	44.5823	-106.5569	23.00	4150	53N	81W	12	ACAD	Sheridan
CC-12AC5Q	207117	Well	44.5823	-106.5568	17.00	4150	53N	81W	12	ACAD	Sheridan
CC-12ACCC	209338	Stream	44.5823	-106.5569		4150	53N	81W	12	ACAD	Sheridan
CC-12AC1B	207113	Well	44.5817	-106.5584	57.00	4220	53N	81W	12	ACBD	Sheridan
CC-12AC2B	207114	Well	44.5817	-106.5584	36.00	4220	53N	81W	12	ACBD	Sheridan
CC-MSP	211060	Spring	44.5847	-106.5607	2.30	4160	53N	81W	12	BADA	Sheridan
CC-12BA4B	208368	Well	44.5824	-106.5628	21.70	4220	53N	81W	12	CBAA	Sheridan
CC-12BA11B	208375	Well	44.5823	-106.5610	158.20	4270	53N	81W	12	CBAB	Sheridan
CC-12BA12B	208376	Well	44.5822	-106.5610	63.90	4270	53N	81W	12	CBAB	Sheridan
CC-12BA2B	208366	Well	44.5824	-106.5620	35.60	4240	53N	81W	12	CBCC	Sheridan
CC-12BA3B	208367	Well	44.5824	-106.5620	137.00	4240	53N	81W	12	CBCC	Sheridan
CC-12BA9B	208373	Well	44.5814	-106.5634	58.40	4260	53N	81W	12	CBDB	Sheridan
CC-12BA10B	208374	Well	44.5818	-106.5615	143.20	4245	53N	81W	12	CCCC	Sheridan
CC-12BA1B	208365	Well	44.5818	-106.5615	42.30	4245	53N	81W	12	CCCC	Sheridan
CC-12BA6B	208370	Well	44.5817	-106.5625	35.00	4225	53N	81W	12	CCDD	Sheridan
CC-12BA7B	208371	Well	44.5817	-106.5625	23.50	4225	53N	81W	12	CCDD	Sheridan
CC-12BA8B	208372	Well	44.5817	-106.5625	5.80	4225	53N	81W	12	CCDD	Sheridan
CC-12BA5B	208369	Well	44.5817	-106.5634	155.60	4260	53N	81W	12	CDBD	Sheridan
CC-12DA1B	207105	Well	44.5771	-106.5495	36.00	4130	53N	81W	12	DAAA	Sheridan
CC-12DA2Q	207106	Well	44.5773	-106.5496	17.00	4130	53N	81W	12	DAAA	Sheridan
CC-12DA3Q	207107	Well	44.5773	-106.5496	18.00	4130	53N	81W	12	DAAA	Sheridan
CC-12DA4Q	207108	Well	44.5772	-106.5496	20.00	4130	53N	81W	12	DAAA	Sheridan
CC-LF	202186	Stream	44.5771	-106.5494		4125	53N	80W	7	CBBC	Sheridan

*Datum NAD27

Appendix A. Monitoring site information including location, aquifer formation, lithology, static water level, and date completed, continued.

Site Name	Aquifer Fm	Informal Unit	Lithology	Static Water Level	Static Water Level Date	Yield	Date Completed
BCLP_P							
BCUP_P							
BC-MF							7/10/03
BC-UF							7/8/03
BCLP_CBM	Ft Union		Coal (Big George)				
BC-15	Alluvium		Sand	6.80	12/13/02	0.0	12/13/02
BC-5	Wastach		Sandstone	17.00	12/13/02	1.0	12/13/02
BC-6	Alluvium		Sand	17.70	12/13/02	1.0	12/13/02
BC-7	Alluvium		Sand	17.20	12/13/02	1.0	12/13/02
BC-8	Alluvium		Sand	17.50	12/13/02	1.0	12/13/02
BC-MS							
BCUP_Q							
BCUP_CBM	Ft Union		Coal (Big George)				
BC-1	Alluvium		Siltstone	10.80	12/15/02	0.3	12/15/02
BC-2	Alluvium		Siltstone	11.10	12/14/02	1.0	12/14/02
BC-3	Alluvium		Siltstone	11.30	12/14/02	0.0	12/14/02
BC-4	Wasatch		Sandstone & siltstone	10.40	12/14/02	0.6	12/14/02
BC-LF							7/10/03
BC-NPF							7/9/03
BC-11	Wasatch		Coal & siltstone	13.30	12/14/02	1.2	12/14/02
BC-12	Alluvium		Sand	14.90	12/14/02	0.0	12/14/02
BC-13	Alluvium		Sand	13.74	1/8/03	0.0	12/14/02
BC-14	Alluvium		Sand	12.50	12/14/02	0.1	12/14/02
BCLP_Q							
BC-16	Alluvium		Sand	Dry	12/15/02	0.0	12/15/02
BC-9	Wasatch		Sandstone & siltstone	26.77	1/8/03	0.0	12/15/02
CC-1CC1B	Wasatch		Sandstone	4.66	10/9/02	3.0	10/9/02
CC-1CC2Q	Alluvium		Sand	3.76	11/7/02	2.0	11/7/02
CC-1CC3Q	Alluvium		Sand	3.96	11/5/02		11/5/02
CC-1CC4Q	Alluvium		Sand	3.95	11/5/02		11/5/02
CC-UW							4/3/03
CC-UTW							9/10/03
CC-SP							
CC-SPCBM	Wasatch		Coal (Roland)				
CC-12AC3Q	Alluvium		Sand	5.85	11/7/02	1.5	11/7/02
CC-12AC4Q	Alluvium		Sand	6.97	11/6/02		11/6/02
CC-12AC5Q	Alluvium		Sand	6.39	11/6/02		11/6/02
CC-12ACCC							
CC-12AC1B	Wasatch	CC	Coal	40.96	10/10/02	0.3	10/10/02
CC-12AC2B	Wasatch	DC	Coal	30.51	10/10/02	1.0	10/10/02
CC-MSP	Alluvium		Gravel	1.22	6/4/04	2.0	6/4/04
CC-12BA4B	Wasatch	FS	Siltstone	Dry	6/10/03		6/10/03
CC-12BA11B	Wasatch	AS	Sandstone	112.34	6/12/03	1.2	6/12/03
CC-12BA12B	Wasatch	FS	Sandstone	61.28	6/12/03	0.1	6/12/03
CC-12BA2B	Wasatch	FS	Sandstone	33.36	6/9/03	0.8	6/9/03
CC-12BA3B	Wasatch	AS	Sandstone	96.37	6/10/03	1.0	6/10/03
CC-12BA9B	Wasatch	FS	Sandstone	44.52	6/11/03	0.6	6/11/03
CC-12BA10B	Wasatch	AS+BC	Sandstone & coal	102.48	6/12/03	1.0	6/12/03
CC-12BA1B	Wasatch	FS	Sandstone	37.62	6/10/03	0.3	6/10/03
CC-12BA6B	Wasatch	GS	Sandstone	16.29	6/11/03	1.0	6/11/03
CC-12BA7B	Wasatch	HS	Sandstone	16.91	6/11/03	0.5	6/11/03
CC-12BA8B	Wasatch	IS	Silty clay	5.67	6/11/03	0.3	6/11/03
CC-12BA5B	Wasatch	AS	Sandstone	119.96	6/20/03	0.4	6/20/03
CC-12DA1B	Wasatch		Sandstone	13.66	10/9/02	0.2	10/9/02
CC-12DA2Q	Alluvium		Sand	11.27	11/6/02	1.0	11/6/02
CC-12DA3Q	Alluvium		Sand	11.88	11/6/02		11/6/02
CC-12DA4Q	Alluvium		Sand	11.94	11/6/02		11/6/02
CC-LF							4/2/03

Appendix B. Water quality data from study sites.

Site Name	Gwic Id	Sample	Site Type	Agency	Sample Date	Water Temp	Lab pH	Lab Specific Conductance	Total Dissolved Solids (mg/L)
CC-12AC1B	207113	2004Q0013	Well	MBMG	7/2/03	13.9	7.89	1902	1252
CC-12AC2B	207114	2004Q0008	Well	MBMG	7/2/03	11.8	7.48	2310	1677
CC-12AC3Q	207115	2004Q0011	Well	MBMG	7/1/03	10.8	7.59	2770	2248
CC-12ACCC	209338	2004Q0010	Stream	MBMG	7/1/03	25.4	7.96	2350	1779
CC-12BA11B	208375	2004Q0005	Well	MBMG	6/27/03	12.6	7.92	1063	632
CC-12BA12B	208376	2004Q0004	Well	MBMG	6/27/03	13.8	7.37	2770	2072
CC-12BA1B	208365	2004Q0002	Well	MBMG	6/27/03	13.2	7.64	3150	2594
CC-12BA1B	208365	2004Q0540	Well	MBMG	6/3/04	17.8	7.75	3320	2538
CC-12BA2B	208366	2004Q0003	Well	MBMG	6/27/03	14.9	7.52	1936	1338
CC-12BA2B	208366	2004Q0536	Well	MBMG	6/3/04	19.4	7.81	3710	3298
CC-12BA3B	208367	2003Q1173	Well	MBMG	6/20/03	13.1	8.26	1059	647
CC-12BA5B	208369	2003Q1171	Well	MBMG	6/20/03	15.5	7.95	1181	765
CC-12BA6B	208370	2003Q1172	Well	MBMG	6/20/03	13.2	7.45	1865	1428
CC-12BA6B	208370	2004Q0317	Well	MBMG	12/4/03	8.8	7.34	1906	1362
CC-12BA6B	208370	2004Q0538	Well	MBMG	6/3/04	9.1	7.59	2150	1346
CC-12BA7B	208371	2003Q1174	Well	MBMG	6/20/03	13.2	7.95	1902	1436
CC-12BA7B	208371	2004Q0318	Well	MBMG	12/4/03	9.9	7.62	6350	6804
CC-12BA7B	208371	2004Q0539	Well	MBMG	6/3/04	8.6	7.89	10590	12421
CC-12BA8B	208372	2004Q0543	Well	MBMG	6/3/04	10.7	8.24	3000	1747
CC-12BA9B	208373	2004Q0001	Well	MBMG	6/27/03	12.2	7.36	2090	1680
CC-12BA9B	208373	2004Q0537	Well	MBMG	6/4/04	17.5	7.63	2190	1685
CC-12DA1B	207105	2004Q0014	Well	MBMG	7/2/03	11.3	7.37	4240	3822
CC-12DA2Q	207106	2004Q0012	Well	MBMG	7/2/03	9.5	7.48	2670	2320
CC-1CC1B	207109	2004Q0009	Well	MBMG	9/16/03		7.69	1603	1125
CC-1CC2Q	207110	2004Q0007	Well	MBMG	7/1/03	1.0	7.56	1818	1378
CC-COAL CREEK	202187	2003Q0909	Stream	MBMG	4/4/03	12.1	7.84	1560	1146
CC-COAL CREEK	202185	2003Q0907	Stream	MBMG	4/4/03	11.1	8.18	1555	1155
CC-COAL CREEK	202187	2004Q0006	Stream	MBMG	7/1/03	18.2	7.83	1152	790
CC-MSP	211060	2004Q0542	Spring	MBMG	6/4/04	9.8	7.81	2890	2384
CC-SP	209363	2004Q0316	CBM Well	MBMG	12/4/03	0.8	8.46	1590	990
CC-SP	209363	2004Q0541	CBM Well	MBMG	6/3/04	12.2	8.97	1482	947
CC-SPCBM	209364	2004Q0319	Well	MBMG	12/4/03	3.8	8.03	1647	995
BCLP_P	209043	2004Q0332	Pond	MBMG	12/18/03	2.2	8.54	1966	1225
BCUP_P	209050	2004Q0339	Pond	MBMG	12/19/03	6.1	8.56	2130	1203
BC-MF	209046	2004Q0343	Stream	MBMG	12/19/03	0.0	8.45	2700	1577
BC-UF	209051	2004Q0342	Stream	MBMG	12/19/03	0.0	8.35	2250	1428
BCLP_CBM	209042	2003Q0791	CBM Well	MBMG	1/9/03	19.9	7.79	2050	1267
BCLP_CBM	209042	2004Q0334	CBM Well	MBMG	12/18/03	21.1	7.75	1940	1288
BC-5	207123	2003Q0794	Well	MBMG	1/10/03	10.7	7.74	2780	2502
BC-5	207123	2004Q0335	Well	MBMG	12/17/03	9.4	7.67	1298	926
BC-6	207124	2003Q0812	Well	MBMG	1/20/03	11.2	7.64	1664	1345
BC-6	207124	2004Q0331	Well	MBMG	12/17/03	4.9	7.22	1312	960
BCUP_Q	209049	2003Q0793	Pond Discharge	MBMG	1/9/03	3.5	8.47	2040	1275
BCUP_Q	209049	2004Q0340	Pond Discharge	MBMG	12/17/03	2.7	8.65	2160	1266
BCUP_CBM	209047	2003Q0792	CBM Well	MBMG	1/10/03	19.5	7.91	2100	1390
BCUP_CBM	209047	2004Q0333	CBM Well	MBMG	12/17/03	20.3	7.56	2050	1284
BC-2	207130	2003Q0814	Well	MBMG	1/20/03	10.1	7.50	1127	768
BC-2	207130	2004Q0336	Well	MBMG	12/17/03	6.1	7.52	1216	830
BC-4	207132	2003Q0811	Well	MBMG	1/20/03	11.1	7.39	1477	1110
BC-4	207132	2004Q0344	Well	MBMG	12/17/03	11.1	7.52	1631	1169
BC-LF	208571	2004Q0345	Stream	MBMG	12/19/03	0.0	8.06	2200	1391
BC-NPF	208572	2004Q0338	Stream	MBMG	12/18/03	1.8	8.05	1936	1246
BC-11	207118	2003Q0813	Well	MBMG	1/20/03	10.3	7.57	1976	1575
BC-11	207118	2004Q0337	Well	MBMG	12/18/03	9.5	7.35	1917	1529
BC-14	207121	2003Q0810	Well	MBMG	1/20/03		7.58	2610	2383
BC-14	207121	2004Q0341	Well	MBMG	12/18/03	9.5	8.19	4110	4202
BCLP_Q	209044	2003Q0795	Pond Discharge	MBMG	1/9/03	4.4	8.27	1857	1246
WR-17A	123796	1991Q1015	Well	MBMG	9/17/91	10.8	7.91	3993	2567
WR-17A	123796	2002Q0279	Well	MBMG	10/3/01	12.7	7.7	4430	3553

Appendix B. Water quality data from study sites, continued.

Site Name	Calcium (mg/l)	Magnesium (mg/l)	Sodium (mg/l)	Potassium (mg/l)	Iron (mg/l)	Manganese (mg/l)	Silica (mg/l)	Bicarbonates (mg/l)	Carbonate (mg/l)	Sulfate (mg/l)
CC-12AC1B	22.2	13.5	389.0	3.3	0.012	0.147	6.78	623.5	0.0	503.0
CC-12AC2B	202.0	118.0	224.0	4.0	0.037	0.073	9.62	598.5	0.0	814.0
CC-12AC3Q	189.0	196.0	266.0	9.5	0.095	<0.005	12.00	612.4	0.0	1261.0
CC-12ACCC	151.0	170.0	221.0	8.4	0.037	0.007	14.60	751.5	0.0	839.0
CC-12BA11B	6.9	4.0	260.0	2.2	0.011	0.012	6.57	685.2	0.0	9.8
CC-12BA12B	163.0	88.3	469.0	8.0	0.092	0.417	12.40	961.4	0.0	843.0
CC-12BA1B	238.0	154.0	410.0	9.6	0.084	0.448	11.00	673.4	0.0	1425.0
CC-12BA1B	220.0	157.0	381.0	9.4	0.127	0.544	10.20	780.8	0.0	1363.0
CC-12BA2B	104.0	58.0	275.0	5.9	0.183	0.565	12.80	635.6	0.0	558.0
CC-12BA2B	259.0	258.0	390.0	9.6	2.010	0.119	26.90	496.5	0.0	2080.0
CC-12BA3B	6.9	3.6	267.0	2.2	0.013	0.010	6.82	674.7	0.0	22.6
CC-12BA5B	11.2	5.8	282.0	2.5	0.040	0.022	7.31	734.9	0.0	90.5
CC-12BA6B	136.0	84.2	230.0	7.6	1.480	0.116	10.10	734.4	0.0	594.5
CC-12BA6B	130.0	80.8	221.0	7.4	0.021	0.057	10.10	613.7	0.0	605.0
CC-12BA6B	122.0	80.6	242.0	7.1	1.430	0.107	10.10	698.7	0.0	536.0
CC-12BA7B	155.0	102.0	203.0	7.0	0.045	0.127	11.20	664.9	0.0	626.8
CC-12BA7B	444.0	520.0	898.0	9.5	0.273	0.069	12.00	634.4	0.0	4575.0
CC-12BA7B	361.0	849.0	2236.0	8.4	0.091	0.059	8.25	642.9	0.0	8604.0
CC-12BA8B	72.0	71.2	605.0	4.0	0.028	0.042	6.05	808.9	0.0	582.0
CC-12BA9B	198.0	133.0	184.0	6.9	0.040	0.242	10.70	778.4	0.0	752.0
CC-12BA9B	192.0	128.0	181.0	7.0	0.931	0.411	12.30	682.4	0.0	824.0
CC-12DA1B	276.0	211.0	665.0	11.6	0.807	1.050	9.17	772.3	0.0	2251.0
CC-12DA2Q	215.0	184.0	261.0	8.2	0.062	0.111	14.20	697.5	0.0	1281.0
CC-1CC1B	94.1	67.2	203.0	5.6	0.748	0.217	8.32	567.3	0.0	464.0
CC-1CC2Q	123.0	129.0	159.0	5.9	0.022	0.051	17.70	586.8	0.0	644.0
CC-COAL CREEK	130.0	105.0	89.4	12.3	0.831	0.303	8.39	542.9	0.0	530.5
CC-COAL CREEK	99.4	99.7	113.0	10.2	0.106	0.042	8.07	416.6	0.0	609.9
CC-COAL CREEK	93.8	74.0	73.9	8.6	0.048	0.048	11.60	475.8	0.0	293.0
CC-MSP	212.0	215.0	247.0	4.7	0.296	0.202	20.30	671.0	0.0	1352.0
CC-SP	11.4	5.8	382.0	3.2	0.503	0.041	9.20	1121.2	12.0	<2.5
CC-SP	7.4	7.4	391.0	3.0	0.114	0.003	8.05	899.4	48.5	22.0
CC-SPCBM	11.7	5.7	393.0	3.3	1.600	0.046	9.76	1128.9	0.0	<2.5
BCLP_P	25.5	22.2	471.0	8.4	0.055	0.005	3.40	1282.2	50.4	5.1
BCUP_P	22.5	21.9	473.0	8.3	0.022	0.002	7.66	1244.4	39.6	7.8
BC-MF	39.0	35.9	567.0	11.0	0.057	0.022	10.00	1523.8	34.8	114.0
BC-UF	43.2	31.1	475.0	8.3	0.064	0.049	7.99	1489.6	14.4	106.0
BCLP_CBM	46.1	19.4	464.0	8.1	8.300	0.109	9.44	1427.4	0.0	<2.5
BCLP_CBM	43.0	22.2	459.0	8.3	0.667	0.020	9.80	1497.0	0.0	<2.5
BC-5	385.0	106.0	195.0	5.4	3.270	0.543	9.01	388.0	0.0	1602.4
BC-5	146.0	42.0	93.0	3.6	1.100	0.163	9.70	491.1	0.0	379.0
BC-6	207.0	60.0	107.0	2.9	0.043	0.032	9.91	300.1	0.0	806.8
BC-6	212.0	49.2	49.8	3.0	0.049	0.004	11.90	620.2	0.0	320.0
BCUP_Q	24.0	21.0	481.0	8.5	0.018	0.014	8.79	1384.7	36.0	5.4
BCUP_Q	22.4	22.3	463.0	8.1	0.022	0.003	7.42	1403.0	36.0	7.7
BCUP_CBM	46.7	21.2	532.0	8.3	3.890	0.091	9.12	1540.5	0.0	<2.5
BCUP_CBM	46.0	20.5	436.0	8.1	0.635	0.044	9.50	1531.9	0.0	<2.5
BC-2	124.0	45.5	59.4	1.3	0.034	0.215	7.99	418.7	0.0	321.1
BC-2	134.0	50.6	63.1	1.6	0.703	0.201	10.00	393.5	0.0	374.0
BC-4	162.0	46.4	112.0	4.2	2.530	0.370	11.70	387.9	0.0	576.8
BC-4	173.0	48.5	115.0	4.1	2.650	0.445	11.90	434.3	0.0	597.0
BC-LF	79.0	39.3	426.0	7.1	0.050	0.018	2.99	1313.9	0.0	181.0
BC-NPF	64.4	30.6	394.0	6.6	0.175	0.105	4.21	1357.9	0.0	69.7
BC-11	224.0	72.1	152.0	3.7	2.330	0.351	9.84	400.2	0.0	906.9
BC-11	228.0	78.8	148.0	3.3	2.230	0.283	9.86	381.9	0.0	868.0
BC-14	364.0	142.0	127.0	1.4	0.051	0.116	9.23	445.8	0.0	1514.9
BC-14	490.0	307.0	328.0	1.5	0.098	<0.010	7.77	416.0	0.0	2848.0
BCLP_Q	25.8	18.1	461.0	8.2	0.175	0.009	9.03	1454.2	0.0	<2.5
WR-17A	20.2	12.1	978.0	7.9	0.126	0.051	8.50	2240.0	0.0	419.0
WR-17A	50.7	154.0	898.0	13.3	0.845	0.085	9.68	950.4	0.0	1890.0

Appendix B. Water quality data from study sites, continued.

Site Name	Chloride (mg/l)	Nitrate (mg/l)	Flroride (mg/l)	Ortho-phosphate (mg/l)	Silver (ug/l)	Alumi-num (ug/l)	Arsenic (ug/l)	Boron (ug/l)	Barium (ug/l)	Berylli-um (ug/l)	Bromide (ug/l)
CC-12AC1B	5.2	<0.5	2.0		<5	<30	<5	80.4	26.8	<2	<500
CC-12AC2B	5.5	<0.5	2.2		<5	<30	<5	124.0	93.9	<2	<500
CC-12AC3Q	7.4	<0.5	2.6		<5	<150	<5	288.0	25.8	<10	<500
CC-12ACCC	<5.0	<0.5	2.5		<5	<30	<5	333.0	3.8	<2	<500
CC-12BA11B	5.5	<0.5	<0.05	<0.05	<1	<30	<1	68.6	77.2	<2	<50
CC-12BA12B	10.0	<0.5	2.7		<5	<150	<5	<150	110.0	<10	<500
CC-12BA1B	10.7	<0.5	<0.05	<2.50	<5	<150	<5	163.0	119.0	<10	<50
CC-12BA1B	7.5	<2.5	<0.5	<0.50	<5	<150	<5	188.0	41.7	<10	<500
CC-12BA2B	8.0	<0.5	1.6		<5	65.5	<5	173.0	173.0	<2	<500
CC-12BA2B	11.3	8.8	<0.5	<0.50	<10	2629.0	<10	<300	128.0	<20	<500
CC-12BA3B	5.1	<0.5	0.7	0.12	<5	<30	<5	71.1	110.0	<2	<50
CC-12BA5B	3.1	<0.5	0.5	0.08	<5	<30	<5	76.8	79.5	<2	<50
CC-12BA6B	<5.0	<0.5	<0.5	<0.50	<5	33.4	<5	213.0	25.3	<2	<500
CC-12BA6B	<5.0	0.7	<0.5	<0.50	<5	<300	<5	235.0	16.1	<2	<500
CC-12BA6B	<5.0	<0.5	<0.5	<0.50	<1	<30	<1	218.0	33.9	<2	<500
CC-12BA7B	<5.0	0.5	<0.5	<0.50	<5	<30	<5	225.0	124.0	<2	<500
CC-12BA7B	16.5	7.4	<1.0	<1.00	<10	<300	<10	321.0	38.5	<20	<1000
CC-12BA7B	26.7	1.2	<2.5	<2.50	<10	327.0	<10	461.0	44.6	<20	<2500
CC-12BA8B	7.1	<0.5	<0.5	<0.50	<5	<150	<5	241.0	186.0	<10	<500
CC-12BA9B	5.7	<0.5	2.1		<5	<30	<5	294.0	124.0	<2	<500
CC-12BA9B	<10.0	<0.5	<1.0	<1.00	<5	62.5	<5	307.0	50.9	<10	<1000
CC-12DA1B	7.8	<0.5	3.8		<10	<300	<10	<300	21.8	<20	<500
CC-12DA2Q	8.4	<0. 5	2.6		<5	<30	<5	237.0	34.0	<2	<500
CC-1CC1B	<5.0	<0.5	1.6		<5	<30	<5	137.0	29.6	<2	<500
CC-1CC2Q	5.6	1.0	1.8		<5	<30	<5	268.0	23.1	<2	<500
CC-COAL CREEK	<5.0	1.2	<0.5	<0.50	<5	<150	<5	<150	93.8	<2	<500
CC-COAL CREEK	6.5	1.9	<0.5	<0.50	<5	<150	5.9	<150	40.5	<2	<500
CC-COAL CREEK	<5.0	<0.5	<0.5		<1	<30	1.4	175.0	38.8	<2	<500
CC-MSP	<10.0	<1.0	<1.0	<1.00	<5	<150	<5	444.0	48.9	<10	<1000
CC-SP	14.0	<0.5	0.1	<0.05	<5	<30	<5	<5	201.0	<2	131
CC-SP	16.4	<0.5	<0.05	<0.05	<1	140.0	1.4	132.0	61.6	<2	155
CC-SPCBM	13.9	<0.5	0.1	0.06	<1	47.2	2.0	122.0	256.0	<2	104
BCLP_P	6.6	<0.5	0.2	<0.05	<5	<30	<5	90.3	607.0	<10	57
BCUP_P	7.2	1.5	0.2	<0.05	<5	<30	<5	95.8	458.0	<2	<50
BC-MF	10.6	4.0	<0.5	<0.5	<5	<30	<5	<150	381.0	<2	<500
BC-UF	7.6	<0.5	0.2	<0.05	<5	<30	<5	92.5	356.0	<2	62
BCLP_CBM	6.2	1.1	<0.05	<0.05	<5	<30	<5	<150	1140.0	<2	<50
BCLP_CBM	5.8	<0.5	0.2	<0.05	<5	<30	<5	97.2	1066.0	<2	75
BC-5	<30.0	1.6	<3.0	<3.0	<5	<150	<5	<150	27.9	<2	<1000
BC-5	8.8	<0.5	<0.05	<0.05	<5	43	<5	<150	27.4	<2	<50
BC-6	<10.0	2.2	<1.0	<1.0	<5	<30	<5	<150	45.2	<2	<1000
BC-6	6.4	0.9	<0.5	<0.5	<5	<30	<5	<150	42.9	<10	<500
BCUP_Q	6.5	1.2	0.4	<0.05	<5	<30	<5	<150	465.0	<2	60
BCUP_Q	6.9	<0.5	0.2	<0.05	<5	<30	<5	92.1	449.0	<2	62
BCUP_CBM	6.0	2.9	<0.05	<0.05	<5	<30	<5	<150	1050.0	<2	<50
BCUP_CBM	5.8	0.7	0.2	<0.05	<5	<30	<5	89.2	1076.0	<2	<50
BC-2	<5.0	0.5	<0.5	<0.5	<5	<30	<5	<150	19.0	<2	<500
BC-2	<5.0	<0.5	<0.5	<0.5	<5	398	<5	<150	25.5	<2	<500
BC-4	<10.0	1.0	<1.0	<1.0	<5	<30	<5	<150	16.2	<2	<1000
BC-4	<5.0	<0.5	<0.5	<0.5	<5	<30	<5	<30	13.4	<2	<500
BC-LF	7.4	<0.5	0.1	<0.05	<5	<30	<5	89.0	396.0	<2	77
BC-NPF	7.0	<0.5	0.1	<0.05	<5	<30	<5	<150	416.0	<2	83
BC-11	<10.0	4.6	<1.0	<1.0	<5	<30	<5	<150	11.5	<2	<1000
BC-11	<5.0	<0.5	<0.5	<0.5	<5	<30	<5	<30	10.7	<2	<500
BC-14	<25.0	<1.0	<2.5	<2.5	<5	<30	<5	<150	28.6	<2	<2500
BC-14	5.2	<0.5	<0.5	<0.5	<10	<300	<10	<300	<20	<20	<500
BCLP_Q	6.2	0.7	0.3	<0.05	<5	<30	<5	<150	441.0	<2	<50
WR-17A	15.9	1.1	0.4	<0.2	<6	<100		<100	45.0		<100
WR-17A	30.5	32.5	<2.5	<2.5	<10	<300	<10	<300	25.4	<20	<2500

Appendix B. Water quality data from study sites, continued.

Site Name	Cadmium (ug/l)	Cobalt (ug/l)	Chromium (ug/l)	Copper (ug/l)	Lithium (ug/l)	Molybdenum (ug/l)	Nickel (ug/l)	Lead (ug/l)	Antimony (ug/l)	Selenium (ug/l)	Strontium (ug/l)	Titanium (ug/l)
CC-12AC1B	<1	<2	<10	<5	45.5	<10	<2	<10	<10	<10		501.0
CC-12AC2B	<1	<2	<10	<5	77.2	<10	<2	<10	<10	<5	2649	<1
CC-12AC3Q	<5	<10	<10	<10	98.3	<50	<10	<10	<10	<5	2533	<5
CC-12ACCC	<1	<2	<10	<5	93.9	<10	3.1	<10	<10	<5	2273	<1
CC-12BA11B	<1	<2	<2	<2	26.6	<10	<2	<2	<2	<1	166	1.0
CC-12BA12B	<5	<10	<10	<10	117.0	<50	<10	<10	<10	<5	2290	<5
CC-12BA1B	<5	<10	<10	<10	130.0	<50	10.6	<10	<10	<5	3532	<5
CC-12BA1B	<5	<10	<10	<10	128.0	<50	17.2	<10	<10	<5	4344	<5
CC-12BA2B	<1	<2	<10	<5	88.4	<10	5.8	<10	<10	<5	1319	4.2
CC-12BA2B	<10	<20	<20	<20	148.0	<100	30.1	<20	<20	28.5	5020	57.8
CC-12BA3B	<1	<2	<10	<5	25.4	<50	<2	<10	<10	<5	159	<1
CC-12BA5B	<1	<2	<10	<5	28.8	<10	3.8	<10	<10	<5	216	<1
CC-12BA6B	<1	<2	<10	<5	102.0	<10	<2	<10	<10	<5	2800	<1
CC-12BA6B	<1	<2	<10	<10	101.0	<10	<2	<10	<10	<5	4970	<1
CC-12BA6B	<1	<2	3.3	5.0	94.5	<10	5.3	<2	<2	<1	2425	<1
CC-12BA7B	<5	<2	<10	<5	97.3	<50	<2	<10	<10	<5	2675	<1
CC-12BA7B	<10	<20	<20	<20	161.0	<100	<20	<20	<20	198.0	8707	<10
CC-12BA7B	<10	<20	<20	<20	178.0	<100	20.2	<20	<20	224.0	9097	<10
CC-12BA8B	<5	<10	<10	<10	53.5	<50	<10	<10	<10	8.8	1167	<5
CC-12BA9B	<1	<10	<10	<5	109.0	<10	12.8	<10	<10	<5	3189	<1
CC-12BA9B	<1	<10	<10	<10	107.0	<50	12.4	<10	<10	<5	3117	6.4
CC-12DA1B	<10	<20	<20	<20	154.0	<100	<20	<20	<20	<10	5248	<10
CC-12DA2Q	<1	<10	<10	<10	83.2	<50	<10	<10	<10	<5	2221	<1
CC-1CC1B	<1	<2	<10	<5	72.4	<10	<2	<10	<10	<5	1308	<1
CC-1CC2Q	<1	<2	<10	<5	81.0	<10	<2	<10	<10	11.9	1844	<1
CC-COAL CREEK	<2	<10	<10	<10	57.6	<50	<10	<10	<10	<5	1340	1.1
CC-COAL CREEK	<2	<10	<10	<10	56.1	<50	13.6	<10	<10	6.4	1370	<1
CC-COAL CREEK	<1	<2	<2	<2	51.1	<10	3.5	<2	<2	<1	997	<1
CC-MSP	<5	<10	<10	<10	84.7	<50	13.7	<10	<10	<5	2416	<5
CC-SP	<1	<2	<10	<5	42.9	<10	<2	<10	<10	<5	325	<1
CC-SP	<1	<2	3.2	4.0	37.2	<10	<2	<2	<2	2.3	182	3.6
CC-SPCBM	<1	<2	3.9	10.1	43.1	<10	<2	<2	<2	6.3	343	<1
BCLP_P	<1	<2	<10	<5	53.7	<10	<2	<10	<10	<5	1136	<1
BCUP_P	<1	<2	<10	<5	56.8	<10	<2	<10	<10	<5	1058	<1
BC-MF	<1	<2	<10	<5	71.4	<10	<2	<10	<10	<5	1294	<1
BC-UF	<1	<2	<10	<5	59.9	<10	<2	<10	<10	<5	1250	<1
BCLP_CBM	<1	<2	<10	<10	59.8	<10	<10	<10	<10	<5	1470	<1
BCLP_CBM	<1	<2	<10	<5	56.3	<10	<2	<10	<10	<5	1593	<1
BC-5	<1	<2	<10	<10	32.0	<10	<10	<10	<10	<5	3270	<1
BC-5	<1	<2	<10	<5	17.2	<10	<2	<10	<10	<5	1335	4.1
BC-6	<1	<2	<10	<10	11.4	<10	<10	<10	<10	<5	1730	1.6
BC-6	<1	<2	<10	<5	14.0	<10	4.1	<10	<10	7.4	982	<1
BCUP_Q	<1	<2	<10	<10	55.3	<10	<10	<10	<10	<5	1100	<1
BCUP_Q	<1	<2	<10	<5	55.5	<10	<2	<10	<10	<5	1057	<1
BCUP_CBM	<1	<2	<10	<10	55.1	<10	<10	<10	<10	<5	1520	<1
BCUP_CBM	<1	<2	<10	<5	52.8	<10	<2	<10	<10	<5	1465	<1
BC-2	<1	<2	<10	<10	37.3	<10	<10	<10	<10	<5	1670	1.8
BC-2	<1	<2	<10	<5	39.3	<10	3.0	<10	<10	<5	1759	11.0
BC-4	<1	<2	<10	<10	43.4	<10	<10	<10	<10	<5	2140	1.6
BC-4	<1	<2	<10	<5	43.6	<10	<2	<10	<10	<5	2280	<1
BC-LF	<1	<2	<10	<5	52.2	<10	2.1	<10	<10	<5	1524	<1
BC-NPF	<1	<2	<10	<5	47.3	<10	<2	<10	<10	<5	1267	<1
BC-11	<1	<2	<10	<10	31.9	<10	<10	<10	<10	<5	2360	1.5
BC-11	<1	<2	<10	<5	31.0	<10	<2	<10	<10	<5	2410	<1
BC-14	<1	<2	<10	<10	42.1	<10	11.3	<10	<10	<5	4760	1.4
BC-14	<10	<20	<20	<20	51.4	<100	<20	<20	<20	<10	9413	<10
BCLP_Q	<1	<2	<10	<10	50.4	<10	<10	<10	<10	<5	999	<1
WR-17A	<6		10	<6	348.0	<40	<20				2150	<8
WR-17A	<20	<20	<20	<20	322.0	<100	<20	<20	<20	41.6	5500	<10

Appendix B. Water quality data from study sites, continued.

Site Name	Thallium (ug/l)	Uranium (ug/l)	Vanadium (ug/l)	Zinc (ug/l)	Zirconium (ug/l)
CC-12AC1B	<1	<3	<10	2.8	<2
CC-12AC2B	<25	<2.5	<10	3.9	<2
CC-12AC3Q	<25	19.8	<25	<10	<10
CC-12ACCC	<25	4.9	<10	<2	<2
CC-12BA11B	<5	<0.5	<5	<2	<2
CC-12BA12B	<25	8.3	<25	34.7	<10
CC-12BA1B	<25	16.3	<25	19.0	<10
CC-12BA1B	<25	5.0	<25	11.2	<10
CC-12BA2B	<25	10.2	<10	7.6	<2
CC-12BA2B	<50	58.1	<50	21.3	<20
CC-12BA3B	<25	<3	<10	<2	<2
CC-12BA5B	<25	<3	<10	11.3	<2
CC-12BA6B	<25	<3	<10	11.7	<2
CC-12BA6B	<25	<3	<10	<2	4.1
CC-12BA6B	<5	15.6	<5	6.0	<2
CC-12BA7B	<25	2.5	<10	27.1	<2
CC-12BA7B	<50	32.9	<50	<20	<20
CC-12BA7B	<50	75.6	<50	<20	<20
CC-12BA8B	<25	46.0	<25	<10	<10
CC-12BA9B	<25	2.9	<10	428.0	<2
CC-12BA9B	<25	21.8	<25	<10	<2
CC-12DA1B	<50	<5	<50	<20	<20
CC-12DA2Q	<25	14.7	<25	<10	<2
CC-1CC1B	<25	<2.5	<10	4.0	<2
CC-1CC2Q	<25	10.1	<10	2.1	<2
CC-COAL CREEK	<25	13.9	<25	<10	<2
CC-COAL CREEK	<25	16.0	<25	<10	<2
CC-COAL CREEK	<5	5.7	<5	<2	<2
CC-MSP	<25	26.8	<25	<10	<10
CC-SP	<25	<3	<10	2.9	<2
CC-SP	<5	3.4	<5	<2	<2
CC-SPCBM	<5	<1	<5	<2	<2
BCLP_P	<25	<3	<10	<2	2.2
BCUP_P	<25	<3	<10	<2	<2
BC-MF	<25	<3	<10	2.6	2.2
BC-UF	<25	<3	<10	<2	2.0
BCLP_CBM	<25	<2.5	<25	<10	<10
BCLP_CBM	<25	<3	<10	5.7	<2
BC-5	<25	5.0	<25	<10	<10
BC-5	<25	10.8	<10	2.3	<2
BC-6	<25	30.9	<25	<10	<10
BC-6	<25	30.4	<10	177.0	<2
BCUP_Q	<25	<2.5	<25	<10	<10
BCUP_Q	<25	<3	<10	<2	2.6
BCUP_CBM	<25	<2.5	<25	38.3	<10
BCUP_CBM	<25	<3	<10	<2	<2
BC-2	<25	23.9	<25	<10	<10
BC-2	<25	25.9	<10	8.9	<2
BC-4	<25	<2.5	<25	<10	<10
BC-4	<25	<3	<10	6.5	<
BC-LF	<25	6.6	<10	<2	2.6
BC-NPF	<25	5.7	<10	<2	<2
BC-11	<25	2.9	<25	<10	<10
BC-11	<25	3.8	<10	<2	<2
BC-14	<25	65.5	<25	<10	<10
BC-14	<50	178.0	<50	<20	<20
BCLP_Q	<25	<2.5	<25	<10	<10
WR-17A			<8	16.0	<8
WR-17A	<50	10.8	<50	<20	<20

Appendix C. Saturated paste extract data from Coal Creek site in Wyoming and from Squirrel Creek site in Montana.

Sample site:	GWIC No.	Date	Latitude	Longitude	Township	Range	Section	Tract	State	Formation
CC-12ba6B	208370	6/11/03	44.5817	-106.5625	53N	81W	12	CCDD	Wyoming	Wasatch

Appendix C. Saturated paste extract data from Coal Creek site in Wyoming and from Squirrel Creek site in Montana, continued.

Sample site:	Depth top	Depth bottom	Sand	Silt	Clay	Texture	pH	conductance	SAR	Calcium
12ba6B	0.0	5.0	11	43	46	Silt clay	8.3	8.80	13.7	25.00
12ba6B	5.0	10.0	9	43	48	Silt clay	8.3	7.52	12.1	22.80
12ba6B	10.0	16.0	11	55	34	Silty-clay loam	8.0	5.60	10.7	14.00
12ba6B	16.0	20.0	45	37	18	Loam	7.8	1.81	4.9	5.26
12ba6B	20.0	22.0	12	66	22	Silt loam	7.8	3.00	3.8	12.40
12ba6B	22.0	25.0	9	70	21	Silt loam	7.8	1.54	2.1	6.01
12ba6B	25.0	26.0	<1	70	30	Silty-clay loam	7.8	1.27	2.0	4.10
12ba6B	26.0	30.0	4	71	25	Silt loam	7.0	3.31	1.6	22.70
12ba6B	30.0	33.0	11	59	30	Silty-clay loam	6.9	4.03	2.9	27.80
12ba6B	33.0	36.0	2	44	54	Silty clay	7.2	3.80	3.3	22.80
CX 50	0.0	5.0					7.4	5.80	3.9	29.10
CX 50	5.0	10.0					7.7	4.40	6.0	22.80
CX 50	18.0	20.0					7.7	5.10	6.3	22.20
CX 50	30.0	38.5					8.0	7.60	14.2	20.50
CX 50	40.0	46.0					8.7	2.10	27.3	0.80
CX 50	50.0	57.2					9.0	1.10	19.3	0.55
CX 50	60.0	70.0					9.0	0.90	25.5	0.28
CX 50	70.0	80.0					9.0	0.70	21.8	0.15
CX 50	80.0	90.0					9.1	0.50	16.7	0.12
CX 50	90.0	100.0					8.9	0.60	25.1	0.19
CX 50	100.0	105.9					8.9	1.00	31.4	0.29
CX 50	106.7	110.0					9.3	0.50	21.7	0.10
CX 50	110.0	117.0					9.2	0.50	16.9	0.12
CX 50	117.0	120.5					8.9	0.50	22.2	0.13
CX 50	120.5	127.0					9.1	0.60	33.5	0.10
CX 50	127.0	135.8					9.3	0.40	21.3	0.13
CX 50	135.8	140.0					9.2	0.60	24.9	0.11
CX 50	140.0	146.0					9.0	0.60	28.8	0.13
CX 50	146.0	154.3					9.1	0.70	36.4	0.06
CX 50	154.3	164.0					9.2	0.70	25.3	0.10
CX 50	164.0	169.9					9.3	0.70	21.6	0.12
CX 50	169.9	179.4					9.2	0.40	10.2	0.26
CX 50	179.4	185.0					9.1	0.40	20.6	0.10
CX 50	185.0	190.0					9.1	0.50	23.6	0.14
CX 50	199.9	205.4					8.7	0.60	28.9	0.21
CX 50	205.4	207.1					9.0	0.60	18.2	0.29
CX 50	207.1	213.5					8.6	0.70	27.9	0.35
CX 50	213.5	217.8					8.7	0.60	26.8	0.17
CX 50	217.8	224.6					8.6	0.70	30.1	0.16
CX 50	224.6	227.6					8.4	0.90	36.7	0.36
CX 50	227.6	234.7					8.5	1.00	40.4	0.23
CX 50	234.7	238.3					8.5	0.80	40.4	0.19
CX 50	238.3	243.7					8.4	1.30	40.6	0.61
CX 50	243.7	251.5					8.6	0.90	30.8	0.19
CX 50	251.5	259.5					8.6	0.80	35.1	0.20
CX 50	259.5	267.5					8.2	1.80	38.0	0.38
CX 50	267.5	269.5					8.1	2.20	36.3	0.46
CX 50	269.5	279.5					8.0	1.50	34.8	1.28
CX 50	279.5	284.6					7.8	3.30	26.0	1.70
CX 50	284.6	291.3					7.0	4.90	21.7	4.70
CX 50	348.1	353.0					7.2	2.60	26.9	1.31
CX 50	374.1	380.6					8.1	1.70	24.9	0.68
CX 50	380.6	386.2					7.9	2.10	16.6	1.71
CX 50	387.9	396.0					6.5	6.40	10.9	26.50
CX 50	396.0	405.4					7.9	2.20	24.9	1.76
CX 50	405.4	409.6					8.6	1.80	28.4	0.73
CX 50	409.6	413.0					7.8	2.80	23.0	3.37
CX 50	414.0	424.0					8.3	2.10	29.6	0.59
CX 50	424.0	431.6					8.4	1.10	21.6	0.57
CX 50	431.6	436.8					7.1	2.60	15.1	8.12
CX 50	436.8	444.0					8.3	2.00	25.1	0.84
CX 50	444.5	454.5					9.0	1.40	22.1	0.36
CX 50	454.5	462.7					8.4	1.10	26.8	0.57
CX 50	462.7	467.2					8.2	1.50	23.1	0.46
CX 50	467.2	471.1					8.3	1.70	29.3	0.60
CX 50	471.1	473.1					7.8	1.50	23.7	0.63
CX 50	473.1	476.1					7.9	0.90	37.8	1.02
CX 50	476.1	478.5					7.1	1.40	36.1	0.88
CX 50	500.2	509.0					7.1	2.30	28.2	4.71

Appendix C. Saturated paste extract data from Coal Creek site in Wyoming and from Squirrel Creek site in Montana, continued.

Sample site:	Magnesium	Sodium	Lime	Sulfate			
12ba6B	77.90	98.00	6.7	8720			
12ba6B	54.70	75.20	8.4	8680			
12ba6B	26.80	48.20	5.9	2830			
12ba6B	4.85	11.00	6.1	358			
12ba6B	12.30	13.50	6.2	794			
12ba6B	6.58	5.19	6.4	426			
12ba6B	5.09	4.24	7.5	316			
12ba6B	22.30	7.46	6.0	1500			
12ba6B	25.70	14.80	6.5	1780			
12ba6B	20.80	15.50	5.5	2230			
CX 50	38.10	22.80					
CX 50	58.60	38.20					
CX 50	60.70	40.80					
CX 50	29.80	71.40					
CX 50	3.25	38.90					
CX 50	0.88	16.30					
CX 50	0.24	13.00					
CX 50	0.09	7.54					
CX 50	0.17	6.36					
CX 50	0.11	9.71					
CX 50	0.09	13.70					
CX 50	0.11	7.04					
CX 50	0.16	6.34					
CX 50	0.14	8.17					
CX 50	0.07	9.78					
CX 50	0.07	6.75					
CX 50	0.19	9.65					
CX 50	0.06	8.89					
CX 50	0.02	7.28					
CX 50	0.03	6.44					
CX 50	0.07	6.67					
CX 50	0.67	6.94					
CX 50	0.10	6.51					
CX 50	0.10	8.17					
CX 50	0.17	12.60					
CX 50	0.16	8.64					
CX 50	0.22	14.90					
CX 50	0.10	9.85					
CX 50	0.07	10.20					
CX 50	0.20	19.40					
CX 50	0.15	17.60					
CX 50	0.09	15.10					
CX 50	0.32	27.70					
CX 50	0.13	12.30					
CX 50	0.10	13.60					
CX 50	0.32	22.50					
CX 50	0.40	23.80					
CX 50	0.91	36.40					
CX 50	2.65	38.40					
CX 50	2.88	42.30					
CX 50	0.83	27.80					
CX 50	0.56	19.60					
CX 50	3.71	27.40					
CX 50	10.20	46.60					
CX 50	1.48	31.70					
CX 50	1.03	26.60					
CX 50	2.51	39.50					
CX 50	0.59	22.70					
CX 50	0.43	15.30					
CX 50	4.42	37.90					
CX 50	0.71	22.10					
CX 50	0.28	12.50					
CX 50	0.37	18.40					
CX 50	0.33	14.50					
CX 50	0.60	22.70					
CX 50	0.49	17.70					
CX 50	0.62	34.20					
CX 50	0.39	28.80					
CX 50	3.00	55.30					

CHAPTER 3

Assessment of the environmental impacts of coalbed natural gas development in the Powder River Basin – Use of coalbed natural gas-produced water for cropland irrigation

Principal Investigator: Terry H. Brown
Senior Scientist: Chris Johnston
Western Research Institute
Laramie, Wyoming

Table of contents

List of figures 72
List of tables 72
List of appendices 72
Abstract 73
Background 73
The chemistry of saline/sodic soils 74
Impact of sodicity/salinity on infiltration rate and hydraulic conductivity 75
The effect of exchangeable magnesium on the physical properties of soils 76
Model for sodic soil behavior 76
Project objectives 77
Methods 77
Laboratory research – column studies 78
Results and discussion 78
Laboratory column study 78
Baseline evaluations 81
Field site characterization and field plot design 82
Conclusions 83
References cited 84
Appendix A 86
Appendix B 90
Appendix C 92

List of figures

1. Dry aggregate wetting stages 76
2. Laboratory set-up for the column studies 78
3. Hydraulic conductivity values for the treated and untreated A-Horizon materials collected from the Leiter Ranch study site 78
4. Hydraulic conductivity values for A-Horizon mixed materials collected from sites 2 and 8 located near the Leiter Ranch study site 79
5. Hydraulic conductivity values of the Leiter Ranch soil material using CBNG produced water and Clear Creek water 79
6. Determination of field infiltration rates using a tension infiltrometer 82
7. The tension infiltrometer unit used for field determinations 82
8. Diagram showing the location of soil amendments at the Cooksley Irrigation study site 82
9. Diagram showing the locations of the CBNG water treatments at the Cooksley Irrigation study site 83
10. Surface water monitoring locations associated with the Cooksley Irrigation study site 83

List of tables

1. Hydraulic conductivity and the resulting chemistry of saturated paste extracts collected from the materials used in the column studies after the treatment application 80
2. Water analysis for baseline conditions 81

List of appendices

A. Chemical analysis of saturated paste extracts collected from the materials used in the column studies after the treatment application 87
B. Soil survey of coalbed methane product water application areas at the Cooksley Ranch and Leiter Ranch study sites 90
C. Baseline water quality data for Clear Creek, Piney Creek, and Fowler 11-18—the CBNG water that will be applied to the research plots at Cooksley Ranch research site 92

Abstract

Water quality issues are at the forefront with regard to the development of coalbed natural gas reserves in the Powder River Basin (PRB). The practice of discharging large volumes of water into drainage channels or using it to irrigate rangeland areas has the potential of causing serious problems with regard to salinity and sodicity of soils. The primary problems associated with salinity are related to the ability of plants to take up water to facilitate the biochemical processes of photosynthesis and plant growth. As the solution electrolyte concentrations of the soil increase, plants dependent on their level of salt tolerance will become less able to absorb the amounts of water needed. As a result, the plants are not able to function at high levels and the plant will grow at slow rates or die.

It is very important to make sure that water applied to soils meets the favorable combination of salinity and sodicity that will allow the plants to grow at good production levels and that will maintain the structure of the soils. Each soil will react differently to the chemistry of the water applied and the method of application. Therefore, a research effort that includes studies of the interactions of various parameters with the soil types found in the area should be conducted so that produced water from coalbed natural gas (CBNG) operations can be used in an environmentally safe manner.

The overall purpose of this research effort is to evaluate the chemistry of produced waters generated at various locations in the PRB with regard to salinity and sodicity and to determine how such waters will impact the physical and chemical nature of soils in the vicinity of active production.

Work accomplished during Year 1 of the project included the literature review, collection of materials for laboratory evaluations, characterization of soils present at the Cooksley Ranch study site and the coalbed natural gas produced water projected to be used for irrigation, installation of field plots using sulfur and gypsum amendments, purchase and installation of a side-roll irrigation system, and installation of the water treatment system that included gypsum injection and acid addition using a sulfur burner. Irrigation was initiated during the latter part of the irrigation season. During Year 2, the research effort was initiated with the application of soil amendments to the field plots followed by the initiation of CBNG produced water. The water treatment activities were also started. The availability of produced water became an issue early in the growing season as the expected quantity of water changed from 300 gpm to 40 gpm. As a result, irrigation activities were modified to include the plot areas only. The areas outside of the research plots were irrigated with Piney Creek water only. As a result, the water availability issue did not impact the integrity of the research effort. Soil samples were collected after the growing season and are currently being analyzed. Infiltration evaluations will be completed during the spring of 2005 prior to the application of amendments to the field site.

Background

Water quality issues are at the forefront with regard to the development of coalbed natural gas (CBNG) reserves in the Powder River Basin (PRB). Large quantities of water are being discharged as part of the process of releasing gas from the coal. The excess of produced water is causing concerns from several points of view. The drawdown of water in the coal aquifers is causing major concerns from landowners and others such as those worried about future generations and the availability of water. In addition, the dilemma of how to use the water in worthwhile, environmentally sound applications is currently under consideration. The practice of discharging large volumes of water into drainage channels or using it to irrigate rangeland areas has the potential of causing serious problems with regard to salinity and sodicity of soils. Some waters currently being disposed of in the PRB are of such quality that land application should not cause any significant problems. However, there is evidence that some of the CBNG-produced waters will cause problems with salinity and sodicity.

The primary problems associated with salinity are related to the ability of plants to take up water to facilitate the biochemical processes of photosynthesis and plant growth. As the solution electrolyte concentrations of the soil increase, plants dependent on their level of salt tolerance will become less able to absorb the amounts of water needed. As a result, the plants are not able to function at high levels and the plant will grow at slow rates or die.

The major impact of sodicity on the soils is associated with soil structure. Soil structure is important to maintain the flow of gases (oxygen) and solution (water plus nutrients) to the plant roots and can cause severe erosion of once-productive soils. Dependent on the characteristics of individual soils, as the level of sodium in the soil increases the physical structure will degrade. High levels of sodium can cause the structure of a soil to completely disperse.

An important aspect of the sodicity and salinity chemistry of soils is that the two are closely related. For example, a highly sodic [high sodium adsorption ratio (SAR)] soil can maintain its soil structure if the salinity level [electrical conductivity (EC)] of the soil is high. However, if the salinity level is low (the water is very clean), the highly

sodic soil will slake and disperse and the structure will be lost. If a soil is characterized by a low SAR, the application of clean water or water characterized by low EC can cause degradation of soil structure. If the electrolyte concentration of the water applied to the soil is high, the soils will maintain their structure.

The dilemma of this system is to make sure that water applied to soils meets the favorable combination of salinity and sodicity that will allow the plants to grow at good production levels and that will maintain the structure of the soils. Each soil will react differently to the chemistry of the water applied and the method of application. Therefore, the research effort that includes studies of the interactions of these various parameters with the soil types found in the area should be conducted so that produced water from CBNG operations can be discharged in an environmentally safe manner.

Several issues must be understood in order to successfully manage CBNG-produced water for land application, including the chemistry of saline/sodic soils and its impact on the infiltration rate and hydraulic conductivity, as well as the effect of exchangeable magnesium on the physical properties of soils. A recent model describes these issues. Following is a brief summary of these issues.

The chemistry of saline/sodic soils

Excessive levels of salts impact large areas of soils around the world. The primary impacts of salts on soil quality are associated with saline and sodic conditions. Saline soil conditions are associated with excess salts usually consisting of chlorides (Cl^{-1}) and sulfates (SO_4^{-2}) of sodium (Na^{+1}), calcium (Ca^{+2}), and magnesium (Mg^{+2}) (Sumner and others, 1998). Saline conditions often have a deleterious effect on plant growth because salts decrease the osmotic potential of soil water, making it difficult for plants to extract water. Sodic conditions are associated with elevated levels of Na on the exchange complex, often responsible for the development of the poor physical conditions in a soil. Thus the impacts of Na result in an inadequate balance between water and air regimes in the soil. This imbalance is caused by restricted water infiltration and transmission properties causing the soil to be too wet or dry for much of the time, resulting in poor root development and plant growth. In addition, sodic soils often are difficult to cultivate and have low load bearing properties. Poor structural stability promotes the sealing of soil pores and crust formation at the soil surface, resulting in soil erosion and pollution of surface water resources.

The definition of a sodic soil in simple terms is a soil that has been adversely impacted physically by the presence of Na adsorbed to the cation exchange sites. The presence of Na in a soil promotes the slaking of aggregates and the dispersion of clay particles. At the same time the impact of Na, as characterized by SAR or ESP, on the physical character of a soil is greatly dependent on the salinity of the soil. It is impossible to estimate the impact of low or high SAR values on the physical state of a soil or spoil material without evaluating the EC or electrolyte concentration of the system (Shanmuganathan and Oades, 1983). Any attempt to set critical ESP or SAR values for land management would be arbitrary unless total cation concentration or EC is taken into consideration simultaneously (Sumner and others, 1998). Research has shown that extremely high SAR values do not cause physical degradation of soil materials if the system also contains high levels of salts. This fact was first demonstrated by research done by Quirk and Schofield (1955). Their work demonstrated that soil materials with an ESP of 40 maintained a stable permeability with an electrolyte concentration of about 30 mmol/L (about EC = 2.1 dS/m). McNeal and Coleman (1966) pointed out that typical arid land soils (having clay mineralogy dominated by 2:1 layer silicates with only moderate amount of montmorillonite) can tolerate ESP values of 15 or greater before serious reductions in hydraulic conductivity occur, if the salt concentration of the percolating solution exceeds 3 mmol/L (0.2 dS/m). Gardner and others (1959) came to the same conclusion dealing with unsaturated soils. Sumner and others (1998) discussed the SAR/EC relationship very thoroughly in their publication. The discussion addresses the fact that the USDA Soil Salinity Laboratory did not address this topic in their recommendations set forth during the late 1950s for the management of sodic soils, even though they were well aware of it. In fact, the definition of sodic soils was published by USSL Staff (1954) without mention of electrolyte concentration in the definition. It was apparent at the time that people were well aware of the impact of salinity on the behavior of sodic conditions; however, apparently these scientists elected to downplay the relationships because of the apparent transient nature of salinity. Sumner and others (1998) noted that if the work of Quirk and Schofield (1955) had been adopted in the United States, a much clearer understanding of sodicity would have resulted. Instead of using electrolyte concentration as an important component of the definition of sodic soils, *Handbook 60*, which was published in 1954 and reprinted in 1969 without emphasizing the importance of salinity and its impact on sodicity, has been and continues to be used as an authority addressing salinity and sodicity issues.

The impact of sodicity on the physical properties of soils is dependent on the electrolyte concentration associated with the system. If salt is added to dispersed clay

in a suspension, the increased electrolyte concentration causes the clay particles to stick together, forming flocs that settle. The minimum electrolyte concentration required to cause flocculation is referred to as the threshold electrolyte concentration (TEC) or flocculation value (FV). This value is dependent on counter-ion valency and clay type. The TEC values for a sodium-montmorillonite were shown to be about 12 mol/m^3 NaCl or 0.86 dS/m and 0.25 mol/m^3 $CaCl_2$ or 0.02 dS/m for calcium montmorillonite (Van Olphen, 1977). Corresponding values for sodium and calcium illites were found to be 40 mol/m^3 to 50 mol/m^3 NaCl and 0.25 mol/m^3, respectively (Arora and Coleman, 1979). These data show that a sodium montmorillonite can be maintained in a flocculated condition if the salt levels of the same ion (Na) are about 1 dS/m. Sodium illites will tend to remain flocculated if salt levels with the same ion (Na) are about 3.6 dS/m. Sposito (1989) indicated through his discussion of the literature that a fully Na-saturated smectite suspension will flocculate if the electrolyte concentration is >8 mol/m^3 (0.6 dS/m) and a suspension of Na illite will do the same if the electrolyte concentration reaches about 50 mol/m^3 (3.6 dS/m). His conclusion is that soil salinity tends to counteract the effect of exchangeable sodium on soil structure. The presence of divalent ions such as Ca would lower the TEC to lower salt concentrations.

The data show that if salinity is maintained at or above the TEC value for a specific material, the physical condition of the material will be maintained in a flocculated state, no matter how high the SAR. The only caveat to this situation is that some materials that have high SAR and EC character can become dispersed at the surface if impacted with water containing low levels of electrolytes from irrigation or rainfall. In addition, mechanical forces resulting from raindrop impact, the flow of water at the surface, or the use of farm equipment could cause clay dispersion. If measures are taken to eliminate these potential impacts to the system, the high-SAR soil/spoil material will usually be maintained in good physical condition. One method of doing this is to treat the surface with an amendment such as gypsum. Another method of protecting the surface against the mechanical forces that can initiate slaking and dispersion is to cover such spoils with topdressing material. This fact was demonstrated during a recent visit to the La Plata Mine. A soil pit was dug at a reclaimed site that had about 10 inches of topdressing material over spoil material that exceeded the current SAR standards. The spoil material had SAR values from 11 to 75 in the top 4 feet with EC values ranging from 3.5 to 7.3 dS/m at various depths within the same depth zone. The roots exhibited no problems growing through this material. In fact, the rooting showed numerous branching and overall good health. The spoil materials to about 4 inches below the topdressing/spoil interface showed evidence of weathering with the development of a very porous structure. Migration of Na at or near the topdressing/spoil interface was not evident, probably because the water present in the profile was readily removed via transpiration. The elevated SAR values associated with the spoil did not have a detrimental impact on plant growth.

It is generally accepted that both high sodium adsorption rations and/or low electrolyte concentrations create soil structural problems; however, we still do not have reliable criteria and standards for predicting how these parameters quantitatively affect structural stability and hydraulic conductivity (K) of soils (Rhoades, 1972). The mechanisms that cause these problems have been postulated to be: 1) swelling of soils, 2) clay dispersion and subsequent plugging of conducting pores by dispersed clay, and 3) failure of soil aggregates. However, the literature demonstrates divergence of opinions relative to the importance of these mechanisms. McNeal and Coleman (1966) and Jayawardane (1979) determined that clay swelling was the dominant mechanism reducing K in sodic soils. Research by Rhoades and Ingvalson (1969), Frenkel and others (1978), Pupisky and Shainberg (1979), Shainberg and others (1981), and Yousaf and others (1987) showed that clay dispersion was the dominant mechanism responsible for the reduction in K. Other scientists such as Waldron and Constantin (1970) and Cass and Sumner (1982) concluded that the reduction in K was primarily related to aggregate slaking caused by internal swelling pressure or from shearing stresses.

As noted previously, the chemistry associated with sodic and saline conditions in soils is very complex. The complexities of sodicity and salinity with regard to the management of soil materials will be discussed in some detail in the following review of the literature. The objective of this work is to show that an understanding of the chemistry associated with sodic/saline conditions relative to water/soil interactions can lead to the successful use of CBNG-produced waters for improving vegetation production in various vegetation communities.

Impact of sodicity/salinity on infiltration rate and hydraulic conductivity

Hydraulic conductivity is less sensitive to sodic conditions as compared to the infiltration rate (IR). The primary factor responsible is the influence of mechanical energy resulting from the impact of raindrops at the surface. This mechanical energy promotes the disintegration of aggregates and the dispersion of clays, resulting in the formation of a structural crust. Crusts are formed as a result of

the physical disintegration of aggregates, while compaction is caused by the impact of the water droplets and chemical dispersion of clays near the surface. Smectitic soils are very sensitive to reduced IR, even at very low ESP levels (ESP<3). A very important factor in the degradation of IR is that rainfall contains very low levels of salts. Therefore, rainfall is responsible for leaching electrolytes from the surface, leaving the surface materials more susceptible to dispersion. K is much less susceptible to degradation, except at the surface, mainly because of the reduced impact of mechanical forces and the electrolyte levels that often occur (Shainberg and others, 1992). The mineral phase associated with arid land materials usually readily weathers, providing electrolytes to the system and enhancing its ability to maintain structure.

This discussion supports the fact that topdressing placed over sodic materials will alleviate the development of poor physical conditions in the sodic materials. The surface layer of material (topdressing) eliminates the mechanical energy input from raindrop impact and/or surface water flow and the low electrolyte water that would promote aggregate slaking and clay dispersion. Weathering of the surface layer and the underlying sodic materials would result in increased electrolyte levels in solution that would prevent dispersion; and the Ca^{+2} present in the solution would tend to self-remediate the sodic condition.

The effect of exchangeable magnesium on the physical properties of soils

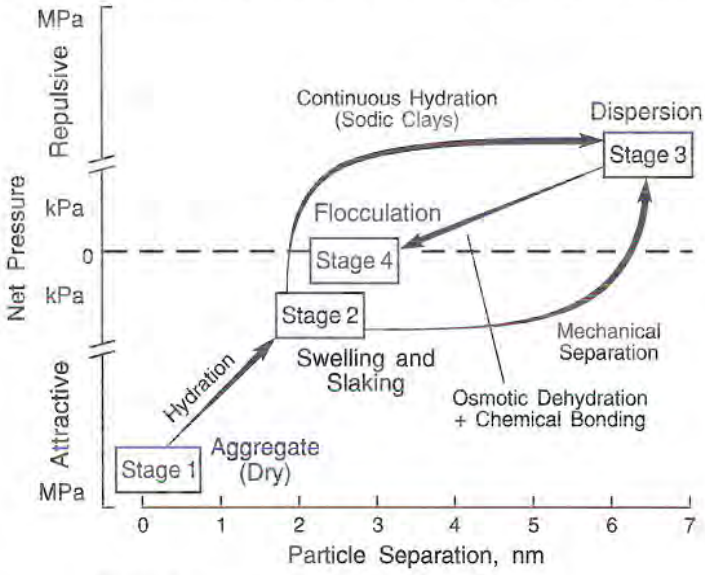
The USSL staff (1954) grouped Ca and Mg together as similar ions beneficial in developing and maintaining soil structure. However, evidence now exists that shows that Mg can cause the deterioration of soil structure under certain conditions. Studies have shown that Na-Mg soils developed lower K characteristics than Na-Ca soils under similar conditions. Research has demonstrated that Mg can impact K through direct effects (specific effects) and through the ability of Mg^{+2} to cause higher exchangeable Na^{+1} levels to develop in the soils as compared to Ca^{+2} (Chi and others, 1977; Emerson and Chi, 1977).

Alperovitch and others (1981) showed that well-weathered soils that do not contain $CaCO_3$ are impacted by the specific effect of Mg^{+2}. Reduction in K and enhanced clay dispersion resulted when Na-Mg soils were leached with distilled water (simulated rain water). The theory behind this finding was that clays saturated with Mg^{+2} are chemically more stable and do not release electrolytes into solution. As a result, the lack of weathering products will allow the system to disperse more easily when leached with water that contains low concentrations of electrolytes. In the same study, exchangeable Mg^{+2} was found not to have a specific effect on the K and clay dispersion in calcareous soils. In these soils, Mg^{+2} enhances the dissolution of $CaCO_3$, increasing the solution electrolyte concentrations and preventing the dispersion of clays and the reduction of K.

Model for sodic soil behavior

In the past, soil scientists have used a model involving the electrical diffuse double-layer theory to explain sodic soil behavior. This explanation was usually conducted using pure clay minerals in saturated systems. However, in natural systems, complex clay systems are bound together into aggregates with silt and sand particles by inorganic and organic compounds and are usually not suspended in water. The slaking of aggregates and the dispersion of clays requires forces other than those that operate in colloidal clay suspensions. Rengasamy and Sumner (1998) have developed a model that describes the processes that take place during the wetting of a dry soil aggregate (**Figure 1**). Their model will be presented herein as a realistic approach describing the influences of sodicity and salinity on the physical nature of natural soil systems.

The model consists of four stages. Dry soil aggregates are held together by inorganic and organic compounds and associated bonds that produce very strong attractive forces. The forces involved include Lifshitz-van der Waals, ionic bonds, hydrogen, hydrophobic, and hard-soft acid-base reactions. As dry aggregates are wetted, solvation or hydration forces become important. The stability of aggregates, and hence the pore systems, depends on attractive and repulsive forces resulting from intermolecular and electrostatic interactions between the soil solution and soil particles



Source: P. Rengasamy and M.E. Sumner, 1998

Figure 1. Stages that take place during the wetting of a dry aggregate.

(Rengasamy and Olsson, 1991). When an aggregate is placed in contact with water, the interactive forces lower the potential energy of water molecules, thus releasing energy for structural changes and as heat. Aggregate slaking, clay swelling, and clay dispersion are the major mechanisms that occur during these transformations.

Thus, as an aggregate is hydrated, the initial attractive forces between clay particles decrease. As hydration increases, the distance between particles increases. In general, if the clay particles are saturated with Ca or Mg, additional hydration does not increase the interparticle distance beyond a few nanometers, resulting in a net force that is attractive and the aggregates are held together by hydrated cations. The swelling resulting from these reactions will occur even with high electrolyte concentrations. Slade and Quirk (1991) found that the change in separation to 1.5 nm is not affected by electrolyte solution (crystalline swelling) and that the separation from 1.5 to 1.9 nm is an osmotic process that includes electrolyte concentrations, charge density, and the location of the charge in the clay minerals. If the clays are saturated by monovalent cations such as Na, the clay particles are separated beyond 7 nm dependent on the ionic strength and the existence of soft-hard acid-base reactions. This results in clay dispersion, shown as Stage 3 in **Figure 1**. Stage 3 can also be reached when a source of mechanical energy is applied to the clay domains that have undergone limited separation. Mechanical energy resulting from raindrop impact and surface water flow can overcome the attractive forces, causing the system to separate. Once the system is completely dispersed the electrostatic repulsive forces, as predicted by the electrical double-layer theory, become important to the physical nature of the system. A dispersed clay system will become flocculated as the difference in the electrical potentials in the inner and outer solutions approach zero and as the clay particles approach each other. The repulsive pressure is balanced by osmotic pressure, and the van der Waals attractive forces become dominate. At this point, the clays become flocculated, as identified as Stage 4 (**Figure 1**).

Since much of the research regarding sodic/saline conditions has been conducted using saturated aqueous systems, some concern exists for whether these studies apply to unsaturated conditions. Since low water content results in low repulsion forces, unsaturated systems would be expected to have higher attractive forces as compared to saturated systems. Rengasamy and Sumner (1998) indicated that spontaneous dispersion takes place when sodic clay is impacted with water of very low electrolyte concentration. However, water content below saturation results in limited swelling and incomplete separation of clay particles with the interparticle distance depending upon the water content. Therefore, aggregate slaking and clay dispersion in unsaturated systems would be limited as compared to saturated systems for specific SAR/EC conditions. Russo and Bresler (1977) demonstrated this fact in their study evaluating hydraulic conductivity with regard to cationic ratio $(Na^{+1}/(Ca^{+2})^{1/2}$ (R), electrolyte concentrations (C), and volumetric water content (θ). This study showed that under specific combinations of these variables the value of the cationic ratio can be estimated for a given hydraulic conductivity. For example, under saturated conditions with C = 0.02 N (approximate irrigation field soil) it is possible to maintain $K \geq 0.5$ cm/s as long as $R \leq 14$. Under the same conditions (C and K), but in unsaturated soils the corresponding value for R is 20. This study shows that water of poorer quality (higher sodicity) can be applied when unsaturated conditions are maintained during irrigation. These studies demonstrate that the negative effect of high SAR and low solution electrolyte levels decreases in dryer soils.

Project objectives

The project was designed to evaluate the chemistry of produced waters generated at various locations in the PRB with regard to salinity and sodicity and to determine how such waters will impact the physical and chemical nature of soils in the vicinity of active production. The research will determine if very poor quality water can be used to improve crop production when used for irrigation projects (sites that will receive irrigation for extended periods of time). It is anticipated that irrigable sites can easily handle quantities of water required to meet evapotranspiration requirements along with the leaching fraction needs. However, water blending (combining CBNG water with good quality surface waters) may be required, especially at sites where soils are considered to be questionable for irrigation purposes.

The specific objectives of the project were to: (1) assess the characteristics of CBNG-produced water and several representative irrigable soils in the PRB; (2) assess the interaction between CBNG-produced waters and soils through leaching studies; and (3) design field trials to verify laboratory assessments of the environmental impact of land disposal of CBNG-produced water.

Methods

The technical approach proposed for this study is based on a combination of laboratory and fieldwork. Year 1 activities covered the literature review, characterization of the baseline soil conditions at the two potential research sites, characterization of CBNG produced water to be used

at the field irrigation site, characterization of surface water samples collected from potentially impacted resources in the immediate area of the irrigation site, conducting leaching studies, and design of the field plots.

A detailed literature review was completed to ensure that the methods and procedures outlined in the Technical Approach represent the "state of the art" rather than duplication of work already completed. This information will be incorporated into a document describing the use of amendments to develop synthetic soil materials suitable for plant growth.

Laboratory research – column studies

Soils materials for the laboratory studies were collected from the Leiter Ranch located near Ucross, Wyoming. The materials were collected and placed in 5-gallon buckets and shipped to Western Research Institute's (WRI's) laboratory in Laramie, Wyoming. The materials were stored at temperatures of about 4 °C (39.2 °F) until used. The materials were also stored at field moisture conditions until prepared for analyses.

A laboratory study was conducted to determine saturated hydraulic conductivity of soil cores prepared using materials from the Leiter Ranch location. Soil amendments and water treatments were used in the laboratory column study to modify the soil/water conditions to determine if irrigation with highly sodic CBNG-produced water could be accomplished without negative impacts to the hydraulic conditions of the soils. The treatments evaluated included combinations of irrigation waters, soil amendments, and water treatment. The combination of treatments consists of the following: (1) irrigating with Piney Creek water; (2) irrigating with a blend of 1/2 Piney Creek water and 1/2 CBNG-produced water; (3) irrigating with CBNG-produced water; (4) soil amendment treatments include no treatment, gypsum, sulfur, gypsum + sulfur and irrigating with CBNG-produced water; and (5) irrigating with CBNG water treated with gypsum (injection) and sulfuric acid (injection).

CBNG-produced water was percolated through reconstructed soil columns for time periods of 4500 minutes (75 hours). The resulting hydraulic conductivities associated with the various treatments were determined. The laboratory set-up for the column studies is shown in **Figure 2**.



Figure 2. Laboratory set-up for the column studies.

Results and discussion

Laboratory column study

The hydraulic conductivity (K) relationships associated with the samples collected and the various soil and water treatments are presented in **Figures 3** and **4** for the Leiter Ranch and a mixture of A horizon materials collected from several locations at the Leiter Ranch, respectively. Data presented in **Figure 3** is associated with the A horizon of the soil profile sampled at the Leiter Ranch. The data provided in this figure represents 4 reps of 2 treatments including the Leiter Ranch soil with and without the application of gypsum at the surface. The data show much higher K values for the treated soils materials versus the untreated materials. This expected result is associated with the increased salt levels in the soil materials caused by the dissolution of the added gypsum and likely the addition of calcium to the system, which would tend to reduce the amount of sodium able to adsorb to the cation exchange sites associated with the soil materials. In addition, because the soils collected from the Leiter Ranch contained high percentage of clays, the impacts associated with the addition of gypsum as an amendment would be expected to be more radical compared to materials containing less clay such as

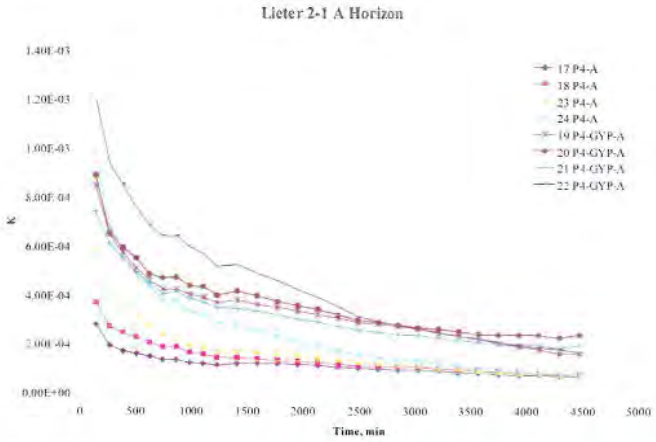


Figure 3. Hydraulic conductivity values for the treated and untreated A-Horizon materials collected from the Leiter Ranch study site using CBNG water produced from the Leiter CBNG production area.



Figure 4. Hydraulic conductivity values for the treated and untreated A-Horizon materials collected from several soils located near the Leiter Ranch study site using CBNG water produced from the Cooksley Ranch CBNG production area.

the materials collected from the mixed A-horizon materials (**Figure 4**).

Results associated with the mixed A-horizon materials shown in Figure 4 provide somewhat of a different result. Initially, the hydraulic conductivities associated with the untreated soil materials were higher than those associated with the treated soil samples. This appears to be opposite of the results found for the Leiter Ranch soil materials. However, near the end of the 4500-minute leaching period both the untreated and the treated samples appear to be characterized with comparable low K values. However, the rate of reduced K associated with the untreated soil materials appears to be high as compared to the treated soil material. It should be noted that one of the treated and one of the untreated samples show much higher K values. However, at the end of the 4500-minute leaching study, the K values associated with the treated sample appear to be leveling off while the K values associated with the untreated sample appear in decline. The differences shown between the Leiter Ranch A-horizon material and the mixed A-horizon materials may be related to the fact that the mixed A-horizon material contained less clay and more sand compared to the Leiter Ranch material. The differences in texture may delay the effects of clay swelling on the K values. As noted previously, the K values associated with the untreated mixed A-horizon material would be expected to decrease with an extended leaching period while K values associated with the treated materials would be expected to level off and possibly increase.

An additional leaching study was conducted using the soil materials collected from the Leiter Ranch study site. In this study, the K evaluations of the soil materials were conducted using only CBNG produced water and Clear Creek water. In addition, amended soil material was evaluated using CBNG water. The results of these evaluations are presented in **Figure 5**. The data show that the K values associated with CBNG produced water decrease substantially if gypsum is not applied to the soil material. In fact, the data show that the K values associated with the application of gypsum to the soil material results in better infiltration using CBNG methane produced water compared to applying Clear Creek water to the soil material. These data show that using gypsum as a soil amendment can allow the use of CBNG produced water in a managed irrigation system. This information provides the justification for the development of a field pilot study to demonstrate that the use of amendments may allow the use of CBNG produced water for irrigation of cropland and upland rangeland.

Saturated paste extracts were determined for the core materials following the leaching periods to acquire a sense of the impact of amendments and CBNG produced water on the chemical nature of the soil materials. The information collected from this analysis also provided an indication of how hydraulic conductivity changes with regard to the chemistry of the soil materials (**Table 1**). The K of the

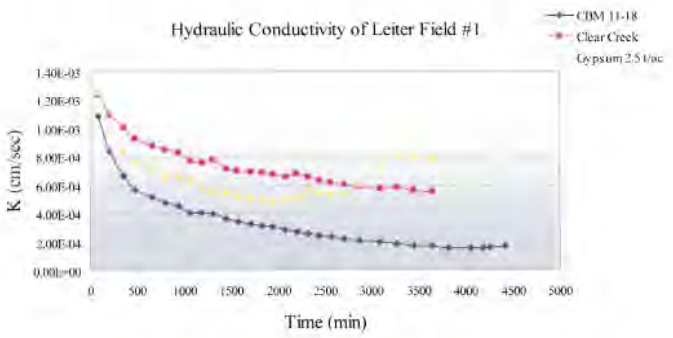


Figure 5. Hydraulic conductivity (K) of the Leiter Ranch soil material using CBNG produced water and Clear Creek water and the K associated with use of CBNG produced water with treated Leiter Ranch soil materials.

soil materials that were leached with Clear Creek water remained very high as compared to the soil cores receiving CBNG water and CBNG water with either soil or water treatments. Of the soil cores that received CBNG water with or without soil or water treatments, the cores treated with a surface application of gypsum were characterized with the highest K. This was a very interesting result since the EC of this treatment was rather low and the SAR values were comparable to the other leachates from treated soil materials. The primary reason for this result is thought to be associated with the presence of the gypsum at the surface, which more efficiently provided salt and Ca at levels required to reduce the slaking of aggregates and the dispersion of clays at the surface of the soil cores.

Table 1. Hydraulic conductivity and the resulting chemistry of saturated paste extracts collected from the materials used in the column studies after the treatment application.

Sample	Water	Treatment	pH s.u.	EC dS/m	Mg ppm	Na ppm	Ca ppm	SAR	alkalinity meq/l	K cm/s
Leiter A 2/8 mix	CC	-	8.38	1.21	57.71	110.24	144.38	1.96	7.27	1.87E-03
Leiter A 2/8 mix	CC	-	8.48	1.21	57.02	65.96	140.65	1.19	6.96	1.88E-03
Leiter A 2/8 mix	CC	-	8.47	1.27	56.80	77.88	138.88	1.41	7.71	1.74E-03
Leiter A 2/8 mix	CC	-	8.45	1.21	56.25	63.83	134.11	1.17	6.93	1.85E-03
Leiter A 2/8 mix	CBNG	-	8.97	1.47	10.18	330.65	25.14	14.05	14.60	7.53E-05
Leiter A 2/8 mix	CBNG	-	9.12	1.48	11.05	352.61	26.47	14.52	15.48	6.65E-05
Leiter A 2/8 mix	CBNG	-	8.34	1.39	9.27	308.30	16.61	15.02	14.10	6.86E-05
Leiter A 2/8 mix	CBNG	2.5 t/ac surface gyp	8.76	1.61	11.02	375.43	32.71	14.49	17.38	7.20E-04
Leiter A 2/8 mix	CBNG	2.5 t/ac surface gyp	8.99	1.68	7.95	405.28	20.06	19.37	18.19	6.89E-04
Leiter A 2/8 mix	CBNG	2.5 t/ac surface gyp	8.91	1.76	14.30	444.13	29.11	16.84	17.44	4.70E-04
Leiter A 2/8 mix	CBNG	2.5 t/ac surface gyp	8.91	1.89	13.58	412.71	23.86	16.70	15.15	6.65E-04
Leiter A 2/8 mix	CBNG	H2SO4 1.68 ml/gal	8.94	3.88	17.29	393.93	43.21	12.80	7.40	1.15E-04
Leiter A 2/8 mix	CBNG	H2SO4 1.68 ml/gal	9.41	4.61	15.25	421.96	41.68	14.21	6.25	2.02E-04
Leiter A 2/8 mix	CBNG	H2SO4 1.68 ml/gal	8.91	4.13	15.03	406.28	41.01	13.79	6.25	1.29E-04
Leiter A 2/8 mix	CBNG	H2SO4 1.68 ml/gal	9.07	3.75	12.57	352.85	36.00	12.89	5.78	1.02E-04
Leiter A 2/8 mix	CBNG	Gyp 193 mg/gal	9.01	4.83	30.39	572.07	43.37	16.28	24.19	1.00E-04
Leiter A 2/8 mix	CBNG	Gyp 193 mg/gal	9.04	4.51	29.79	528.65	37.37	15.64	23.54	6.79E-05
Leiter A 2/8 mix	CBNG	Gyp 193 mg/gal	8.98	4.86	29.75	574.56	51.52	15.77	24.57	2.20E-04
Leiter A 2/8 mix	CBNG	Gyp 193 mg/gal	9.06	4.37	29.54	481.58	43.02	13.84	21.84	5.95E-05

The quantity of salt deposited in the soil materials and the chemical nature of the materials resulting from the various treatments is also shown in **Table 1** with the complete data set provided in **Appendix A**. Salinity values, represented by EC, were relatively low for materials leached with Clear Creek water and CBNG produced water, and for soil materials surface treated with gypsum. Materials leached with water treated with sulfuric acid and gypsum were characterized with relatively high salt levels. The sulfuric acid treatment would be expected to increase salt levels in the soil materials by removing alkalinity from the CBNG produced water resulting in less precipitation of Ca and possibly Mg, and by increasing the dissolution of calcite present in the soil materials. The gypsum treatment increased salt levels likely due to the enhanced dissolution of gypsum because of the fine-grain nature of the gypsum particles and the more intimate relationship between the particles and water.

The pH levels of the soil materials leached with CBNG water treated or untreated were about the same with values near 9, while the saturated paste extracts of soil materials leached with Clear Creek water were lower at values near 8.5. Such pH values usually result in relatively low Ca levels in solution as calcite dissolution decreases substantially as pH values increase.

Soil materials leached with CBNG-produced water all were characterized with rather high SAR values. The materials leached with CBNG-produced water without treatment had SAR values similar to the materials treated with surface applications of gypsum or water treated with either acid or gypsum. Calcium levels tended to decrease with the addition of CBNG-produced water undoubtedly as a result of the high levels of alkalinity associated with the CBNG water. High alkalinity enhances the precipitation of calcite. However, the levels of Ca found in the soils leached with water treated with either sulfuric acid or gypsum appeared to be higher compared to samples leached with untreated water or samples treated with a surface application of gypsum. As noted previously, the addition of sulfuric acid to the water is expected to remove bicarbonate from the water prior to the leaching process. As a result, the bicarbonate will not be available to react with soluble Ca forming calcite and enhancing the amount of Ca found in solution. The reason for the relatively high levels of Ca associated with the soil materials leached with CBNG water with injected gypsum is likely associated with the increased reactivity of the gypsum applied in this manner. The

alkalinity found in the saturated paste extract did not seem to react with the relatively high levels of Ca found in the soil solution. The reason for this finding will require additional evaluation. However, the result might be explained by some work accomplished by Rhoades (1968). This study showed that the increases in Ca + Mg content produced by mineral weathering processes were greater than the decreases produced by lime precipitation processes caused by the interaction of Ca^{+2} and HCO_3^{-1} in solution. The dissolution of minerals present in the soil environment may provide Ca^{+2} to solution at rates larger than the formation of calcite by the Ca^{+2} and HCO_3^{-1} reaction.

Magnesium levels found in the leachates also varied significantly. The levels of Mg were highest in leachates resulting from the application of Clear Creek water to the soil materials. The lowest Mg levels were associated with the soils leached with CBNG water without treatment, which compared closely to the leachates resulting from the soils treated with a surface application of gypsum. The decreased levels of Mg found in the saturated extracts may be associated with the precipitation of Mg compounds from solution primarily carbonates and probably due to the removal of Mg from the soil core during leaching. The Mg levels associated with soil materials treated with acid were slightly higher compared to the surface gypsum application, while the levels found in leachates associated with the gypsum injection water treatment were much higher compared to the other treatments. In the case of acid treated water, the increase in soluble Mg levels may be associated with the dissolution of carbonates containing rather high levels of Mg such as magnesite and dolomite. The high levels of Mg resulting from the application of water injected with gypsum may be associated with Mg being present in the gypsum used for the treatment.

The Na levels found in the leachates tended to match Mg levels. The highest increase in Na levels was associated with water injected with gypsum with lesser amounts associated with acid injected water and the surface application of gypsum. Leachates associated with soil materials treated with CBNG water without treatment yielded the lowest concentrations of Na. All soil cores receiving CBNG produced water were characterized with high Na levels present in the saturated paste extracts. There does not appear to be any indication that Na levels were impacted by leaching of Na from the cores. The prevention of Na accumulation might be expected to occur due to adsorption competition with Ca and Mg.

Baseline evaluations

Detailed baseline evaluations were conducted at two potential research locations for the use of CBNG-produced water for managed irrigation. The first step in the baseline process was to map the soils at each site using a very detailed scale. The detailed soil survey including soil analysis for each of the study locations is presented in **Appendix B**. The results of the soil survey were to be used to determine the best site for the research project. The soil survey indicated that the Cooksley Ranch study site was the preferred irrigation site primarily because of the texture of materials present at the site. However, in this case the final site determination was based on water availability rather than the baseline conditions characterizing the sites. The availability of water at the Leiter Ranch was questionable. Therefore, the Cooksley Ranch site became the official study site for the project.

The CBNG water quality data is shown in **Table 2**. The CBNG water is characterized with a SAR of about 24 and a relatively low EC of 1.4 µS/cm. The quality of this water falls in the middle of road compared to other CBNG waters common to the PRB. A more complete data list is presented in **Appendix C**.

The baseline infiltration characteristics of the soils at Cooksley Ranch were conducted using a double-ring infiltrometer and the tension infiltration unit as noted in the methods section. The data collected using the tension infiltrometer were found to be more repeatable as compared to the data generated using the double ring unit. Repeatability of data collected using the double-ring infiltration unit was a major problem as data collected within a few feet was sometimes an order of magnitude different. Therefore, the tension infiltrometer data will be used for comparisons between treatments in the field plots.

Infiltration measurements were collected at four locations in each treatment plot. The data show seemingly high variability of infiltration rate associated with each plot. However, in the area of soil physics the variability shown in this data set are very typical and rather good. **Figures**

Table 2. Water analysis for baseline conditions.

Sample ID	pH s.u.	EC µS/cm	TDS mg/L	ALK mg/L	SAR	HCO_3^{-1} mg/L	CO_3^{-1} mg/L	Cl mg/L	F mg/L	SO_4^{-2} mg/L	Ca mg/L	Mg mg/L	K mg/L	Na mg/L	Fe mg/L
Clear Creek	8.3	954	760	201	1.1	226	9.3	4.2	0.19	302	105	45.4	5.8	55.1	90
Piney Creek	8.3	636	470	207	0.7	237	7.5	2.5	0.19	137	74.8	29.5	5.8	28.1	100
Fowler 11-18	8.3	1380	910	802	24.3	853	61.5	12.8	0.94	<1.0	8.9	3.9	3.1	344	560

6 and **7** are photographs showing the field infiltration determinations using the tension infiltrometer.

Field site characterization and field plot design

Detailed Order II soil surveys were completed at two locations in the Powder River Basin to evaluate soil suitability for application of CBNG product water



Figure 6. Determination of field infiltration rates using a tension infiltrometer.



Figure 7. The tension infiltrometer unit used for field determinations.

(**Appendix B**). Test-pits were excavated and soil profiles described to aid in the classification of predominant soil types and suitability for water application within each location. Soil samples were collected from representative profiles and analyzed for chemical and physical parameters. Analyses included pH, electrical conductivity (EC), calcium, magnesium, sodium, and textural class with percent sand, silt, and clay. In addition, tension infiltrometer and double ring permeameter tests were completed within each location area to estimate hydraulic conductivity and bulk density was determined by excavation. Using the above information, the Cooksely location was selected as the research plot for CBNG product water application.

Water samples collected from CBNG sources were placed in 5-gallon containers for laboratory testing using techniques reducing the incorporation of oxygen into the water during collection. Field determinations included T, pH, EC, and Eh. Samples collected for characterization purposes were filtered using 0.45 µm filters where required and maintained at near 4 °C during shipment to the laboratory. Sample containers were preconditioned as required by EPA (Environmental Protection Agency) methods for the various constituents. Water to be used for laboratory studies was held in cold storage until used.

The experimental design of the field test locations is provided in **Figures 8** and **9**. The research plot was designed using randomization of the locations of amendment applications and irrigation water type. Soil samples were collected and analyzed within each study plot to characterize baseline soil chemistry (pH, EC, Ca, Mg, Na, SAR, SO_4, HCO_3, and CO_3). In addition, baseline soil hydraulic properties were determined, including the determination of saturated hydraulic conductivity, using a tension infiltrometer and soil water retention functions, using gravimetric techniques. A split-plot in space statistical design was selected for the Cooksley project area. This design allows for analysis of interactions between soil and product water treatments on soil chemical and physical properties. Randomized study plots were established within the project area and baseline chemical and physical soil properties were measured. Chemical analysis included pH, EC, calcium, magnesium, sodium, sulfate, chloride, and alkalinity. Unsaturated K was measured using tension infiltrometer measurements at -10 and -6 cm tensions. Saturated K was estimated using Wooding's equation for unconfined infiltration rates into a soil from a circular source. Baseline

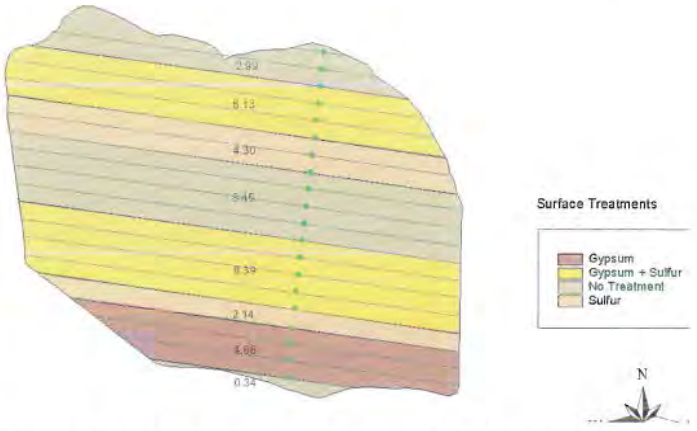


Figure 8. Diagram showing the location of soil amendments at the Cooksely irrigation study site.

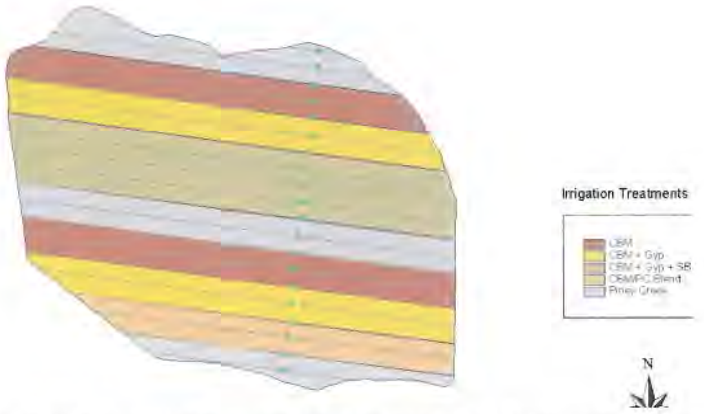


Figure 9. Diagram showing the locations of the CBNG water treatments at the Cooksely irrigation study site.



Figure 10. Surface water monitoring locations associated with the Cooksely irrigation study site.

data were analyzed statistically to determine variation between treatment plots prior to treatment application.

A major concern associated with irrigation using CBNG produced water is the potential of contaminating adjacent surface water resources and ground water aquifers at the irrigation site. As a result, monitoring locations were established to assess potential contamination of adjacent surface water resources that might result from the CBNG irrigation activities. Surface water quality monitoring locations have been established on Piney Creek and the irrigation ditch that flows east through Jack Cooksley's property to monitor any impact that the irrigation activities may have on adjacent surface water resources. Monitoring locations are positioned upstream of the CBNG irrigation research project and along the eastern boundary of Jack Cooksley's property. Baseline water samples were collected from the four locations and the samples were analyzed for pH, EC, TDS, alkalinity, Ca, Mg, Na, K, SO_4, Cl, CO_3, and HCO_3. Periodic monitoring, including sample collection and analysis, will continue throughout the research study period. Frequent monitoring of water pH and EC will be conducted using field measurement devices. Water monitoring locations are shown in **Figure 10** by the blue diamonds. A Gee passive capillary lysimeter was installed along with dielectric soil moisture probes to evaluate leaching fraction, drainage water quality, and irrigation efficiency. Groundwater monitoring will be constructed in the alluvial aquifer located beneath the research plot area to determine whether or not irrigation water is impacting the aquifer.

Soil treatments will be applied to the plots prior to the initiation of irrigation activities. Soil treatments were elemental sulfur at 0.5 t/acre, gypsum at 1.5 t/acre, sulfur (0.5 t/acre) plus gypsum (1.5 t/acre), and no treatment. Product water treatments included the removal of bicarbonate using a sulfuric acid injection system, injection of solution grade gypsum, blending with typical irrigation water, no treatment, and typical irrigation water as the control.

Conclusions

The project was designed to evaluate the chemistry of produced waters generated at various locations in the PRB with regard to salinity and sodicity and to determine how such waters will impact the physical and chemical nature of soils in the vicinity of active production. The research will determine whether poor-quality CBNG-produced water can be used to improve crop production when used for irrigation. The data collected from the laboratory studies showed that the use of amendments allows the application of CBNG produced water to soil materials without reducing the K characteristics as compared to soils leached with Clear Creek water. The data also provides an indication that the application of soil amendments to the surface of the soil prior to the application of CBNG-produced water may cause less impact on K as compared to water treatments. Additional research is required before this observation can be substantiated. Information developed in the laboratory research activities provides justification for the development of a field pilot study to demonstrate whether or not amendments will allow the use of CBNG produced water for irrigation of cropland and upland rangeland without detrimental impact to the physical and chemical conditions of treated soils. The field study will also assess whether or not irrigation with CBNG produced water can be done without impact to the surface and groundwater resources at or near irrigation sites. The field study was implemented with funding provided by the Western Research Institute's Jointly Sponsored Research Program with the United States Department of Energy that is governed by Cooperative

Agreement DE-FC26-98FT40323. Wolverine Energy is the commercial client contributing funding and in-kind contributions to the project. The field component of the project will be reported by Western Research Institute in cooperation with the U.S. Department of Energy and Wolverine Energy.

References cited

Alperovitch, N., Shainberg, I., and Keren, R., 1981, Specific effect of magnesium on the hydraulic conductivity of sodic soils: Journal of Soil Science, v. 32, p. 543-554.

Arora, H.S., and Coleman, N.T., 1979, The influence of electrolyte concentration on flocculation of clay suspensions: Soil Science, v. 127, p. 134-139.

Cass, A., and Sumner, M.E., 1982, Soil pore structural stability and irrigation water quality: II, Sodium stability data: Soil Science Society of America Journal, v. 46, p. 507-512.

Chi, C.L., Emerson, W.W., and Lewis, D.G., 1977, Exchangeable calcium, magnesium, and sodium and the dispersion of illites in water. I—Characterization of illites and exchange reactions: Australian Journal of Soil Resources, v. 15, p. 243-253.

Emerson, W.W., and Chi, C.L., 1977, Exchangeable calcium, magnesium, and sodium and the dispersion of illites in water. II—Dispersion of illites in water: Australian Journal of Soil Resources, v. 15, p. 255-262.

Frenkel, H., Goertzen, J.O., and Rhoades, J.D., 1978, Effects of clay type and content, exchangeable sodium percentage, and electrolyte concentration on clay dispersion and soil hydraulic conductivity: Soil Science Society of America Journal, v. 48, p. 32-39.

Gardner, W.R., Mayhugh, M.S., Goertzen, J.O., and Bower, C.A., 1959, Effect of electrolyte concentration and ESP on diffusivity of water in soils: Soil Science, v. 88, p. 270-274.

Jayawardane, N.S., 1979, An equivalent salt solutions method for predicting hydraulic conductivities of soils for different salt solutions: Australian Journal of Soil Resources, v. 17, p. 423-428.

McNeal, B.L., and Coleman, N.T., 1966, Effect of solution composition on soil hydraulic conductivity: Soil Science Society of America Proceedings v. 30, p. 308-312.

Pupisky, H., and Shainberg, I., 1979, Salt effects on the hydraulic conductivity of a sandy soil: Soil Science Society of America Journal, v. 43, p. 429-433.

Quirk, J.P., and Schofield, R.K., 1955, The effect of electrolyte concentration on soil permeability: Journal of Soil Science, v. 6, p. 163-178.

Rengasamy, P., and Sumner, M.E., 1998, Processes involved in sodic soils, *in* Sumner, M.E., and Naidu, R., editors, Sodic soils: Distribution, properties, management, and environmental consequences: Oxford University Press, New York, New York, p. 35-50.

Rengasmy, P., and Olsson, K.A., 1991, Irrigation and sodicity: Australian Journal of Soil Resources, v. 31, p. 821-837.

Rhoades, J.D., 1968, Leaching requirement for exchange sodium content: Soil Science Society of America Proceedings, vol. 32, p. 652-656.

Rhoades, J.D., 1972, Quality of irrigation water: Soil Science, v. 113, p. 277-284.

Rhoades, J.D., and Ingvalson, R.D., 1969, Macroscopic swelling and hydraulic conductivity properties of four vermiculite soils: Soil Science Society of America Proceedings, v. 33, p. 364-369.

Russo, D., and Bresler, E., 1977, Analysis of the saturated and unsaturated hydraulic conductivity in mixed sodium and calcium soil systems: Soil Science Society of America Journal, v. 41, p. 706-712.

Shainberg, I., Levy, G.J., Rengasamyu, P., and Frenkel, H., 1992, Aggregate stability and seal formation as affected by Drops' impact energy and soil amendments: Soil Science, v. 154, p. 113-119.

Shanmuganathan, R.T., and Oades, J.M., 1983, Modification of soil physical properties by addition of calcium compounds: Australian Journal of Soil Resources, v. 21, p. 285-300.

Slade, P.G., and Quirk, J.P., 1991, The limited crystalline swelling of smectite in $CaCl_2$, $MgCl_2$, and $LaCl_3$ solutions: Journal of Colloid Interface Science, v. 144, p. 18-26.

Sposito, G., 1989, The chemistry of soils: Oxford University Press, New York, New York, 304 p.

Sumner, M.E., Rengasamyu, P., and Naidu, R., 1998, Sodic soils: A reappraisal, *in* Sumner, M.E., and Naidu, R., editors, Sodic Soils: Distribution, properties, management, and environmental consequences: Oxford University Press, New York, New York, p. 3-17.

U.S. Salinity Laboratory Staff, 1954, Diagnosis and improvement of saline and alkali soils: U.S. Department

of Agriculture Handbook No. 60, U.S. Government Printing Office, Washington, D.C., 160 p.

Van Olphen, H., 1977, An introduction to clay colloid chemistry, 2nd edition: John Wiley, New York, New York, 318 p.

Waldron, L.J., and Constantin, G.K., 1970, Soil hydraulic conductivity and bulk volume changes during cyclic calcium-sodium exchange: Soil Science, v. 110, p. 81-85.

Yousaf, M., Ali, O.M., and Rhoades, J.D., 1987, Dispersion of clay from some salt-affected, arid land soil aggregates: Soil Science Society of America Journal, v. 56, p. 1257-1260.

Appendix A

Appendix A. Chemical analysis of saturated paste extracts collected from the materials used in the column studies after the treatment application. Extract results are for WRI 7/24/03.

ID	Sample	Water	Treatment	pH s.u.	EC dS/m	Sat %	Mg ppm	Mg meq/l	Na ppm	Na meq/l	K ppm	K meq/l	Ca ppm	Ca meq/l	SAR	alkalinity meq/l	alkalinity meq/l	F ppm	Cl ppm	PO_4 ppm	NO_3 ppm	SO_4 ppm	K cm/s	K cm/s
CC-1	Leiter A horizon 2/8 mix	Clear Creek	-	8.38	1.21		57.71	4.75	110.24	4.79	28.90	0.74	144.38	7.20	1.96	7.27	0.00	0.00	6.75	0.00	3.94	321.97	1.87E-03	6.72
CC-3	Leiter A horizon 2/8 mix	Clear Creek	-	8.48	1.21		57.02	4.69	65.96	2.87	10.24	0.26	140.65	7.02	1.19	6.96	0.00	0.00	9.01	0.62	2.04	327.96	1.88E-03	6.77
CC-6	Leiter A horizon 2/8 mix	Clear Creek	-	8.47	1.27		56.80	4.68	77.88	3.39	9.69	0.25	138.88	6.93	1.41	7.71	0.00	0.00	6.14	0.55	1.73	337.78	1.74E-03	6.26
CC-7	Leiter A horizon 2/8 mix	Clear Creek	-	8.45	1.21		56.25	4.63	63.83	2.78	9.97	0.26	134.11	6.69	1.17	6.93	0.00	0.00	6.58	0.00	0.26	325.22	1.85E-03	6.66
CBNG-4	Leiter A horizon 2/8 mix	Fowler 11-18	-	8.97	1.47		10.18	0.84	330.65	14.38	6.93	0.18	25.14	1.25	14.05	14.60	0.00	0.25	33.33	0.42	0.10	10.62	7.53E-05	0.27
CBNG-5	Leiter A horizon 2/8 mix	Fowler 11-18	-	9.12	1.48		11.05	0.91	352.61	15.33	8.19	0.21	26.47	1.32	14.52	15.48	0.00	0.20	31.41	0.00	0.12	9.18	6.65E-05	0.24
CBNG-8	Leiter A horizon 2/8 mix	Fowler 11-18	-	8.34	1.39		9.27	0.76	308.30	13.40	5.31	0.14	16.61	0.83	15.02	14.10	0.00	0.21	33.22	0.75	7.23	10.36	6.86E-05	0.25
CBNG-9	Leiter A horizon 2/8 mix	Fowler 11-18	2.5 t/ac surface gyp	8.76	1.61		11.02	0.91	375.43	16.32	6.65	0.17	32.71	1.63	14.49	17.38	0.00	0.23	21.54	1.71	1.39	18.37	7.20E-04	2.59
CBNG-10	Leiter A horizon 2/8 mix	Fowler 11-18	2.5 t/ac surface gyp	8.99	1.68		7.95	0.65	405.28	17.62	4.50	0.12	20.06	1.00	19.37	18.19	0.33	0.20	18.97	1.95	3.33	4.37	6.89E-04	2.48
CBNG-11	Leiter A horizon 2/8 mix	Fowler 11-18	2.5 t/ac surface gyp	8.91	1.76		14.30	1.18	444.13	19.31	10.04	0.26	29.11	1.45	16.84	17.44	0.00	0.13	32.71	0.00	30.76	83.95	4.70E-04	1.69
CBNG12	Leiter A horizon 2/8 mix	Fowler 11-18	2.5 t/ac surface gyp	8.91	1.89		13.58	1.12	412.71	17.94	9.55	0.24	23.86	1.19	16.70	15.15	0.00	0.39	67.48	0.00	7.88	294.19	6.65E-04	2.40
1079-44-1	Leiter A horizon 2/8 mix	Fowler 11-18	H2SO4 1.68 ml/gal	8.94	3.88	40.50	17.29	1.42	393.93	17.13	8.02	0.21	43.21	2.16	12.80	7.40	0.00	13.99	17.65	0.00	4.11	612.76	1.15E-04	0.41
1079-44-2	Leiter A horizon 2/8 mix	Fowler 11-18	H2SO4 1.68 ml/gal	9.41	4.61	43.00	15.25	1.26	421.96	18.35	6.87	0.18	41.68	2.08	14.21	6.25	0.00	0.00	18.93	4.23	0.00	702.50	2.02E-04	0.73
1079-44-5	Leiter A horizon 2/8 mix	Fowler 11-18	H2SO4 1.68 ml/gal	8.91	4.13	42.50	15.03	1.24	406.28	17.66	6.79	0.17	41.01	2.05	13.79	6.25	0.00	21.35	16.86	0.00	4.38	667.53	1.29E-04	0.46

Appendix A. Chemical analysis of saturated paste extracts collected from the materials used in the column studies after the treatment application. Extract results are for WRI 7/24/03, continued.

ID	Sample	Water	Treatment	pH	EC	Sat	Mg	Mg	Na	Na	K	K	Ca	Ca	SAR	alkalinity	alkalinity	F	Cl	PO_4	NO_3	SO_4	K	K
				s.u.	dS/m	%	ppm	meq/l	ppm	meq/l	ppm	meq/l	ppm	meq/l		meq/l	meq/l	ppm	ppm	ppm	ppm	ppm	cm/s	cm/s
1079-44-8	Leiter A horizon 2/8 mix	Fowler 11-18	H2SO4 1.68 ml/gal	9.07	3.75	40.50	12.57	1.03	352.85	15.37	5.13	0.13	36.00	1.80	12.89	5.78	0.00	0.00	18.53	0.95	4.92	571.66	1.02E-04	0.37
1079-44-3	Leiter A horizon 2/8 mix	Fowler 11-18	Gyp 193 mg/gal	9.01	4.83	43.60	30.39	2.50	572.07	24.87	20.07	0.51	43.37	2.16	16.28	24.19	0.00	5.95	24.65	0.00	9.26	18.08	1.00E-04	.036
1079-44-4	Leiter A horizon 2/8 mix	Fowler 11-18	Gyp 193 mg/gal	9.04	4.51	41.60	29.79	2.45	528.65	22.98	8.91	0.23	37.37	1.86	15.64	23.54	0.00	7.06	16.45	0.00	0.26	15.52	6.79E-05	0.24
1079-44-6	Leiter A horizon 2/8 mix	Fowler 11-18	Gyp 193 mg/gal	8.98	4.86	40.40	29.75	2.45	574.56	24.98	11.61	0.30	51.52	2.57	15.77	24.57	0.00	6.53	27.99	0.00	3.86	33.53	2.20E-04	0.79
1079-44-7	Leiter A horizon 2/8 mix	Fowler 11-18	Gyp 193 mg/gal	9.06	4.37	40.80	29.54	2.43	481.58	20.94	10.08	0.26	43.02	2.15	13.84	21.84	0.00	0.13	23.89	0.00	4.00	39.21	5.95E-05	0.21
CC-14	Clear Creek	Clear Creek	-	8.77	0.89		37.13	3.06	54.98	2.39	4.63	0.12	87.05	4.34	1.24	3.76	0.00	0.06	8.37	0.62	5.28	262.33	4.65E-04	1.67
CC-15	Clear Creek	Clear Creek	-	8.66	0.96		42.66	3.51	59.95	2.61	4.17	0.11	98.92	4.94	1.27	3.89	0.00	9.52	9.42	0.00	0.00	310.72	5.50E-04	1.98
CC-19	Clear Creek	Clear Creek	-	8.79	0.86		37.37	3.08	54.66	2.38	4.79	0.12	92.25	4.60	1.21	3.87	0.00	0.06	8.44	1.10	3.89	259.57	5.20E-04	1.87
CC-20	Clear Creek	Clear Creek	-	8.79	0.99		45.05	3.71	63.90	2.78	4.18	0.11	95.64	4.77	1.35	4.07	0.00	0.06	9.34	0.75	5.08	319.50	7.44E-04	2.68
CBNG-13	Fowler 11-18	Fowler 11-18	-	9.34	1.35		8.36	0.69	314.43	13.67	2.28	0.06	10.32	0.51	17.63	13.81	0.33	0.49	30.92	1.69	3.44	5.18	1.18E-04	0.42
CBNG-16	Fowler 11-18	Fowler 11-18	-	9.44	1.39		10.49	0.86	337.31	14.67	3.14	0.08	16.62	0.83	15.94	14.59	0.60	0.39	29.00	2.14	0.07	7.23	2.77E-04	1.00
CBNG-17	Fowler 11-18	Fowler 11-18	-	9.12	1.32		10.30	0.85	305.92	13.30	2.59	0.07	11.53	0.58	15.77	13.32	0.37	0.55	26.51	0.83	4.00	17.18	1.20E-04	0.43
CBNG-18	Fowler 11-18	Fowler 11-18	-	9.30	1.29		8.84	0.73	312.38	13.58	2.87	0.07	18.67	0.93	14.91	13.39	0.40	0.55	22.82	1.07	0.05	6.45	1.28E-04	0.46
CBNG-21	Fowler 11-18	Fowler 11-18	2.5 t/ac surface gyp	9.00	1.73		17.28	1.42	379.57	16.50	4.51	0.12	43.73	2.18	12.29	9.07	0.00	0.00	13.91	0.00	0.00	387.48	4.17E-04	1.50
CBNG-22	Fowler 11-18	Fowler 11-18	2.5 t/ac surface gyp	9.14	1.64		8.62	0.71	411.53	17.89	6.45	0.16	15.60	0.78	20.74	17.28	0.31	0.59	28.65	1.33	3.01	19.96	8.65E-04	3.11
CBNG-23	Fowler 11-18	Fowler 11-18	2.5 t/ac surface gyp	9.19	2.18		15.52	1.28	502.85	21.86	4.38	0.11	8.26	0.41	23.79	15.01	0.00	0.52	26.62	0.00	7.01	351.00	7.29E-04	2.62
CBNG-24	Fowler 11-18	Fowler 11-18	2.5 t/ac surface gyp	9.18	1.31		8.73	0.72	309.38	13.45	3.36	0.09	14.20	0.71	15.92	12.82	0.00	0.42	21.45	0.45	3.75	41.24	7.36E-04	2.65

Appendix A. Chemical analysis of saturated paste extracts collected from the materials used in the column studies after the treatment application. Extract results are for WRI 7/24/03, continued.

ID	Sample	Water	Treatment	pH	EC	Sat	Mg	Mg	Na	Na	K	K	Ca	Ca	SAR	alkalinity	alkalinity	F	Cl	PO_4	NO_3	SO_4	K	K
				s.u.	dS/m	%	ppm	meq/l	ppm	meq/l	ppm	meq/l	ppm	meq/l		meq/l	meq/l	ppm	ppm	ppm	ppm	ppm	cm/s	cm/s
1079-44-10	Leiter Bt horizon 2/8 mix	Fowler 11-18	H2SO4 1.68 ml/gal	9.14	4.09	42.50	15.43	1.27	403.00	17.52	2.35	0.06	52.36	2.61	12.58	6.02	0.00	0.00	14.57	0.00	0.00	644.22	3.51E-04	1.26
1079-44-12	Leiter Bt horizon 2/8 mix	Fowler 11-18	H2SO4 1.68 ml/gal	9.16	4.20	42.30	16.74	1.38	417.13	18.14	2.54	0.06	56.26	2.81	12.54	7.49	0.00	0.00	14.81	0.00	0.26	648.20	3.04E-04	1.09
1079-44-15	Leiter Bt horizon 2/8 mix	Fowler 11-18	H2SO4 1.68 ml/gal	9.15	4.08	41.60	19.65	1.62	384.42	16.71	1.68	0.04	65.87	3.29	10.67	7.28	0.00	0.00	14.09	0.00	7.72	634.41	3.44E-04	1.24
1079-44-16	Leiter Bt horizon 2/8 mix	Fowler 11-18	H2SO4 1.68 ml/gal	9.12	4.20	41.20	21.63	1.78	402.01	17.48	2.09	0.05	72.17	3.60	10.66	8.19	0.02	0.00	14.38	0.00	0.00	636.01	4.02E-04	1.45
1079-44-9	Leiter Bt horizon 2/8 mix	Fowler 11-18	Gyp 193 mg/gal	9.37	2.65	37.40	12.08	0.99	291.22	12.66	1.12	0.03	28.79	1.44	11.49	12.85	0.30	0.39	19.23	0.88	0.13	32.56	1.39E-04	0.50
1079-44-11	Leiter Bt horizon 2/8 mix	Fowler 11-18	Gyp 193 mg/gal	9.28	2.97	40.50	9.86	0.81	347.28	15.10	1.71	0.04	11.90	0.59	18.02	14.02	0.42	0.45	20.38	0.88	0.19	34.72	3.08E-04	1.11
1079-44-13	Leiter Bt horizon 2/8 mix	Fowler 11-18	Gyp 193 mg/gal	9.42	2.78	39.00	10.41	0.86	321.13	13.96	1.58	0.04	16.91	0.84	15.14	13.22	0.49	0.51	23.50	1.86	5.04	35.24	1.82E-04	0.66
1079-44-14	Leiter Bt horizon 2/8 mix	Fowler 11-18	Gyp 193 mg/gal	9.31	2.66	39.30	10.12	0.83	309.08	13.44	4.57	0.12	19.17	0.96	14.21	12.70	0.32	0.25	17.95	1.48	0.00	26.90	1.94E-04	0.70
1079-44-17	Leiter A horizon site 2	P-4	-	9.30	3.49	41.70	19.33	1.59	955.35	41.54	8.29	0.21	9.71	0.48	40.78	36.41	1.72	0.25	73.49	0.00	0.00	41.88	6.71E-05	0.24
1079-44-18	Leiter A horizon site 2	P-4	-	9.30	3.69	42.00	20.25	1.67	989.68	43.03	9.34	0.24	12.79	0.64	40.08	38.31	1.35	0.38	89.18	0.00	0.26	55.79	7.22E-05	0.26
1079-44-23	Leiter A horizon site 2	P-4	-	9.32	3.88	41.30	15.26	1.26	1042.71	45.34	7.80	0.20	11.58	0.58	47.34	39.96	0.89	0.63	87.64	0.00	0.39	76.25	6.89E-05	0.25
1079-44-24	Leiter A horizon site 2	P-4	-	9.40	3.66	42.70	14.51	1.19	984.98	42.83	7.31	0.19	8.75	0.44	47.42	38.48	2.20	0.38	78.90	0.00	0.26	50.20	7.34E-05	0.26
1079-44-19	Leiter A horizon site 2	P-4	4.0 t/ac surface gyp	9.03	3.40	41.00	13.13	1.08	863.20	37.53	6.34	0.16	16.43	0.82	38.50	32.88	0.45	0.51	69.80	0.00	0.26	146.56	159. E-04	0.57
1079-44-20	Leiter A horizon site 2	P-4	4.0 t/ac surface gyp	8.97	3.84	39.90	15.04	1.24	978.59	42.55	7.98	0.20	20.96	1.05	39.81	33.91	0.17	0.25	62.77	0.00	0.26	257.58	2.35E-04	0.85
1079-44-21	Leiter A horizon site 2	P-4	4.0 t/ac surface gyp	8.92	3.75	40.60	16.67	1.37	937.89	40.78	8.14	0.21	24.90	1.24	35.66	28.15	0.00	0.25	65.87	0.00	0.13	499.62	1.92E-04	0.69
1079-44-22	Leiter A horizon site 2	P-4	4.0 t/ac surface gyp	9.12	3.85	41.70	17.26	1.42	1072.04	46.61	8.01	0.20	18.51	0.92	43.05	36.20	0.20	0.25	61.56	0.00	0.26	312.84	1.64E-04	0.59

Appendix B—Soil survey of coalbed natural gas product water application areas at the Cooksley Ranch and Leiter Ranch study sites

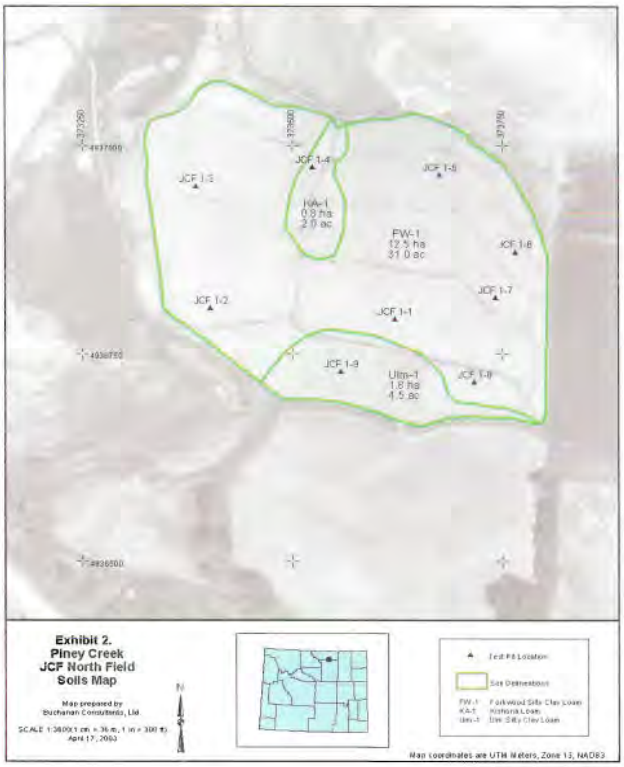
Introduction

Wolverine Operations has selected a 52.6-acre field near Leiter, Wyoming and a 37.5-acre field along Clear Creek, Wyoming the Cooksley Ranch for irrigation with coalbed natural (CBNG) product water. Historically, these areas have been cultivated and used for grazing and harvesting of hay grass. A soil survey was completed by the Western Research Institute (WRI) to evaluate the extent and proportion and to document the physicochemical properties of the major soil types within each area and to assess their suitability for irrigation with CBNG product water. Preliminary analyses of soil chemistry and soil texture have been completed by WRI and are included with this report.

Methods

The Leiter and Clear Creek fields were traversed by a soil scientist and test-pits were randomly located in each area (**Exhibits 1** and **2**, respectively). The location of all test sites was recorded using a global positioning system (GPS). At each site a test-pit was excavated to a depth of approximately 48 inches and the soil profile was described. Descriptions included depth, texture-by-feel, consistency, structure, effervescence, percentage of coarse fragments, and visible salts for each soil horizon. Also noted were soil type, slope, aspect, and any other characteristics pertinent to pedon classification or suitability determinations.





Soil samples were collected from randomly selected soil profiles. Soil samples were analyzed by WRI for pH and electrical conductivity (EC), and texture with percent sand, silt, and clay. Saturated paste extracts were submitted to Green Analytical in Durango, Colorado for analysis of calcium, magnesium, sodium, potassium, sodium adsorption ratio (SAR), alkalinity, chloride, and sulfate.

Soil boundaries were drawn on an orthogonal photograph base-map to reflect field observations as test-sites were described. After mapping was complete, the revised soil boundaries were digitized and soil maps were prepared at a scale of 1:3600 using ArcView®.

Results

A soil survey was conducted for the 52.6-acre Leiter Field #1 and the 37.5-acre Cooksley Ranch study site in Sheridan County, Wyoming. The purpose of this survey was to identify the extent and proportion of soils in each area and to determine their suitability for application of CBNG product water. The soils in both areas formed predominately in mixed alluvium from sedimentary rock sources. The following are the soil-mapping units identified in each area:

Leiter Field #1

- Forkwood loam
- Hiland fine sandy loam

Cooksley Ranch study site

- Forkwood silty clay loam
- Kishona loam
- Ulm silty clay loam

The extent and proportion of soils in the Leiter Field #1 and Cooksley Ranch study site are shown on Exhibits 1 and 2, respectively. The A-horizon and Bt-horizons were selected for sampling from four test-pit locations in the Leiter Field #1 and one test-pit in the Cooksley Ranch study site. The results from the laboratory analyses for the Leiter and Cooksley Ranch fields are provided in **Tables A** and **B**, respectively. Analysis of extractable cations, hydraulic conductivity, and soil texture are being conducted by WRI. A supplementary report of laboratory results and data interpretation will be submitted upon completion. Additional information regarding the physical and chemical properties of soils within the Leiter and Cooksley Ranch fields was summarized from the Soil Survey of Sheridan County, Wyoming (USDA-NRCS, 1986) (**Table C**).

The Leiter Field #1 is composed of two soil mapping units: Forkwood loam and Hiland fine sandy loam. The predominant soil type identified in the Leiter Field is Forkwood, which represents 97% (51.2 acres) of the survey area. The minor soil type located in the southwestern part of the survey area is Hiland. This map unit represents 3% (1.4 acres) of the survey area. The Hiland soil does not have limitations for irrigation. The primary limitations for irrigation in the Leiter Field are clay content in the surface horizons and platy structure of the A-horizon associated with the Forkwood mapping unit. Fine-textured materials have greater potential for clay dispersion and aggregate dispersion than coarser-textured soils. Investigation of the Leiter Field shows a platy structure of the A-horizon (surface) largely throughout the Forkwood mapping unit. The formation of platy structure is likely the result of compaction from high intensity grazing and rain-drop impacts to the soil surface when low vegetation cover is present. In addition, the Leiter Field contains a high density of annual plants that may proliferate under an irrigated regime. Cultivation and replanting of the Leiter Field may be warranted to ameliorate the compacted surface condition and presence of annual species.

The Cooksley Ranch study site is composed of three soil mapping units: Forkwood silty clay loam, Kishona loam, and Ulm silty clay loam. Forkwood silty clay loam is the predominant map unit and represents 83 % (31 acres) of the survey area. Kishona and Ulm soils make up 5% (2 acres) and 12 % (4.5 acres) of the survey area. The Ulm mapping unit in the Cooksley Ranch study site represents the greatest limitations to this site because of elevated clay concentrations throughout the profile. Clay content in the surface horizons ranges from 28 to 50% and will typically result in a low permeability condition. Clay content of the Forkwood and Kishona soils ranges from 20 to 35%, but these soils are

Table A. Leiter Field #1—Results from laboratory analysis of soil samples collected from the Leiter Ranch study site.

Location	Sample date	Sample depth	pH units	EC mmho/ cm	% Sat	Calcium meq/l	Magne-sium meq/l	Sodium meq/l	SAR	% Sand	% Silt	% Clay	Class	Bicar-bonate meq/l	Car-bonate meq/l	Chlo-ride meq/l	Sulfate meq/l	Potas-sium meq/l
Leiter 1-1	04/03/03	0-7"	8.51	0.57	60.57	3.76	2.53	0.45	0.25	18.7	44.6	36.7	SICL	3.6	0.1	0.59	0.67	0.38
Leiter 1-1 DUP	04/03/03	0-7"	8.76	0.59	45.60	3.63	2.48	0.67	0.38	.	.	.	.	3.3	0.1	0.93	0.65	0.40
Leiter 1-2	04/03/03	7-15"	8.93	0.80	36.03	5.24	3.33	2.02	0.97	35.7	38.6	25.7	L	6.0	0.2	0.62	1.17	0.31
Leiter 1-3	04/03/03	15-30"	8.94	0.64	39.16	2.48	1.58	3.50	2.46	22.6	43.8	33.5	CL	3.2	0.1	0.51	3.00	0.09
Leiter 2-1	04/03/03	0-5"	8.31	0.67	40.40	3.85	2.75	0.84	0.46	29.2	39.3	31.5	CL	2.6	0.1	1.07	1.12	0.29
Leiter 2-2	04/03/03	5-15"	8.74	0.50	45.50	3.11	1.99	1.06	0.66	32.7	38.8	28.5	CL	3.7	0.1	0.39	<0.10	0.12
Leiter 2-3	04/03/03	15-30"	8.93	0.71	52.23	3.30	2.10	3.17	1.93	24.9	44.0	31.1	CL	4.1	0.1	1.44	1.54	0.10
Leiter 3-1	04/03/03	0-6"	8.66	0.63	35.50	4.15	2.39	1.26	0.70	53.4	25.9	20.7	SCL	5.3	0.0	0.82	0.75	0.38
Leiter 3-2	04/03/03	6-18"	8.74	0.36	44.53	1.54	0.99	1.60	1.42	35.6	28.3	36.1	CL	1.7	0.0	0.65	1.12	<0.10
Leiter 3-2 DUP	04/03/03	6-18"	8.5	0.38	44.36	1.53	1.00	1.71	1.52	.	.	.	.	1.7	0.0	0.54	1.17	<0.10
Leiter 4-1	04/03/03	0-6"	7.97	0.69	.	3.28	2.65	1.17	0.68	40.2	33.8	26.0	L	1.6	0.0	1.24	1.17	0.35
Leiter 4-2	04/03/03	6-12"	8.62	0.47	31.33	1.85	1.52	1.86	1.43	38.8	38.2	22.9	L	2.0	0.0	1.13	0.71	0.11
Leiter 4-3	04/03/03	12-24"	8.97	0.76	42.86	1.41	1.25	3.50	3.03	32.5	31.1	36.3	CL	1.9	0.0	0.96	0.54	<0.10

Table B. Cooksely Ranch Study Site — Results from laboratory analysis of soil samples collected from the Cooksley Ranch study site.

Location	Sample date	Sample depth	pH units	EC MMHO/ CM	% Sat	Calcium meq/l	Magne-sium meq/l	Sodium meq/l	SAR	% Sand	% Silt	% Clay	Class	Bicar-bonate meq/l	Car-bonate meq/l	Chlo-ride meq/l	Sulfate meq/l	Potas-sium meq/l
CR 1-1-1	04/03/03	0-8"	8.77	0.86	49.91	6.64	2.47	1.91	0.89	19.7	49.8	30.4	SICL	6.8	0.4	0.68	2.81	0.48
CR 1-1-2	04/03/03	8-20"	8.66	0.61	40.25	4.12	1.94	1.29	0.74	20.9	53.6	25.5	SIL	333.3	0.2	0.82	1.92	0.16

structurally more stable than their counterparts in the Leiter Field. This is largely because of the management practices that have been employed at the two sites.

Conclusion

Field investigation and laboratory analysis show that soils in the Leiter Field may have limitations for irrigation due to clay content and compacted surface zones. Cultivation of this site may improve surface conditions for infiltration. The Cooksley Ranch site has few limitations for irrigation, however low permeability conditions may exist in the Ulm mapping unit. Hydraulic conductivity of these materials is being evaluated and will be presented upon completion.

Table C. Physical and chemical properties of Leiter Field #1 and Cooksley Ranch soils[1].

Soil series	Horizon	Depth/ inches	Hydro. group	Clay %	Moist P_b g/cm^3	Permeability in/hr	Avialable water capacity	Soil reacton pH	Salinity mmhos/ cm	Shrink/ swell potential
Hiland	A	0-2	B	8-18	1.25-1.35	2.0-6.0	0.10-0.13	6.6-7.8	<2	Low
	Bt1	2-8		20-35	1.25-1.35	0.6-2.0	0.14-0.16	7.4-7.8	<2	Moderate
	Bt2	8-26		20-35	1.25-1.35	0.6-2.0	0.14-0.16	7.9-9.0	<2	Low
	Bt3	26-35		10-20	1.35-1.45	2.0-6.0	0.10-0.14	7.9-9.0	<2	Low
	Bk	35-48		10-20	1.35-1.45	2.0-6.0	0.10-0.14	7.9-9.0	<2	Low
Forkwood	A	0-4	B	12-25	1.15-1.25	0.6-2.0	0.15-0.17	6.6-7.8	<2	Low
	Bt1	4-15		25-35	1.25-1.35	0.6-2.0	0.19-0.21	6.6-7.8	<2	Moderate
	Bt2	15-25		20-32	1.25-1.35	0.6-2.0	0.16-0.18	7.9-9.0	<2	Low
	Btk	25-31		20-32	1.25-1.35	0.6-2.0	0.16-0.18	7.9-9.0	<2	Low
	Bk	31-44		20-32	1.25-1.35	0.6-2.0	0.16-0.18	7.9-9.0	<2	Low
	Bky/Cky	44-60		20-32	1.25-1.35	0.6-2.0	0.16-0.18	7.9-9.0	<2	Low
Ulm	Ap	0-4	C	28-35	1.15-1.25	0.6-2.0	0.17-0.21	6.6-7.3	<2	Moderate
	Bt1	4-18		35-50	1.20-1.30	0.06-0.2	0.17-0.21	6.6-7.8	<2	High
	Bt2	18-25		30-42	1.20-1.30	0.2-0.6	0.17-0.21	7.9-9.0	<2	High
	Btk	25-33		30-42	1.20-1.30	0.2-0.6	0.17-0.21	7.9-9.0	<2	High
	Ck	33-53		30-42	1.20-1.30	0.2-0.6	0.17-0.21	7.9-9.0	<2	High
Kishona	A	0-5	B	20-27	1.20-1.30	0.6-2.0	0.15-0.17	7.4-8.4	<2	Low
	Bw/k	5-11		20-35	1.20-1.35	0.6-2.0	0.16-0.20	7.9-9.0	<4	Moderate
	C	11-55		20-35	1.20-1.35	0.6-2.0	0.16-0.20	7.9-9.0	<4	Moderate

[1] Data taken from the Soil Survey of Sheridan County, Wyoming (USDA-NRCS, 1986)

Appendix C

Appendix C. Baseline water quality data for Clear Creek, Piney Creek, and Fowler 11-18–The CBNG water that will be applied to the research plots at Cooksley Ranch study site.

Sample ID	Date Sampled	Time Sampled	PH s.u.	EC umhos/cm	TDS mg/L	TDS Calc mg/L	ALK mg/L	HARD mg/L	SAR	BICARB mg/L	BICARB meq/L	CARB mg/L	CARB meq/L
Clear Creek	3/26/2003	1000	8.3	954	760	640	201	449	1.1	226	3.7	9.3	0.31
Piney Creek	3/26/2003	1400	8.3	636	470	400	207	308	0.7	237	3.89	7.5	0.25
Fowler 11-18	3/26/2003	1200	8.3	1380	910	850	802	38	24.3	853	13.98	61.5	2.05

Sample ID	Date sampled	Time sampled	Hydrox mg/L	Hydrox meq/L	CL mg/L	CL meq/L	Fluoride mg/L	Fluoride meq/L	SO_4 mg/L	SO_4 meq/L	CA mg/L	CA meq/L	MG mg/L
Clear Creek	3/26/2003	1000	<1.0	NA	4.2	0.12	0.19	0.01	302	6.29	105	5.24	45.4
Piney Creek	3/26/2003	1400	<1.0	NA	2.5	0.07	0.19	0.01	137	2.85	74.8	3.73	29.5
Fowler 11-18	3/26/2003	1200	<1.0	NA	12.8	0.36	0.94	0.05	<1.0	NA	8.9	0.44	3.9

Sample ID	Date sampled	Time sampled	MG meq/L	K mg/L	K meq/L	NA mg/L	NA meq/L	CATSUM meq/L	ANSUM meq/L	BALANCE %	DISS_FE mg/L
Clear Creek	3/26/2003	1000	3.74	5.8	0.15	55.1	2.4	11.53	10.44	4.96	90
Piney Creek	3/26/2003	1400	2.43	5.8	0.15	28.1	1.22	7.53	7.06	3.22	100
Fowler 11-18	3/26/2003	1200	0.32	3.1	0.08	344	14.96	15.8	16.45	2.02	560

CHAPTER 4

Strontium isotopic tracing of the effects of coal bed natural gas (CBNG) development on shallow and deep groundwater systems in the Powder River Basin, Wyoming

Carol D. Frost
Elizabeth Brinck
Department of Geology and Geophysics
University of Wyoming
Laramie, Wyoming

Table of contents

List of figures 94
List of tables 94
Abstract 95
Introduction 95
Geologic background 96
Geologic setting of the study sites 96
Analytical details 97
Results 99
Discussion 99
Distinguishing CBNG product water from ambient water 99
Tracing the infiltration of CBNG water from ambient water 100
Beaver Creek site 100
Coal Creek site 102
Identifying the effects of CBNG water upon water quality using strontium concentration as a corollary for total dissolved solids 102
Evaluate the possibility of leakage in deep aquifers 103
Groundwater ages of coal sandstone aquifers 103
Future work 105
Conclusions 105
Acknowledgements 106
References cited 106

List of figures

1. Geologic map of the Powder River Basin in Wyoming and Montana 97
2. Topographic map of Beaver Creek 98
3. Topographic map of Coal Creek 98
4. Graph summarizing the $^{87}Sr/^{86}Sr$ ratios and strontium concentrations of water samples from Beaver Creek 100
5. Graph showing initial measurements of $^{87}Sr/^{86}Sr$ and strontium concentration at Coal Creek 101
6. Graph of the strontium concentration trend with time for one well at each of the three well sites at Beaver Creek 101
7. Graph showing the $^{87}Sr/^{86}Sr$ and strontium concentrations of the wells within the pond at Coal Creek and the CBNG sample (open circle) for three sampling dates 102
8. Graph of strontium ratio versus depth within the off-channel pond at Coal Creek 103
9. Graphs of strontium concentration and TDS versus time for well BC-14 at Beaver Creek's lower well site and for well 7b within the pond at Coal Creek 104

List of tables

1. Strontium isotopic and concentration data from the Beaver Creek site 99
2. Strontium isotopic and concentration data from the Coal Creek site 100

Abstract

Water withdrawn during coal bed natural gas (CBNG) production poses a variety of economic, environmental, and policy issues in Wyoming and Montana. To minimize co-produced water it is important to develop a means of verifying that groundwater is withdrawn solely from the mined coal seam and not from adjacent aquifers. In addition, where this water is discharged to the surface it is important to be able to trace this water as it infiltrates and interacts with the near surface aquifers in order to mitigate potential environmental effects. Strontium isotopes are effective fingerprints of the aquifer from which water originates and tracers of the interaction of waters from different aquifers and the surface and near-surface environment. This study explores the extent to which the strontium isotopic fingerprint can be used to trace CBNG water and its impacts following discharge on the surface. Our results suggest that strontium isotopic and elemental tracers are effective in tracking the infiltration of CBNG produced water and monitoring increases in total dissolved solids. Additionally, strontium isotopes have the potential to indicate aquifer leakage into the mined coal seam if monitored directly at individual production wells.

Introduction

Coalbed natural gas (CBNG) development is increasing rapidly in the Powder River Basin (PRB) of Wyoming and Montana. In the U.S., 96% of commercial CBNG production originates in unmined coal seams while only 4% comes from active or abandoned coal mines (Creedy and Tilley, 2003). CBNG development in the PRB originally focused on the shallow coals just west of the active coal mines along the eastern margin of the basin near Gillette, Wyoming. The development is expanding to the west and north and to a limited extent to other basins within Wyoming. Of the 348.2 billion cubic feet (BCF) of coalbed natural gas produced in 2003, 346.0 BCF was from the PRB, where it was withdrawn from more than 12,000 wells (De Bruin and others, 2004).

CBNG wells in the PRB are completed open-hole and casing is set to the top of the coal seam. A downhole submersible pump extracts groundwater from the coal seam. This depressurizes the coal, allowing the natural gas, mainly in the form of methane, to separate from the coal and water and travel up an annular pipe to the surface. A typical well produces 15,000 gallons of water per day, which is discharged to the surface (Wyoming Oil and Gas Conservation Commission, 2004). Water production from CBNG activity in the PRB from the beginning of CBNG activity through August 2004 totals 115 billion gallons (Wyoming Oil and Gas Conservation Commission, 2004). Disposal of this water is an important environmental, agricultural, and legislative issue.

Specific topics of concern in relation to disposal of CBNG produced waters include effects of drawdown in coal seams and adjacent aquifers, rate and location of recharge to the aquifers, and the impacts of discharged CBNG water upon surface waters, drainages, and soils (Rice and others, 2002). In addition, understanding what effect the discharged CBNG water will have upon shallow groundwater and surface water quality is problematic. Complications stem from variations in local hydrology, geology, and stream chemistry (Clark and others, 2001). Additional complications in the discharge of CBNG produced waters arise from Wyoming's Department of Environmental Quality (WDEQ) regulations that require the class of groundwater be protected in all situations (Wyoming Department of Environmental Quality, 2004).

A first step in addressing these concerns is to identify the specific aquifers with which the discharged water is interacting. Tracking the CBNG water as it is discharged into surface drainages or retention ponds and infiltrates into the shallow groundwater system would accomplish this. It has been shown that water originating from distinct geologic settings may have unique chemical characteristics that can be used to trace the source of the water (Clark and others, 2001). However, chemical parameters, even in combination with stable isotopic ratios of oxygen and hydrogen, have proven insufficient in distinguishing groundwater in coal aquifers from that in other sandstone aquifers in the PRB (Frost and others, 2002a).

Radiogenic isotope concentrations and ratios have long been used for tracing geologic and environmental processes. Strontium isotopes have been used to identify the sources of strontium in throughfall (Graustein and Armstrong, 1983) as well as to constrain residence time in watersheds (Bullen and others, 1996). Additionally, strontium isotopes have been shown to be effective tracers of aquifer interactions (Frost and Toner, 2004). The strontium concentration in conjunction with the ratio of radiogenic ^{87}Sr to stable ^{86}Sr has been shown to be an effective fingerprint that distinguishes coal-seam water from other ground and surface water. Frost and others (2002a,b) have shown that coal and sandstone aquifers have distinctive strontium isotopic compositions that successfully fingerprint these aquifers whereas other stable isotopes and major ion chemistry do not.

Strontium is an appealing candidate for isotopic tracing because it does not fractionate during evaporation or precipitation and small variations in $^{87}Sr/^{86}Sr$ can be measured precisely ($\pm$ 0.00001). Additionally, the radiogenic isotope ^{87}Sr is a product of the radioactive decay of ^{87}Rb,

such that its concentration will vary greatly depending upon the age and original Rb content of the source. Groundwater obtains strontium through interaction with the aquifer material and therefore has as great a range of ^{87}Sr to ^{86}Sr as does geologic material. Therefore when applying this tool to CBNG/near surface groundwater interactions it is likely that the deep coal aquifer will have a measurably different ratio than that of shallow alluvial groundwaters.

The objectives of this part of research funded by the Western Resources Project (WRP) Foundation were to use strontium isotopic tracing to study the fate and impact of coalbed natural gas product waters on shallow aquifers, and to evaluate the possibility of leakage in deep aquifers. This study was undertaken at two sites: first, a site of where CBNG produced water is discharged into two in-channel disposal ponds in the Beaver Creek area, approximately fifty miles southwest of Gillette, Wyoming and second, an off-channel disposal site adjacent to Coal Creek near Ucross, Wyoming. We have used strontium isotope data to:

1. distinguish CBNG water from surface and shallow groundwater,
2. trace the infiltration of CBNG water through the near surface aquifers, and
3. correlate strontium concentration changes with changes in water quality.

Geologic background

The PRB is a sedimentary basin in northeastern Wyoming and southeastern Montana. Laramide foreland thrust tectonics during Paleocene and Eocene times formed the PRB (Hunter, 1999), which is bounded on the west by the Big Horn Mountains and Casper Arch and on the east by the Black Hills. The axis of this asymmetrical basin trends north-northwest and is west of the basin center, creating shallowly dipping beds on the eastern margin (approximately 0.5-5°) and steeply dipping beds on the western edge (approximately 20-25°; Denson and others, 1980; Flores and Bader, 1999). Numerous coals seams occur in the Pleistocene Fort Union Formation and the Eocene Wasatch Formation. Both formations consist of sandstone, siltstone, and mudstone, with minor coal, conglomerate, limestone, and carbonaceous shale. Coal seams range from a few inches to more than 200 feet, with an average thickness of 25 feet. The Fort Union and Wasatch formations were deposited in a fluvial environment consisting of braided and meandering streams, floodplain lakes, and alluvial plains along basin margins. The stratigraphic relationship of coal seams is very complex; the beds merge, split, and pinch-out within short distances. The thickest and most laterally continuous coal beds are associated with a coal zone present in the upper part of the Fort Union Formation, known as the Wyodak-Anderson coal zone (Flores and Bader 1999). Much of the coalbed natural gas activity is concentrated in this zone.

Geologic setting of the study sites

Two geologically distinct CBNG mining locations were chosen by the WRP investigators to represent two different produced water discharge configurations: an on-channel discharge site near the center of the PRB, and an off-channel discharge site along its eastern edge (**Figure 1**). The on-channel research site is located on the ephemeral headwaters of Beaver Creek, a tributary of the Powder River, approximately 50 miles southwest of Gillette, Wyoming. The off-channel site is a pond that has been excavated one-half kilometer up-gradient from Coal Creek, also a tributary to the Powder River, near Ucross, Wyoming. The off-channel pond was constructed to prevent any overland flow.

Beaver Creek is one of the many tributaries to the Powder River and the WRP field site centers on one of Beaver Creek's ephemeral tributaries. CBNG in this area is produced from the Wyodak-Anderson coal zone, including the thick "Big George" seam. The study site extends for a mile along this ephemeral drainage and includes two CBNG on-channel ponds (**Figure 2**). Producers began to fill the lower pond on November 10, 2002, and the upper pond on November 20, 2002. Several CBNG production wells are tied together to discharge the product water into each of these excavated holding ponds. After the upper pond filled, around December 8, 2002 (Payne, 2004), water began flowing down the once-ephemeral stream channel.

Monitoring wells were installed by the WRP cooperative (Payne and Saffer, 2005; Wheaton and Brown, 2005) (**Figure 2**). A set of monitoring wells were placed up-gradient (south) from both of these ponds at the "upper well site" in order to allow sampling of groundwater that is unaffected by the CBNG discharge. Additional nested monitoring wells were placed between the two ponds at the "middle well site" and down-gradient (north) of both ponds at the "lower well site." Water sampling at two CBNG produced water discharge points, the two ponds, and the three monitoring well fields began in January 2003, one month after the upper pond had filled. Additional samples have been collected at approximately three-month intervals to the present. In each of the three well locations, samples were collected from wells completed within the alluvial layer as well as those completed in the underlying Wasatch Formation. In addition, water samples were also collected at two of the four weirs within the stream, one downstream of the upper pond and one downstream of the lower pond.

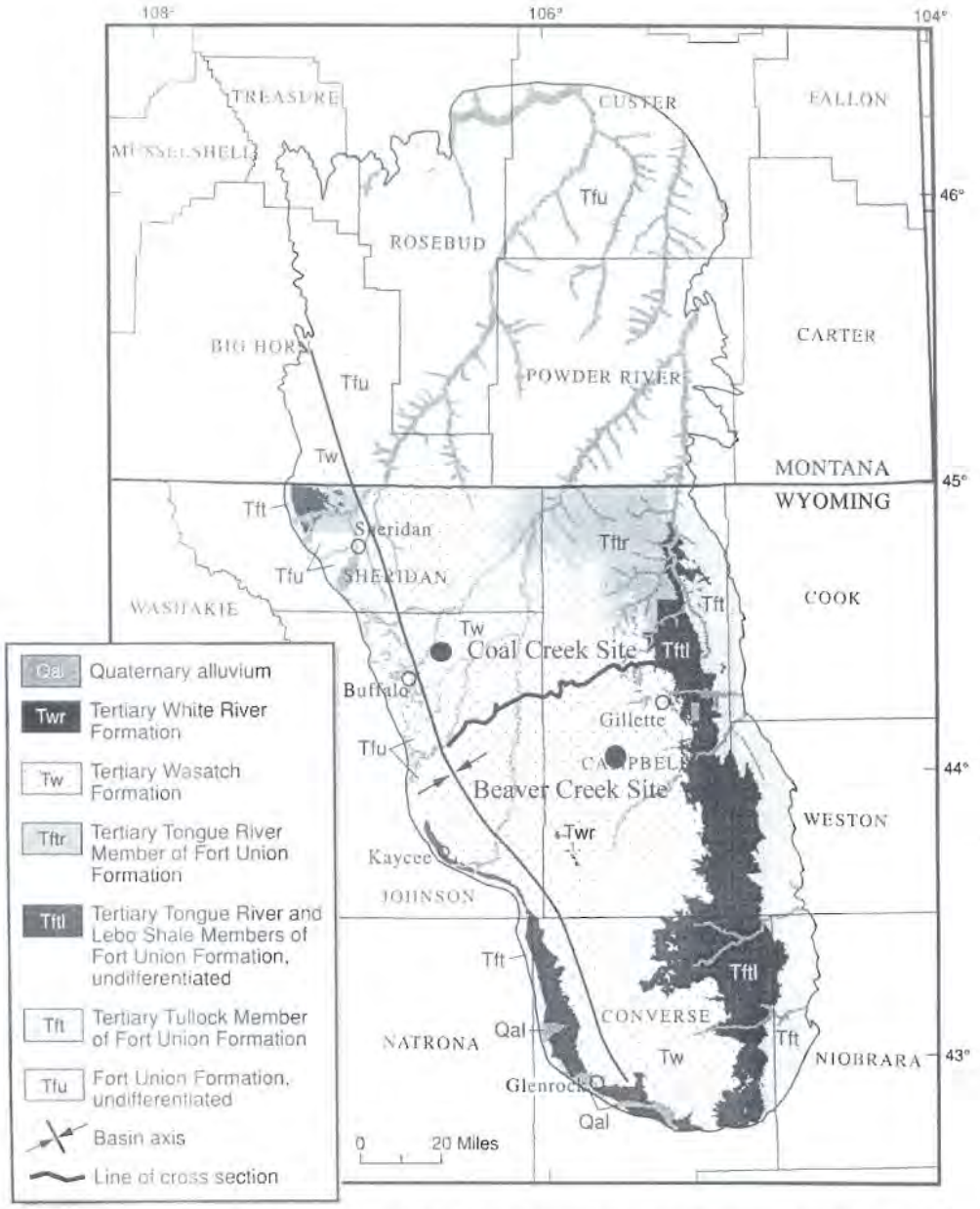


Figure 1. Geologic map of the Powder River Basin in Wyoming and Montana showing the approximate locations of the two WRP study sites: Coal Creek, near Ucross, Wyoming and Beaver Creek, near Gillette, Wyoming. From Rice and others (2002).

The majority of CBNG wells in the Ucross area target gas in the Eocene Roland Coal of the Wasatch Formation, although some are completed within the Anderson and deeper Fort Union coals. The off-channel, Coal Creek reservoir began filling a year after the Beaver Creek location, in January 2004. At the Coal Creek site, wells were installed along Coal Creek (down-gradient from the CBNG pond), surrounding the pond, and within the pond (Wheaton and Brown, 2005) (**Figure 3**). Wells along the stream are up to 57 feet deep, wells surrounding the pond reach depths of up to 160 feet, and within the pond a nested set of wells are completed at depths of 5, 23, and 35 feet Initial water samples were collected from each of the wells and the surface water before filling of the pond began, and periodic sampling continues.

Analytical details

Water samples from monitoring wells were collected after two casing volumes of water were removed; samples from flowing CBM discharge points, the ponds, and streams were collected directly. Temperature and pH were measured in the field, samples were filtered through a 0.45 micron filter, and kept cool and dark until laboratory analysis.

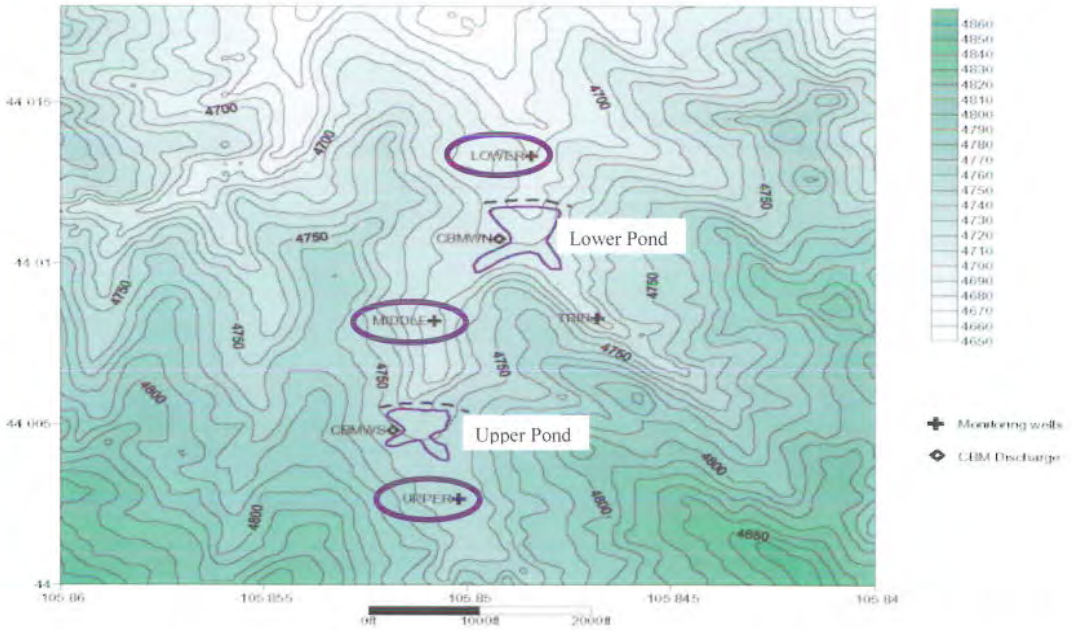


Figure 2. Topographic map of Beaver Creek showing the locations of the two on-channel CBNG discharge ponds and the three nested well locations up-gradient from the ponds, between the two ponds and down-gradient from both ponds. The middle well site, between the two ponds, is within the stream channel, while the lower well site, down-gradient from the ponds, is located on the creek's flood plain. Base map prepared by A. Payne.

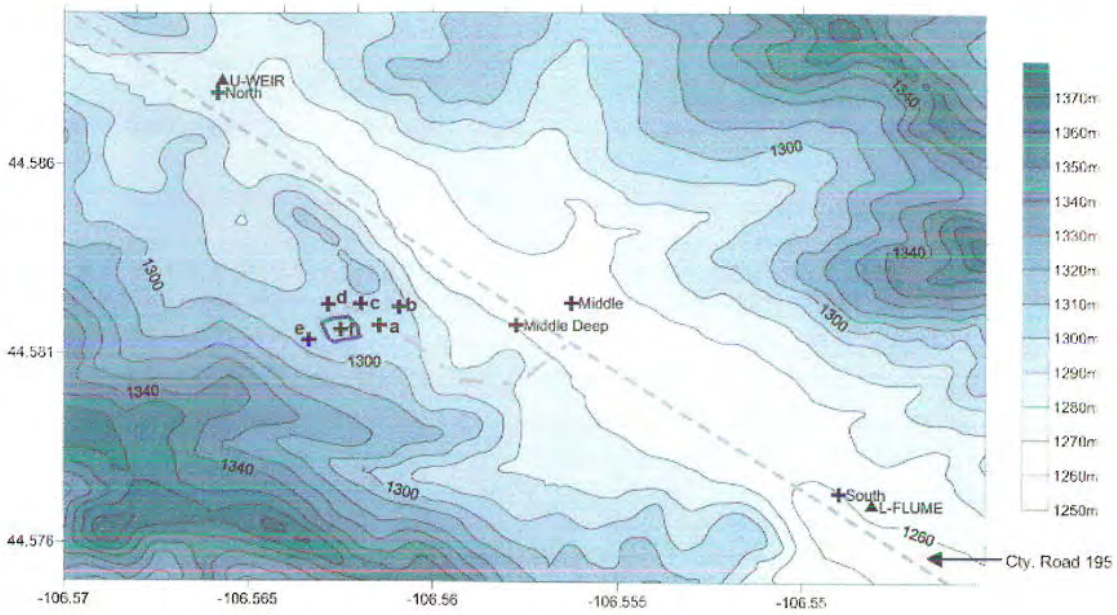


Figure 3. Topographic map of Coal Creek showing the location of the off-channel CBNG discharge pond, and the wells along the creek, surrounding the pond and within the pond. Base map prepared by A. Payne.

Strontium was isolated from a filtered, 3 ml aliquot of each water sample using Teflon columns filled with Eichrom® Sr-Spec resin and the Sr isotopic composition determined by thermal ionization mass spectrometry at the University of Wyoming. The internal precision of $^{87}Sr/^{86}Sr$ isotope measurements is ± 0.00001. 76 analyses of NBS 987 strontium standard measured during the course of this study gave an average value of $^{87}Sr/^{86}Sr$ = 0.71026 ± 0.00002 (2 standard deviations). All analyses were normalized to an $^{86}Sr/^{88}Sr$ value of 0.1194. Analytical blanks were 0.2 ng or lower, negligible compared to sample sizes of at least 0.1 microgram strontium. An additional 1-ml aliquot of each sample was spiked with an ^{84}Sr-enriched tracer and Sr concentration determined by isotope dilution. Sr concentrations are reproducible at the 1% level.

Results

Water samples have been collected on eight different dates over a period of twenty months at Beaver Creek (**Table 1**). In general, the CBNG product water and the upper well site (baseline) water have remained constant in terms strontium concentration and $^{87}Sr/^{86}Sr$ ratio throughout the monitoring period. From the time it was first sampled in January 2003, the middle well site water samples have had $^{87}Sr/^{86}Sr$ ratios intermediate between the ambient water ratio and the CBNG water ratio. The lower well site has shown dramatic fluctuations in strontium concentration and over time only a slight shift in $^{87}Sr/^{86}Sr$ ratio towards that of the CBNG water.

CBNG mining in the Coal Creek area began in January 2003. Initial baseline samples were taken the spring and summer preceding the filling of the pond, and thrice since (**Table 2**). The initial samples taken from the wells surrounding the pond show more variation in $^{87}Sr/^{86}Sr$ ratio than one would generally expect from wells in such close proximity. We tentatively attribute this variability to insufficient flushing of the wells after completion and prior to sampling. After filling of the pond began, samples have been collected only from those wells that showed an increase in water level and from wells along the stream. The only changes in strontium concentration and $^{87}Sr/^{86}Sr$ ratio detected to date are in samples from wells within the pond.

Discussion

Distinguishing CBNG product water from ambient water

At both the Beaver Creek and the Coal Creek sites CBNG-produced water is easily distinguished from ambient shallow groundwater and surface water by the $^{87}Sr/^{86}Sr$ ratio. **Figure 4** is a summary of the results from Beaver Creek showing the distinction between CBNG water and the ambient water, as well as evidence for the interaction between CBNG water and the near-surface environment, as discussed in a later section. The CBNG water, shown by black diamonds, is easily distinguished from the ambient water, represented by open squares. In the Beaver Creek location, the water co-produced during CBNG mining is more radiogenic (higher $^{87}Sr/^{86}Sr$ ratio) than the ambient water.

The opposite is seen in the Coal Creek area, where the ambient water (black squares) is more radiogenic than

Table 1. Strontium isotopic and concentration data from the Beaver Creek site.

				January 2003		April 2003		August 2003		October 2003		December 2003		February 2004		May 2004		August 2004	
Stream Location	ID	Formation	Depth (ft)	Sr ppm	$^{87}Sr/^{86}Sr$	Sr ppm	$^{87}Sr/^{86}Sr$	Sr ppm	$^{87}Sr/^{86}Sr$	Sr ppm	$^{87}Sr/^{86}Sr$	Sr ppm	$^{87}Sr/^{86}Sr$	Sr ppm	$^{87}Sr/^{86}Sr$	Sr ppm	$^{87}Sr/^{86}Sr$	Sr ppm	$^{87}Sr/^{86}Sr$
Upper	UP-CBM	Ft. Union		1.36	0.71401			1.40	0.71388	1.23	0.71391	1.21	0.71391	1.19	0.71402	1.09	0.71397	1.15	0.71415
	UP-Q	surface	0	0.87	0.71397	0.99	0.71406	0.75	0.71394	0.75	0.71394	0.74	0.71393			0.63	0.71397		
	BC-2	Alluvium	18	1.32	0.71279	2.48	0.71255	1.54	0.71278	1.38	0.71275	1.77	0.71260			1.34	0.71276	1.40	0.71275
	BC-4	Wasatch	31.5	2.29	0.71262	1.63	0.71271	1.90	0.71260	1.80	0.71259	1.10	0.71274			1.88	0.71258	1.75	0.71260
	BC-4	duplicate		1.56	0.71277														
	BC-4	duplicate		1.88	0.71260														
Middle	M-SS	surface	0			1.28	0.71380	0.68	0.71388	0.58	0.71390	0.85	0.71374			0.60	0.71342		
	BC-5	Wasatch	38	1.70	0.71312					0.85	0.71324	1.02	0.71312			0.95	0.71323	1.03	0.71316
	BC-6	Alluvium	25.8	1.59	0.71343	0.94	0.71346					0.69	0.71329						
	BC-6	duplicate		0.67	0.71344														
	BC-7	Alluvium	25					1.19	0.71311	1.09	0.71311					0.93	0.71311	0.98	0.71310
	BC-8									0.61	0.71322								
Lower	LP-CBM	Ft. Union		1.29	0.71411			1.36	0.71422	1.20	0.71420	1.08	0.71423	1.14	0.71423	1.22	0.71436	1.26	0.71441
	LP-Q	surface	0	0.99	0.71403			0.83	0.71415	0.71	0.71416	0.78	0.71416			0.74	0.71428		
	L-SS	surface	0			1.02	0.71344	0.75	0.71392	0.65	0.71381	0.91	0.71370			0.62	0.71392	0.44	0.71382
	BC-11	Wasatch	38	4.97	0.71269	1.37	0.71274	2.30	0.71278	2.01	0.71276	1.94	0.71271			1.93	0.71273	1.92	0.71272
	BC-11	duplicate		3.35	0.71271														
	BC-13									5.79	0.71291								
	BC-14	Alluvium	15	4.72	0.71282	5.00	0.71283	12.32	0.71289	7.49	0.71287	6.58	0.71289	6.90	0.71287	7.19	0.71289	7.68	0.71293
	BC-14	duplicate		4.72	0.71282														

Table 2. Strontium isotopic and concentration data from the Coal Creek site.

				March/April 2003		June/July 2003		December 2003		February 2004		June 2004	
Location	ID	Formation	Depth (ft)	Sr ppm	$^{87}Sr/^{86}Sr$	Sr ppm	$^{87}Sr/^{86}Sr$	Sr ppm	$^{87}Sr/^{86}Sr$	Sr ppm	$^{87}Sr/^{86}Sr$	Sr ppm	$^{87}Sr/^{86}Sr$
upper Coal Creek	CCUW	surface	0	1.38	0.71408	0.87	0.71400				frozen		
	CCUC	surface	0	0.16	0.71399						frozen		
	1cc2q	Alluvium	17			1.49	0.71402			1.78	0.71402		
	1cc3q									1.08	0.71400		
	1cc4q	Alluvium	19.5	1.33	0.71393								
	1cc1b	Wasatch	27	0.80	0.71298	1.14	0.71397			0.94	0.71387		
middle Coal Creek	CCMC	surface	0	0.29	0.71403					1.41	0.71404		
	MSP (spring)	surface	0							2.16	0.71397	1.87	0.71406
	12ac3q	Alluvium	14			1.87	0.71405						
	12ac3q	duplicate				2.13	0.71405						
	12ac4q	Alluvium	23	0.96	0.71364								
	12ac1b	Wasatch	57			0.42	0.71390						
	12ac2b	Wasatch	40			2.22	0.71409						
lower Coal Creek	CCLC	surface	0	0.46	0.71400								
	12da2q	Alluvium	17	2.19	0.71399	2.71	0.71409			1.89	0.71408		
	12da1b	Wasatch	36			3.13	0.71385			1.91	0.71406		
upper pond	12ba5b		156			0.17	0.71340						
	12ba9b		59			2.62	0.71406					2.33	0.71419
within pond	12ba6b		36			2.21	0.71421	1.97	0.71422			1.81	0.71423
	12ba7b		23			2.14	0.71398	6.74	0.71424			7.24	0.71429
	12ba8b		5				dry		dry		dry	0.84	0.71330
lower pond	12ba1b		43			3.05	0.71368						
	12ba2b		34			1.18	0.71295						
	12ba3b		141			0.13	0.71383						
	12ba10b		151			0.76	0.71366			0.60	0.71410		
	12ba11b		160			0.14	0.71439						
	12ba12b		65			1.96	0.71344						
Pond	SP (pond)	surface	0					0.24	0.71183			0.14	0.71248
CBM	SP-CBM							0.24	0.71178				

the CBNG produced water (open circle) (**Figure 5**). The higher ratio in the ambient surface and near-surface water is most likely attributable to proximity of the study site to the radiogenic Precambrian rocks exposed in the Bighorn Mountains. Additionally, groundwater contained within the Eocene coals being mined for natural gas in this area typically has less radiogenic Sr isotope compositions than Ft. Union coals (Pearson, 2002). Although the $^{87}Sr/^{86}Sr$ ratios of waters produced from coals and ambient surface and near-surface waters are different from each other in these two locations, at each site the CBNG water is readily distinguishable from the ambient water.

Tracing the infiltration of CBNG water from ambient water

Beaver Creek site

CBNG produced water has been discharged at Beaver Creek from December 2002 to the present. Hydrologic monitoring at the site shows that infiltration of CBNG water has led to increased ground water levels in the monitoring wells at the middle and lower sites, and that ground water is mounded along the channel within the study site downstream

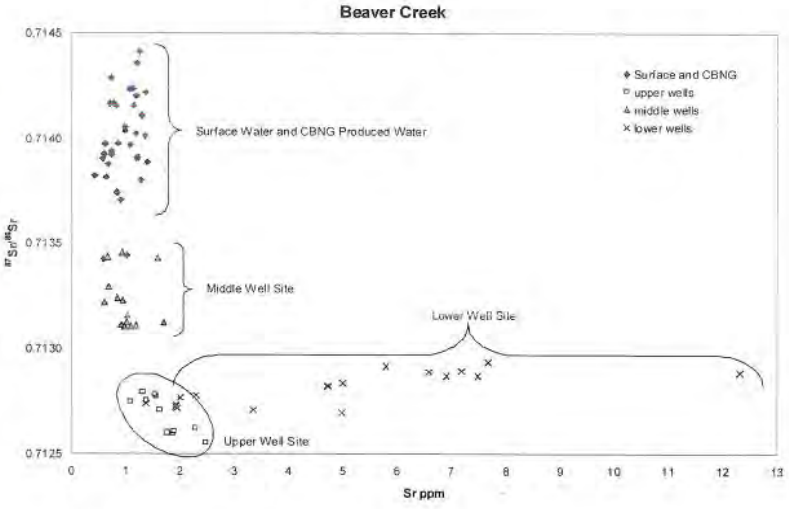


Figure 4. Graph summarizing the $^{87}Sr/^{86}Sr$ ratios and strontium concentrations of water samples from Beaver Creek. The CBNG water, pond samples and creek samples, represented by black diamonds, are the most radiogenic samples. The upper wells water samples, represented by open squares, are unaffected by the infiltration of CBNG water and used for baseline comparisons. Samples from the middle wells, located within the channel (grey triangles), have an $^{87}Sr/^{86}Sr$ ratio between that of the CBNG water and baseline water indicating a mixing of strontium, approximately half of which is from CBNG water and half from shallow sources. Water from the lower wells, represented by crosses, show a slight increase in ratio towards that of the CBNG water and a significant increase in strontium concentration. This increase may be related to the location of the wells on the flood plain as opposed to within the channel.

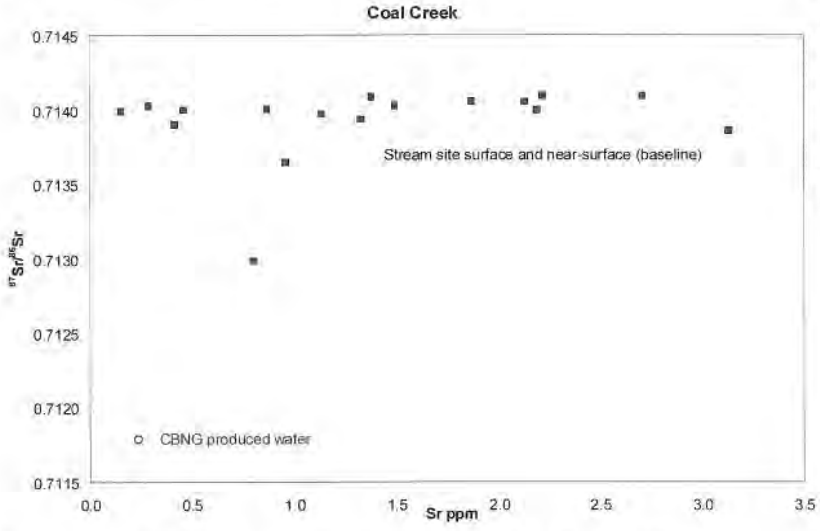


Figure 5. Graph showing initial measurements of $^{87}Sr/^{86}Sr$ and strontium concentration at Coal Creek. The wells along the stream and the surface water, represented by black squares, represent the most radiogenic measurements at this site. The CBNG produced water, represented by the open circle, is the least radiogenic sample. Mixing of CBNG water with the ambient water in this area should result in intermediate $^{87}Sr/^{86}Sr$ values.

of the upper pond (Payne, 2004; Payne and Saffer, 2005). This infiltration is also evident from the Sr isotopic data.

As noted above, the CBNG produced waters, represented by black diamonds on **Figure 4**, have more radiogenic strontium ratios (higher $^{87}Sr/^{86}Sr$) than do the ambient groundwater samples (open squares) measured at the upper well site location. This difference makes it possible to track the interactions of these waters. The interaction is shown in groundwater collected down-gradient from the CBNG discharge at the middle well site (gray triangles). The groundwater in these wells has an intermediate strontium isotopic ratio lying between the measured ratios of CBNG and ambient water. This intermediate ratio suggests that approximately half of the strontium in these well waters is introduced from produced water, and half from the near-surface environment. This ratio was achieved within 32 days of the upper pond filling, indicating that CBNG water reached 38-foot-depths by this time. Thirty-two days, therefore, represents a maximum infiltration time to the water table. This estimate agrees well with the results of the two-layer infiltration model of Payne (2004) and Payne and Saffer (2005).

Wells sampled farther downstream at the lower well site, represented by crosses on **Figure 4**, have shown only modest increases in ratio towards that of the CBNG input water but have shown significant changes in concentration. The strontium concentration of water from the lower alluvial well spiked in August 2003 and has continued to slowly increase from December 2003 to the present (**Figure 6**).

The large fluctuations in strontium concentration at the lower site and the relative absence of such changes in concentration at the middle site may be related to the locations of the wells. At the middle site the wells were drilled in the stream channel itself in a location that experiences annual flushing of soluble salts in the soil profile. The lower site monitoring wells lie 18 to 45 feet off

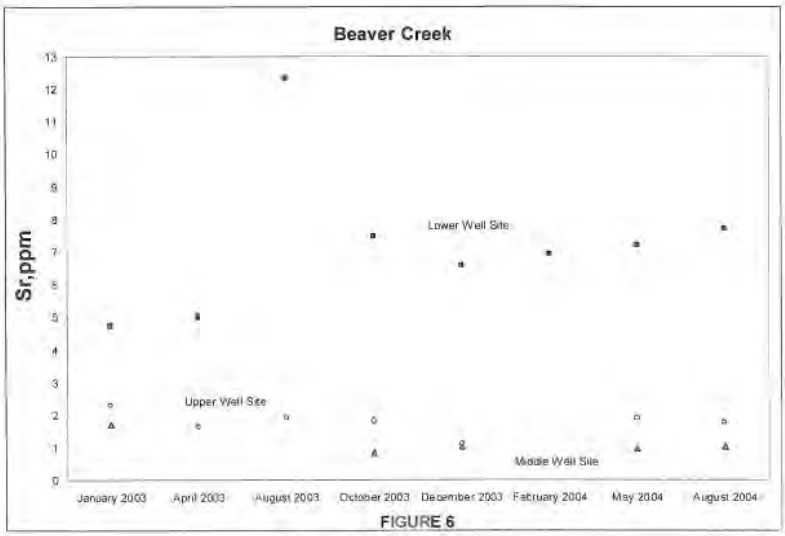


Figure 6. Graph of the strontium concentration trend with time for one well at each of the three well sites at Beaver Creek: the upper and middle wells are completed in the Wasatch Formation and the lower site well is completed in the alluvium. Whereas the upper and middle well sites show very little fluctuation during the 20 month monitoring period, the lower well shows a spike in concentration in August, 2003, followed by a decrease in concentration until December, 2003. Since that time the concentration has been steadily increasing.

the channel on a terrace several feet above the channel. The soil on this flood plain builds up soluble salts between rare flooding events. This area is now impacted by groundwater mounding related to CBNG discharge (Payne, 2004), and this groundwater is dissolving some of these soluble salts, leading to the observed increased concentrations of Sr and other major ions.

Coal Creek site

To date, Sr isotopic ratios from Coal Creek and the associated monitoring wells along the creek have remained constant. Limited data have been obtained from the monitoring wells around the discharge pond because many of those wells have been dry during sampling dates. However, it appears that some of the initial heterogeneity in Sr isotopic composition measured shortly after the wells were completed has disappeared. Since December 2003, the monitoring wells have yielded groundwater with $^{87}Sr/^{86}Sr = 0.7141$ to 0.7143. We therefore tentatively attribute the initial variability to insufficient flushing of the wells after completion and prior to sampling.

Water from two of the three monitoring wells within the pond at the Coal Creek site have strontium characteristics suggesting CBNG impacts directly below the pond itself. These wells in the middle of the pond are 5 and 23 feet deep. The 5-foot deep well was dry for the first four sampling dates, and the first water sample was collected in June 2004, resulting in a single data point on **Figure 7**. At that time it yielded water with $^{87}Sr/^{86}Sr = 0.7133$, a ratio intermediate between the shallow groundwater and the CBNG-produced water. We interpret this to reflect CBNG water infiltration beneath the pond. **Figure 8** shows Sr data from the pond and the monitoring wells within the pond, which indicates an increase in $^{87}Sr/^{86}Sr$ ratio with depth below the pond surface. The pond sample plotted was collected 0.25 foot above the floor of the pond.

There is an order of magnitude less Sr in the CBNG water than in the near surface groundwater. This means that the Sr isotopic ratio of CBNG produced water will change dramatically with only small inputs of Sr from the near-surface sources. In the shallowest well beneath the Coal Creek retention pond there is a slight increase in strontium concentration compared to the discharge CBNG water that we attribute to dissolution of local soluble salts. The addition of this strontium reduces the CBNG strontium ratio to one closer to that of the strontium ratio of ambient shallow groundwater. By the time the water has infiltrated to the depth of the middle well, the concentration has increased from approximately 2 ppm to approximately 7.5 ppm, the strontium in the CBNG water has been swamped by strontium from the shallow aquifer materials, and the strontium isotope ratio is indistinguishable from the ratio in shallow groundwater that contains no CBNG component (**Figure 7**).

Identifying the effects of CBNG water upon water quality using strontium concentration as a corollary for total dissolved solids

Strontium is chemically similar to calcium and is typically found in concentrations proportional to those of calcium. Wheaton and Brown (2005) have shown that the presence of infiltrating CBNG water correlates with an increase in total dissolved solids (TDS) in the aquifers subject to infiltration. Changes in TDS due to dissolution of calcium bearing minerals such as calcite and gypsum will also be manifest as increases in strontium concentration. This is seen in water from the lower site at Beaver Creek

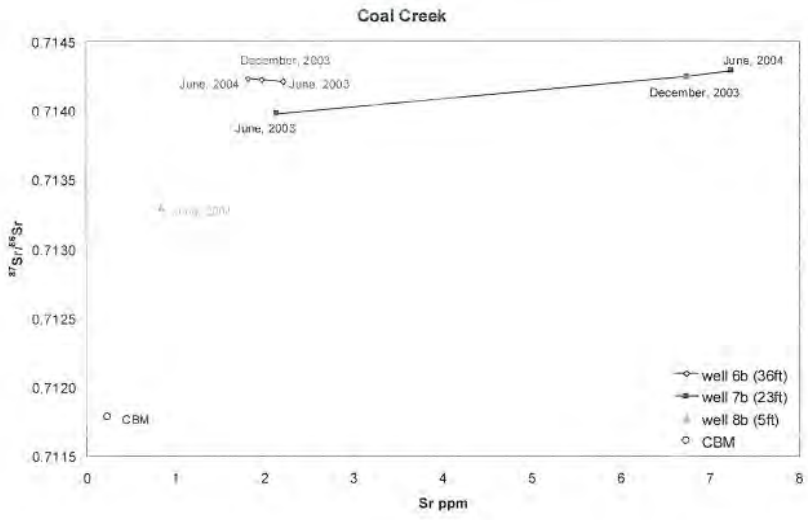


Figure 7. Graph showing the $^{87}Sr/^{86}Sr$ and strontium concentrations of the wells within the pond at Coal Creek and the CBNG sample (open circle) for three sampling dates. The shallowest well, represented by a grey triangle, was dry until the June, 2004 sampling date. The deepest well, represented by open diamonds, shows little change over the year of sampling, while the middle well, represented by black squares, shows an increase both in Sr isotope ratio and in concentration.

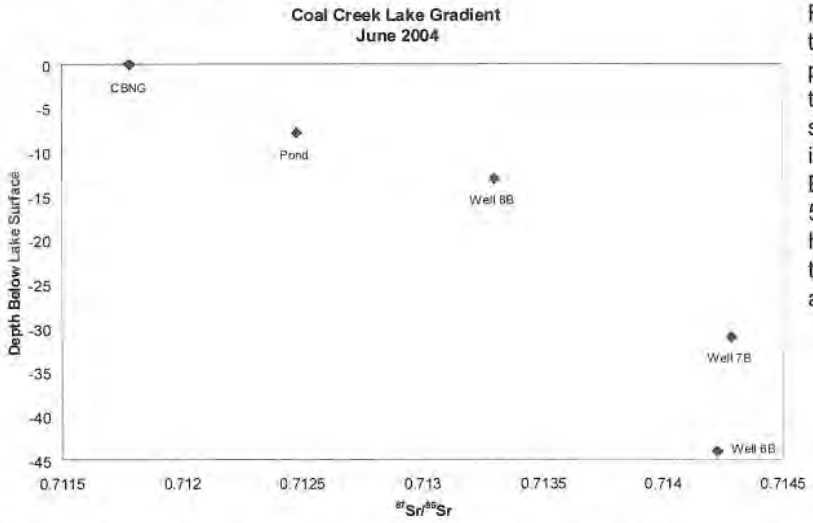


Figure 8. Graph of strontium ratio versus depth within the off-channel pond at Coal Creek. The water sample plotted at the surface is the CBNG discharge water. Water is within 0.25 feet of the floor of the pond (the "pond" sample) has incorporated some of the local strontium, as is indicated by a shift towards a more radiogenic ratio. By the time the water from the pond infiltrates to a well 5 feet below the floor of the pond it acquires an even higher ratio. Water in the deepest two wells has a strontium isotope ratio that is indistinguishable from that of the ambient shallow groundwater.

(**Figure 4**) as well as in samples taken from the wells within the Coal Creek pond (**Figure 7**).

Water samples from the lower well site at Beaver Creek, represented by crosses in **Figure 4**, show only slight increase in ratio but a dramatic increase in concentration over time. An early spike in concentration followed by a gradual climb is evident on a plot of strontium concentration versus time (**Figure 6**). Major ion chemistry performed by Montana State University shows corresponding increases in TDS (**Figure 9**) (Montana Bureau of Mines and Geology, 2004). As was explained in a preceding section, the concentration differences between Beaver Creek's middle and lower sites are interpreted as the result of their proximity to the stream channel. The middle wells are within the channel and are flushed annually during spring snowmelt. The lower wells only see flushing during major flooding events. Similarly at the Coal Creek site, the area below the pond had never experienced sustained saturated flow before the introduction of CBNG water, allowing for large amounts of soluble salts to accumulate.

These results suggest that CBNG water discharge into existing drainages may be less detrimental to the water quality of underlying shallow aquifers than discharge into off-channel containment ponds. Continued monitoring of both sites should provide the data required in order to predict how long it will take after the introduction of CBNG water to see decreases in TDS as soluble salts are removed from the system. Our monitoring over nearly two years at the Beaver Creek middle and lower sites shows that soluble salts continue to be incorporated into infiltrating CBNG waters. The flushing process will presumably take longer at the off-channel sites where larger amounts of soluble salts have accumulated.

Evaluate the possibility of leakage in deep aquifers

CBNG discharge water was monitored for shifts in strontium ratio that would indicate aquifer leakage. Drawdown of adjacent aquifers caused by water withdrawal from coal seams should be marked by a decrease in the Sr isotopic ratio of the produced water (Frost and others, 2002a). At the Beaver Creek site, variations in the $^{87}Sr/^{86}Sr$ of the produced water were observed, but because several wells are tied to a common discharge point and the proportion of water produced from individual wells changed with time, it is impossible to make any conclusions based on this observation. During 2003 two wells (API 49-005-44186 and 49-005-44124) were discharging into the upper pond. In the summer of 2004, 49-005-44124 was removed and replaced with well 49-005-34573. Changes also occurred in the wells discharging into the lower pond: three wells (API 49-005-49986, 49-005-44126, and 49-005-50127) discharged into the lower pond from November 2002 until April 2004 at which time three more wells were added. The water produced from these three new wells was split between the lower pond and another pond to the east. Records on water production from individual production wells and their discharge points are insufficient to interpret the Sr isotopic ratio data from the discharge points into the Beaver Creek ponds. To monitor for aquifer leakage using strontium isotope it would be best to monitor individual wells directly, before the water was mixed with other wells for disposal. Unfortunately, access to individual well stems is not readily available.

Groundwater ages of coal sandstone aquifers

Estimating the age of the water in the coal seams mined for natural gas is important for understanding recharge rates. CBNG wells withdrew 23.8 billion gallons of water in 2003 alone (Wyoming Oil and Gas Conservation Commission,

2004). In situations where pumping rates exceed the rate of recharge, aquifers will become depleted and drawdown may promote leakage from overlying or underlying aquifers. In the PRB, residents rely on groundwater for domestic, agricultural, and industrial use. If drawdown due to excessive withdrawal of water during CBNG mining causes water levels to drop in aquifers commonly used for domestic uses, conflicts between mineral rights and water rights may result. Knowing the approximate age of the water in the coal aquifers is critical to estimating recharge rates and predicting potential drawdown.

We attempted to obtain carbon-14 dates on groundwater from three wells: two CBNG wells tapping the Big George coal seam in the Double Tanks field of Beaver Creek and discharging into the upper pond (only one of which, API 49-005-34573, S34 T47N R75W, yielded ^{14}C data), and one artesian well tapping a sandstone aquifer at Rose Draw, just west of the Powder River (S19 T52N R77W). Five gallons of water were collected from the CBNG wells and ten gallons from the sandstone well. Sodium hydroxide (10N) was added in the field until the water was pH 11 or greater to convert all the dissolved inorganic carbon to carbonate. Barium chloride was added to convert all the carbonate and sulfate into barium carbonate and barium sulfate. In the lab, this solution was decanted and the precipitate collected under a nitrogen atmosphere.

Radiocarbon dates are based on the premise that ^{14}C is introduced from the atmosphere into groundwater during recharge, and that the percent of the initial ^{14}C that remains when the groundwater is sampled is a function of age. The dating of groundwater is complicated by the presence of carbon incorporated into the groundwater subsequent to recharge, including carbon introduced by carbonate dissolution or from methane in the aquifer. The $^{13}C/^{12}C$ ratio (expressed as delta-^{13}C) of water may be used to correct the measured activity of ^{14}C for these additional sources of carbon. Accordingly, the precipitates were analyzed both for delta-^{13}C and for carbon-14 at Brigham Young University (BYU). Delta-^{13}C values of +20.5, +22.3, and +8.7 per mil were measured for the two CBNG wells and the sandstone well respectively. Assuming that all the bicarbonate in the Big George coal waters is derived from methane-CO_2 equilibration, then the delta-^{13}C of the methane is approximately –55 per mil, a value typical of methanogenic carbon. This in turn suggests that the carbon budget in Big George groundwaters is dominated by methane. It is not surprising, therefore, that the ^{14}C value of the one CBNG well chosen for ^{14}C counting on BYU's ultra-low counter (the well with delta-^{13}C of +20.5) yielded a result of -0.3 +/- 0.3 percent modern carbon (pmc). Although taken at face value this result could be interpreted to suggest that the water is older than the effective dating range of ^{14}C (about 30,000 years), we must conclude that the method is not appropriate for groundwater samples in which the bicarbonate budget is dominated by methanogenic sources.

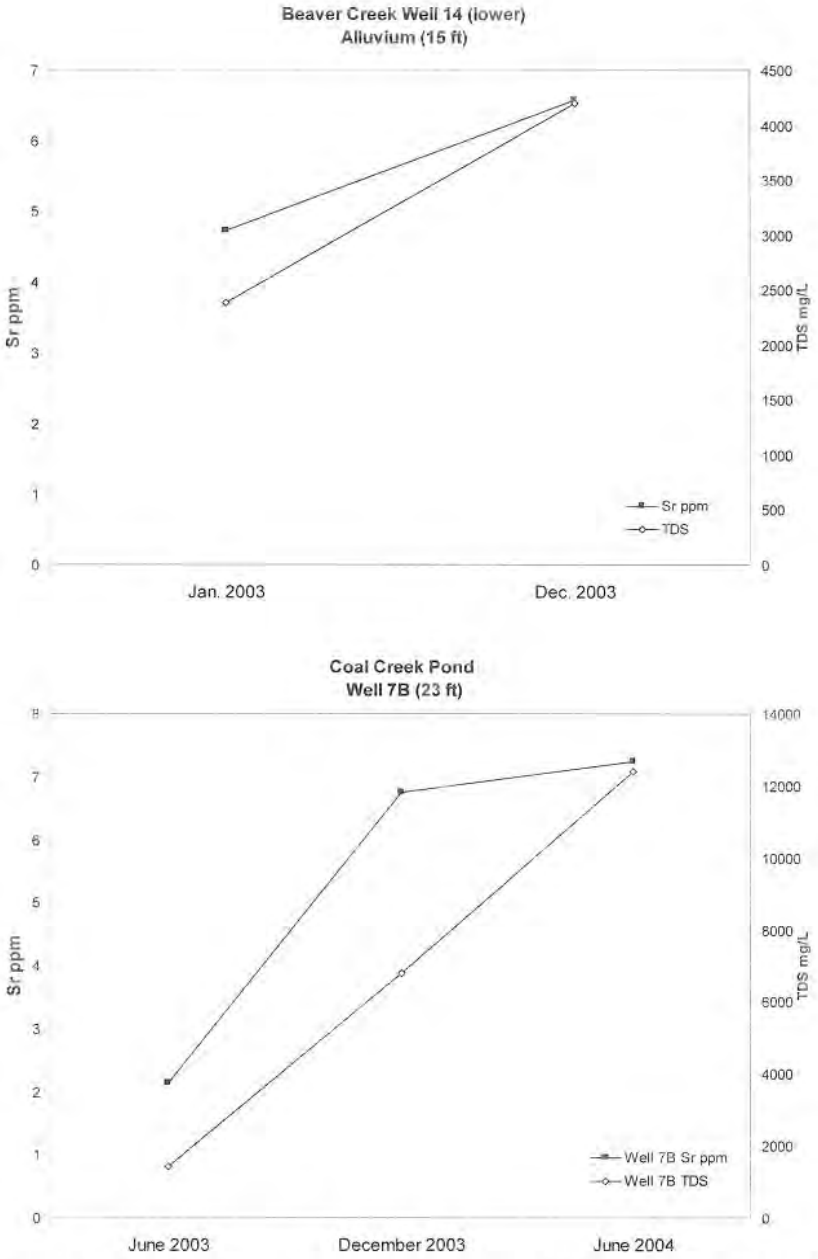


Figure 9. Graphs of strontium concentration and TDS versus time for well BC-14 at Beaver Creek's lower well site (top) and for well 7b (bottom) within the pond at Coal Creek. In both of these situations increases in TDS are correlated with increases in strontium concentrations.

The water from the Rose Draw sandstone well has delta -^{13}C of +8.7, which most likely reflects a mixed system of carbon from methane and carbon from recharge. Its raw ^{14}C activity of +7.8 +/- 0.8 pmc is interpreted to suggest that the maximum mean age of the groundwater in this aquifer is 21,000 years. The true age will be younger because only a portion of the carbon is from surface recharge. This estimate, though extremely rough, is within the range of age estimates for groundwaters in the vicinity of the Powder River by Pearson (2002). His estimate based upon extrapolation from the maximum distance from the eastern recharge zone that tritium is detected in groundwater was a minimum of 2000 to 6000 years. Based upon rudimentary calculations using Darcy's law and published parameters for hydraulic conductivity Pearson (2002) determined that groundwaters in coal seams below the Powder River would likely be in the age range of 7500 to 75,000 years.

Future work

We plan future studies of the soil and alluvium at the lower well site at Beaver Creek in order to better understand to sources of soluble salts that are contributing to the increase in TDS and strontium concentration. This work will include paste extracts and step dissolution analyses. The step dissolution will consist of identifying the exchangeable fraction through treatment with a $MgCl_2$ solution, the carbonates with NaOAc leaching, the carbonates, sulfides, gypsum, phosphates, and hydrated oxides through HCl leaching, and the silicates with HF and $cHNO_3$ leaching (Tessier and others, 1979). Carbonate species are prevalent in the PRB, so by isolating the source of changes in strontium concentration it should be possible to predict the types of soils that will result in high levels of TDS. These soils could then be avoided for use as CBNG product water disposal sites in the future.

The Coal Creek site will continue to be monitored to see whether the plume of high TDS progresses to the deepest well within the pond. Additionally, we will continue to monitor the wells surrounding the pond to see if we detect the movement of the CBNG water laterally. It may be possible to detect CBNG water influence by monitoring increases in strontium concentration even if there is no discernable change in strontium ratio.

Conclusions

We have shown strontium tracers to be a powerful tool for tracing the interaction of water discharged during coalbed natural gas production as it interacts with the surface and near-surface environment. The fundamental characteristic that allows this tracer to be applied is the ^{87}Sr/^{86}Sr ratio, which is markedly different in the CBNG water to that of the surface and near-surface waters in the PRB. We have used this tool to trace the infiltration of product water and show a connection between changes in TDS and strontium concentration

Through the use of strontium isotope tracing, this study successfully detected CBNG produced water within the alluvial and Wasatch aquifers at the middle site at Beaver Creek within one month after the upper pond filled. A ^{87}Sr/^{86}Sr signal from CBNG water was also detected in the lower wells at Beaver Creek, but the CBNG water did not raise the ambient water's ratio to the same extent as seen at the middle site. We attribute this to the dissolution of the soluble salts in the off-channel soils at the lower site. The dissolution of these salts may also account for the increases in strontium concentration seen at the lower well site. Major ion chemistry data from this site shows a parallel rise in total dissolved solids.

Strontium tracing at Coal Creek shows the influence of CBNG water directly below the excavated pond. As soon as water was present in the shallowest well within the pond, it showed an intermediate strontium ratio composition between the CBNG discharged water and the local water. In this well, local geologic materials contributed a strontium ratio similar to that recorded in shallow, ambient groundwater in the area, increasing the sampled water's strontium ratio from the CBNG ratio. By the time the CBNG water reaches the middle well within the pond, the local strontium ratio dominates. This effect is also seen in these wells' strontium concentrations. The shallowest well has slightly more strontium than the discharged CBNG water, while the middle site has significantly more strontium than the discharged CBNG water. The deepest well within the pond does not show the influence of CBNG water, perhaps due to an aquitard in place between the middle and deepest well (Wheaton and Brown, 2005). The major ion chemistry of these samples also shows corresponding increases in TDS.

The results of our study also suggest that changes in strontium concentration are correlated to changes in total dissolved solids and that both are related to the amount of soluble salts in near-surface soils and regolith. Both strontium and TDS are higher when CBNG water infiltrates in the off-channel locations studied: the lower well site at Beaver Creek and the disposal pond at Coal Creek. This is tentatively attributed to the greater build-up of soluble salts in areas that do not experience annual saturated flow. The middle site at Beaver Creek is within a stream channel that, prior to CBNG discharge, received saturated flow annually, whereas the lower site's placement on the flood plain experienced saturated flow only during major flooding

events. Similarly, Coal Creek's off-channel pond was placed in geologic material that had rarely experienced saturated flow prior to the introduction of CBNG water.

Acknowledgements

Peter Valley and Aaron Payne assisted with sample collection during the first six months of this study, and Peter Valley is thanked for technical assistance with the strontium isotopic analyses during the same period. Drs. Steve Nelson and Alan Mayo with their laboratory staff at the Department of Geology, Brigham Young University generously provided the radiocarbon analyses. Since July 2003 this study has been the responsibility of Elizabeth Brinck, Ph.D. student on the project. It is thanks to her insight and effort that this study was completed and this report became reality.

References cited

Bullen, T.D., Krabbenhoft, D.P., and Kendall, C., 1996, Kinetic and mineralogic controls on the evolution of groundwater chemistry and $^{87}Sr/^{86}Sr$ in a sandy silicate aquifer, northern Wisconsin, U.S.A.: Geochimica et Cosmochimica Acta, v. 60, no. 10, p. 1807-1821.

Clark, M.L., Miller, K.A., and Brooks, M.H., 2001, U.S. Geological Survey monitoring of Powder River Basin stream-water quantity and quality: U.S. Geological Survey Water-Resources Investigations Report 01-4279, 8 p.

Creedy, D. and Tilley, H., 2003, Coalbed methane extraction and utilization. Journal of Power and Energy: Proceedings of the Institution of Mechanical Engineers, v. 217 part A, p. 19-25.

De Bruin, R.H. Lyman, R.M., Jones, R.W., Cook, L.W., 2004, Coalbed methane in Wyoming. Wyoming State Geological Survey Information Pamphlet 7 (revised), 19 p.

Denson, N.M., Dover, J.H., and Osmonson, L.M., 1980, Structure contour and isopach maps of the Wyodak-Anderson coal bed in the Reno Junction-Antelope Creek area, Campbell and Converse counties, Wyoming: U.S. Geological Survey Miscellaneous Investigations Map I-1194.

Flores, R.M., and Bader, L.R., 1999, Fort Union coal in the Powder River Basin, Wyoming and Montana: A synthesis: U.S. Geological Survey Professional Paper 1625A, Chapter PS, 49 p. on CD-ROM.

Frost, C.D., Pearson, B.N., Ogle, K.M., Heffern, E.L., Lyman, R.M., 2002a, Sr isotopic tracing of aquifer interactions in an area of coal and methane production, Powder River Basin, Wyoming: Geology, v. 30, p. 923-926.

Frost, C.D., Viergets, J.E., Pearson, B.N., Heffern, E.L., Lyman, R.M., and Ogle, K.M., 2002b, Sr isotopic identification of coal and sandstone aquifers and monitoring of aquifer interactions in an area of active coal bed methane production, Powder River Basin, Wyoming: Wyoming Geological Association 52nd Field Conference Guidebook, p. 107-121.

Frost, C.D., and Toner, R.N., 2004, Strontium isotopic identification of water-rock interaction and groundwater mixing: Ground Water, v. 42, 418-432.

Graustein, W.C., and Armstrong, R.L., 1983, The use of strontium-87/strontium-86 ratios to measure atmospheric transport into forested watersheds: Science, v. 219, p. 289-292.

Hunter, J., 1999, Fluvial architecture and paleo-ground water infiltration of the Fort Union Formation near the Highland Uranium Mine, southern Powder River Basin, Wyoming, *in* Miller, W.R., editor, Coalbed methane and the Tertiary geology of the Powder River Basin, Wyoming and Montana: Wyoming Geological Association 50th Annual Field Conference Guidebook, p. 119-139.

Montana Bureau of Mines and Geology, Montana Tech of The University of Montana, Ground-Water Information Center, <http://mbmggwic.mtech.edu/>, accessed December 2004.

Payne, A.A., 2004, Surface water hydrology and shallow groundwater effects of coalbed methane development, upper Beaver Creek drainage, Powder River Basin, Wyoming: M.S. thesis, Department of Geology and Geophysics, University of Wyoming, Laramie, 116 p.

Payne, A.A., and Saffer, D.M., 2005, Surface water hydrology and shallow groundwater effects of coalbed natural gas development, upper Beaver Creek drainage, Powder River Basin, Wyoming, *in* Zoback, M.D., editor, Western Resources Project Final Report—Produced groundwater associated with coalbed natural gas production in the Powder River Basin: Wyoming State Geological Survey Report of Investigations No. 55, p. 5-44.

Pearson, B.N, 2002, Sr isotope ratio as a monitor of recharge and aquifer communication, Paleocene Fort Union Formation and Eocene Wasatch Formation, Powder River Basin, Wyoming and Montana: M.S. thesis, Department of Geology and Geophysics, University

of Wyoming, Laramie, 151 p.

Rice, C.A., Bartos, T.T., and Ellis, M.S., 2002, Chemical and isotopic composition of water in the Fort Union and Wasatch Formations of the Powder River Basin, Wyoming and Montana: Implications for coalbed methane development: The Rocky Mountain Association of Geologists, Coalbed Methane of North America–II, p. 53-70.

Tessier, A., Campbell, P.D.C., and Bisson, M., 1979, Sequential extraction procedure for the speciation of particulate trace metals: Analytical Chemistry, v. 51, n. 7, p. 844-850.

Wheaton, J., and Brown, T.H., 2005, Predicting changes in groundwater quality associated with coalbed natural gas infiltration ponds, *in* Zoback, M.D., editor, Western Resources Project Final Report—Produced groundwater associated with coalbed natural gas production in the Powder River Basin: Wyoming State Geological Survey Report of Investigations No. 55, p. 45-70.

Wyoming Department of Environmental Quality, <http://deq.state.wy.us/wqd/>, accessed December 2004.

Wyoming Oil and Gas Conservation Commission, <http://wogcc.state.wy.us/, accessed December 2004>.

CHAPTER 5

Time-lapse seismic monitoring of coalbed natural gas production: A case study from the Powder River Basin

Jerry M. Harris and Martins Akintunde
Department of Geophysics
Stanford University
Stanford, California

Table of contents

List of figures 110
Abstract 111
Introduction 111
Geologic background 113
Time-lapse methodology 113
Time-lapse feasibility analysis—Modeling acoustic changes in coal 114
Crosswell seismic data acquisition 115
Data processing 117
Traveltime tomography 118
Data interpretation 123
Future work 124
Conclusions 124
References cited 124

List of figures

1. Map of the U.S. showing the location of the Powder River Basin 112
2. Acoustical microscope image of a coal sample shows cleats and microstructure 112
3. Schematic diagram of coalbed natural gas completion in the Powder River Basin 113
4. Conceptual time history of CBNG production 113
5. Gassmann-predicted changes in P-wave velocity with pressure for coal 114
6. Computed fluid and coal properties versus water/methane saturation at a pressure of 5 Mpa 114
7. Estimated changes in velocity with pressure and saturation (upper) 115
8. P-wave velocity's behavior in saturated coal as a function of differential pressure 115
9. Cross-well survey geometry 116
10. Plot of common receiver point (CRP) profile showing direct P-waves and tube waves 116
11. Plot of common source point (CSP) profile showing direct P-waves and tube waves 117
12. Plot of common source point (CSP) profile showing direct P-waves at large vertical offset 117
13. (a) The zero-offset CVO profile (baseline survey, depth vs. time in seconds) includes only sources and detectors at the same depth. (b) The coal zone is easily delineated by its low velocity, i.e., larger traveltime 118
14. A display of zero-offset sections for the three data sets showing evidence of production-induced changes within the coal reservoir and high repeatability of events outside the reservoir 119
15. A common receiver point profile shows typical direct P-wave picks 119
16. Traveltime maps of P-wave picks (in msec) from the baseline surveys 1, 2, and 3 120
17. Traveltime difference maps of P-wave picks (in msec) between surveys 120
18. Schematic showing 3-D deviations of the source and receiver wells 121
19. Baseline tomogram with gamma ray logs (insets are tomogram-derived velocity logs) 121
20. Cross-plots of baseline velocity and gamma ray in the two wells showing subsurface heterogeneity and spatial distribution of velocity within the coal layer and other subsurface strata 122
21. Baseline and repeat tomograms (from left: survey 1, survey 2, and survey 3) 122
22. Measured difference tomograms from the time-lapse surveys 123
23. Measured water head pressure as a function of time with markers for surveys 1, 2, and 3 124
24. Measured gas pressure as a function of time with markers for surveys 1, 2, and 3 124

Abstract

The growing significance of the Powder River Basin's (PRB's) coalbed natural gas (CBNG) to U.S. domestic energy supplies has heightened interest in its exploitation. Systematic and continued development of this resource requires improved characterization of the CBNG production process and improved resource management practices for efficient gas production in an environmentally sound manner. In situ monitoring strategies of the type described herein will help optimize these processes. The main objective of this study is to monitor time-variant changes in coal during dewatering. This will be accomplished by measuring the changes in the velocity of seismic waves during natural gas production. Dewatering causes a decrease in pore pressure resulting in an increase in gas saturation. Gas lowers the velocity of seismic waves whereas a decrease in pore pressure increases velocity. Knowledge of the spatial distribution of gas and changes in pore pressure will be helpful in identifying the source of produced water and the spatial efficiency of the dewatering process.

This study is based on three cross-well seismic surveys executed at a test site near Casper, Wyoming. The surveys were run between a pair of monitoring wells that straddle a completed CBNG production well. The monitoring wells were provided for our surveys with the help of the U.S. Bureau of Land Management (BLM), ConocoPhillips, and the Western Resources Project (WRP). Our first survey was completed in December 2002 before dewatering began and thus provided the baseline image or tomogram of the coal between the wells. The second and third surveys were run in July 2003 and June 2004 respectively. Changes in the P-wave traveltimes can be seen in unprocessed seismograms though tomography was used to produce an image of the velocity changes between wells from the traveltime changes.

From the baseline tomogram, we have delineated four major lithologic units that are typical of the Upper Cretaceous sediments in the PRB. From the time-lapse surveys, we detected decreases in seismic velocity within the coal consistent with spatially heterogeneous increases in gas saturation. Moreover, we observed velocity increases above the coal, presumably as a result of dewatering the overlying formation. These seismic observations demonstrate feasibility to monitor a CBNG production process and that the observed changes are consistent with theoretically derived coal-physics models and short-term observations from gas production data.

Introduction

Globally, coal constitutes a major portion of the world's mineral energy resources. It serves as a source for electricity generation, heat and coking coal for iron and steel making. Coal is formed by the physiochemical alteration of peat (coalification) by processes involving bacterial decay, compaction, heat, and time. It is a readily combustible rock containing more than 50% of carbonaceous material by weight. Also, coal contains gas, about 90% of it methane, hence the name Coalbed natural gas (CBNG). The types of coal, in increasing order of alteration (or rank) are lignite (brown coal), sub-bituminous, bituminous, and anthracite. Porosity in coal varies considerably (1.6% to 25%) depending on the coal's rank (King and Wilkins, 1994). Also, coal exhibits low density, low seismic velocity, low magnetic susceptibility, and low radioactivity. Its electrical resistivity is higher when compared with surrounding sediments.

The Powder River Basin (PRB) (**Figure 1**) accounts for 800 billion short tons of coal and is estimated to produce 25 trillion cubic feet of gas—about 20% of the CBNG being produced in the U.S. The PRB coals are biogenic, permeable, shallow, and low-rank. They are characterized by higher moisture content and lower carbon content when compared with high-rank bituminous coals. Located in the central part of the PRB of Wyoming and Montana, the Big George is currently one of the world's most established coal fields. Our test site is located near Casper, Wyoming where the Big George, along with the Wyodak, is a major CBNG producer.

Methane is stored in the coal by adsorption in the pores, as free gas in the pore space and cleats, and/or through dissolution in pore water. The microstructure and cleat system (**Figure 2**) of coal play vital roles in storage and flow of gas. Coalbed natural gas reservoirs are dual storage reservoirs consisting of primary and secondary storage systems. The primary storage system makes up perhaps 98% of the reservoir volume and contains organic matter, inorganic material, inherent water, and gas stored within very small pore spaces. Primary gas storage is dominated by sorption phenomena because of the small size of the pores. During sorption, the molecules that are within very close proximity to solid surfaces are attracted to the solid and are packed closer than expected from the pressure conditions. The primary porosity is relatively impermeable and mass transfer is dominated by diffusion. Commercially productive coal reservoirs contain well-developed secondary storage dominated by natural fractures (**Figure 2**). These natural fractures are very significant to flow and the commercial productivity of CBNG reservoirs. Flow through the secondary storage system is due to pressure gradients between the fracture system and production wells. The majority of gas in a coal gas reservoir desorbs and diffuses through primary storage, and then flows through the cleats to producing wells (Mavor and others, 2002).

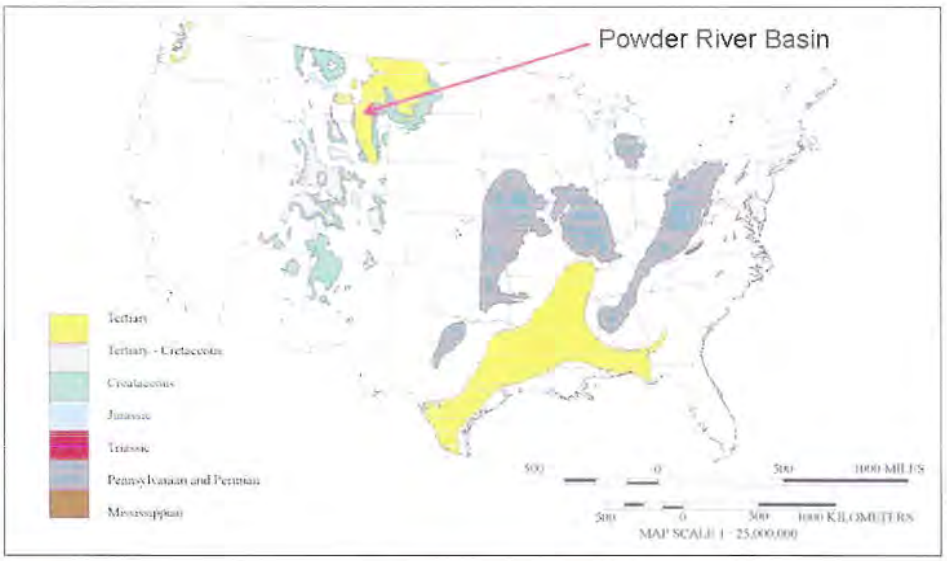


Figure 1. Map of the U.S. showing the location of the Powder River Basin.

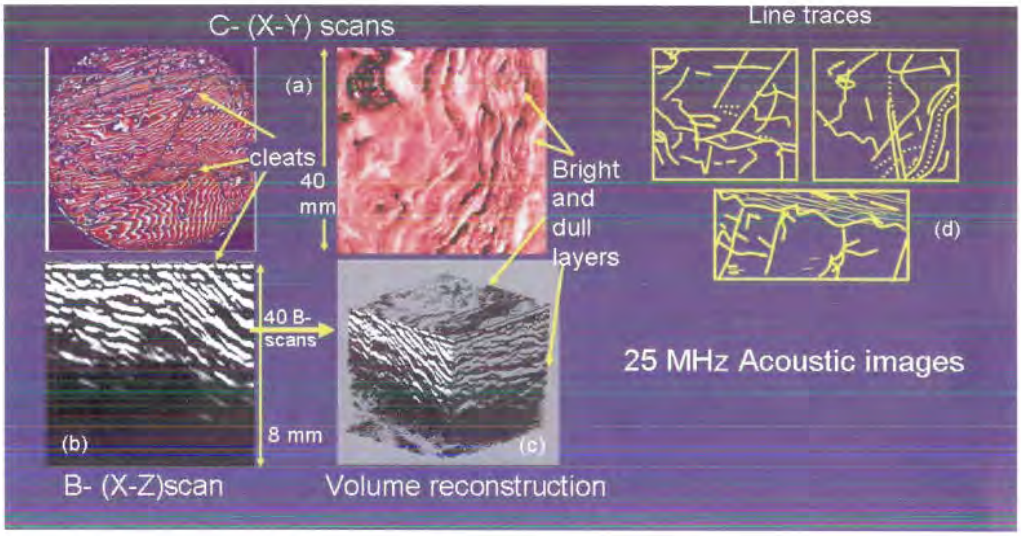


Figure 2. Acoustical microscope image of a coal sample shows cleats and microstructure (from Prasad, 2001).

The common practice for primary CBNG recovery in the PRB is to depressurize the coal by pumping water from production wells. The wells are completed by installing casing to the top of the coal, reaming the coal, and then leaving the coal open to the hole (**Figure 3**).

Time-lapse monitoring depends on changes in the acoustic properties of coal during dewatering. The acoustic properties are most sensitive to changes in pore pressure and fluid saturation. The conceptual time history for producing CBNG is given in **Figure 4**. At the initial stage of dewatering, gas production is negligible, but then increases and stabilizes as dewatering progresses. Richardson and Lawton (2002) showed that the dewatering process affects the acoustic and elastic properties of the CBNG reservoir, causing appreciable acoustic impedance changes between the coal-bearing layer and the surrounding strata. These changes in turn affect the amplitude and traveltimes of reflected and transmitted waves, paving the way for seismic mapping. Monitoring applications rely on saturation and pressure changes that dominantly affect the velocities of P-waves and S-waves in the reservoir.

Historically, the first quantitative data set on time-lapse reservoir monitoring emanated from rock physics measurements at Stanford University in the mid 1980s. Laboratory measurements on heavy-oil saturated core samples showed large decreases in seismic rock velocity when the viscous oil was heated (Nur and others, 1984; Wang and Nur, 1986, and Nur, 1989). Other notable time-lapse reservoir monitoring studies in the last two decades concentrated on steam injection (Pulin and others, 1987; Lumley, 1996; Jenkins and others, 1997). Others include fireflood EOR process (Greaves and Fulp, 1987), a North Sea gas cap expansion project (Johnstad and others, 1995), and a West Texas CO_2 injection project (Harris and others, 1995). It is, however, pertinent to note that recent and current efforts on time-lapse seismic reservoir monitoring have focused

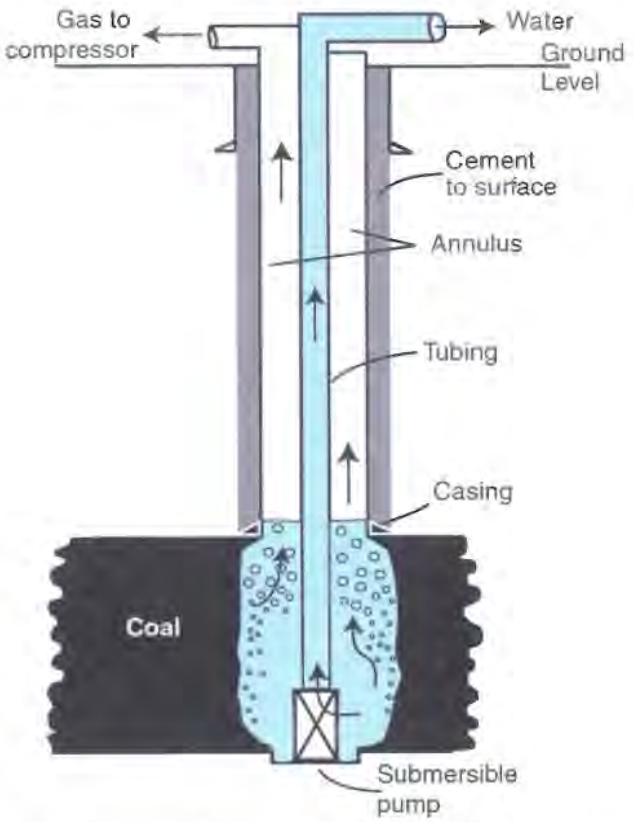


Figure 3. Schematic diagram of coalbed natural gas completion in the Powder River Basin. Water is removed by installing a submersible pump in the open coal bed. Gas is transported to the surface in the space between the tubing attached to the submersible pump and the well casing and the produced water is discharged via the tubing (modified from De Bruin and others, 2000).

mostly on hydrocarbon reservoirs (Tura and Lumley, 1998; Tura and Lumley, 1999; Landro and others, 2003; Landro, 2001; Harris and others, 1995). This history underscores the significance of a test of time-lapse monitoring to the CBNG dewatering process. Continued and systematic development of the CBNG resource requires an improved understanding of the efficiency of the dewatering process and knowledge of the spatial distribution of gas and pressure drawdown between wells.

In this study, cross-well seismic surveys were designed to image production-induced changes in P-wave velocity associated with primary CBNG production. The pre- and post-CBNG production cross-well surveys were executed in December 2002, August 2003, and June 2004 respectively.

Geologic background

Geologically, the PRB is an intermontane foreland arch basin formed during the Laramide Orogeny. It is located in southeast Montana and northeast Wyoming (**Figure 1**), characterized by rocks of Late Cretaceous to early Tertiary age. The basin is flanked by the Bighorn Mountains on the west, the Casper arch-Laramie Mountains on the southwest and south, the Hartville uplift on the southeast, the Black Hills on the east, and the Miles City arch on the northeast, all formed during the Laramide Orogeny (Flores, 2004). Also, it is a thick sequence of sedimentary rocks formed in a large down warp within the Precambrian basement. Sediments range from Paleozoic at the bottom through Mesozoic to Tertiary at the top. The basin started evolving about 60 million years ago, when it was just a flat, sea-level plain, muddy from a retreating sea that had covered Wyoming for 40,000,000 years. Over the next 14 million years, the basin rose to its present 3000 feet with the Bighorn Mountains and the Black Hills rising thousands of feet higher. Following were episodes of geological processes favoring sediment accumulation into pure peat. Further effects of temperature, erosion, and deposition transformed the peat into some of the thickest, low-ash coals in the world. More geological details are contained in Larson (1989), De Bruin and others (2000), Randall (1989), Rice and others (2000) and Flores (2004).

Time-lapse methodology

This study has four objectives that are germane to monitoring projects:

1. Estimate the magnitude of the anticipated changes;
2. Execute field surveys with a high degree of repeatability;
3. Process the data in a manner that resolves small time-lapse changes; and
4. Interpret seismic changes in terms of the dewatering process.

We completed a coal physics feasibility analysis, acquired and processed three cross-well field seismic data sets, and carried out image analysis and interpretation. The methods and their results are discussed in the following sections.

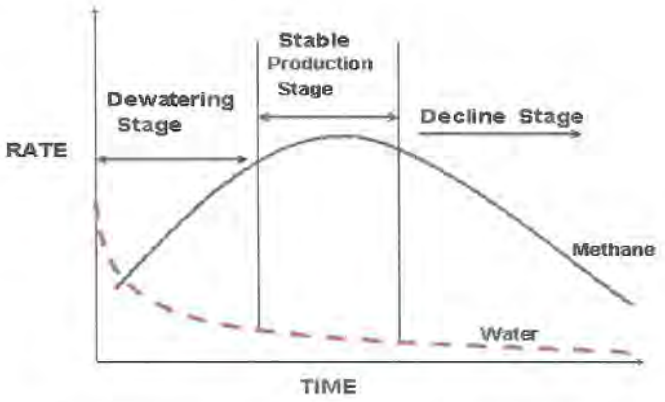


Figure 4. Conceptual time history of CBNG production (modified from Ayers, 2002).

Time-lapse feasibility analysis—Modeling acoustic changes in coal

Prior to the first field experiment, we carried out a modeling study to predict changes in P-wave velocity in coal when saturated with water and methane. We extracted P-wave velocities for dry coal and their pressure dependence from laboratory measurements on a bituminous, Permian coal sample (Yu and others, 1993). The Yu sample has a porosity of 2.9% and a density of 1.35g/cc. We modeled the data using Gassmann's equation (Gassmann, 1951), appropriate fluid properties and physics relationships for P-wave velocity, effective fluid modulus, and density of a fluid-saturated rock (Mavko and others, 1998). The Gassmann model relates the fluid-saturated moduli to the matrix moduli and fluid properties. It permits estimation of velocity of fluid-saturated rocks from measured dry rocks and vice versa. Also, it is equivalent to the low-frequency limit of Biot's theory (Mavko and others, 1998). Additionally, the Gassmann theory is strictly valid for low (quasi-static) frequencies. Our analysis assumes free gas, homogeneous saturations and does not account for the effects of gas adsorption or desorption.

Figure 5 shows the results of this analysis for four saturation levels at various pressures. The influence of increasing differential pressure is to close thin cracks and penny-shaped pores and to make better contact between particles in the coal. At 100% water (H_2O), depicted by the blue curve, the Gassmann-derived P-wave velocity increases considerably above the dry values. The Gasmann-derived curve for the 100% water saturated coal compares favorably with the laboratory measured velocity data (Yu and others, 1993). There are observed discrepancies, at the lower pressures, that overestimate the magnitude of the measured changes. The addition of methane (CH_4) into the water-coal mixture decreases the P-wave velocity due to the high compressibility of free gas and a slight density effect. Quantitatively, the magnitude of the changes in P-wave velocity due to CH_4 would depend partly on the water/methane saturation and partly on pore pressure. For shallow reservoir conditions (lower differential pressures) typical of the shallow coals in the PRB, the predicted changes in velocity range from about 5 to 15%. Furthermore, the observed changes in P-wave velocity are largest at low differential pressure (Wang and others, 1998).

To relate changes in velocity to changes in saturation and pore pressure, we extended the Gassmann analysis to a sensitivity study. **Figure 6** displays the computed fluid density, fluid bulk modulus, saturated coal density, and saturated coal bulk modulus versus water/methane saturation. We then used these parameters to estimate the saturated velocities at an assumed reference pressure of 5 Mpa as shown in **Figure 7**. Subsequently, we calculated changes in velocity as functions of changes in pressure (ΔP) and water saturation (ΔS_w) (**Figure 7**). Also in **Figure 7** we show a sensitivity plot of velocity ΔV_p with water/methane saturation and pressure. The changes in velocity are largest as a small amount of gas is added to water. While the Gassmann model predicts significant changes that should be observable in the field, the predictions are not strictly valid for the PRB's Big George shallow coals. Coal, depending on its rank and geology, may exhibit significant variations.

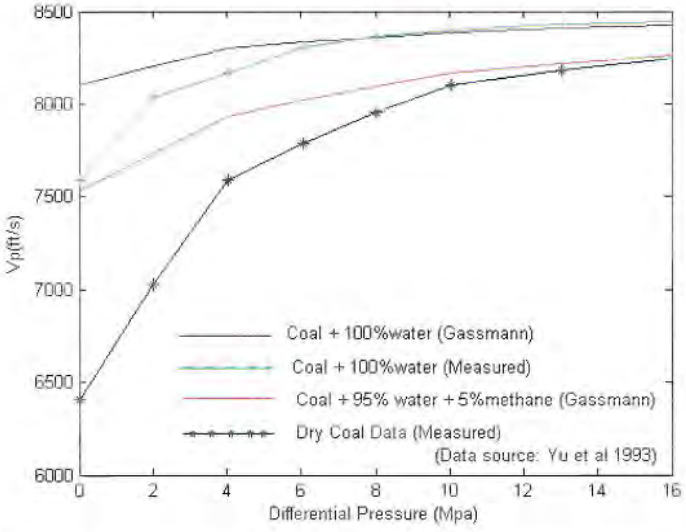


Figure 5. Gassmann-predicted changes in P-wave velocity with pressure for coal. Dry data (black) from Yu and others (1993); 100% water saturation from Yu (green). The blue and red curves were computed using the Gassmann model.

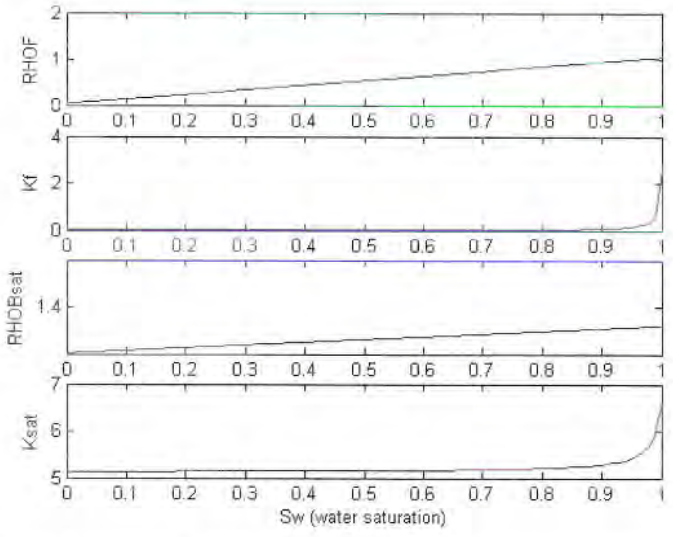


Figure 6. Computed fluid and coal properties versus water/methane saturation at a pressure of 5 Mpa. Fluid density (RHOF), fluid modulus (Kf), saturated coal bulk density (RHOBsat), and saturated coal bulk modulus (Ksat).

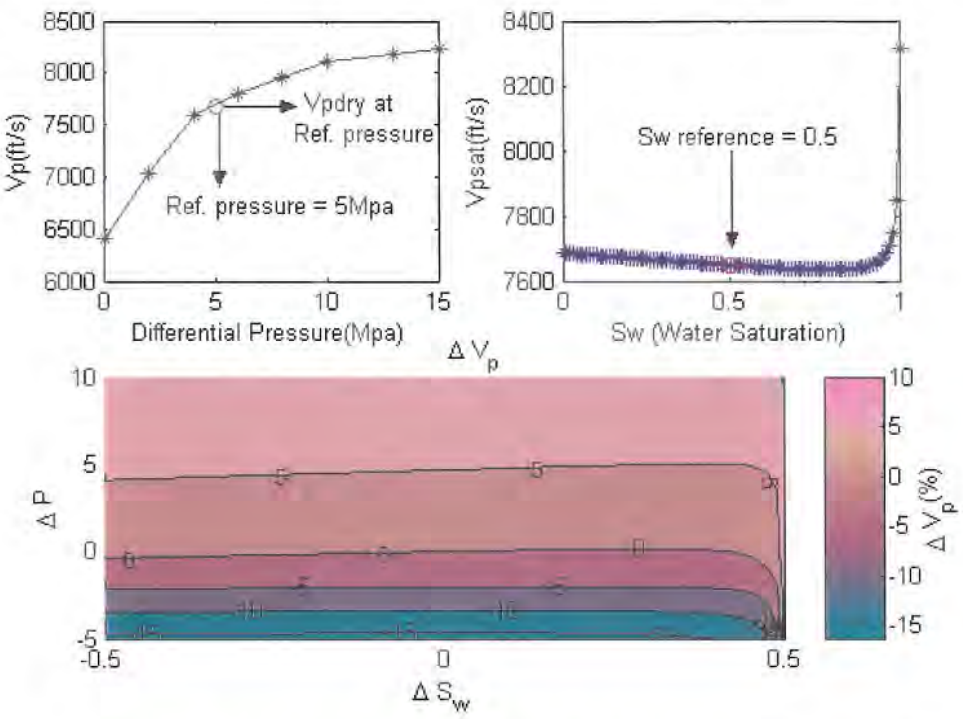


Figure 7. Estimated changes in velocity with pressure and saturation (upper). Sensitivity plot (lower) of velocity (ΔVp) as a function of changes in pressure (ΔP) and changes in water/gas saturation (ΔS_w).

The predicted velocity changes are summarized in **Figure 8**. First, we will have a drop in velocity due to gas from desorption. Then the velocity increases as pore pressure continues to drop during dewatering.

Crosswell seismic data acquisition

We used the crosswell geometry for the monitoring surveys because of the availability of two monitoring wells. Although the surface geometry would have provided better coverage, surface surveys were not permitted at the site nor was there sufficient budget for surface seismic surveys. All the crosswell surveys were run between two monitoring wells spanning 150 feet and straddling the ConocoPhillips production well (CP 23-35). The geometry is illustrated in **Figure 9**. The source and receiver wells are labeled 23-35BG and 23-35W, respectively. The baseline or reference survey was acquired in December 2002, shortly after the production well was completed and before pumping began. The first monitoring survey was run in July 2003 and the second about twelve months later in June 2004. Each of the surveys covered about 600 feet of well depth or about four times the well spacing. The large vertical apertures provide an adequate range of ray angles we need for quantitative imaging. Shots were fired from a piezoelectric down-hole source every 1.25 feet using a sweep signal of 200-1600 Hz. The signals were detected with a six-element array of hydrophones positioned inside the receiver well. The survey was recorded in common receiver "fans," where the hydrophone array was fixed and the source scanned up the adjacent well. The receiver is then repositioned and the scan repeated.

A typical common receiver point (CRP) profile is shown in **Figure 10**, where direct P-wave first arrivals and tube waves are visible. The data can be resorted to yield common source point (CSP) profiles like the one shown in **Figure 11**, where again direct P-waves and tube waves can

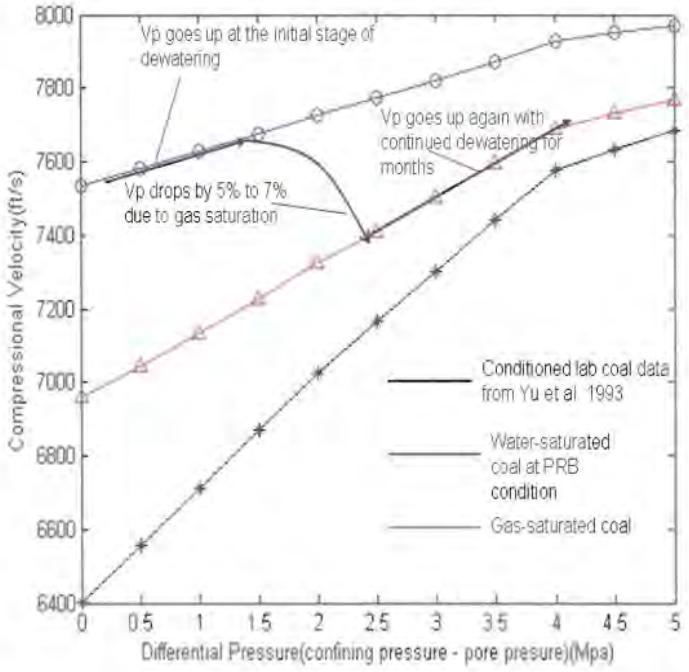


Figure 8. P-wave velocity's behavior in saturated coal as a function of differential pressure.

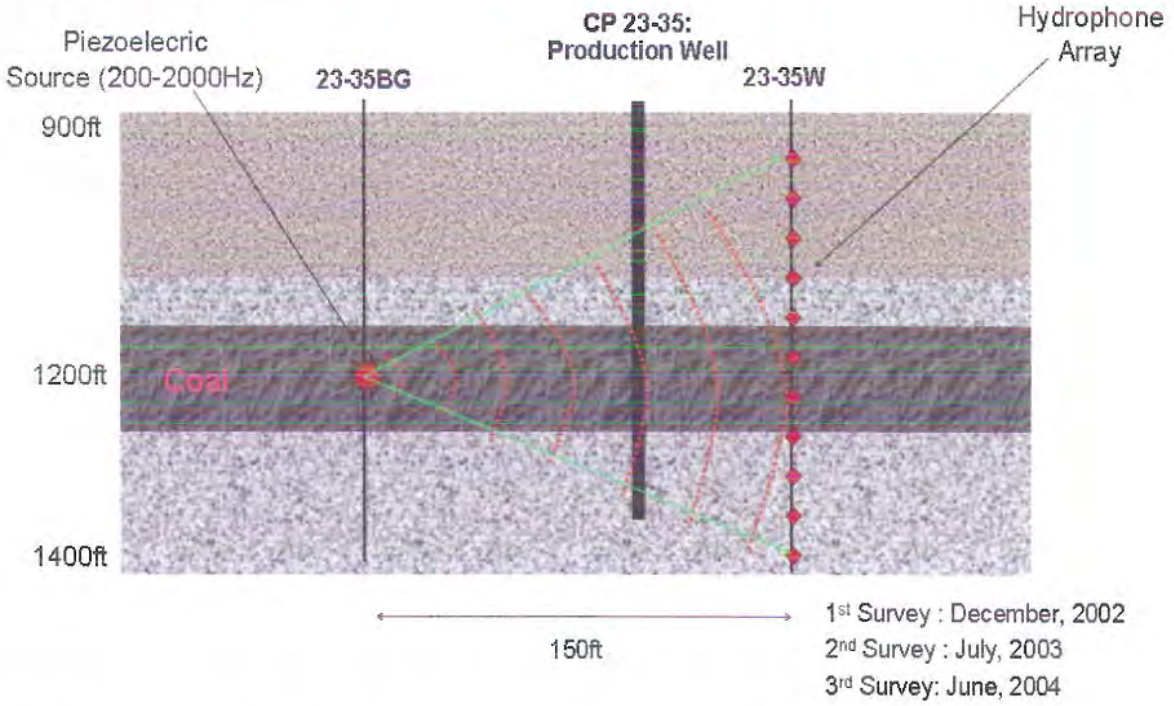


Figure 9. Crosswell survey geometry. The CBNG surveys have approximately 182 source positions by 116 detector positions. The survey took less than 24 hours to record.

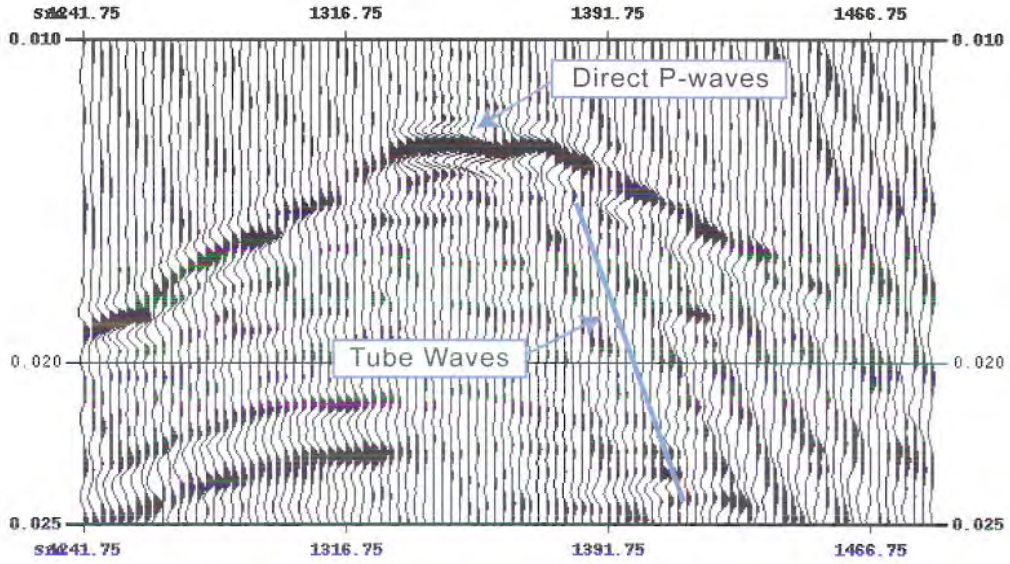


Figure 10. Plot (about 100 traces) of common receiver point (CRP) profile showing direct P-waves and tube waves.

be seen. Ineither CRP or CSP profiles, the direct arrival path increases hyperbolically with increasing source to receiver offset (straight rays in homogeneous media); therefore, the direct wave traveltime has hyperbolic moveout. For large offsets, the direct and reflected events asymptote a straight line that has the moveout of the medium's velocity (**Figure 12**).

Data from the crosswell seismic survey can also be viewed as common mid-point (CMP) and common vertical offset (CVO) profiles. In the CVO profile, the travel paths of direct P-waves are nearly constant and therefore their moveout is nearly zero (exactly zero in homogeneous media). The zero-offset CVO profile from our site is shown in **Figure 13**. This profile is very useful in that stratigraphic delineation of zones of different seismic velocity is easily identified. In the CMP profile, direct arrivals have twice the hyperbolic

moveout. The CMP—CVO domain offers an advantage for both picking traveltimes and wavefield separation, i.e., direct arrivals are more easily separated from other arrivals in this domain. In picking, the CVO direct arrivals are maximally flat, while in CMP direct arrivals have roughly twice the moveout. The CSP—CRP and CMP—CVO comprise the two major domains or four major data sets for analysis and processing crosswell seismic profiles.

Data processing

The seismic velocity of coal is lower than velocities of the surrounding strata; therefore, coal is easily delineated by its larger traveltime in the CVO profile (**Figure 13**). This CVO from the baseline survey is shown again in **Figure 13** (rotated 90°) along side the CVO's from the repeat surveys. Together, the three CVO's illustrate the excellent repeatability of the crosswell surveys as well as the small though distinctive changes with time. Intuitively, we

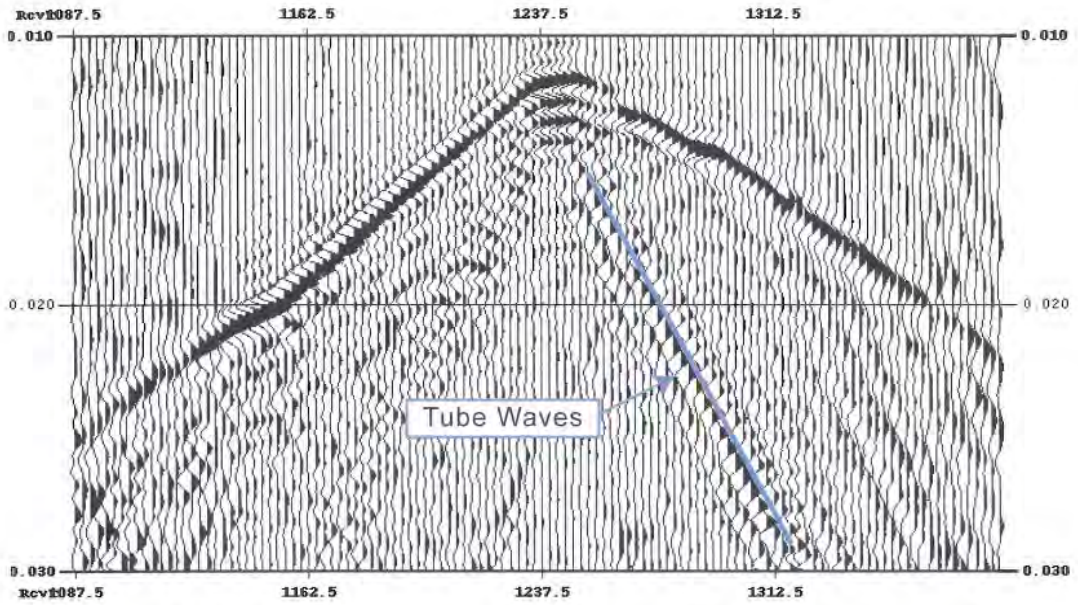


Figure 11. Plot (about 120 traces) of common source point (CSP) profile showing direct P-waves and tube waves.

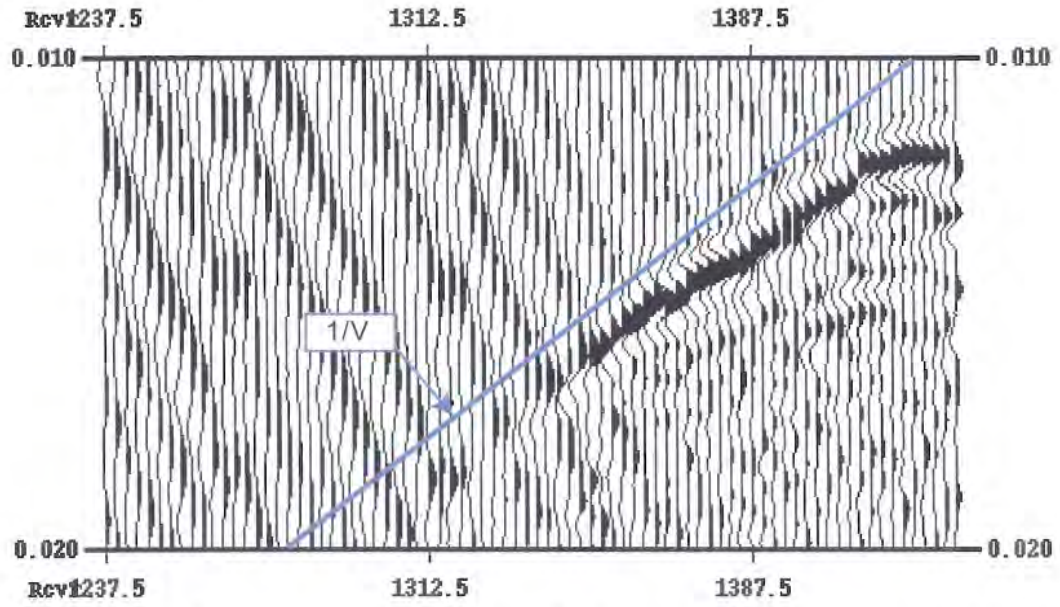


Figure 12. Plot (about 90 traces) of common source point (CSP) profile showing direct P-waves at large vertical offset. At such large offsets, the moveout of direct wave has a slope that asymptotes the average velocity of the medium.

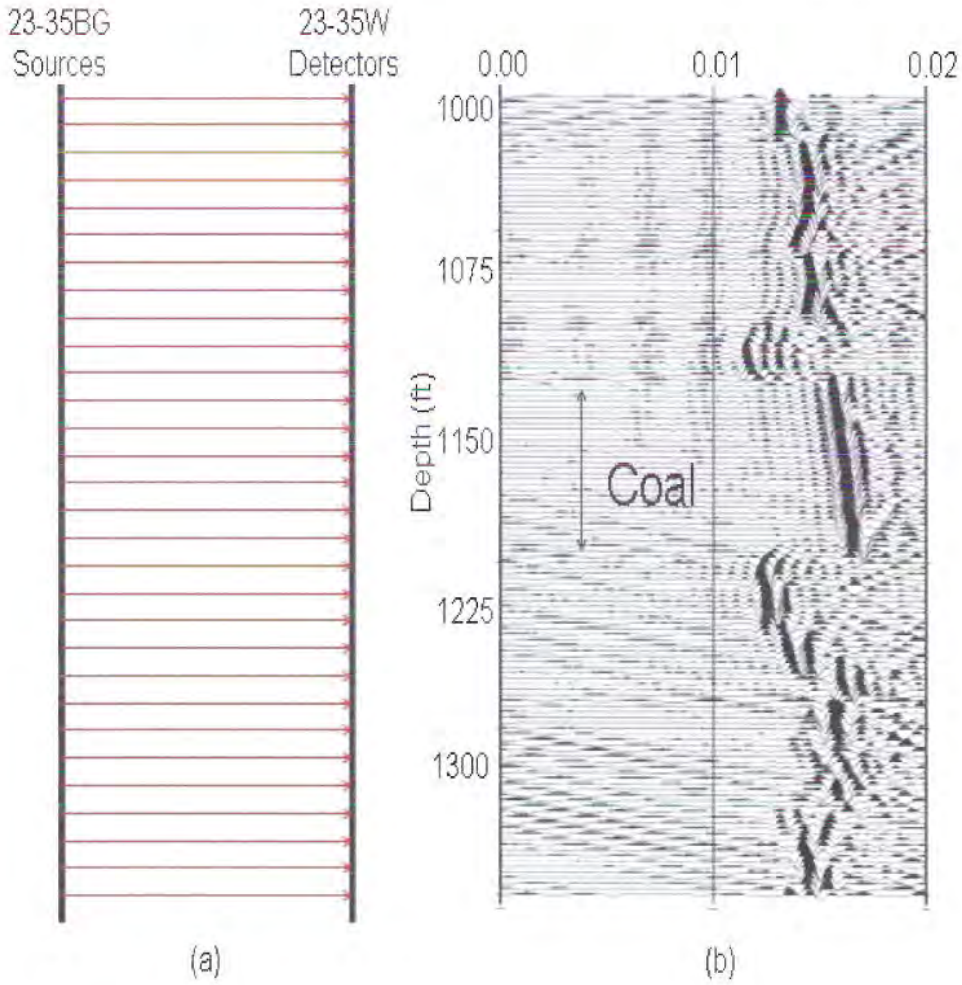


Figure 13. (a) The zero-offset CVO profile (baseline survey, depth vs. time in seconds) includes only sources and detectors at the same depth. (b) The coal zone (1150 to 1240 feet) is easily delineated by its low velocity, i.e., larger traveltime.

hypothesize that seismic events in strata well above and well below the coal will be time-invariant, while events within the coal reservoir will change during dewatering. We test this hypothesis with the CVO's as follows: First, we place red markers on seismic events in the baseline survey, both within and outside the coal zone as shown in the upper plot of **Figure 14**. We then project the skeletal baseline markers onto the repeat surveys 2 and 3 as shown in the middle and lower plots in **Figure 14**. We allow, however, for the possibility that a small static time shift may exist between the surveys by referencing the baseline skeleton at an assumed time-invariant event at about 1400 feet as shown. The event at approximately 1000 feet (above the coal) is seen to repeat with no detectable change in traveltime, while events within the coal show small though obvious changes. The first repeat shows a small increase in traveltime (lower velocity) in the coal whereas the second repeat shows a subsequent decrease in traveltime (higher velocity). As can be seen, the velocity in the coal in the second repeat is nearly the same as the baseline value. Though these production-induced changes are small, they are real and statistically significant for time-lapse processing and interpretation. It is worth repeating that the observed differences in strata above and below the coal are quite negligible, showing that events outside the coal reservoir are repeatable and no significant changes have occurred well above and below the coal zone.

Traveltime tomography

We then pre-processed the data to enhance the first arrivals for picking (**Figure 15**). To ensure consistency, we manually picked more than 21,000 seismic traces in the CSP—CRP and CMP—CVO domains. The picks are displayed in the traveltime maps shown in **Figure 16** for all three surveys. The difference maps use the baseline survey as a reference (**Figure 17**). Evidence of production-induced changes in traveltimes within the coal reservoir can be seen in the difference maps. Although these changes are not uniform within the coal, they appear to be controlled by changes in fluid saturation, for example, gas with dewatering. Estimating velocities from these acoustic traveltimes constitutes traveltime tomography or velocity inversion.

Tomography is the process of inverting the measured traveltimes for an image of velocity, or more specifically

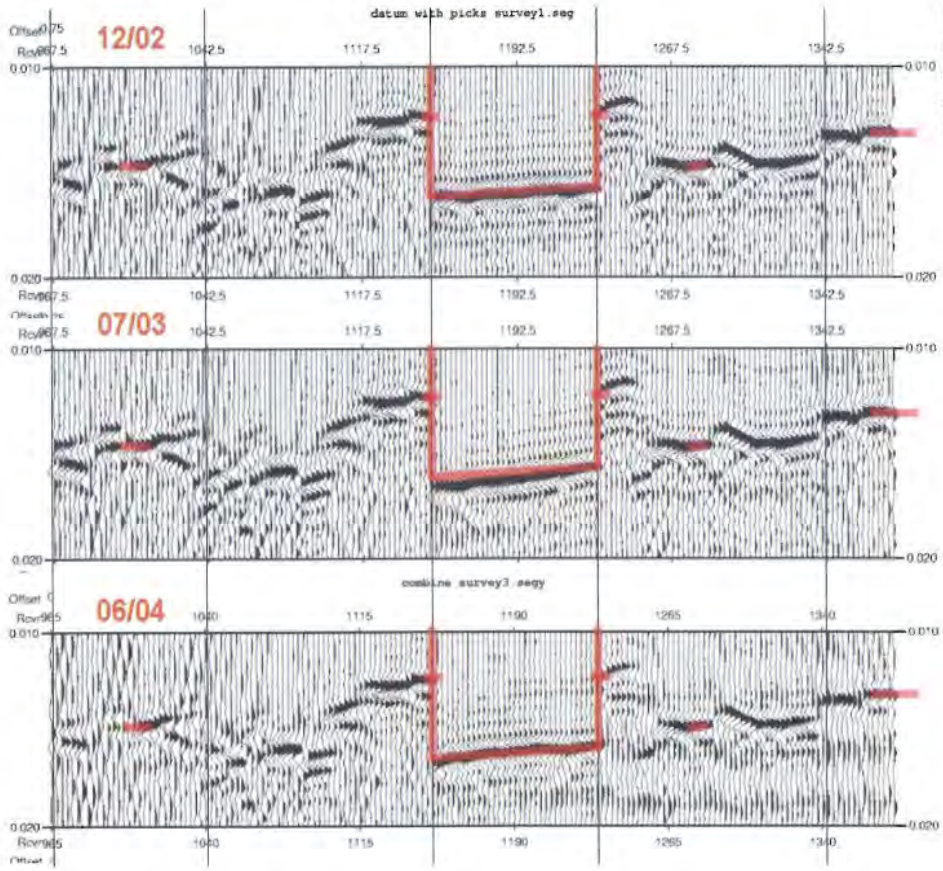


Figure 14. A display of zero-offset sections for the three data sets showing evidence of production-induced changes within the coal reservoir and high repeatability of events outside the reservoir.

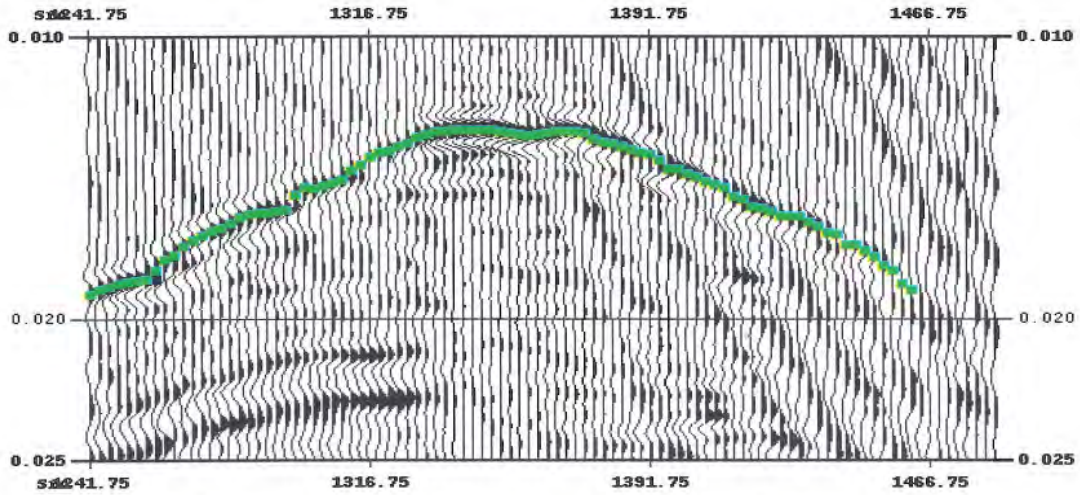


Figure 15. A common receiver point profile shows typical direct P-wave picks (in green).

for slowness (inverse velocity). The tomographic process is based on ray theory,

$$t = \int_l S(x,z)dl \,, \qquad (1)$$

where t is the measured traveltime and S(x,z) is the 2-D slowness. The integration is carried out along the raypath l. Tomography involves inverting equation (1), from a vector of measured traveltimes, for the slowness distribution. This inversion is highly non-linear because the raypaths and slowness are both unknown (Nolet, 1987; Peterson and others, 1985).

We approximate the non-linearity with a sequence of linear steps by assuming we know the raypaths in a known slowness model $S_0(x,z)$ and invert for a perturbation $\Delta S(x,z)$, i.e.,

$$S(x,z) = S_0(x,z) + \Delta S(x,z) \,, \qquad (2)$$

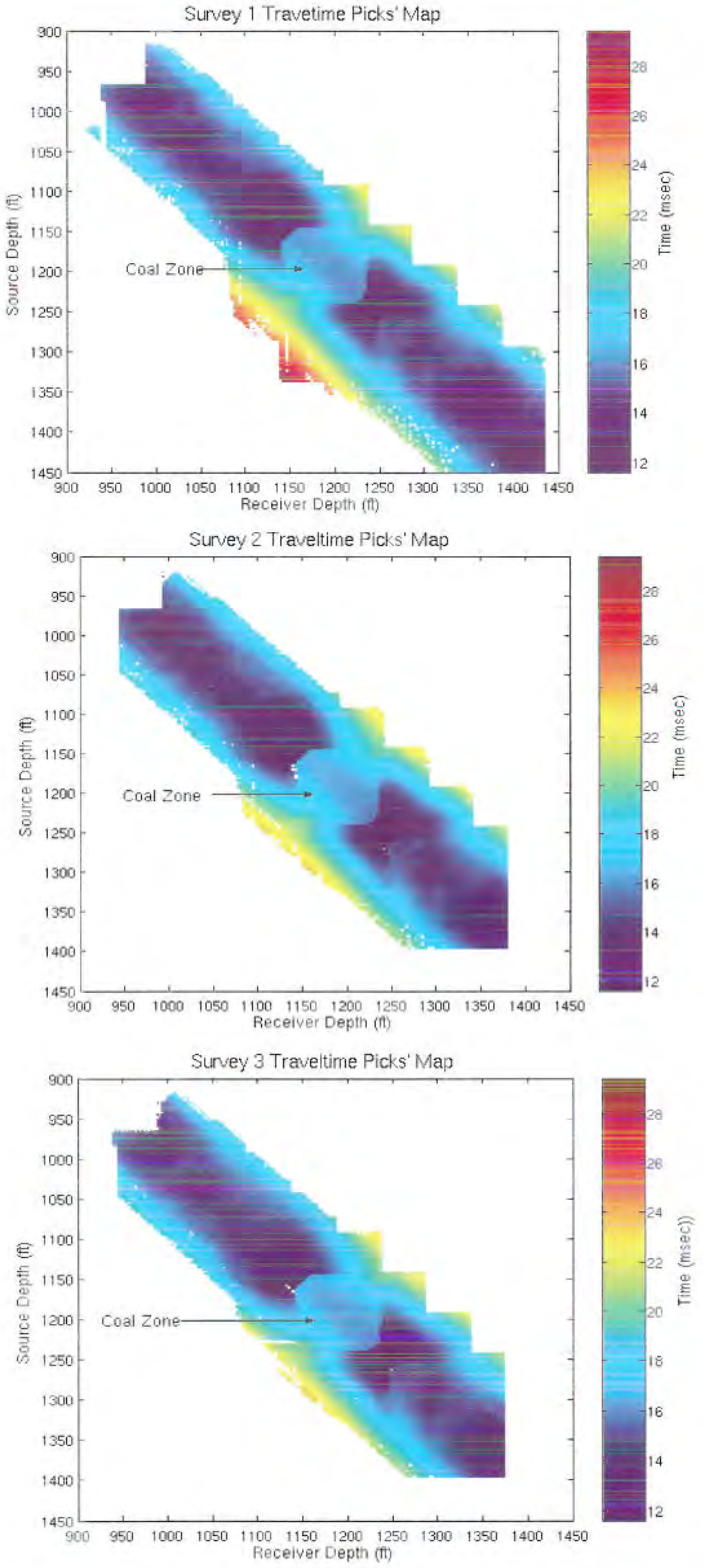


Figure 16. Traveltime maps of P-wave picks (in msec) from the baseline surveys 1, 2, and 3. The coal zone is easily delineated as the low velocity zone at about 1200 feet.

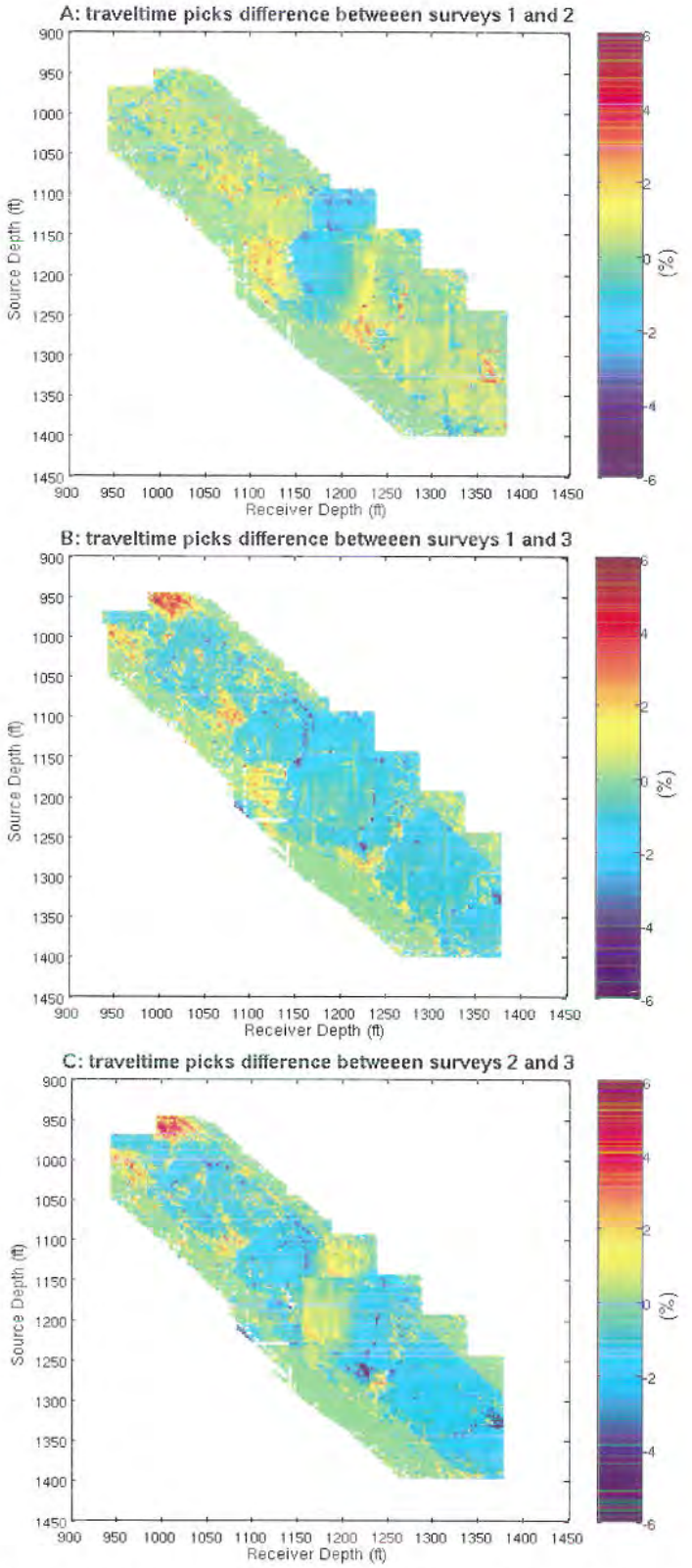


Figure 17. Traveltime difference maps of P-wave picks (in msec) between surveys.

then iterate until the computed traveltimes match the measured traveltimes. The resulting linear inversion problem is

$$\Delta t = \int_{l_0} \Delta S(x,z) dl \ , \quad (3)$$

where $\Delta t = t - t_0$ is the difference between the measured and a calculated traveltime for the known slowness model.

Prior to processing, we needed to consider the 3-D deviations of the wells by applying necessary corrections that allow for a projection of the deviations on to a 2-D plane (**Figure 18**). This is necessary to ensure realistic velocity estimates from the 2-D inversion. Well deviations can cause artificial anisotropy that can impact the inversion and consequently the interpretation.

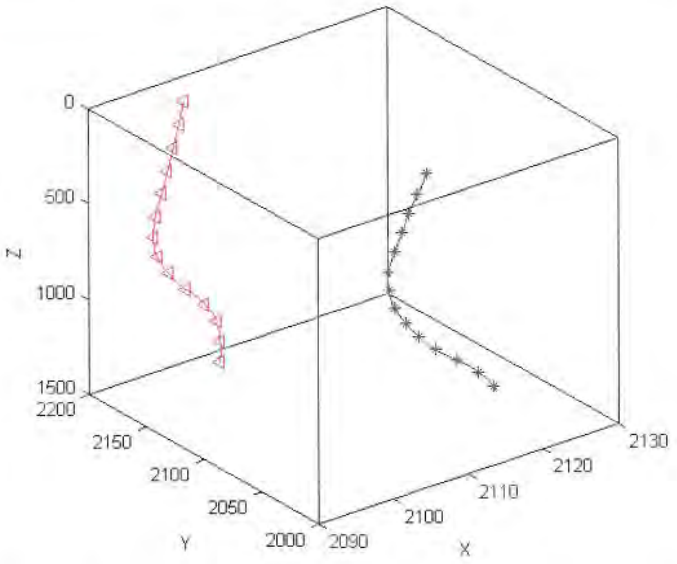


Figure 18. Schematic showing 3-D deviations of the source (in red) and receiver (in blue) wells.

For this study, the picked traveltimes were imported into TOMOXpro® where 2-D tomography was performed. The algorithm performs a non-linear traveltime inversion and reconstructs velocity models for any survey geometry. A 1-D velocity model was used to start the 2-D inversion. This 1-D initial model was constructed from zero-offset data. This approach was used in processing the baseline survey. For the second and third surveys, we used the output of the baseline survey as the starting model and used the same inversion algorithm to get their respective tomograms. The resulting 2-D tomogram for the baseline survey is shown in **Figure 19**, where we plotted the gamma ray logs for the observation wells alongside to validate qualitative geologic interpretation in conjunction with the baseline tomogram.

A cross-plot of the baseline velocity data with the gamma ray data for each of the observation wells further shows consistency in geologic interpretation in which with the low-velocity and low-radioactive coal is easily identified (**Figure 20**). The baseline and repeat tomograms exhibit the same geologic characteristics (**Figure 21**). To permit quantitative estimation of changes in P-wave velocity due to CBNG production, we computed the differences between baseline and repeat tomograms and obtained the results shown in **Figure 22**.

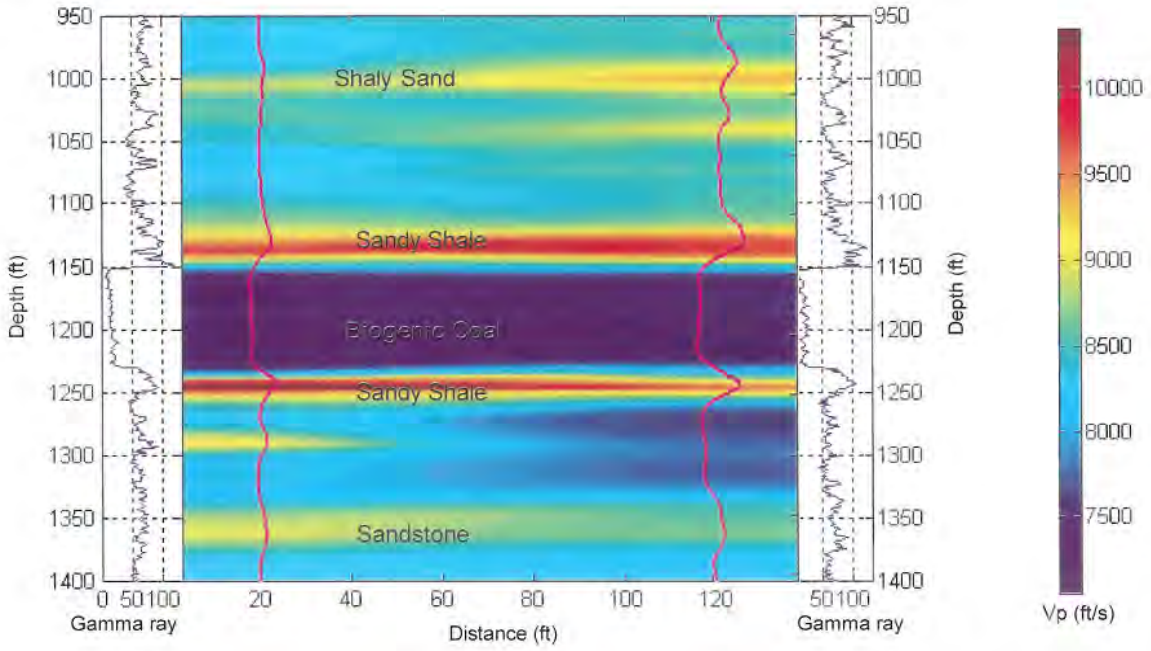


Figure 19. Baseline tomogram with gamma ray logs (insets are tomogram-derived velocity logs).

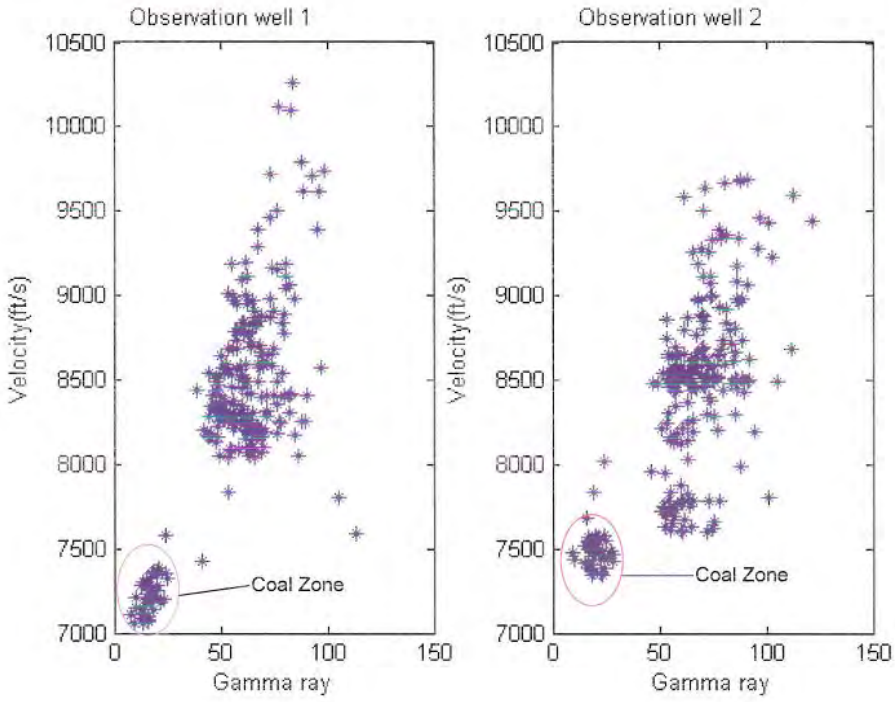


Figure 20. Cross-plots of baseline velocity and gamma ray in the two wells showing subsurface heterogeneity and spatial distribution of velocity within the coal layer and other subsurface strata.

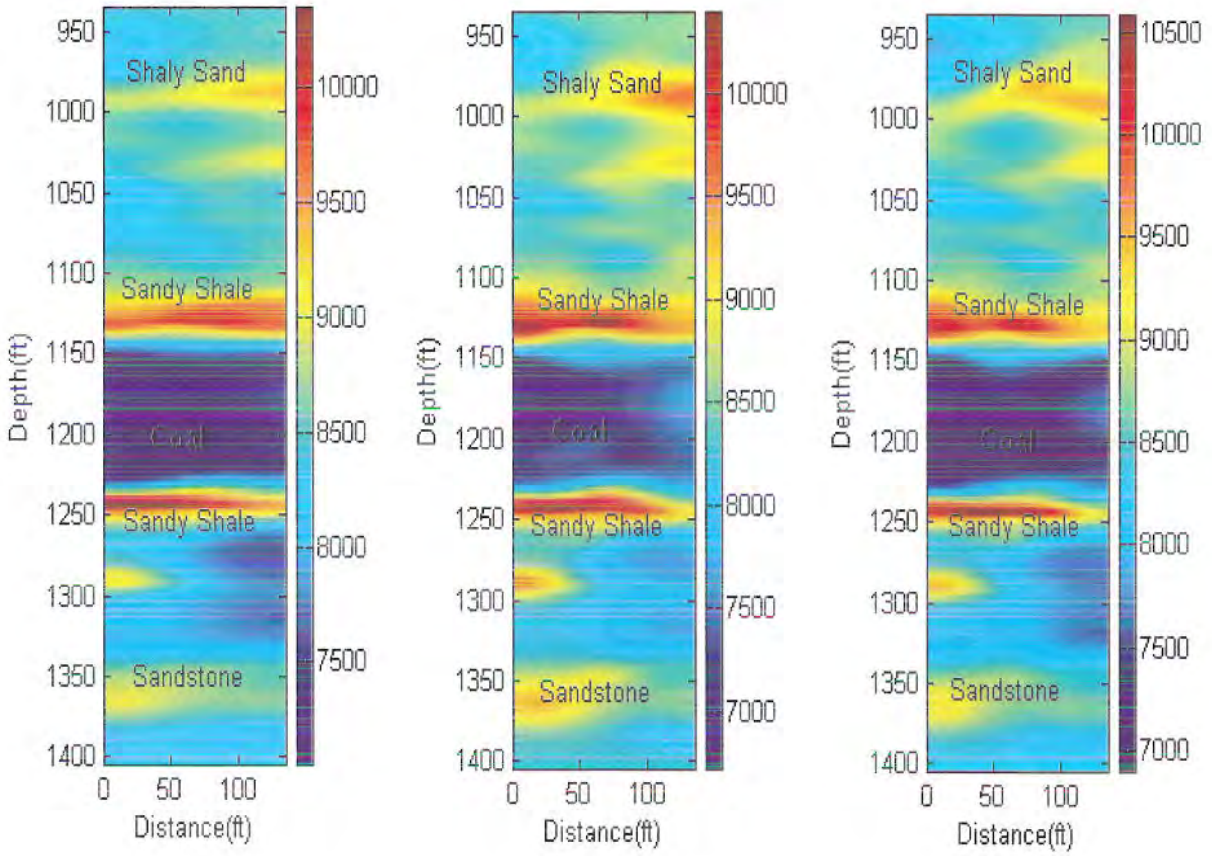


Figure 21. Baseline and repeat tomograms (from left: survey 1, survey 2, and survey 3).

Data interpretation

Four distinct geologic units can be identified from the baseline tomogram (**Figure 19**). They include shaly-sand, sandy-shale, coal, and sandstone. Of interest to us is the low-velocity Big George coal zone at a depth of around 1150 to 1240 feet. The coal is confined above by a low permeability sandy-shale. Qualitative interpretation of the gamma ray logs plotted alongside the baseline tomogram shows geological features similar to the ones observed in the tomograms. This good correlation corroborates the quality of the tomographic inversion process.

The difference tomograms are shown in **Figure 22** along side the baseline. The first difference tomogram (ΔVp_1) was computed between the baseline of December 2002 and first repeat survey of July 2003 (after about eight months of dewatering). The second difference tomogram (ΔVp_2) was computed between the first repeat of July 2003 and second repeat of June 2004 (after about 19 months of continuous dewatering). The third difference tomogram (ΔVp_3) comes from the first and second repeat surveys.

The first difference (ΔVp_1) shows a reduction in Vp of about 4% to 5% within the coal zone over the first eight months of dewatering, most likely due to an increase in partial gas saturation due to methane desorption. The second difference shows an increase in velocity over the next 11 months (between surveys 2 and 3), perhaps due to hardening caused by continued depressurization. These changes are not uniform due to the heterogeneous nature of the coal bed. Interestingly, the observed small changes in pore pressure (**Figure 23**) had considerable effect on the P-wave velocity. As shown in **Figure 23**, the pore pressure

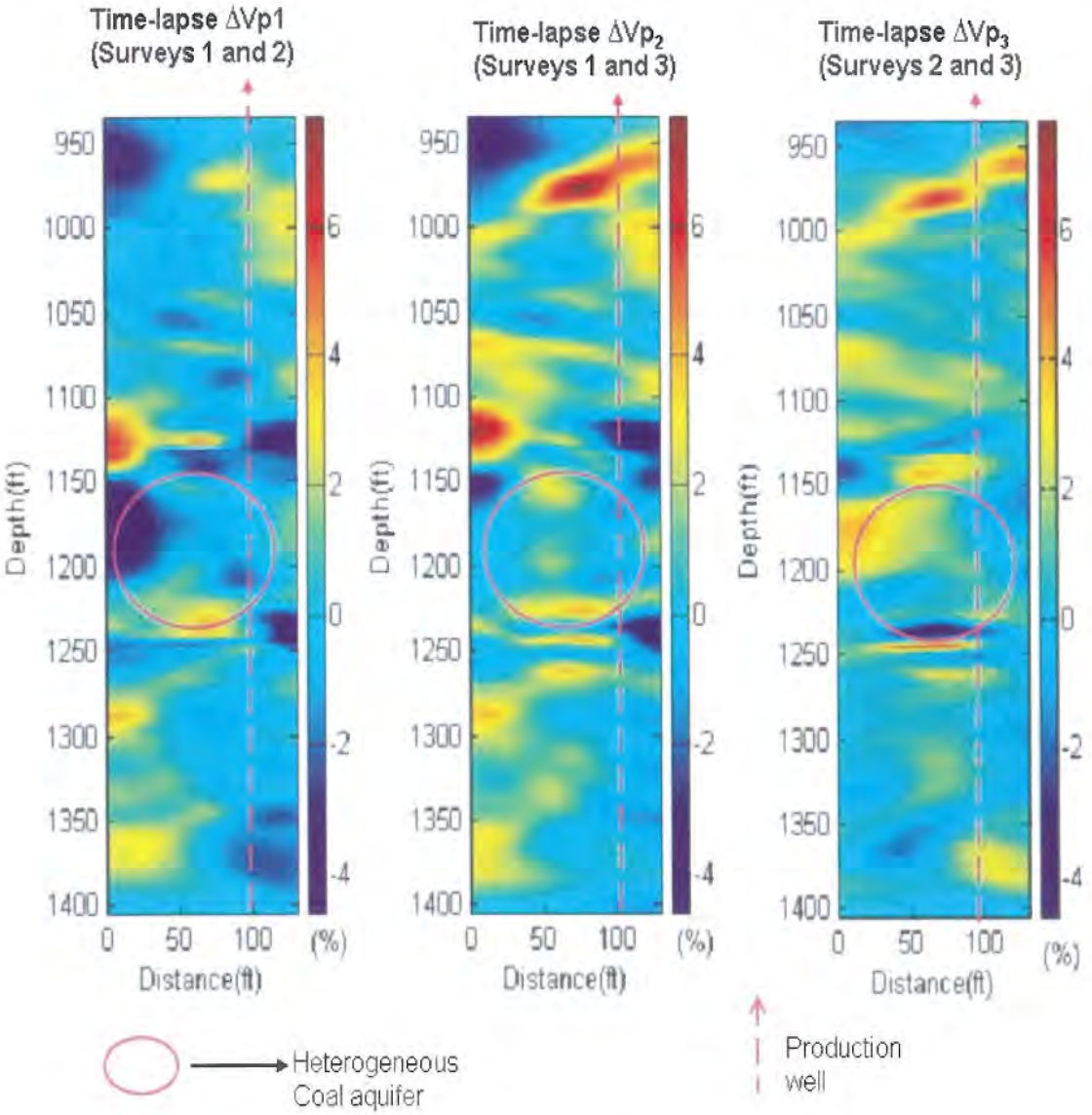


Figure 22. Measured difference tomograms from the time-lapse surveys.

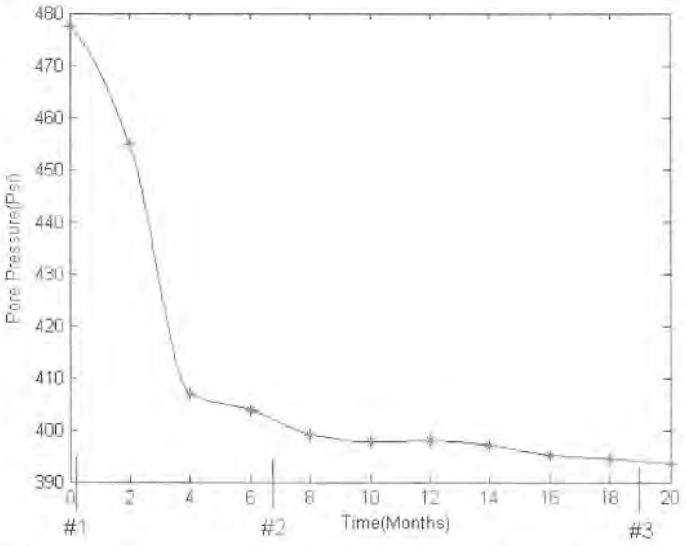


Figure 23. Measured water head pressure as a function of time with markers for surveys 1, 2, and 3.

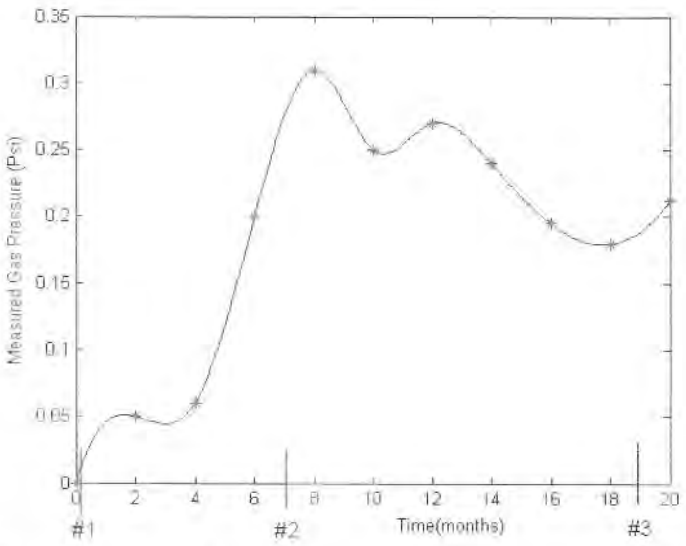


Figure 24. Measured gas pressure as a function of time with markers for surveys 1, 2, and 3.

drops more than 70 Psi (0.5 Mpa) between the first and second surveys, and by only about 7 psi (0.09 Mpa) between the second and third surveys.

The measured gas pressure data (**Figure 24**) shows that gas production increased between the first and second surveys, justifying the observed reduction in P-wave velocity. Gas production reduced between the second and third surveys, corroborating the observed subsequent increase in P-wave velocity. This indicates that the changes in P-wave velocity in the coal depend primarily on gas saturation caused by the dewatering process.

There are also observed changes in velocity both above and below the coal zone. These changes might be due to pressure-related fluid drainage and/or migration through hydraulically active fractures (Colmenares and Zoback, 2005, this volume). In particular, the observed changes above the coal zone might be due to water coming from the overlying sandy-shale possibly caused by hydraulic fracturing during well completion. There is no gas in this caprock, suggesting that the observed increases in P-wave velocity above the reservoir level are due to pressure decreases.

Future work

Observed processing artifacts in the difference tomograms necessitate an improvement in the traditional crosswell tomography and time-lapse analysis approach. Based on the foregoing, we will pursue development of an integrated, acquisition-adaptive traveltime inversion scheme. This is a novel processing method that would give a high quality, repeatable seismic image of the reservoir and an unambiguous geologic interpretation closely linked to reservoir properties. We would reprocess the data sets with this proposed integrated processing method. Also, more surveys would be acquired and processed to provide monitoring of changes as a function of time. Verification involving laboratory measurements, reservoir simulation, and seismic repeatability tests constitute part of our future plans.

Conclusions

We have imaged and quantitatively characterized production-induced changes in P-wave velocity at the PRB's Big George Coal using time-lapse crosswell seismic surveys. The results show that the P-wave velocity first decreases approximately 6% in the coal layer due to an increase in gas saturation then increases 4 to 5% due to further drops in pore pressure. Though these changes are small and non-uniform due to the heterogeneous nature of the coal aquifer, they are significant and can be seen in both the raw seismograms as well as the tomograms. Our observations further suggest that produced water comes from the overlying sandy-shale and that pressure drawdown in the coal is not spatially efficient.

References cited

Ayers, W.B., 2002, Coalbed gas systems, resources, and production and a review of contrasting cases from the San Juan and Powder River basins: AAPG Bulletin, v. 86, no. 11, p. 1853-1890.

Colmenares, L.B., and Zoback, M.D., 2005, Geomechanics and the effectiveness of wellbore completion methods of coalbed natural gas (CBNG) wells in the Powder River Basin: Implications for water and gas production, *in* Zoback, M.D., editor, Western Resources Project Final Report—Produced groundwater associated with

coalbed natural gas production in the Powder River Basin: Wyoming State Geological Survey Report of Investigations No. 55, p. 127-157.

De Bruin, R.H., Lyman, R.M., Jones, R.W., and Cook, L.W., 2000, Coalbed methane in Wyoming: Wyoming State Geological Survey Information Pamphlet 7, 19 p.

Flores, R.M. 2004, Coal bed methane in the Powder River Basin, Wyoming and Montana: An assessment of the Tertiary-Upper Cretaceous coalbed methane total petroleum system: U.S. Geological Survey Digital Data Series DDS-69-C, Version 1.0.

Gassmann, F., 1951, Elastic waves through a packing of spheres: Geophysics v. 16, no. 4. p. 673-685.

Greaves, R.J., and Fulp, T.J., 1987, Three-dimensional seismic monitoring of an enhanced oil recovery process: Geophysics, v. 52, no. 9, p. 1175-1187.

Harris, J.M, Nolen-Hoeksema, R.G., Langan, R.T., Van-Schaack, M., Lazaratos, S.K., and Rector, J.W., 1995, High resolution cross well imaging of a west Texas carbonate reservoir: Part1- Project summary and interpretation: Geophysics, v. 60, no. 3, p. 667-681.

Jenkins, S.D., Waite, M.W., and Bee, M.F., 1997, Time-lapse monitoring of the Duri steamflood: A pilot and case study: The Leading Edge, v. 16, p. 1267-1273.

Johnstad, S.E., Seymour, R.H., and Smith, P.J., 1995, Seismic reservoir monitoring over the Oseberg field during the period 1989-1992: First Break, v. 13, v. 169-183.

King, J.G., and Wilkins, _, 1994, Proceedings for Conference on Ultrafine Structural Coals and Cokers, British Coal Utilisation Research Association (BCURA), London, England, p. 46.

Landro, M., 2001, Discrimination between pressure and fluid saturation changes from time-lapse seismic data: Geophysics, v. 66, no. 3, p. 836-844.

Landro, M., Veire, H.H., Duffaut, K., and Najjar, D., 2003, Discrimination between pressure and fluid saturation changes from marine multicomponent time-lapse seismic data: Geophysics, v. 68, no. 5, p. 1592-1599.

Larson, V.E., 1989, Preliminary evaluation of coal bed methane geology and activity in the Recluse area, Powder River Basin, Wyoming: Quarterly Review of Methane from Coal Seams Technology, v. 6, no. 3-4, p. 2-10.

Lumley, D.E., 1995, 4-D seismic monitoring of an active steamflood: 65th Annual International Meeting, Society of Exploration Geophysicists, Expanded Abstracts, p. 203-206.

Lumley, D.E., 1996, Seismic time-lapse monitoring of subsurface fluid flow: Ph.D. dissertation, Stanford University, Stanford, California, 168 p.

Mavko, G., Mukerji, T., and Dvorkin, J., 1998, The rock physics handbook: Tool for seismic analysis in porous media: Cambridge University Press, Cambridge, Massachusetts. 339 p.

Mavor, M.J., Gunter, W.D., Robinson, J.R., Law, D.H., and Gale, J., 2002, A paper presented at the Society of Petroleum Engineers (SPE) Gas Technology Symposium held in Calgary, Alberta, Canada.

Nolet, G., editor, 1987, Seismic tomography: With applications in global seismology and exploration geophysics: D. Reidel Publishing Company, Dordrecht, Holland, 400 p.

Nur, A., 1989, Four-dimensional seismology and (true) direct detection of hydrocarbons: The petrophysical basis: The Leading Edge, v. 8, no. 9, p. 30-36.

Nur, A, Tosaya, C., and Thanh, D.V., 1984, Seismic monitoring of thermal enhanced oil recovery processes: 54th Annual International Meeting, Society of Exploration Geophysicists, Expanded Abstracts, session RS.6.

Peterson, J.E., Paulson, B.N.P., and McEvilly, T.V., 1985, Application of algebraic reconstruction techniques to crosswell seismic data: Geophysics, v. 50, no. 10, p. 1566–1580.

Prasad, M., 2001, Mapping impedance microstructure in rocks with acoustic microscopy: The Leading Edge, v. 20, no. 2, p. 172-179.

Pullin, N., Matthews, L., and Hirsche, K., 1987, Techniques applied to obtain very high resolution three-dimensional seismic imaging at an Athabasca tar sands thermal pilot: The Leading Edge, v. 6, no. 12, p. 10-15.

Richardson, S.E., and Lawton, D.C., 2002, Time-lapse seismic imaging of enhanced coal bed methane production: A numerical modeling study: CREWES Research Report 14, p. 17.1–17.13.

Randall, A.G., 1989, Shallow Tertiary gas production, Powder River Basin of Wyoming's coal bed methane: *in* Eisert, J.L., editor, Gas resources of Wyoming: Wyoming Geological Association 40th Field Conference Guidebook, p. 83-96.

Rice, C.A., Ellis, M.S., and Bullock, J.H., Jr., 2000, Water co-produced with coalbed methane in the Powder River

Basin, Wyoming: Preliminary compositional data: U.S. Geological Survey Open-File Report 00-372, 20 p.

Tura, A., and Lumley, D.E., 1998, Subsurface fluid flow properties from time-lapse elastic wave reflection data: Mathematical Methods in Geophysical Imaging, v. 5, p. 125-138.

Tura, A., and Lumley, D.E., 1999, Estimating pressure and saturation changes from time-lapse AVO data: 69th Annual International Meeting, Society of Exploration Geophysicists, Expanded Abstracts, p. 1655-1658.

Yu, G., Vozoff, K., and Durney, D.U., 1993, The influence of confining pressure and water saturation on dynamic elastic properties of some Permian coals: Geophysics, v. 58, no. 1, p. 30-38.

Wang, Z., and Nur, A., 1986, Effect of temperature on wave velocities in sands and sandstones with heavy hydrocarbons: 56th Annual International Meeting, Society of Exploration Geophysicists, Expanded Abstracts, session BHG1.2., p. 3-5.

Wang, Z., Cates, M.E., and Langan, R.T., 1998, Seismic monitoring of a CO_2 flood in a carbonate reservoir: Geophysics, v. 63, no. 5., p. 1604-1617.

CHAPTER 6

Geomechanics and the effectiveness of wellbore completion methods of coalbed natural gas (CBNG) wells in the Powder River Basin: Implications for water and gas production

Lourdes Colmenares and Mark D. Zoback
Department of Geophysics
Stanford University
Stanford, California

Table of contents

List of figures 128
List of tables 129
Abstract 131
Introduction 131
Geologic background 132
Note about Big George Coal 134
Drilling and completion overview 134
Hydraulic fracturing 135
Least principal stress 136
Data analysis per area 136
Area A 137
Area B 137
Areas B1, B2, and C (not shown) 137
Area D 137
Variation of the least principal stress (S3) across the basin 138
Possible causes for the variation of S3 in the basin 142
Thickness 142
Pore pressure changes 142
Relationship between hydraulic fracture orientation and water and gas production 144
Water and gas production in specific areas of the basin 147
Area D (Big George coal) 147
Area D (Wyodak Coal) 147
Area B2 (Anderson coal) 148
Area B1 and B (Anderson coal) 149
Area B (Wall Coal) 149
Area C (Anderson Coal) 150
Area A (Roland Coal) 150
How does the relation between hydraulic fracture orientation and cleat system affect the water and gas production? 150
In areas of vertical hydraulic fracturing: why do some wells have large water production and others low water production? 151
Stratigraphy 151
Thickness 151
Depth 151
Pore pressure and gas production 152
Temporal and spatial variations in pore pressure 153
Recommendations to achieve best well completion practices 155
Summary and conclusions 155
Acknowledgements 156
References cited 156

List of figures

1. Location of the PRB showing counties, cities, CBNG wells and methane prospect areas 133
2. Standard completion method in the CBNG wells in the Powder River Basin using under-reaming 135
3. (a) Water-enhancement test from a CBNG well in the PRB. (b) Schematic illustration of an extended Leak-off Test 136
4. Hydraulic fractures always propagate perpendicular to the orientation of the least principal stress 136
5. Water-enhancement test data from 550 wells were obtained from the locations delineated by thick lines 138
6. Magnitude of S_3 in the Powder River Basin versus depth for Area A and Area B 139

7. Magnitude of S_3 in the Powder River Basin versus depth for the Big George coal in Area D 140
8. Magnitude of S_3 in the Powder River Basin vs. depth for the Wyodak coal in Area D 140
9. Map showing variation of S_3/S_V for (a) Anderson coal and (b) Big George coal 141
10. Map showing variation of S_3/S_V for (a) Canyon coal and (b) Wyodak coal 141
11. (a) S_3/S_V versus thickness for Big George coal. (b) Thickness of Big George 142
12. S_3/S_V versus thickness for Anderson, Canyon, Wall, and Wyodak coals 143
13. Pore pressure interpolation for (a) Big George and (b) Wyodak coals 143
14. Average gas production versus average water production for Anderson, Canyon, Wall, Wyodak, and Big George coals 145
15. Gamma Ray logs showing Big George and Wyodak coals 146
16. Water and gas production from the Big George coal for wells with horizontal fractures in Area D 147
17. Water and gas production from the Big George coal for wells with vertical fractures in Area D 147
18. Water and gas production from the Wyodak coal for wells with horizontal fractures in Area D 148
19. Water and gas production from the Wyodak coal for wells with vertical fractures in Area D 148
20. Water and gas production from the Anderson coal for wells with horizontal fractures in Area B2 148
21. Water and gas production from the Anderson coal for wells with vertical fractures in Area B2 149
22. Water and gas production from the Anderson coal for wells with horizontal fractures in Area B 149
23. Water and gas production from the Wall coal for wells with horizontal fractures in Area B 150
24. Water and gas production from the Wall coal for wells with vertical fractures in Area B 150
25. Average water production versus thickness for the Big George and Wyodak coals 151
26. Average water production versus depth for the Big George coal. 152
27. Plots of water and gas production versus time and delta pressure (hydrostatic pressure minus observed pressure) for different wells in the Big George coal 152
28. (a) Cross-plot of P_{obs}/P_{hyd} versus time. (b) Map of P_{obs}/P_{hyd} for Big George coal 153
29. Elevation versus delta pressure for Big George coal. (a) Ungrouped data. (b) Same data grouped in four different groups. (c) Fluid level versus delta pressure for the four groups 154
30. (a) Variations of fluid elevation and topography for Groups 1 through 4. (b) Location of the wells that conform the different groups. The elevation contours are in meters 154
31. Logically, changes of pressure occur after dewatering starts 155

List of tables

1. Number of data points used to make the interpolation of S3/SV for each coal seam 141

Abstract

The shallow depth and relatively low cost of coalbed natural gas (CBNG) wells in the Powder River Basin (PRB) have resulted in widespread use of open-hole/single horizon completion procedures. A common completion technique used by most operators in the PRB is to drill to the top of the coal seam, case and cement the wellbore, and then drill the coal section. After drilling, the coal section is under-reamed to enlarge the hole and to minimize the effects of any formation damage. In many cases, water is then pumped into the wellbore to "clean it out" and "enhance" production.

After analyzing pressure and flow rate data during these operations, it is clear that "water-enhancement" activities result in hydraulic fracturing of the coal. To determine whether vertical hydraulic fracture growth might extend into adjacent formations (and potentially result in both excess CBNG water production and inefficient depressurization of coals), water-enhancement test data from approximately 550 wells have been analyzed to obtain the magnitude of the least principal stress (S_3) in the coal seams. These data indicate that vertical fracture growth (S_3 corresponds to the minimum horizontal stress) does occur in many parts of the basin whereas the hydrofrac growth appears to be horizontal (S_3 corresponds to the overburden stress) in other areas. In addition, water production from wells with horizontal fractures is minimal and excessive water production is always associated to wells with vertical hydraulic fractures. In these wells with exceptionally high water production, the time at which gas production starts is significantly delayed relative to wells with vertical fractures and low water production, which are excellent gas producers. In general, wells with vertical fractures produced more gas than wells with horizontal fractures.

Wells with vertical fractures tend to be excellent gas producers, which implies that the face cleats in the coals must be efficiently connected by the induced vertical fracture. It has also been identified that horizontal hydraulic fracturing is typical toward the Sheridan area. This may be a significant finding, as water injection wells are perhaps needed in the near future in this region because the water has a high content of sodium and will need to be properly disposed. Thus, knowing that there is no vertical connection between the coal seam that is being produced and the sand layers where the water may be injected is particularly important for the operators of the area if water injection activities are undertaken here.

It appears that coal thickness affects the S_3 magnitudes. In general, in areas where a coal seam has a thickness greater than 60 feet S_3 is equivalent to the minimum horizontal stress, and therefore fractures propagate in the vertical direction. This implies that by identifying the areas where a coal seam is thicker than 60 feet, areas of vertical fracture propagation would also be identified. In order to minimize CBNG water production, recommendations for better well completion practices have been outlined here. In areas of known vertical fracture propagation it is necessary to limit the injection during the water enhancement tests in order to prevent propagation of induced fractures into the overlying water-bearing formations.

In areas where S_3 is unknown, a minifrac (approximately 2 bpm for about 2 min) should be done to determine the magnitude of S_3 and thus whether fracture propagation would be vertical or horizontal. If S_3 corresponds to the overburden, horizontal fracture propagation will occur and the water enhancement activities can proceed as usual. As many wells with horizontal fractures tend to be poor gas producers, it is also suggested that such wells are hydraulically fractured (and propped) to enhance gas production. If the shut-in pressure is significantly less than the overburden, vertical hydraulic fracture growth is implied and significantly reduced pumping is advised. This would be beneficial from the perspective of minimizing produced waters and decreasing the time for initial gas production.

Introduction

Most coalbed natural gas in the U.S. has been produced from the San Juan Basin of New Mexico and Black Warrior Basin of Alabama. In recent years, the Powder River Basin (PRB) has gained in importance as production and number of producing wells has increased tremendously.

The PRB of Wyoming and Montana is the site of the fastest growing domestic natural gas play, mostly from the development of coalbed natural gas (CBNG) from the Wyodak and Big George coal beds of the Fort Union Formation. Nearly 4 billion cubic feet (BCF) per day of CBNG are currently being produced in the U.S., with about 20% or 800 million cubic feet (MMCF) per day of it coming from the PRB. Within the next 10 years, as much as 75% of the growth in CBNG production in the U.S. is expected to occur in this region. Since 1996, the amount of producing wells has increased from around 30 to approximately 12,000 in the basin and it is anticipated that in the next decade the amount of producing wells will increase to between 20,000 and 50,000. Along with the growth in CBNG production has been the growth in produced water, as part of dewatering and depressurizing the coal formations, which enables the coals to release their adsorbed methane. CBNG water production has increased since 1996 from about 100 thousand barrels (MBBL) per day to 1.6 million barrels per day

in 2003 (Wyoming Oil and Gas Conservation Commission, 2004). Coalbed natural gas wells in the PRB are generally pumped constantly, removing as much as 400 barrels per day per well (De Bruin and others, 2000). The production history of a typical CBNG well in the basin shows that even after gas production is initiated, large volumes of water are still being produced. Production from water-bearing coal seams can yield significant volumes of water, enough to make it difficult or infeasible to dewater the formation sufficiently to initiate CBNG flow (U.S. Environmental Protection Agency, 2002). Even though the water is generally of potable quality in the center of the basin, it becomes more saline toward the north and south. Therefore, the disposal of such great amounts of water produced by CBNG wells is a major environmental issue, especially in areas where the produced water has a high content of sodium.

At the moment production is concentrated along two main bands in the basin (**Figure 1**). Development toward the Sheridan area has started but it is not as developed as in Campbell and Johnson counties of Wyoming. Coalbed natural gas production has migrated toward the western part of the basin, compared to its initial times (1980s to early 1990s) when production was concentrated in Campbell County. Since about 12,500 wells have been drilled to date, with 50,000 wells total expected in the next decade, water disposal constitutes a major environmental challenge. At the present, 150 barrels of water are produced per well per day, with 50,000 wells in the basin, water production will rise to 7.5 million barrels per day. The goal of this study is to evaluate wellbore completion practices to determine if there are ways to produce less CBNG water and still achieve adequate coal depressurization for CBNG production. Minimizing water production would have appreciable beneficial consequences.

Geologic background

The PRB is bounded to the east by the Black Hills uplift, to the west by the Bighorn uplift and Casper arch, to the south by the Laramie and Hartville uplifts, and the Miles City arch and the Cedar Creek Anticline separate it from the Williston Basin to the north (**Figure 1**). The long axis of the basin is generally aligned NW-SE, and is 18,000 feet deep. Sediments range from Paleozoic at the bottom through Mesozoic to Tertiary at the top of the basin. The basin is a large asymmetrical syncline with its axis near the west side of the basin.

Several periods of deposition by marine and fluvial-deltaic processes have occurred within the basin during the Cretaceous and Tertiary periods. These Cretaceous and lower Tertiary rocks have a total thickness of up to 15,000 feet (Montgomery, 1999). Coal is found in the Paleocene Fort Union and Eocene Wasatch formations. Most of the coal beds in the Wasatch Formation are continuous and thin (6 feet or less) although, locally, thicker deposits have been found (De Bruin and others, 2000). The Fort Union Formation (Paleocene) extends over 22,000 square miles in the PRB. It is overlain by the Wasatch Formation (Eocene) and underlain by the Lance Formation (Upper Cretaceous) in the central part of the basin, and is more than 5200 feet thick along the basin axis.

In ascending stratigraphic order, the Fort Union Formation is divided into the Tullock, Lebo, and Tongue River Members. The Tullock Member is 740 feet thick, the Lebo Member 2600 feet thick, and the Tongue River Member 1860 feet thick. The Fort Union Formation outcrops on the eastern side of the basin, east of Gillette, and on the western side of the basin, north and south of Buffalo. Most of the coal beds in this formation are part of the upper Tongue River Member, which is typically 1500 to 1800 feet thick, and up to a composite total of 350 feet of coal can be found in various beds. The thickest of the individual coal beds is over 200 feet (Flores and Bader, 1999). Coal beds are interspersed with sandstone, conglomerate, siltstone, mudstone, and limestone.

Most CBNG wells in the Powder River Basin are in the Tongue River Member of the Fort Union Formation, in the Wyodak-Anderson coal zone, which contains up to 32 different coal beds according to some authors (Ayers, 1986), including the Big George in the central part of the basin (Flores and Bader, 1999). Most of the coal beds are found within 2500 feet of the ground surface. The Wyodak coal bed gets progressively deeper and thicker toward the west. The thickness of the Wyodak coal bed ranges from 42 to 184 feet. Most of the CBNG wells in the PRB are within the Wyodak coal zone near Gillette. The Big George coal bed is located in the central and western part of the PRB. Although the Big George is stratigraphically higher than the Wyodak, owing to the structure of the basin, the Big George, in the center part of the basin, is deeper than the Wyodak at the eastern margin of the basin.

The stratigraphic correlation of coal beds composing the Wyodak-Anderson coal zone is complex. Part of the problem originated from the use of the same names by various investigators for coal beds that are not stratigraphically correlative within the PRB. In addition, many local names were applied to coal beds in isolated areas, beds that were later physically correlated across the basin. Compounding these problems, no biostratigraphic studies were conducted to confirm or refute these physical correlations basin-wide. One solution to these stratigraphic correlation problems was

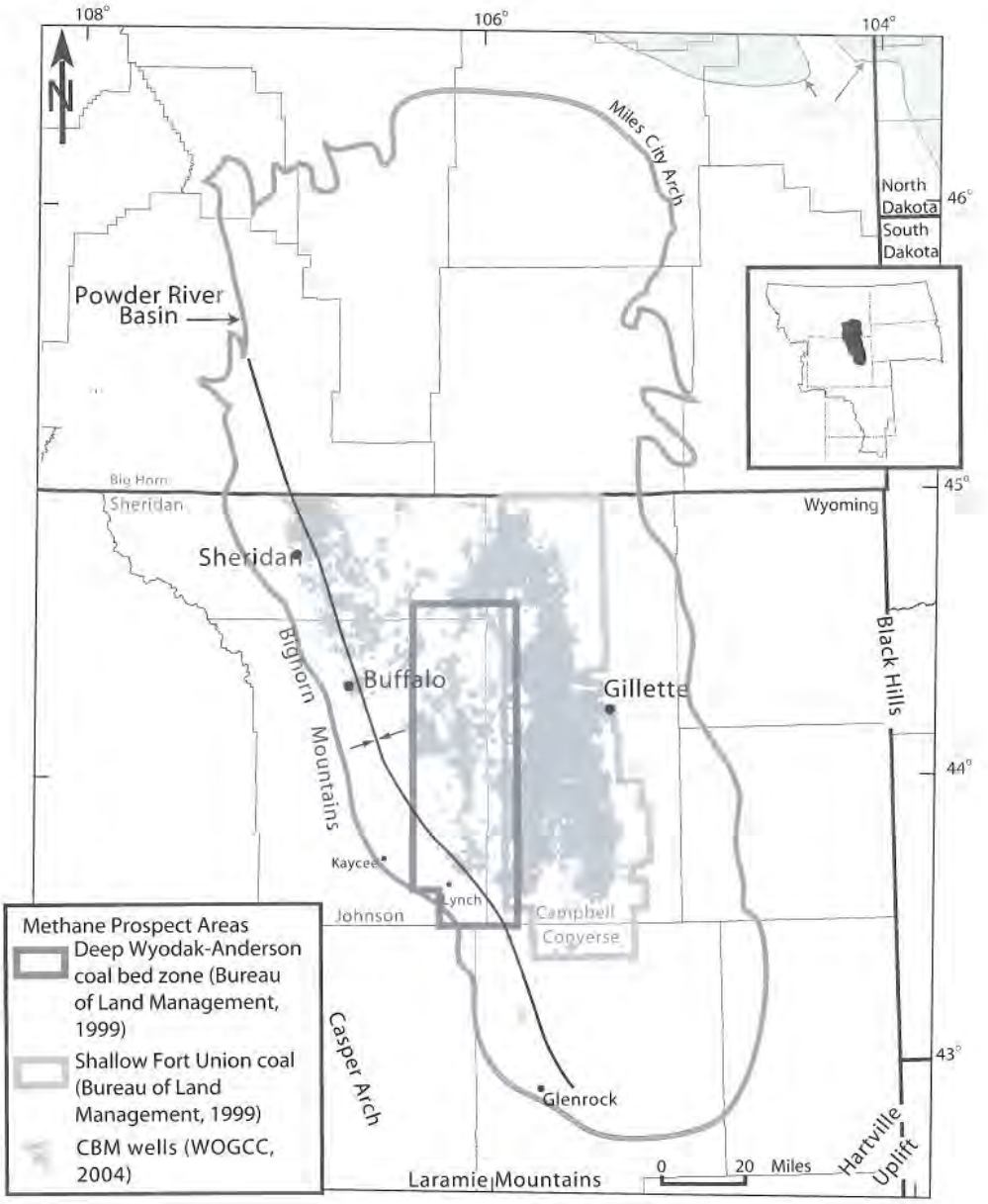


Figure 1. Location of the PRB showing counties, cities, CBNG wells and methane prospect areas (modified from Flores and Bader, 1999).

to lump all the coal beds and associated rocks into a single coal zone. This coal zone was named the Wyodak-Anderson coal zone by Averitt (1975) and was correlated basin-wide by Glass (1980). It has also been called the Wyodak coal, or the Anderson and Canyon coal beds coalesced (Flores and Bader, 1999).

The complexity of correlation is displayed by splitting and merging of the Wyodak-Anderson coal zone according to Flores and Bader (1999). Splitting of coal beds in the Wyodak-Anderson coal zone generates two beds (the lower Wyodak bed comprising the merged Canyon and Werner coals, and the upper Wyodak bed comprising the merged Smith, Swartz, and Anderson coal), three beds (Anderson or Dietz 1, Dietz 2, and Dietz 3), five beds (lower and upper Anderson and lower, middle, and upper Canyon beds), six beds (Smith, Swartz, Anderson, upper and lower Canyon, and Werner beds), or as many as eleven beds (Sussex beds). Overall, successive splitting and merging of beds in this coal zone basin-wide from overlapped, offset, zigzag, and shingled segments, results in older Wyodak-Anderson coal beds (for example, the Big George coal) in the west-central part of the basin than on the basin margins (for example, Smith, Anderson, Dietz, Canyon, School, and Badger coal) (Flores and Bader, 1999).

Most of the coal in the PRB is subbituminous in rank, which is indicative of a low maturity level. Some lignite, lower in rank, has also been identified. The thermal content of the coals found in the Powder River Basin is typically 8300 Btus per pound (U.S. Environmental Protection Agency, 2002). Coal in the PRB was formed at relatively shallow depths, at relatively low temperatures. Most of the methane generated under these conditions is biogenic, which means that it was formed by bacterial decomposition of organic matter. The coals from the Wasatch and Fort Union formations tend to be less thermally mature than the Tertiary coal beds located in the deeper parts of the Wind River, Bighorn, Hanna, and Green River coal fields of Wyoming (De Bruin and Lyman, 1999). Consequently, coal in the PRB contains less methane per unit volume than many other coal deposits in other parts of the country. The gas is typically more than 95% methane, the remainder being mostly nitrogen and carbon dioxide. This resource was overlooked for many years because it was thought to be too shallow for the production of significant amounts of methane. However, the relatively low gas contents of PRB coal is compensated by the thickness of the coal deposits. Because of the thickness of the deposits and their accessibility, commercial development of CBNG has been found to be economical. In the PRB, two different CBNG sources are commonly developed: (1) gas extraction from methane-charged dry sand layers overlying or interbedded with the coals, and (2) conventional methane extraction from the water saturated coal seams (U.S. Environmental Protection Agency, 2002).

Note about Big George Coal

The Big George coal, as defined and interpreted by Flores and Bader (1999), is the amalgamation of different coals, and is between 45 and 200 feet thick. The Big George, as so defined, exists only in the central part of the basin, that is, it directly indicates the location. According to what the operators of the basin have called Big George, this coal seam ranges from 5 feet to 200 feet in thickness, which does not coincide with the interpretation of Flores and Bader (1999). However, the interpretation of the operators and what they report to the Wyoming Oil and Gas Conservation Commission (WOGCC) has been adopted because making the reconciliation between the operators' interpretation and the interpretation of the U.S. Geological Survey is an extremely daunting, if not impossible, task and beyond the scope of this study.

It is very important to mention that the identification of coal seams in this study has been taken from what the operators report to the WOGCC website. Therefore, certain names may not coincide with Flores and Bader's (1999) interpretation of coals in the basin. However, a complete basin-wide reconciliation between all the different names for a certain coal bed does not exist yet so the WOGCC interpretation was chosen as a guide. Currently, efforts are taking place to reconcile the coal nomenclature (Jones, 2005), but, until these reconciliations are completed, some ambiguity remains regarding coal beds classified as Big George by different sources. In an attempt to reduce some of the uncertainty, Gamma Ray (GR) logs were analyzed, where available, to establish correlations across wells of the Big George and the Wyodak coals since they are thick and have a distinct GR response. Based on this analysis, we feel confident that the operators' definition and interpretation of these coal beds is consistent (see the section on Relationship between hydraulic fracture orientation and water and gas production for a more detailed description of the GR analysis). This GR-based distinction of coal beds is harder, if not impossible, for the thinner coals. Nevertheless, the possible confusion in definition of these coal beds should be kept in mind for future analyses.

Drilling and completion overview

The following is a standard drilling and completion procedure followed by the operators (**Figure 2**) in the PRB when under-reaming the coal seam.

The well is spudded with a 14 3/4" surface bit and drilled to 10% of the total well depth or a minimum of 95 feet (29 m). Then, a surface casing (10 3/4") is put in place and cemented. After cementing the surface casing, operators drill the next section down to the top of the coal. This section is drilled with water as a drilling fluid; sometimes gel is added to make the water more viscous, which improves the cleaning capacity of the drilling fluid. As a result, more debris can be transported out of the well. A 7-inch production casing is then put in place and cemented. The operators pay special attention to achieve a good high-quality cement job for this casing shoe, in order to prevent the CBNG from escaping the well, and also to prevent communication with overlying aquifers. Because of this, a cement bond log is run to ensure the quality of the cement job.

Initially, the coal section and an extra 10 feet (3 m) below the coal are drilled with a 6 1/4-inch bit. The drill fluid used is identical to the previous section (water with gel). After finishing the 6 1/4-inch hole through the coal, a GR log is run in order to accurately locate the extent of the coal seam. After logging, the diameter of the coal section is enlarged with an under-reamer to a final diameter of 14 inches. When there is more than one economical coal seam, operators under-ream the bottom coal bed and perforate the upper ones. Afterwards, the coal is water-enhanced. This procedure implies the pumping of 2500 gpm or 60

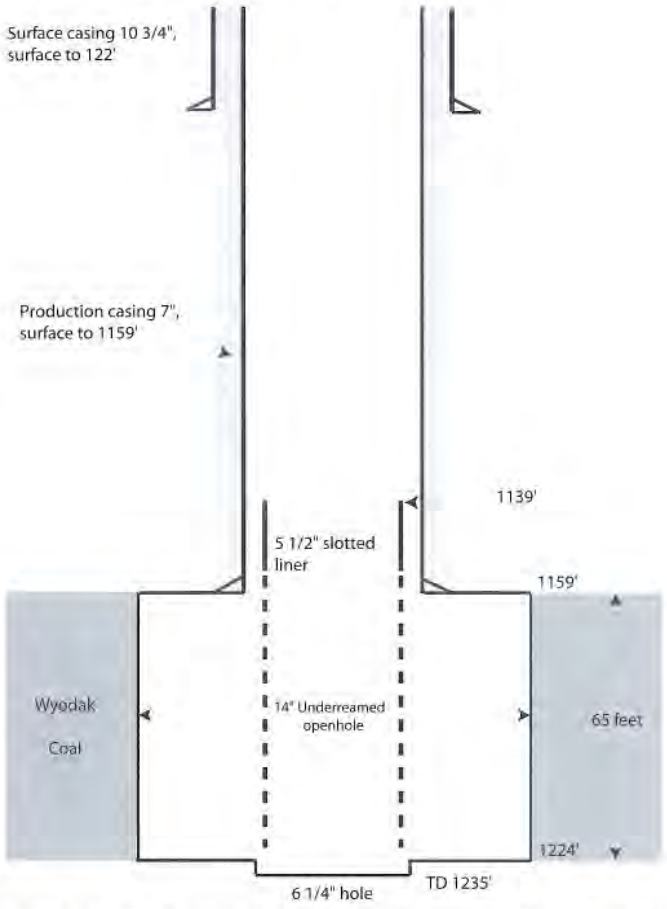


Figure 2. Standard completion method in the CBNG wells in the Powder River Basin using under-reaming. Some operators prefer not to use the slotted liner.

bpm of water into the coal for approximately 15 minutes. It is possible that during this process the coal is hydraulically fractured. Some operators use a 5 1/2-inch slotted liner in the open hole section of the well, as shown in **Figure 2**. This slotted liner is used to prevent debris migrating up the hole and blocking the flow. To finalize the completion of the well, a submersible water pump and the wellhead are installed. The tubing, with a submersible electric water pump, is inserted to allow the water to flow from the bottom of the hole. CBNG exits the well through the annulus formed by the casing and the tubing. The well is capped to control the flow of methane gas. Wells are often dewatered for several months before producing significant quantities of methane gas.

Hydraulic fracturing

During the early years of CBNG development in the PRB (1980s to early 1990s), gas exploration and development companies completed wells with and without hydraulic fracture techniques. Early wells were completed without fracturing treatments, particularly wells targeting gas reserves in coals interspersed between sandstone layers. However, the Quarterly Review (U.S. Environmental Protection Agency, 2002) reported that in one well, Rawhide 15-17, located north of Gillette, Wyoming, an "open frac" hydraulic fracturing was performed using 13,000 lbs of 12/20-mesh sand in 3500 gallons of gelled water. Several wells installed in the early 1990s by Betop, Inc. were fractured using 4000 to 15,000 gallons of a solution with 2% potassium chloride (KCl) in water. Sand was used to prop the fractures open in five of these wells (U.S. Environmental Protection Agency, 2002). However, hydraulic fracturing experienced little success in this basin. It was argued that fractured wells produced poorly because the permeable, shallow sub-bituminous coals collapsed under the pressure of the overburden after they were dewatered.

The PRB contains coals of high permeability. Consequently, drilling fluid (typically water) is lost when drilling the coal beds. Many times drilling mud is used to prevent loss of circulation. Because of this high permeability, most coal bed wells in the Fort Union Formation can be drilled and completed without the use of hydraulic fracturing. In the past, water or sand/water mixtures have been used to fracture the coal (U.S. Environmental Protection Agency, 2002).

The operators in the PRB routinely perform a procedure called "water-enhancement" and it is intended to create pathways in the coal for easier flow of water and gas into the well. This procedure results in the fracturing of the coal. In **Figure 3a** a water-enhancement test plot from the PRB is shown. The upper and lower panels show the flow rate in gallons per minute (gpm) and barrels per min (bpm) respectively. The middle panel shows the pressure-time history while the water was being pumped into the well. When a fracture is produced during the water-enhancement procedure, the pressure-time history from the water-enhancement test (middle panel in **Figure 3a**) is similar to the pressure-time history of an extended Leak-off Test (**Figure 3b**). The water-enhancement test data show that large volumes of water are pumped into the coal while the pressure remains constant. This indicates the formation of a hydraulic fracture and its propagation. The extent of a hydraulic fracture is controlled by the pumping pressure and the variation of the least principal stress with depth. We have also confirmed that such "enhancement" activities result in hydraulic fracturing of the coal through direct interviews with the different operators in the PRB.

Even though hydraulically fracturing the coal might be intended to render good results for CBNG production, if such a fracture is vertical and extends up into adjacent strata through a confining unit, it could result in both excess CBNG water production, as migration of groundwater

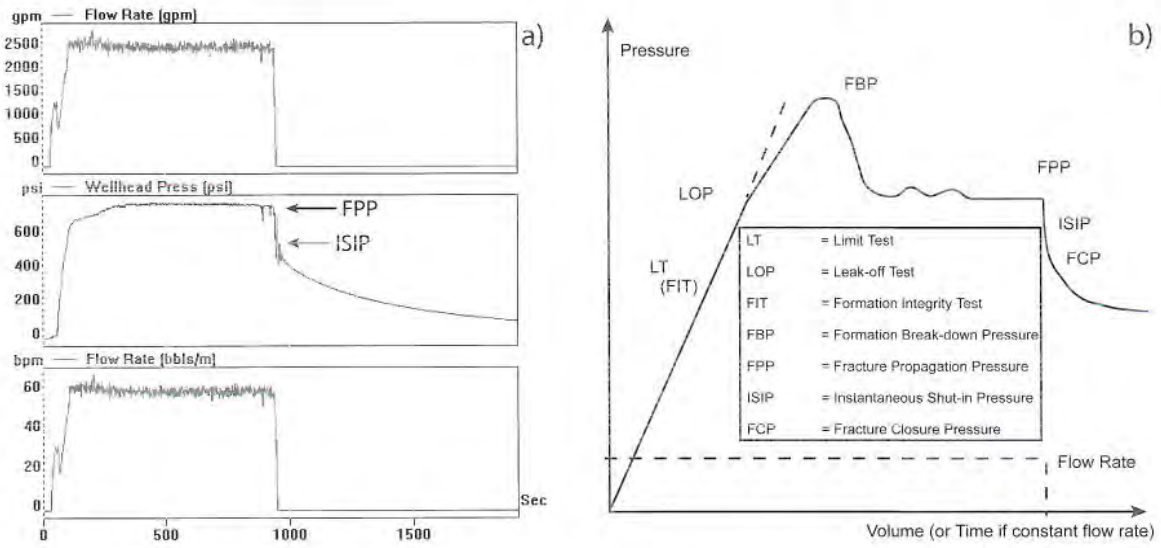


Figure 3. (a) Water-enhancement test from a CBNG well in the PRB. (b) Schematic illustration of an extended Leak-off Test (after Zoback and others, 2003).

toward the producing well occurs, and inefficient depressurization of coals. Avoiding this can result in great benefits for the operators and the environment.

To determine the direction of propagation of a hydraulic fracture it is necessary to know the magnitude of the least principal stress (S_3) since a hydraulic fracture will always propagate perpendicular to the orientation of S_3 (**Figure 4**). Therefore, if S_3 corresponds to the minimum horizontal stress, this indicates that the hydraulic fracture propagates in a vertical plane and if S_3 corresponds to the overburden stress, this indicates that the hydraulic fracture will propagate in the horizontal plane. Even though the water enhancement tests in the PRB are not made with the intention of determining the magnitude of S_3, they are a useful resource since it is possible to determine such magnitude from these tests.

It has been suggested that after a relatively short period of production (several months), an appreciable amount of the water produced from CBNG wells may come from the formations adjacent to the coal seams (personal communication with several operators, 2002 through 2003). It seems that one factor possibly exacerbating this is the vertical growth of hydraulic fractures during the drilling and completion of CBNG wells. We will test this by analyzing the relationship between hydraulic fracture orientation and water and gas production.

Least principal stress

Data analysis per area

As mentioned earlier, the magnitude of the least principal stress can be obtained from the water-enhancement tests. Figure 3a shows that at the surface the Fracture Propagation Pressure (FPP) is 750 psi and the Instant Shut-in Pressure (ISIP) is 600 psi. To determine the magnitude of the least principal stress at the depth of this test, it is neces-

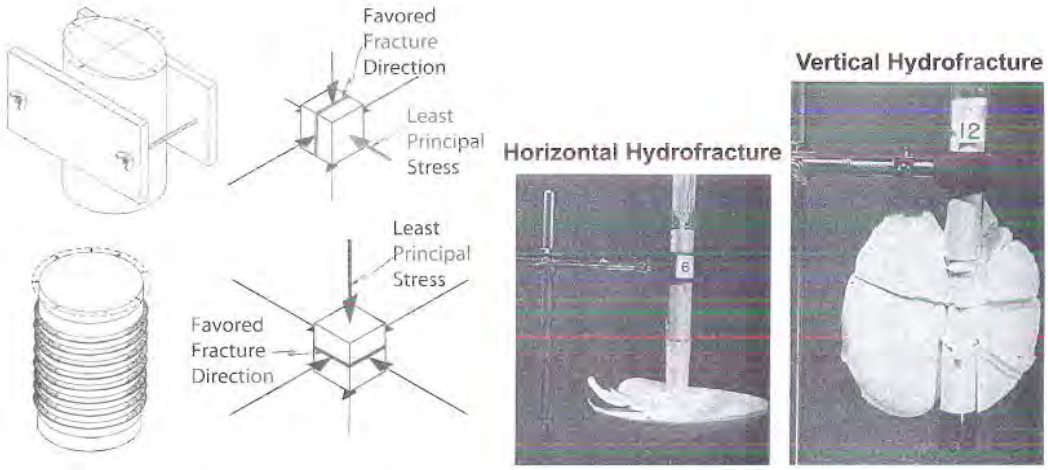


Figure 4. Hydraulic fractures always propagate perpendicular to the orientation of the least principal stress.

sary to add the pressure in the wellbore due to the column of wellbore fluid.

To date, we have analyzed water-enhancement tests from 550 wells, and obtained the magnitude of the least principal stress (S_3) for 372 of these wells. The well locations are shown in **Figure 5**. **Figures 6** to **8** show the analyzed data, which have been grouped by location (areas A, B, B1, B2, C, and D shown in **Figure 5**). The colors represent the producer coal interval in the respective wells, the black line is the overburden stress or S_v, and the gray line corresponds to the hydrostatic pressure or P_{hyd} (0.44 psi/ft).

The magnitude of S_v can be calculated by integration of rock densities from the surface to the depth of interest, z, that is

$$S_v = \int \rho(z) g dz \approx \bar{\rho} g z$$

where $\rho(z)$ is the density as a function of depth, g is the gravitational acceleration constant and $\bar{\rho}$ is mean overburden density. Since density logs were not available, a mean overburden density was assumed equal to 2.3 g/cc, which reflects the different lithologies that can be found above the coal (i.e. mudstones, shales, sandstones).

It is important to note that in some of the figures that follow, the ISIP's fall above the line denoting the overburden stress, which indicates that the magnitude of S_3 is greater than the magnitude of the overburden. Possible causes are the shallow depth of the measurements or the large volumes of water used in the water-enhancement test. At shallow depths the overburden might not be one of the principal stresses and therefore the ISIP's could be larger than the overburden. With respect to the other possible cause, since water enhancement tests are not originally intended to determine the magnitude of S_3, the large flow rate used in the tests could create friction effects that might disguise the actual magnitude of S_3. To reduce the uncertainty in determining the magnitude of S_3, water-enhancement tests made at lower flow rates (1 to 4 bpm instead of 60 bpm) would be more suitable for the determination of the least principal stress.

Area A

All the data from the 12 wells in Area A (**Figure 5**) come from the Roland coal, which is at a depth between 600 and 800 feet (**Figure 6a**). The magnitude of the least principal stress is approximately equal to the overburden. Therefore, since the overburden corresponds to the least principal stress, the hydraulic fractures produced in this area propagate in a horizontal plane. This may be a significant finding, as water injection wells are perhaps needed in the near future in this region because the water has a high sodium content and will need to be properly disposed. Thus, knowing that there is no vertical connection between the coal seam that is being produced and the sand layers where the water may be injected is particularly important for area operators if water injection activities are undertaken here.

Area B

The data in Area B (**Figure 5**) are from 50 wells that are producing from either the Anderson, Cook, Canyon, Smith, Stray, or Wall coals (**Figure 6b**). Down to a depth of 850 feet (Anderson, Cook, Canyon, Smith, and Stray coals), the magnitude of the least principal stress appears to correspond to the overburden, which indicates horizontal propagation of the hydraulic fractures. This implies that the coals just mentioned are not connected to adjacent formations, an important aspect to know if injection is needed in this area. In the Wall coal, between 850 and 1200 feet, the magnitude of the least principal stress is generally below the overburden. Therefore, for the Wall coal, most hydraulic fractures would appear to propagate in the vertical direction.

Areas B1, B2, and C (not shown)

Area B1 (**Figure 5**) is just to the west of Area B and all nine wells are in the Anderson coal. Water enhancement tests from these wells indicate that the least principal stress is clearly the minimum horizontal stress as it is well below the vertical stress. Therefore, the fractures propagate vertically. It is important to note that for these wells the Anderson coal is about 200 feet deeper than in Area B.

West of area B1, stress data from the Anderson coal in Area B2 (**Figure 5**) show that the least principal stress can either be the overburden (five wells) or the minimum horizontal stress (13 wells). This indicates that both types of hydraulic fractures are produced in this area. At this location, the Anderson coal spans from a depth of 500 to 1000 feet deep.

South of Area B, the magnitude of the least principal stress from 13 wells in the Anderson and Canyon coals in Area C (**Figure 5**) corresponds to the minimum horizontal stress. Thus, vertical hydraulic fracturing is expected in this region. In Area C the Anderson coal spans between 600 and 1000 feet, similar to Area B2.

Area D

In Area D (**Figure 5**) the data come from 61 wells in the Big George and Wyodak coals. For the Big George coal, all the wells located in T47N, R75W and most of the wells in T46N, R74W (**Figure 7a**) have water enhancement tests that indicate that the least principal stress corresponds to the minimum horizontal stress, i.e. the fractures would be expected to propagate vertically (**Figure 7b**). All the wells

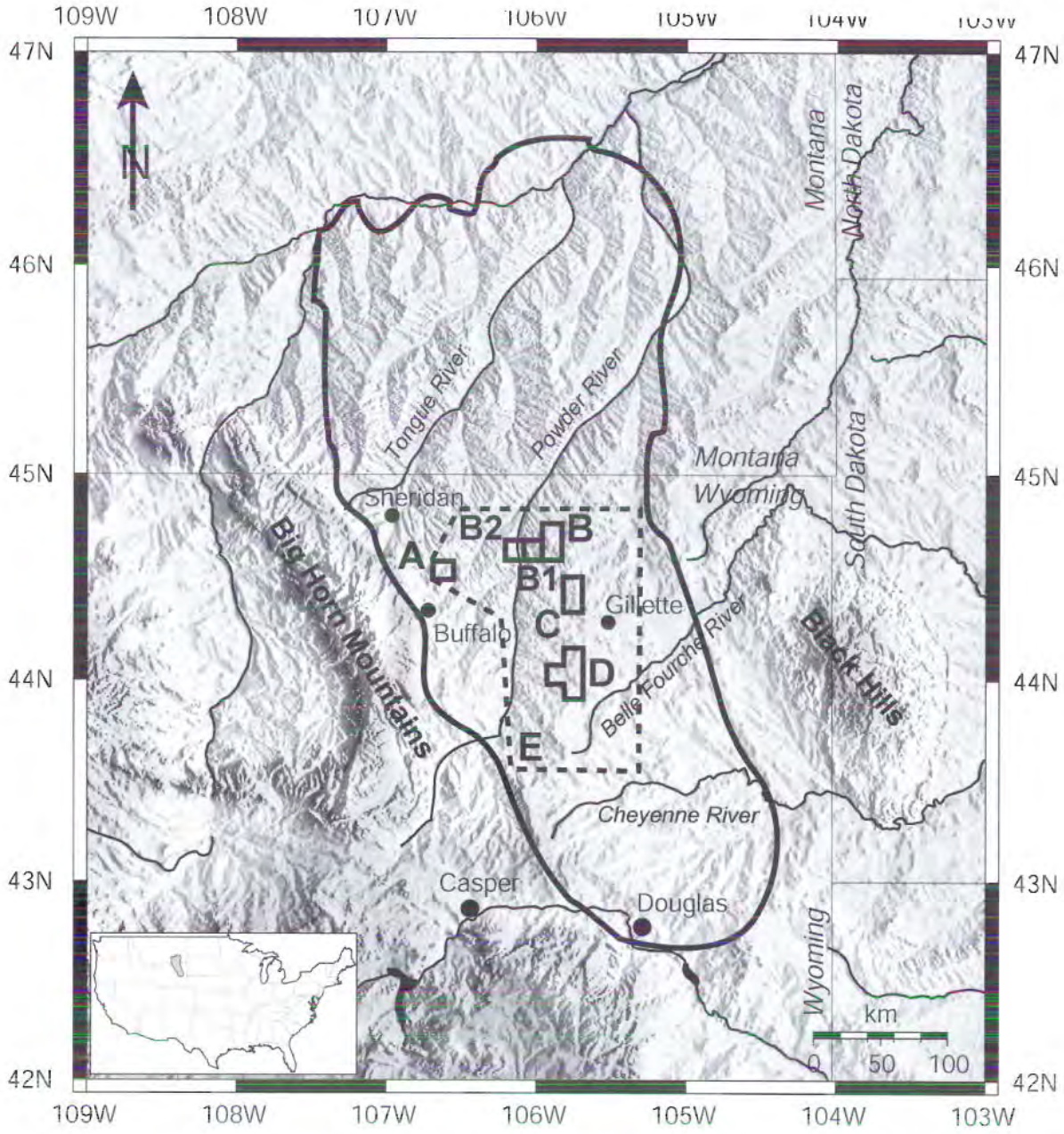


Figure 5. Water-enhancement test data from 550 wells were obtained from the locations delineated by thick lines. The letters identify the grouping of the fields in the areas we analyzed. The data from Figures 6 to 8 all come from areas A to D. The dashed line encompasses the total area (E), from where all the data were obtained.

located in T47N R74W and some of the wells located in T46N R74W (**Figure 7a**) show that the magnitude of the least principal stress corresponds to the overburden, i.e. the fractures propagate horizontally (**Figure 7c**). For the Wyodak coal a geographic differentiation is also seen. As can be observed in **Figure 8a**, in the wells located in sections 1, 2, 11, 12, 13, 14, 23, 24, 26 and 36 of T48N R74W (**Figure 8b**), the fractures propagate vertically. In sections 15 and 21, of the same township (**Figure 8b**), the fractures are expected to propagate horizontally (**Figure 8c**).

Variation of the least principal stress (S_3) across the basin

As mentioned earlier, the magnitude of the least principal stress has been determined from water-enhancement tests for wells targeting different coal seams in the basin. Maps of the occurrence of vertical and/or horizontal fractures in the central part of the basin have been made for each coal. However, water-enhancement test data have come only from about 550 wells, representing 4% of the total amount of wells in the PRB. Therefore, more data are needed to make the maps more complete.

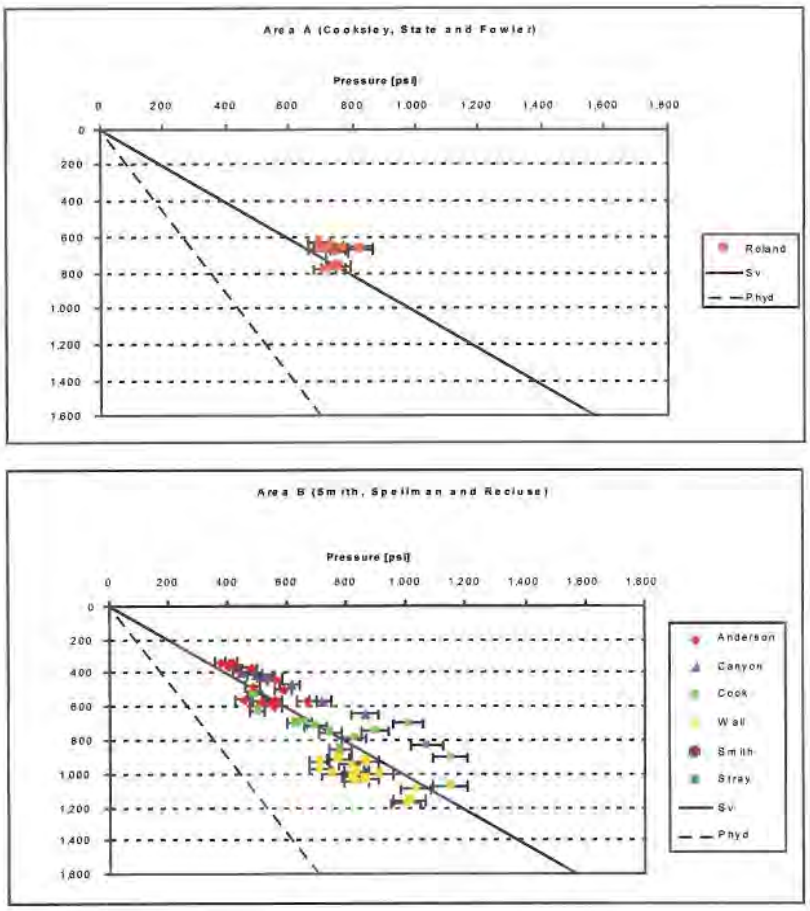


Figure 6. Magnitude of S_3 in the Powder River Basin versus depth for Area A and Area B. The data has been plotted per geographic location and the color denotes the coal seam where the test was performed. The location of areas A and B can be seen in Figure 5.

In **Figures 9** and **10**, the blue color represents areas where the fractures are horizontal, that is $S_3 = S_V$ ($S_3/S_V = 1$). The red shades represent areas where the fractures are vertical, that is $S_3 = S_{hmin}$, ($S_3/S_V < 1$). These maps were made using the interpolation tool from GMT (the Generic Mapping Tool; Wessel and Smith, 1995). The areas that do not have any points are areas where there is no control over the interpolation and should be interpreted carefully, hence, the question marks. The interpolation for each coal was made with the numbers of points outlined in **Table 1**. Many of the wells (data points) are situated very close to each other, so the symbols for some wells overlap or plot on top of each other.

In **Figures 9** and **10** it can be seen that vertical and horizontal fractures occur in many areas of the basin. However, it seems that north of Gillette and Buffalo, horizontal fracturing is more common than vertical fracturing. It appears that for places where the coal is thinner, there is more possibility of horizontal fracturing. For instance, in Big George (**Figure 9**) and Wyodak (**Figure 10**), which are thick coals, areas with vertical fractures are more common than areas with horizontal fractures. Conversely, for Anderson, Canyon, Cook, Werner, and Wall (the last three not shown in here), which are thinner coals, areas with horizontal fractures seem to be more common.

The reliability of the maps could be improved if more least-principal stress data are acquired and also if a consensus on the naming of coals could be reached to ensure a consistent classification.

These maps are potentially very useful for future developments in the basin. The operators could use the maps as tools to easily identify areas where potential fractures could propagate in the vertical or horizontal plane. If the operators know in advance that they would cause vertical fracture growth with their enhancement techniques, they could then limit the amount of water they use in the tests to hopefully limit the extent of vertical fracture propagation.

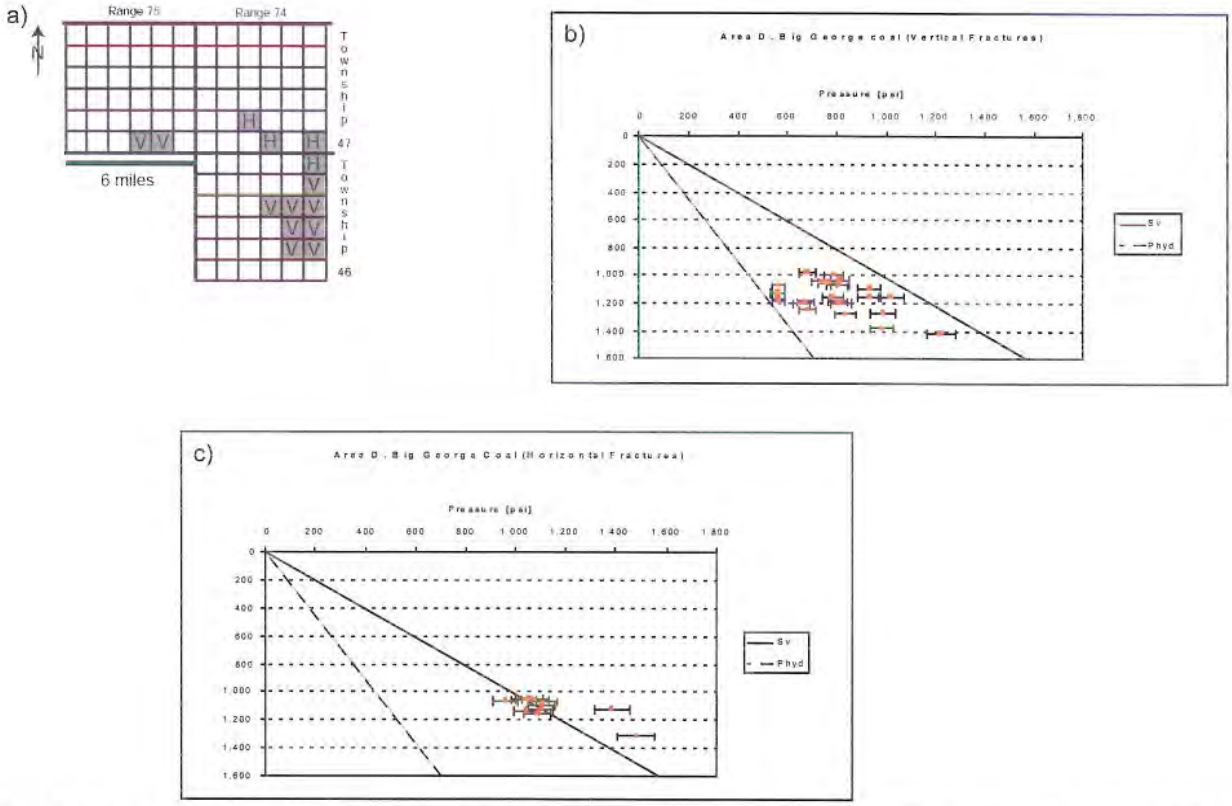


Figure 7. Magnitude of S_3 in the Powder River Basin versus depth for the Big George coal in Area D. (a) Occurrence of horizontal (H) and vertical (V) hydraulic fractures in Area D. The location of this area can be seen in **Figure 5**. (b) S_3 corresponds to the minimum horizontal stress. (c) S_3 corresponds to the vertical stress.

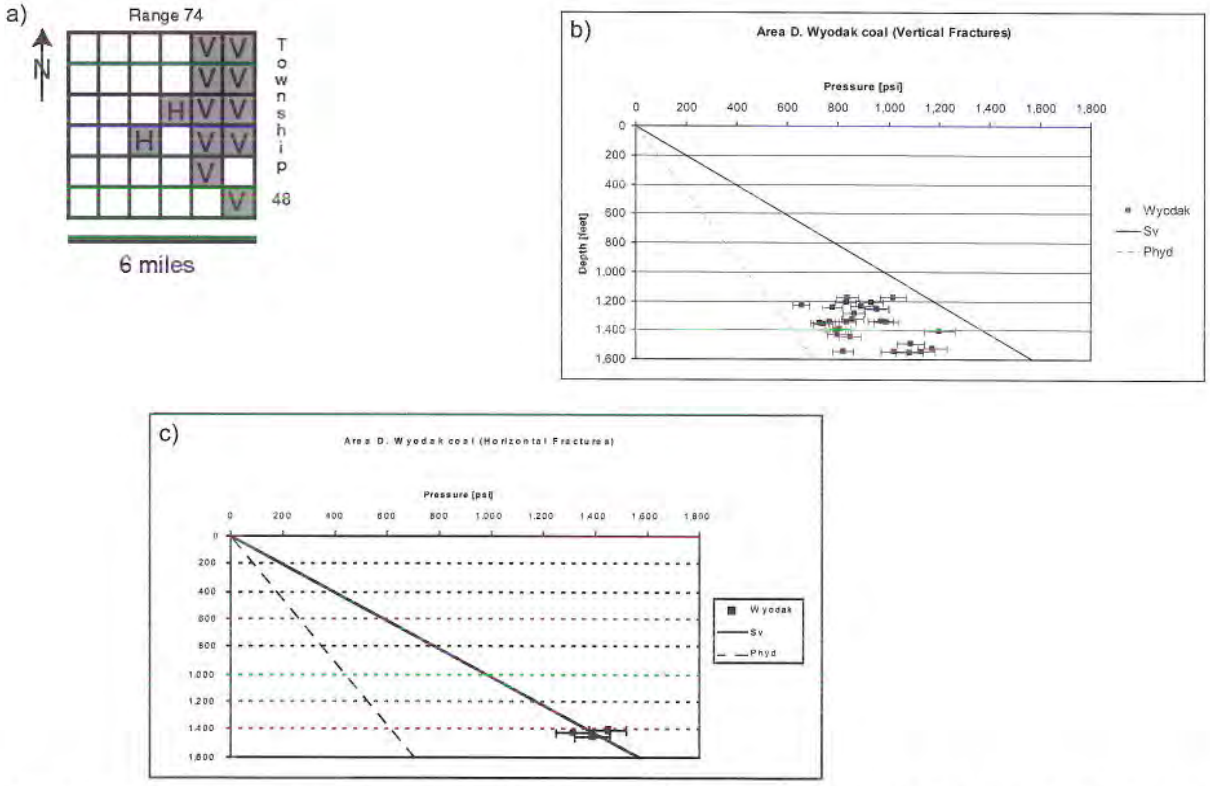


Figure 8. Magnitude of S_3 in the Powder River Basin vs. depth for the Wyodak coal in Area D. (a) Occurrence of horizontal (H) and vertical (V) hydraulic fractures in Area D. The location of this area can be seen in **Figure 5**. (b) S_3 corresponds to the least horizontal stress. (c) S_3 corresponds to the vertical stress.

Table 1. Number of data points used to make the interpolation of S_3/S_v for each coal seam.

Coal seam	# of data points
Anderson	79
Big George	76
Canyon	44
Cook	14
Wall	38
Werner	9
Wyodak	91

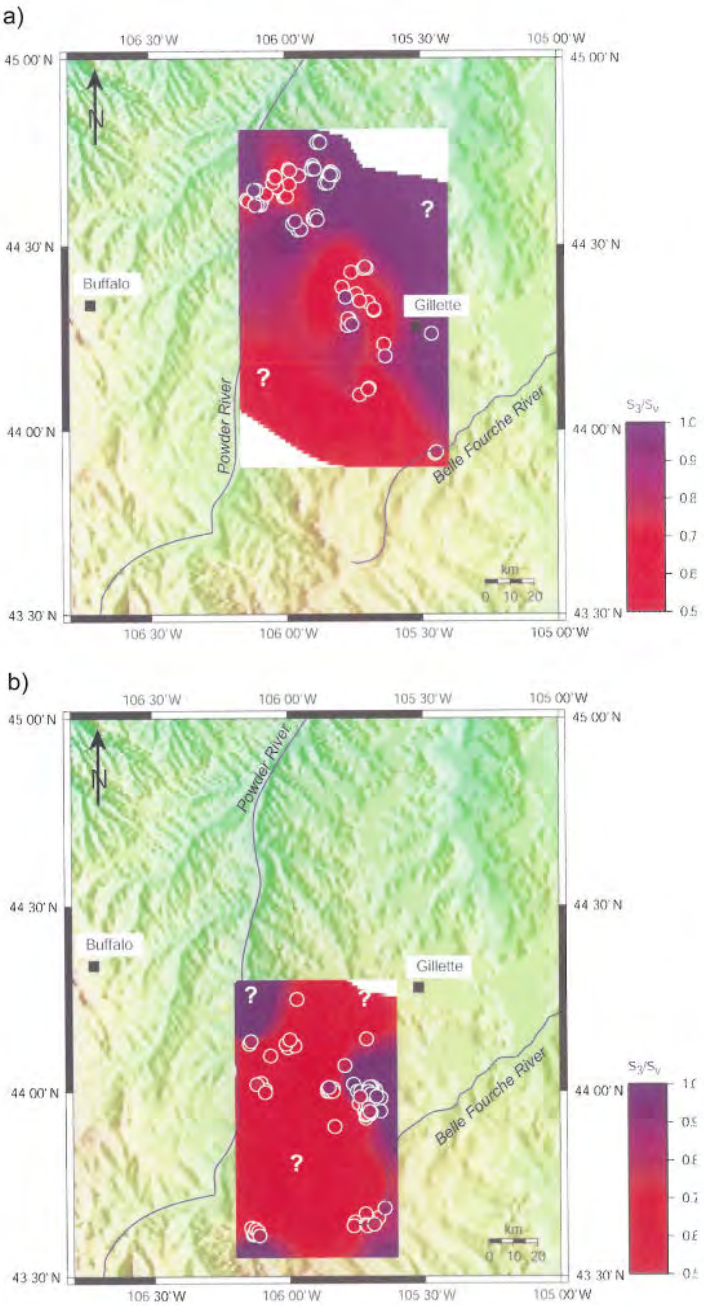


Figure 9. Map showing variation of S_3/S_v for (a) Anderson coal and (b) Big George coal. The circles are actual data points. If S_3/S_v = 1, horizontal fractures are expected. If S_3/S_v < 1, vertical fractures are expected.

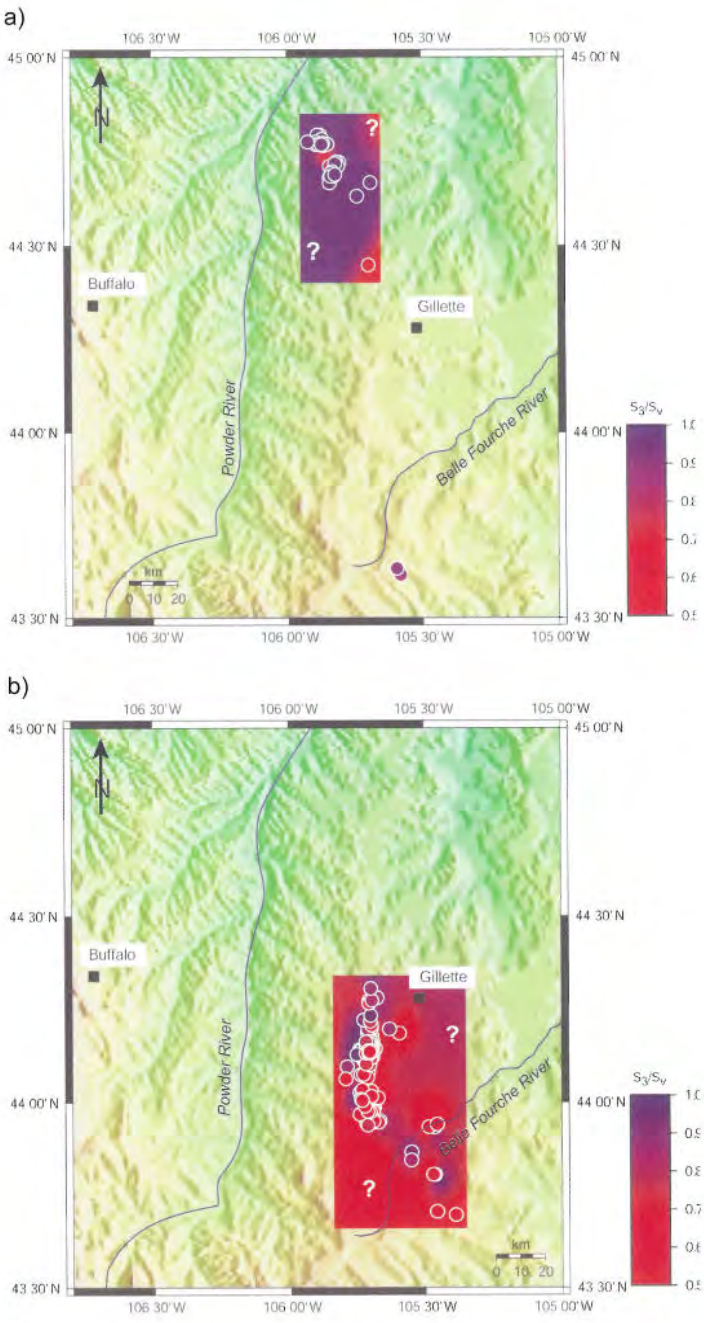


Figure 10. Map showing variation of S_3/S_v for (a) Canyon coal and (b) Wyodak coal. The circles are actual data points. If S_3/S_v = 1, horizontal fractures are expected. If S_3/S_v < 1, vertical fractures are expected.

Possible causes for the variation of S_3 in the basin

Thickness

The differential stress appears to be larger in thicker coals than in thinner coal beds (**Figures 11a** and **12**). This means that in thicker coals the difference between the overburden and the least principal stress is large and the propagation of fractures occurs in the vertical direction. For thinner coals, the difference between S_V and S_3 is smaller and S_V is often the least principal stress, in which case fractures propagate in the horizontal direction.

For thinner coals it is possible to obtain magnitudes of S_3 equivalent to S_V and also equivalent to the minimum horizontal stress. However, the difference between S_V and the minimum horizontal stress is not large, i.e. assuming that S_V is S_1, the differential stress is small. For thicker coals the magnitude of the least principal stress is equivalent to the minimum horizontal stress and the difference between S_3 and S_V is large, which indicates that the differential stress is also large.

For the Big George coal there seems to be a direct relationship between thickness and the magnitude of S_3 (**Figure 11**). In fact, when the Big George coal is thicker than 47 feet, only vertical fractures occur in this coal. Mapping the thickness of the Big George coal (**Figure 11b**) and comparing it with the map of S_3/S_V (**Figure 9**) it can be seen that the region in the central part of the map is most probably a vertical-fracture-prone area because the thickness of the Big George coal at this location is much greater than 47 feet.

For the other coals (Anderson, Canyon, Wall, and Wyodak), the magnitude of S_3/S_V is less than 0.9 at thickness greater than 60 feet, which implies that only fractures propagating in the vertical plane will occur at thickness greater than 60 feet in these coals. There is not enough data available to make any interpretations about thickness and fracturing in the Werner coal.

Pore pressure changes

Even though changes in pore pressure might not necessarily imply large changes in the magnitude of S_3, it was necessary to investigate this hypothesis. **Figure 13** shows maps with interpolated values of P_{obs}/P_{hyd} (observed pressure over hydrostatic pressure) for the Big George and Wyodak coals respectively. The magnitude of S_3/S_V is also shown. If $P_{obs} = P_{hyd}$ then $P_{obs}/P_{hyd} = 1$ but if $P_{obs} < P_{hyd}$ then $P_{obs}/P_{hyd} < 1$ indicating subhydrostatic conditions.

As well numbers have increased in the basin, depressurization of the Wyodak-Anderson coal bed has also increased (Meyer, 1999). This explains why the Big George coal is almost entirely in subhydrostatic conditions, with the exception of small areas in the central part of the region. It can also be seen that the Big George coal becomes more subhydrostatic toward the east, where CBNG operations

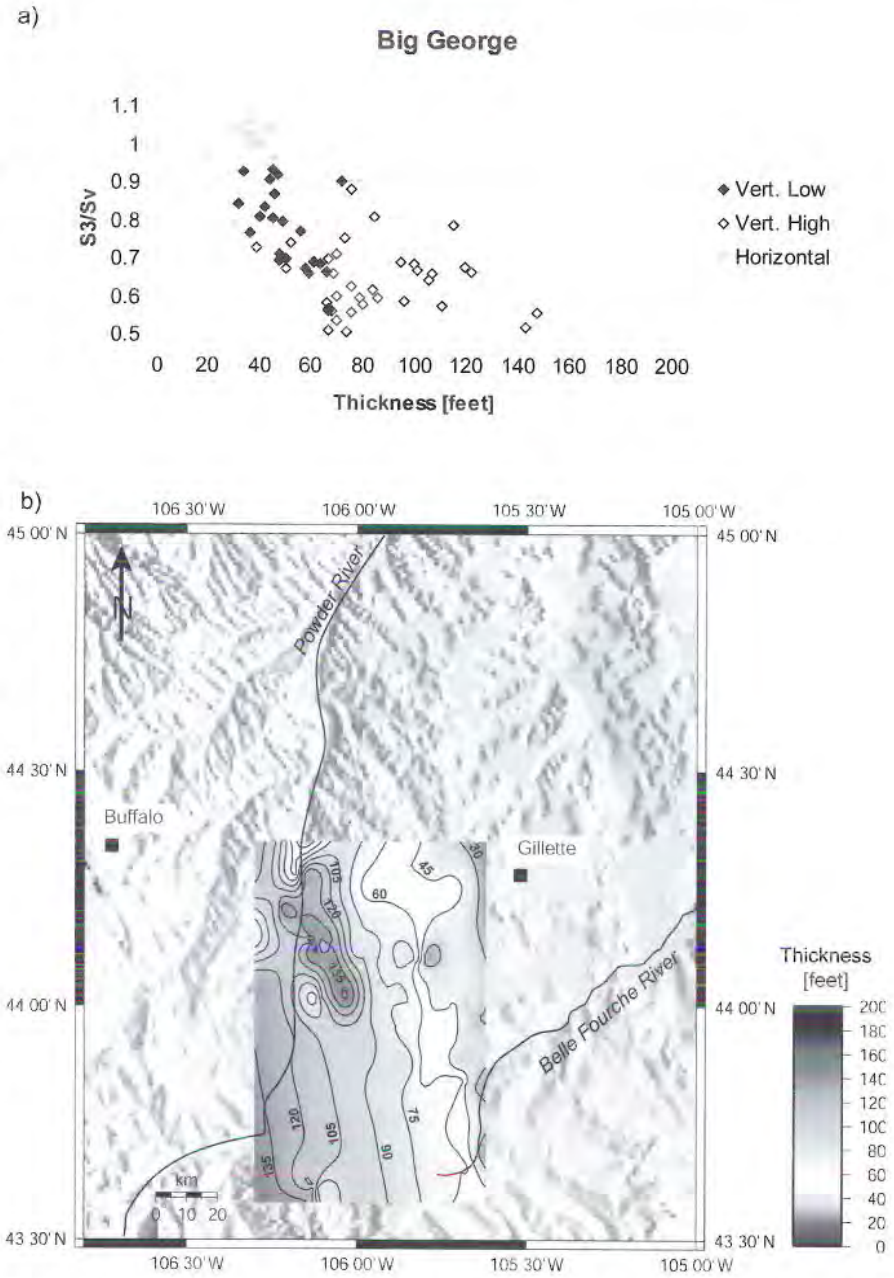


Figure 11. (a) S_3/S_V versus thickness for Big George coal. (b) Thickness of Big George. Note that towards the center of the map, Big George is thicker.

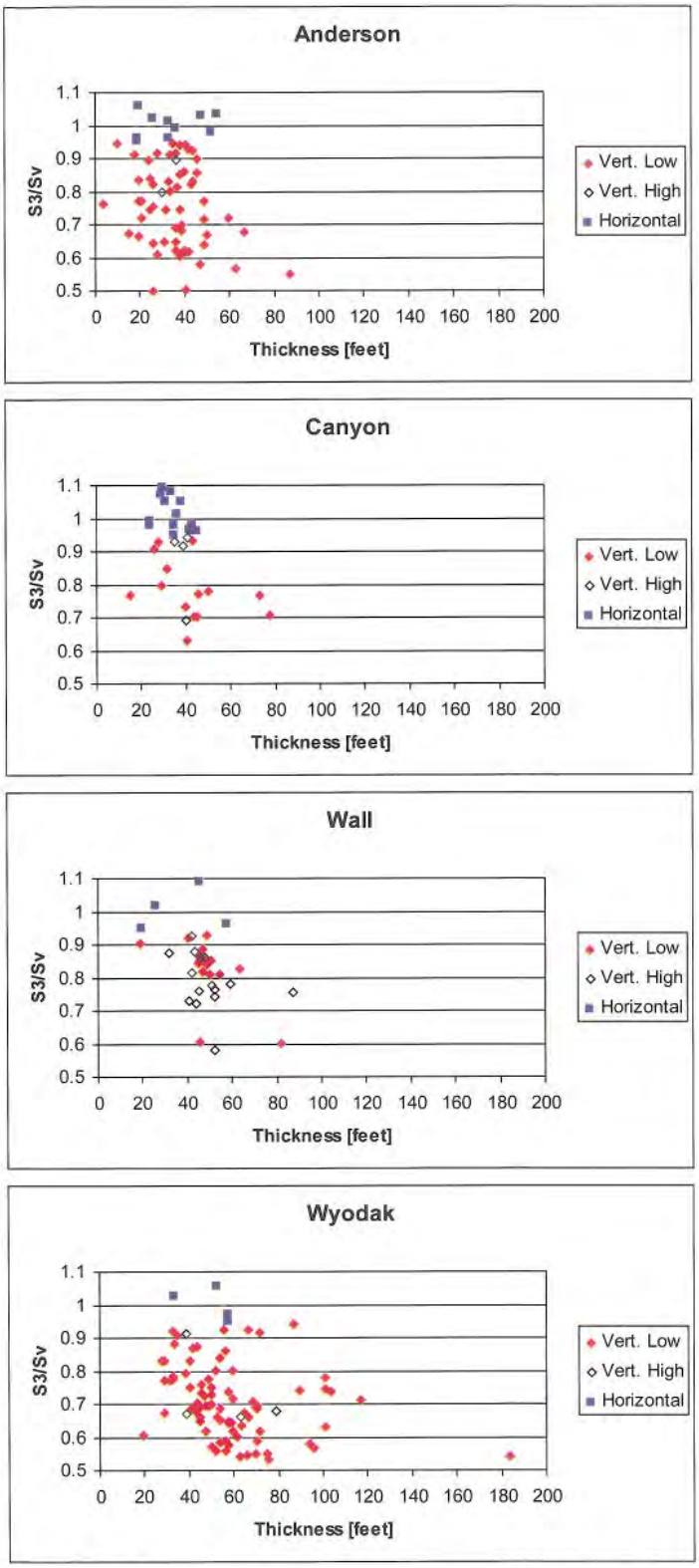


Figure 12. S_3/S_V versus thickness for Anderson, Canyon, Wall, and Wyodak coals. Low and high corresponds to low water production and high water production respectively.

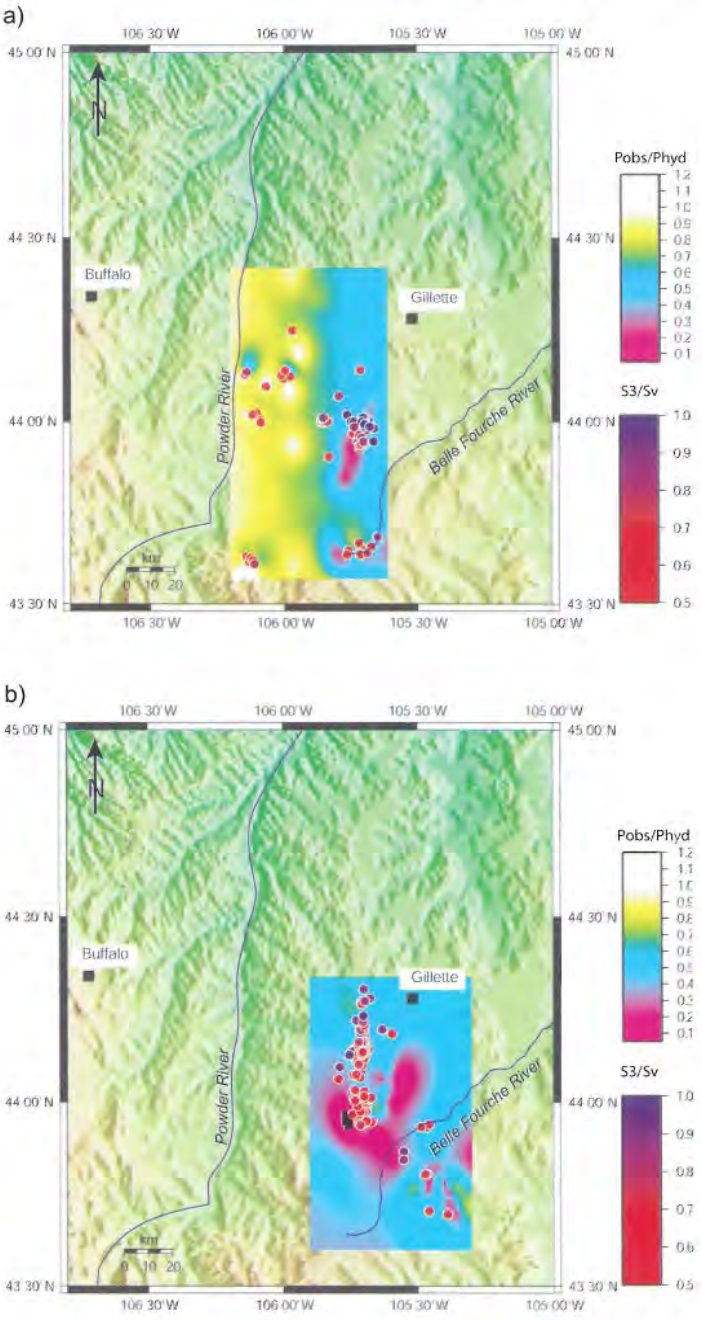


Figure 13. Pore pressure interpolation for (a) Big George and (b) Wyodak coals. Data points denote value of S_3/S_v.

started a decade ago. However, vertical fractures and horizontal fractures occur under no specific pore pressure condition. Vertical fractures occur in places under subhydrostatic, as well as hydrostatic conditions. For the Wyodak coal, the ratio of P_{obs}/P_{hyd} does not exceed 0.7, which means that the entire coal in this area is under subhydrostatic conditions. However, it is possible to have both vertical and horizontal fractures.

From the above analysis it is apparent that there is no correlation between the magnitude of S_3 and pore pressure.

Further analysis is required on a more comprehensive data set in order to confirm this conclusion.

Relationship between hydraulic fracture orientation and water and gas production

As shown in the previous section, the magnitude of the least principal stress and therefore the type of hydraulic fracture varies across the basin. If the vertical hydraulic fractures propagate into an aquifer layer (and if these fractures remain open through time), a hydraulic connection between the coal and the aquifer layer would be established. As a result, a large water production and either a delay in gas production or a lower gas production rate in wells with vertical fractures are expected, compared to wells with horizontal fractures. The operators report water and gas production data for each well to the WOGCC once the well has been put into production. The analysis was made depending on the availability of these data. Thus, there are more wells with least principal stress data than with water and gas production data.

The plots in this section show average gas production in thousand cubic feet (MCF) per month versus average water production in barrels per month (**Figure 14**). Each symbol represents a well, and the color indicates the orientation of the hydraulic fracture, i.e., red is for vertical fractures and blue is for horizontal ones. **Figure 12** shows that within each coal seam there seems to be more wells with vertical fractures than with horizontal fractures. It can also be seen that wells with horizontal fractures always produce low water volumes (less than 7000 barrels per month). In addition, large water production is always associated to wells with vertical fractures. It is important to note that wells with vertical fractures can produce low water volumes and/or large water volumes. However, wells with vertical fractures producing large volumes of water are poor gas producers, while wells with vertical fractures producing small volumes of water tend to be excellent gas producers (i.e., a well producing more than 3000 MCF per month). It is important to keep in mind that the presented data come only from a subset of wells in the basin. Nevertheless, the fact that the relationships are consistent among the different coals seams increases the confidence in these findings.

When looking at **Figure 14**, it is interesting to note that wells with horizontal fractures, even if they are good gas producers, never get to produce as much gas as wells with vertical fractures. The only exception to this is the Werner coal. However, the data for this coal come from only nine wells, which is not sufficient to make any comparisons.

In the following paragraphs, we will discuss the regional trends of water and gas production for the individual coals. As can be seen in **Figure 14**, the Anderson coal in general is not a big water producer. Only three wells produce more than 7000 barrels per month. From the 71 wells we analyzed in the Anderson coal, 27% have horizontal fractures and 73% have vertical fractures. 79% of the water production and 78% of the gas production is produced by wells with vertical fractures, which means that fracture geometry has hardly any impact on water and gas production in this coal. Only about 15% of the wells with vertical fractures in the Anderson coal actually produce large amounts of water.

For the Canyon coal, 34 wells were analyzed, of which 47% have vertical fractures. It is interesting to note that the water production for this coal is almost identical for wells with vertical fractures and wells with horizontal fractures. However, 69% of the gas production comes from wells with vertical fractures, which suggests that wells with vertical fractures are better gas producers than wells with horizontal fractures.

For the Wall coal, 36 wells were analyzed; 81% of these wells have vertical fractures and produce 91% of the water and 86% of the gas. Wells with vertical fractures that produce large amounts of water represent 39% of all the wells and they produce 60% of the water and 44% of the gas from this coal.

For the Big George coal, 74 wells were analyzed, of which 82% have vertical fractures. In total, wells with vertical fractures produce 95% of the water and 99% of the gas. It is important to point out that only half of the wells with vertical fractures are responsible for the bulk of water production (85% of the total amount of produced water) but these large water producers still only account for 45% of the total amount of gas produced from the Big George coal. The remaining 54% of gas production by wells with vertical fractures is from wells with low water production.

There were 85 wells analyzed from the Wyodak coal and 91% had vertical fractures. From this 91%, 5% had high water production. It is curious to note that even though the Big George coal and the Wyodak coal are similar in thickness, their gas and water production differ greatly. For the wells in the Wyodak coal, those with vertical fractures and large water production are only responsible for 13% of the total amount of water produced from this coal. This means that 78% of the water is produced by wells with vertical fractures and low water production, and these same wells produce 92% of the gas from the coal. This seems to imply that the high water production from wells in the Big George coal is not just related to thickness, since the Wyodak coal has a similar thickness and yet, does not produce as much

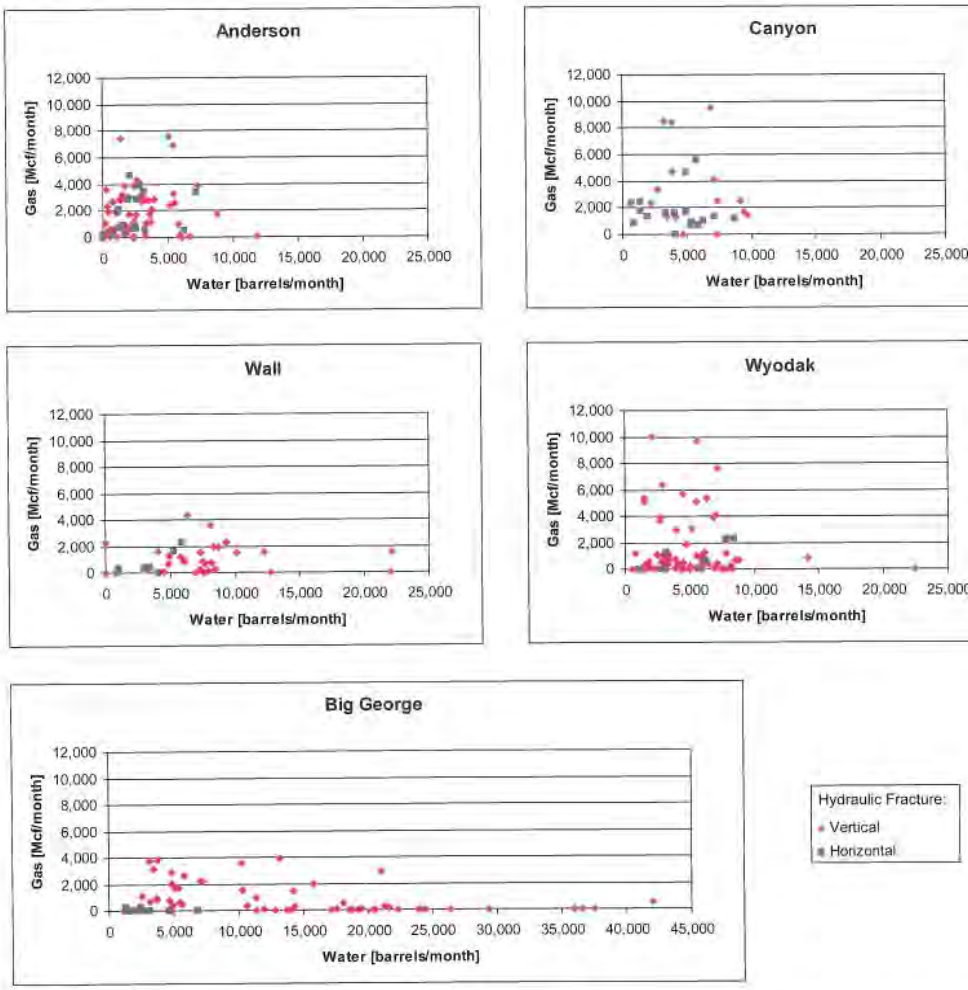


Figure 14. Average gas production versus average water production for Anderson, Canyon, Wall, Wyodak, and Big George coals. The gas production scale for all the plots is the same. The water production scale is the same for all the coals except for Big George coal and it is from 0 to 25,000 and from 0 to 45,000 barrels per month, respectively.

water. At the same time, the Wyodak coal is a better gas producer, perhaps because the depressurization of the coal is more efficient, or because its gas content may be much higher than the Big George coal.

As can be seen in **Figure 14**, wells in the Big George coal produce a maximum of 4000 MCF per month while the wells in the Wyodak coal can produce 10,000 MCF per month. Even the large water producers in the Wyodak coal do not produce as much water as those in the Big George coal (23,000 barrels per month compared to 43,000 barrels per month respectively). A possible explanation for the high water production by Big George wells can be given by comparing Gamma Ray logs between the Big George and Wyodak coals. The GR log in the Big George coal has a blocky signal that is easily identifiable in all the wells analyzed. Conversely, in the Wyodak coal, the GR signal shows more variations, suggesting that interbedded shale stringers lie within this coal (**Figure 15**).

The shales might be acting as flow barriers impeding the flow of water toward the well. If the water cannot flow to the well, then depressurization does not occur. This process is expected to reduce gas production unless the shale stringers also contain gas thereby contributing to the overall gas production from the Wyodak coals. Thus, the presence of shale may explain why the Wyodak coal is not a big water producer and at the same time produces large amounts of gas. The shale stringers in the Wyodak coal can also be acting as barriers for fracture propagation and since the Big George does not have such barriers, the fractures might be propagating into adjacent formations allowing for a hydraulic connection.

The Big George coal is an amalgamation of the Anderson and Canyon coals, however, it does not produce as much gas as the individual Anderson and Canyon coal beds (**Figure 14**). Possibly, the free gas that used to be present in the various coals has escaped out of the coal toward overlying formations (sands, shales). It is known that some sands across the basin contain gas, which are economically extractable (U.S. Environmental Protection Agency, 2002). Therefore, the idea of the Big George coal being under-saturated of methane is a plausible one. This could be another possible factor responsible for the Big George coal producing less gas than the Wyodak coal. In addition, if the Big George coal is hydraulically connected to overlying forma-

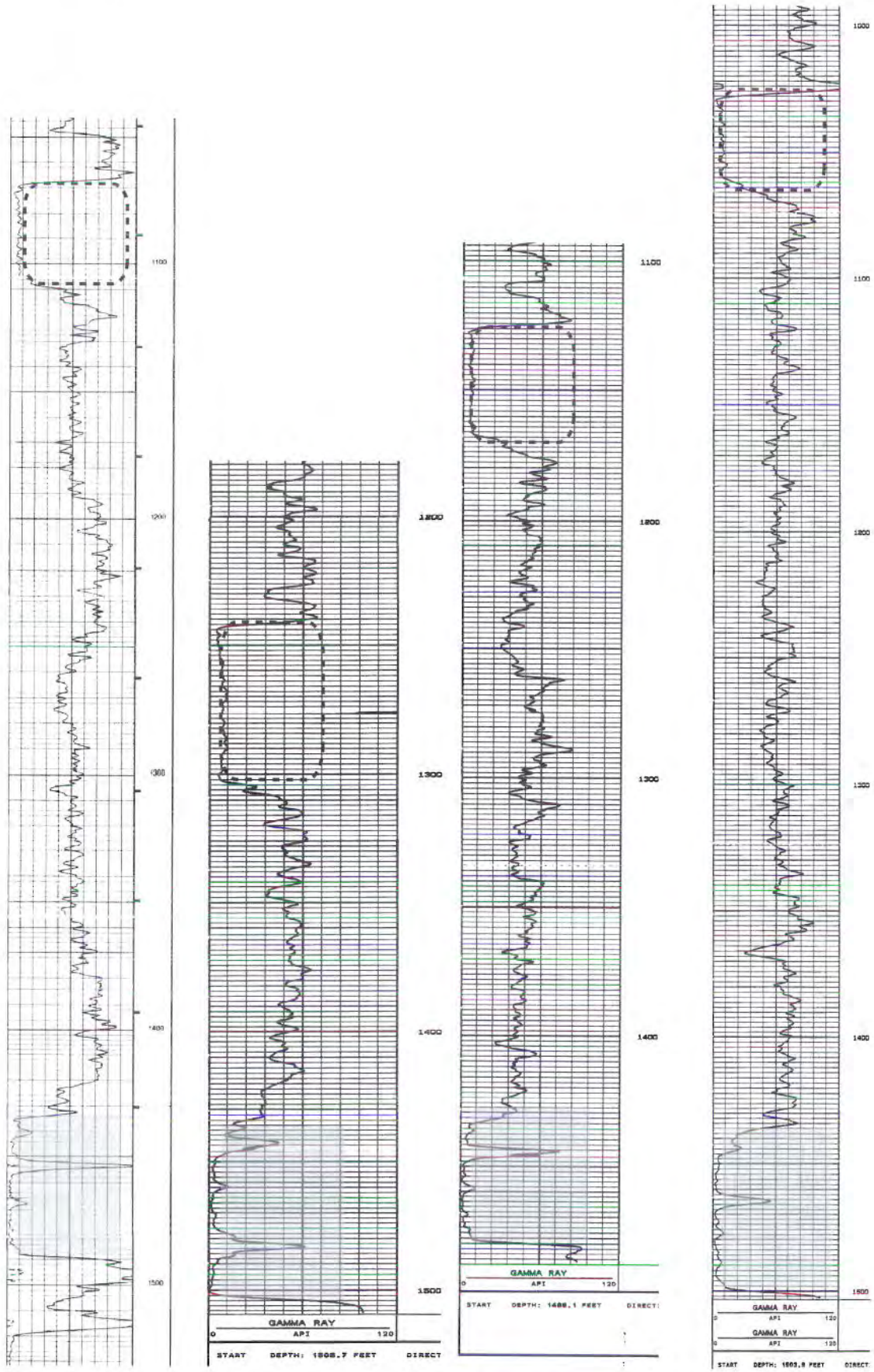


Figure 15. Gamma Ray logs showing Big George (dashed line) and Wyodak (gray) for wells: 534670, 539081, 539123, 545693, respectively. Source: WOGCC Web site.

tions it is being dewatered inefficiently and this could also account for the lower gas production.

Water and gas production in specific areas of the basin

In this section, the wells for a given coal are analyzed in an area-specific manner to determine if the relationships seen in the previous section are not only regional but can also apply to smaller areas. **Figures 16** through **24** show plots of water and gas production (barrels and MCF respectively) for each area that has been analyzed. The plots also indicate whether the data come from wells with vertical or horizontal hydraulic fractures. All the wells show water and gas production since the time production started; in this way it is easier to establish comparisons among wells. The water and gas production data for all the wells were obtained from the WOGCC website.

Area D (Big George coal)

There is a marked contrast in water production depending on the type of hydraulic fracture produced in the Big George coal as can be seen in **Figures 16** and **17** (data for wells with horizontal and vertical fractures, respectively). Wells with vertical fractures produce more water than wells with horizontal fractures. In fact, 71% of the CBNG water from the Big George coal is produced by only 32% of the wells (those enclosed in the blue dashed box in **Figure 17**), all of which are characterized by vertically propagating hydraulic fractures. The same wells that produce 71% of the CBNG water in this area have been in production for at least 16 months and still show no gas production. Actually, gas production seems to only occur in wells (with horizontal or vertical fractures) that produce less than 10,000 barrels of water in a given month. Wells with vertical fractures that produce low water volumes are excellent gas producers. Even though for some of these wells gas production is delayed between 4 to 14 months, it can also be seen that these wells produce 12 times more gas than wells with horizontal fractures. Therefore, wells with vertical fractures that produce low water volumes are better gas producers than wells with horizontal fractures.

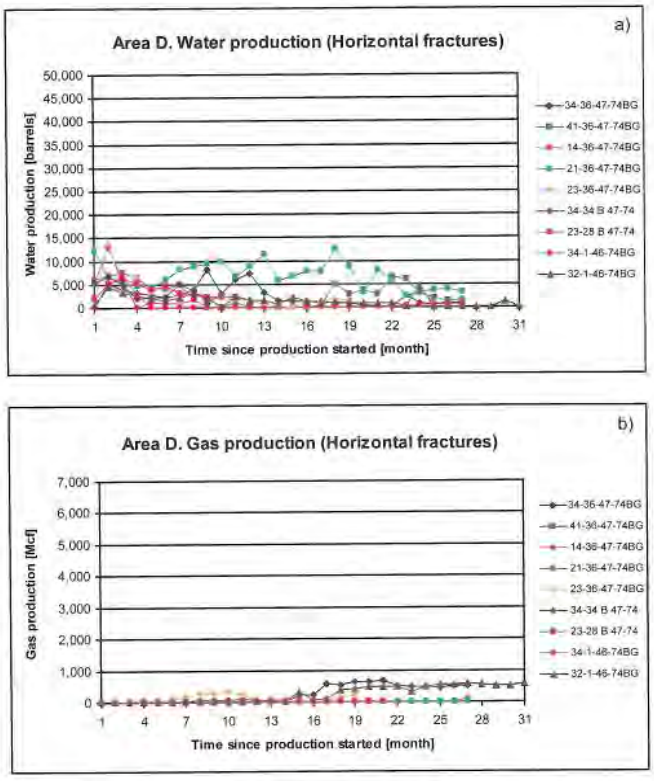


Figure 16. Water and gas production from the Big George coal for wells with horizontal fractures in Area D. (a) Water production and (b) gas production. Water production is low and gas production is immediate but low (compare to gas production from wells with vertical fractures in Figure 17b).

Area D (Wyodak Coal)

For the Wyodak coal (**Figures 18** and **19**), the difference in water production between wells is not as large as

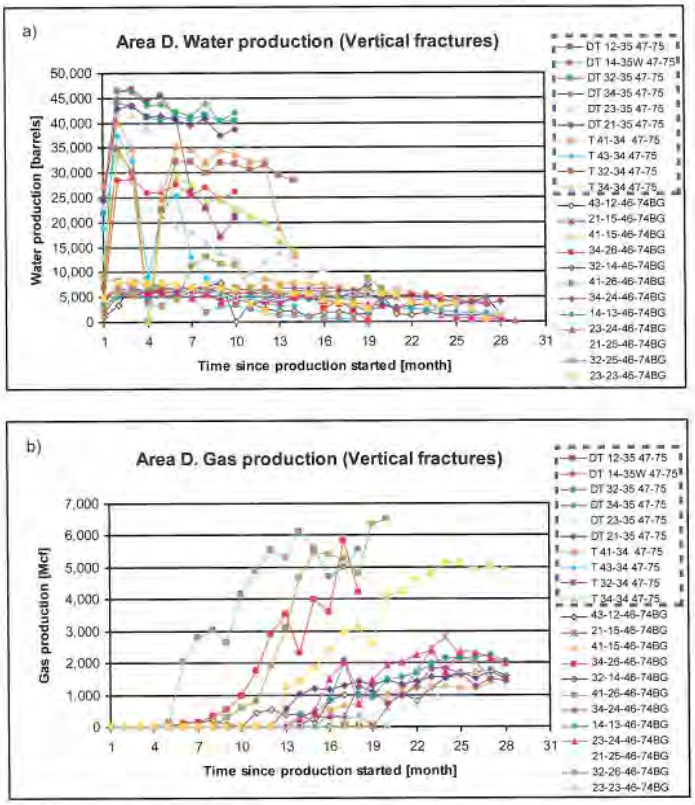


Figure 17. Water and gas production from the Big George coal for wells with vertical fractures in Area D. (a) Water production and (b) gas production The water production in wells with vertical fractures is about 7 to 10 times larger than that of the wells with horizontal fractures (Figure 16). All the wells enclosed by the dashed black box produce more than 10,000 barrels in a month and have not produced any gas. For wells producing less than 10,000 barrels in a month of water gas production is large but delayed by at least 5 months.

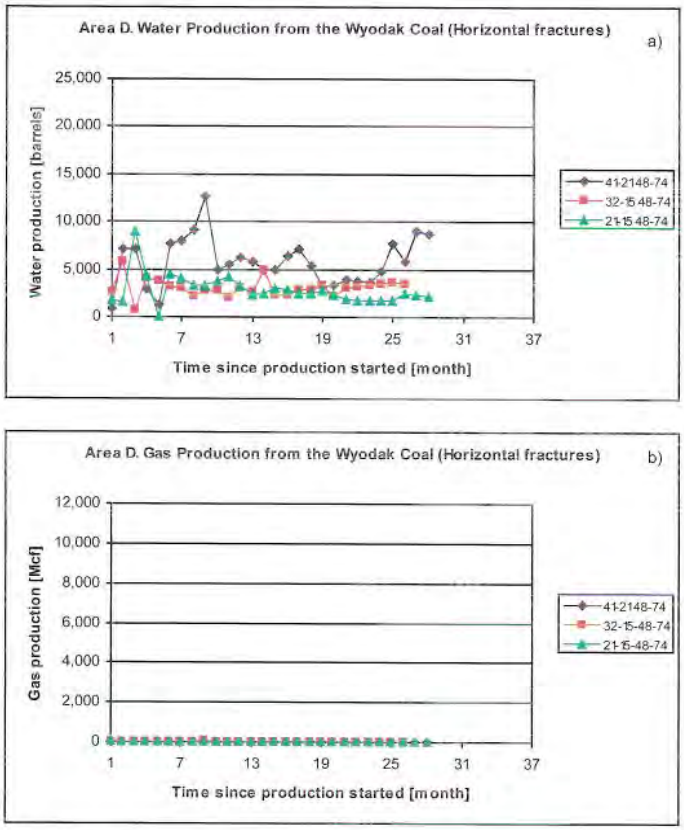


Figure 18. Water and gas production from the Wyodak coal for wells with horizontal fractures in Area D. (a) Water production and (b) gas production. Note that even though water production is low, gas production is nearly zero.

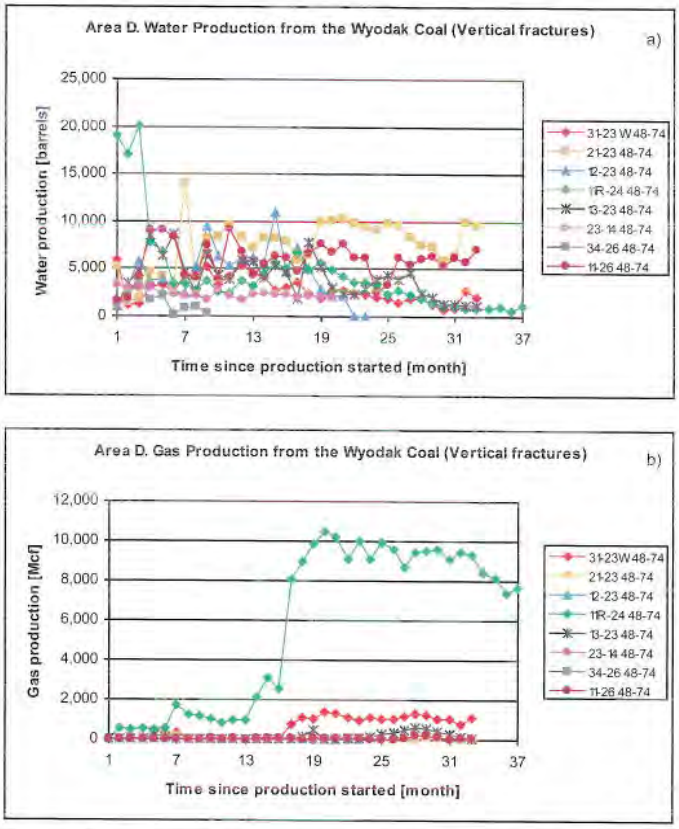


Figure 19. Water and gas production from the Wyodak coal for wells with vertical fractures in Area D. (a) Water production and (b) gas production.

in the Big George coal. However, the average water rate in wells with horizontal fractures is at least 2000 barrels per month lower than for the wells with vertical fractures. In this area, few wells with vertical fractures are producing gas, but they produce more gas than wells with horizontal fractures (e.g. 7 MCF, 173 MCF, and 68 MCF by the 19th month). These wells might not be depressurized enough for methane to desorb but it will be interesting to compare gas production between the wells with horizontal fractures and wells with vertical fractures in the future. Already four of the wells with vertical fractures are producing more gas than wells with horizontal fractures.

Area B2 (Anderson coal)

In Area B2, the water production of wells with horizontal fracturing (**Figure 20**) ranges from 0 to 6000 barrels, with only one well having an anomalous water production rate of 12,000 barrels after nine months of being in production (3-34-54-77). In general, the gas production of these wells increases with time, as can be seen in **Figure 20**, and the maximum gas production was about 9000 MCF in well 1-35-54-77.

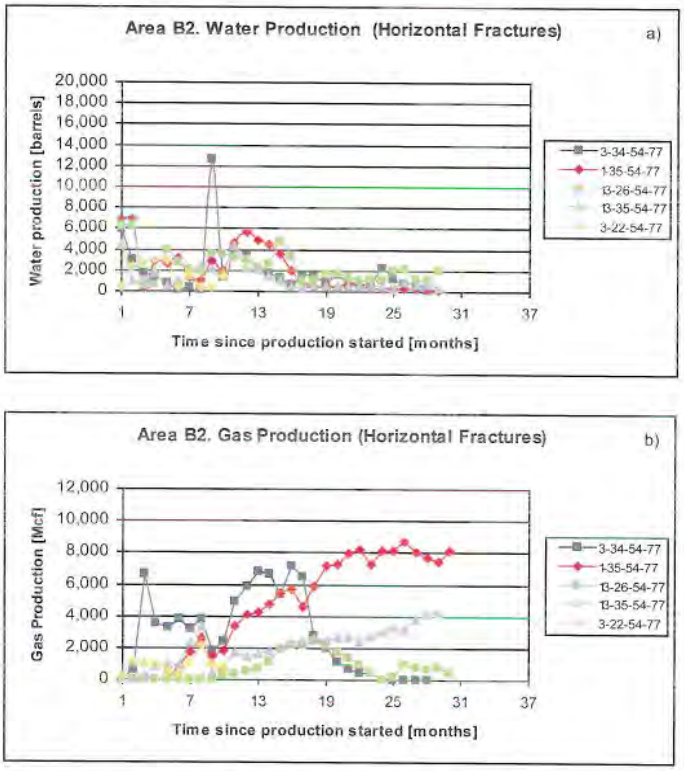


Figure 20. Water and gas production from the Anderson coal for wells with horizontal fractures in Area B2. (a) Water production and (b) gas production.

Wells with vertical fractures (**Figure 21**) that reached a water production rate of more than 6000 barrels per month in the first 12 months, either have delays in gas production of about 12 months (e.g. 5-35-54-77, 3-35-54-77, 11-26-54-77, and 15-35-54-77) or show no gas production at all (e.g. 13-28-54-77 and 3-33-54-77). Interestingly, wells with vertical fractures that have water production rates less than 6000 barrels per month produce gas immediately, reaching a gas production of 6000 MCF in the first 12 months of production (15-34-54-77, 15-24-54-77, and 1-22-54-77).

Area B1 and B (Anderson coal)

Water production of more than 8000 barrels per month in the first seven months is more common in wells with vertical fractures than in wells with horizontal fractures (**Figure 22**). Even though water production is greater in wells with vertical fractures in Area B1 than in wells with horizontal fractures in Area B, gas production is immediate and in general, they all have similar trends in gas production, which increases up to the 13th month of production and then declines over time. However, wells with vertical fractures produce at least 3000 MCF per month but they also reach 4000 and even 11,000 MCF per month compared to the steady and lower gas production from the wells with horizontal fractures (between 1000 and 4000 MCF per month). Since gas production in the wells with vertical fractures was not affected by water production, that is, production of large water volumes did not imply a delay in gas production, the large water volumes produced here in the first seven months might just have been part of a normal dewatering process. After all, these wells do not produce as much water as the wells with vertical fractures in Area B2 (**Figure 21**). It is interesting to note that wells with vertical fractures are better gas producers than wells with horizontal fractures as has also been found for the Big George coal.

Area B (Wall Coal)

As can be seen in **Figures 23** and **24**, there is a marked difference in water production between wells with horizontal fracturing and some of the wells with vertical fracturing. The wells Smith 5-1W, 5-18W, 11-1W, 14-1W, and 6-1W (**Figure 24**) produce almost four times more water than the two wells with horizontal fractures (**Figure 23**). These wells with high water production also produce the least amount of gas among all the wells with vertical fractures, e.g. Smith 14-1 (**Figure 24**). In some cases, gas production is delayed by at least 15 months and water production can be as high as 15,000 barrels. Interestingly, Smith 3-1 W (**Figure 24**), which has vertical fractures, has an average water production of only 5000 barrels per month, similar to the wells with horizontal fractures (**Figure 23**), and its gas production is high (approximately 10,000 MCF). A possible expla-

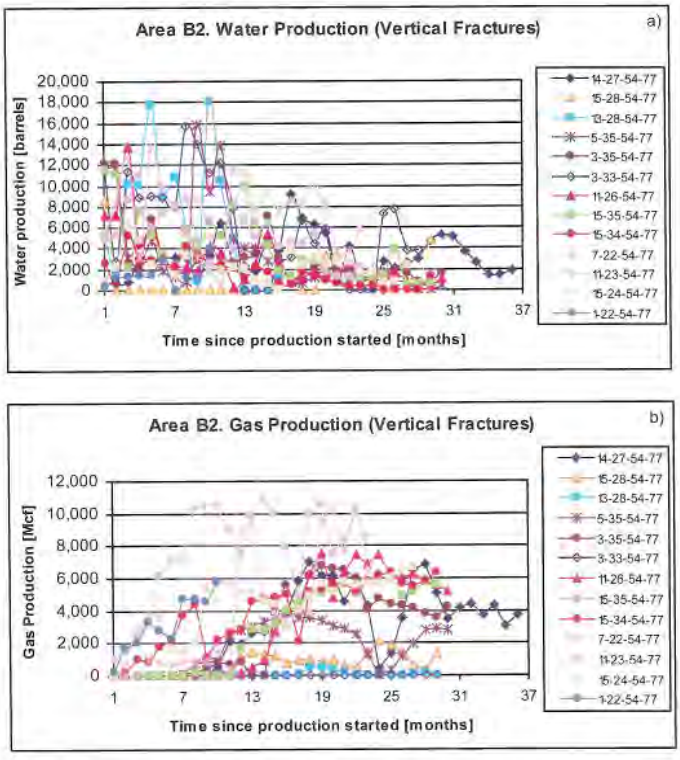


Figure 21. Water and gas production from the Anderson coal for wells with vertical fractures in Area B2. (a) Water production and (b) gas production.

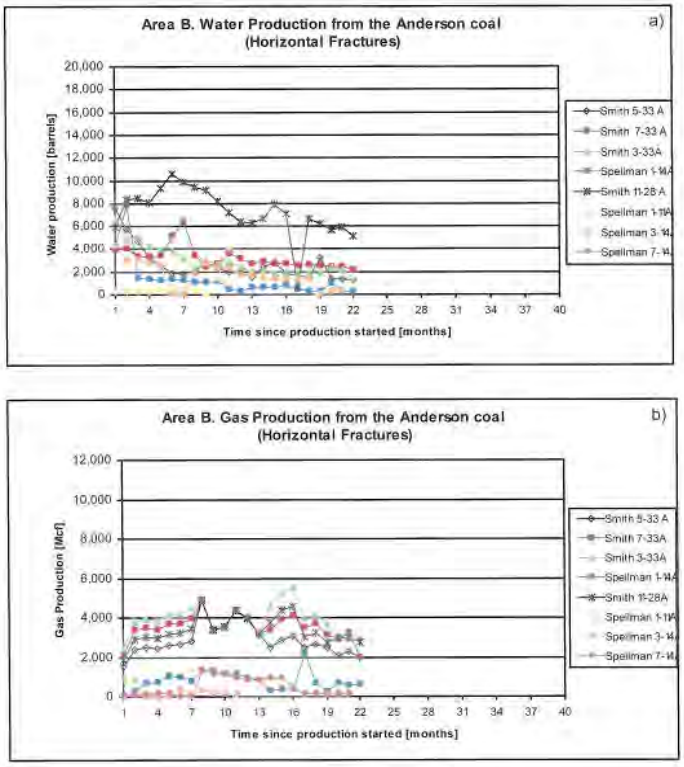
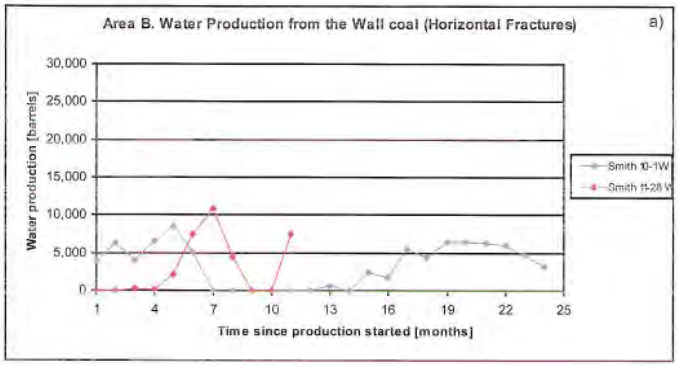


Figure 22. Water and gas production from the Anderson coal for wells with horizontal fractures in Area B. (a) Water production and (b) gas production.



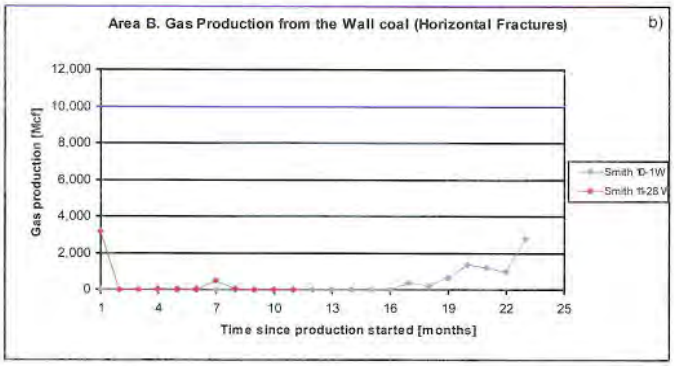
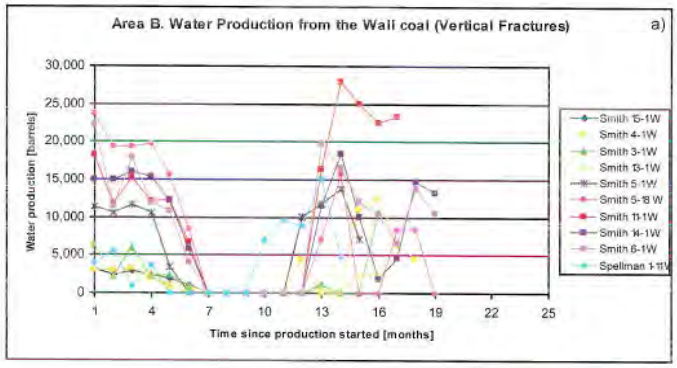


Figure 23. Water and gas production from the Wall coal for wells with horizontal fractures in Area B. (a) Water production and (b) gas production.



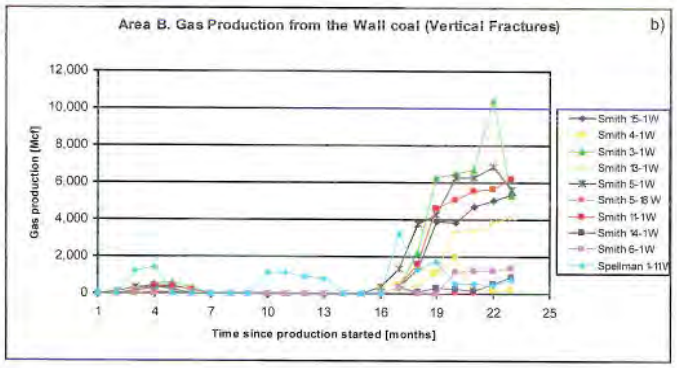


Figure 24. Water and gas production from the Wall coal for wells with vertical fractures in Area B. (a) Water production and (b) gas production.

nation for what is observed in Smith 3-1W is that the vertical fracture may not be extending into the aquifer layer, so water production from the aquifer layer is not being tapped, preventing high water production.

Area C (Anderson Coal)

Even though water production rates are not too high in these wells, in wells with lower water production, more gas is produced. However, the maximum gas production reached in this area (4500 MCF for well 9-27-51-74) is about half of what is being produced in area B2 (**Figure 21**) for the same coal (the Anderson coal). In addition, most of the wells in Area C are only producing an average of 1000 MCF per month, which is relatively low compared to the gas production in areas B1 and B2 (**Figure 21**). This could be due to inefficient depressurization of the coal, or the Anderson coal could be under-saturated of methane in this area.

Area A (Roland Coal)

Water production from the Roland coal in Area A started at about 1000 barrels per month and increased to between 2500 and 6000 barrels per month for the different wells, with some periods of zero production interspersed. These wells show no gas production. We are unable to compare this water production with other wells because none of the other wells we have analyzed are producing from the Roland coal.

How does the relation between hydraulic fracture orientation and cleat system affect the water and gas production?

Fluid flow in coal beds occurs through the natural fractures, or cleats. Cleats are systematic, orthogonal fracture systems that commonly are perpendicular to bedding. They commonly form during coalification and the face (dominant) cleat orientation reflects the far-field stress present during their formation. Tectonic postcoalification fractures also may be present. The face cleat is more continuous than the subordinate butt cleat and in general, cleat density is greatest in thin, bright, low-ash coals (Ayers, 2002). Cleats are perpendicular to the bedding of the coal seam.

Wells with induced vertical hydraulic fractures are, in general, better gas producers than wells with induced horizontal hydraulic fractures. Therefore, the vertical fractures must have a strike nearly perpendicular to the strike of the face cleats, which would imply an efficient connection of several face cleats through the vertical hydraulic fracture. Wells with horizontal hydraulic fractures that produce relatively good amounts of gas (more than 3000 MCF per month), must be producing free gas and gas from the cleats,

which get connected by the horizontal hydraulic fracture. However, horizontal fractures do not seem to be the most efficient pathway for flow of methane from the coal into the well.

There are wells with horizontal hydraulic fractures in the Anderson and Canyon coals that produce more gas than wells with horizontal fractures in the Big George and Wyodak coals. Interestingly, the Anderson and Canyon coals are thinner and shallower than the Big George and Wyodak coals. The cleat density may be larger in the thinner coals than in the thicker coals and the amount of free gas is generally higher in shallower coals than in deeper coal. These could explain why horizontal fractures in thinner coals are better conduits than in thicker coals and therefore, this could also explain why wells with horizontal fractures in thinner coals are better gas producers than wells with horizontal fractures in thicker coals.

In areas of vertical hydraulic fracturing: why do some wells have large water production and others low water production?

One of the goals of this study is to understand why some wells with vertical fractures have excessive water production, while water production is low in adjacent wells. We have identified three different factors that may be responsible for this observation: stratigraphy, thickness, and depth.

Stratigraphy

Excess CBNG water production could result from the propagation of the vertical fractures into overlying strata, creating a hydraulic connection between the formations. GR logs from a number of wells with vertical fractures in Area D have been analyzed. It was expected that wells with vertical fractures and excessive water production would be overlain by sand bodies, which behave as aquifers, and would therefore yield a large amount of water once the coals began to be dewatered. With respect to the wells with vertical fractures and low water production, it was expected that the coals in these wells were overlain by shales, which have low permeability, and therefore yield less water than sands.

Some of the wells with vertical fractures and large water production rates have sand bodies overlying the coal. However, other wells with vertical fractures and large water production rates have shales overlying the coal. Furthermore, wells with vertical fractures and low water production rates were either overlain by shales or sands. Thus, no obvious relationship between stratigraphy and water production can be established. In the future, the availability and analysis of a more extensive GR log dataset may yet reveal whether a relationship does exist between vertical fracture growth and stratigraphy.

Thickness

As can be seen in **Figure 25a**, there is a general trend that the thicker the Big George coal, the greater the water production. However, at a given thickness, say 70 feet, the average water production for different wells ranges from 0 to 40,000 barrels per month. For the Wyodak coal (**Figure 25b**), water production is generally low, despite the large thickness of the coal seam. Even where the coal is thicker than 100 feet, the average water production is less than 8000 barrels per month. This implies that coal seam thickness is not an obvious indicator for the amount of water a coal will end up producing.

Depth

Figure 26 shows a plot of water production versus depth for the Big George coal seam. The plot shows that wells with vertical fractures and high water production rates occur at any depth between 750 and 1500 feet. Therefore, there appears to be no direct correlation between high water production and depth.

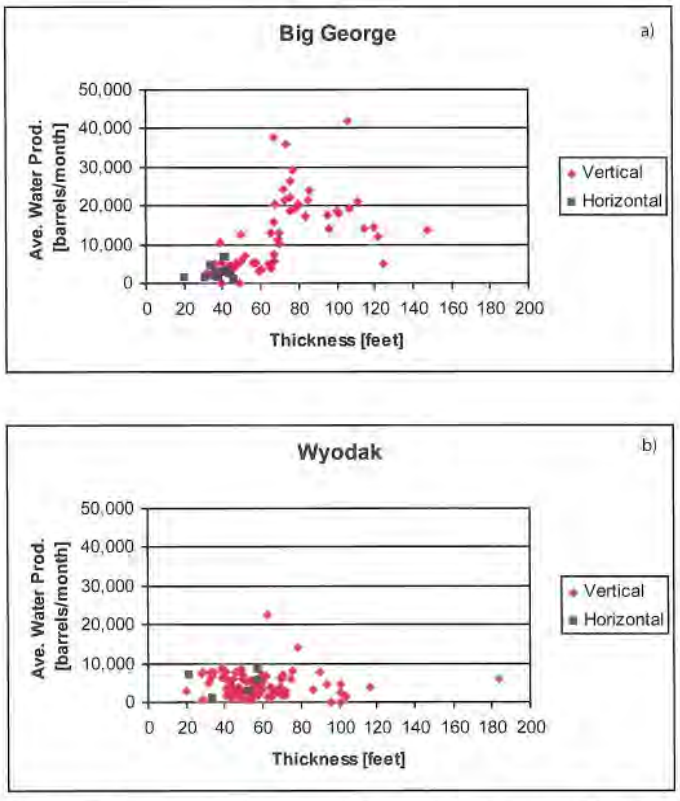


Figure 25. Average water production versus thickness for the (a) Big George and (b) Wyodak coals.

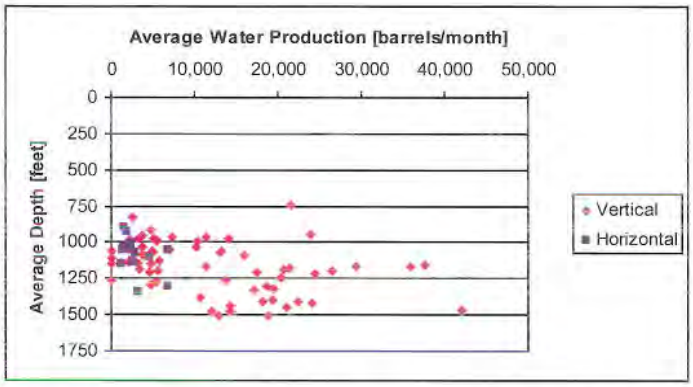


Figure 26. Average water production versus depth for the Big George coal.

None of the investigated factors (stratigraphy, coal thickness, depth) appear to affect the amount of water that is produced in wells with vertical fractures. At this time and considering the factors just mentioned, the prediction of water production in these wells is still not viable.

Pore pressure and gas production

It is known that methane desorbs from the coal once the pressure in the coal decreases. The aim of this section is to investigate the amount of depressurization required for methane desorption to occur. The data presented in this section come from the Big George coal. Figure 27 shows the water and gas production data for each well and also the changes in delta pressure with time. Delta pressure is equivalent to hydrostatic pressure minus observed pressure, which indicates that with time, the observed pressure should be lower due to the dewatering (and depressurizing) of the coal and therefore the delta pressure should increase.

Well SRU2 (**Figure 27a**) shows a change of about 200 psi in delta pressure with ongoing depletion, due to water production, but even after three years it is still not producing any gas. Even though depressurization is implied, the large water production rate (about 35,000 barrels per month) indicates that depressurization might not be taking place effectively. The coal at this site may be in connection with overlying strata.

For well Roush (**Figure 27b**), a change in delta pressure of approximately 30 psi was not enough for the methane to desorb from the coal. The change in 30 psi occurred during the first year of production and gas production started a year after that. Dewatering for 18 months was necessary for this well to start producing gas.

Well Oh (**Figure 27c**) has horizontal fractures and is located in T46N, R73W, adjacent to Area D. In the first six months of production, the delta pressure changed by 25 psi. However, this well has been in production for four years and gas production has still not begun. This indicates that the initial change in pore pressure was not large enough for the methane to be desorbed. In addition, delta pressure might still not be increasing sufficiently for the methane to desorb at all. This well confirms the previous findings, that is, wells with horizontal fractures in the Big George coal produce low water volumes and gas production is low or absent.

For some wells, a 25 psi change in pressure is enough for the gas to desorb, while for others it is not large enough. In fact, even a large change like 200 psi in the case of SRU2 was not large enough for the methane to desorb. It appears that something more complicated might be taking place in this well. The coal at this site may be in hydraulic connection

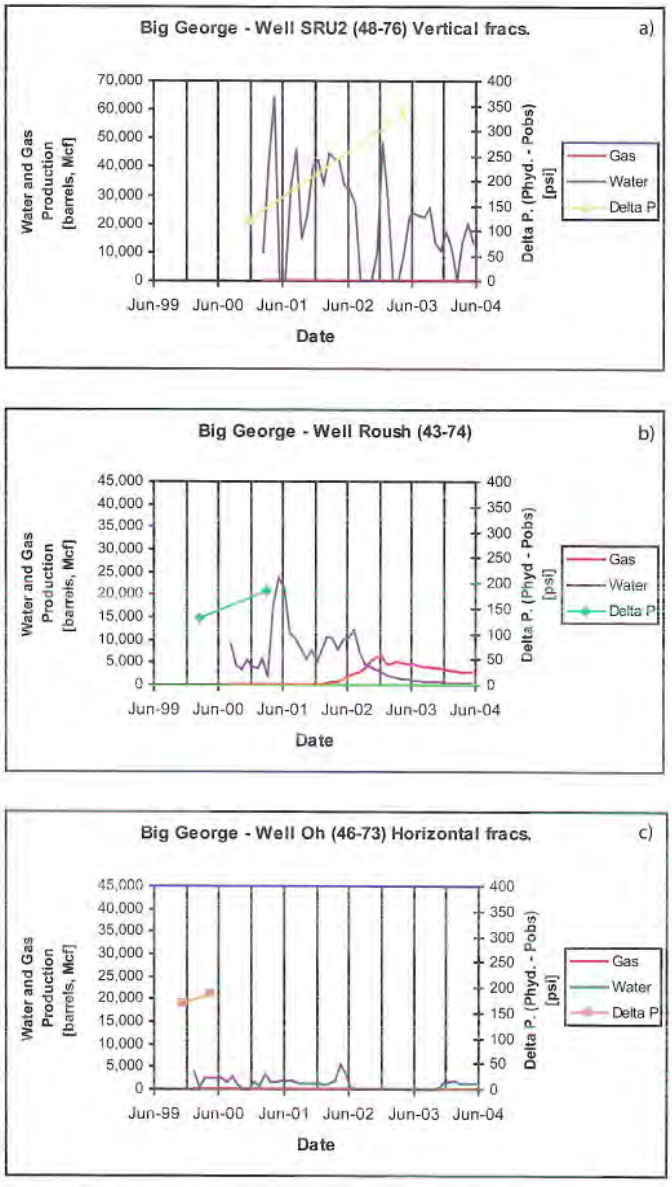


Figure 27. Plots of water and gas production versus time and delta pressure (hydrostatic pressure minus observed pressure) for different wells in the Big George coal.

with adjacent strata, which would explain the large volumes of water produced and the absence of gas production.

Temporal and spatial variations in pore pressure

Figure 28a is a crossplot of P_{obs}/P_{hyd} versus time when the measurement was made and shows no correlation between changes in pore pressure and time for the Big George coal. **Figure 28b** shows a map of interpolated P_{obs}/P_{hyd} with data points over the top. Each symbol represents the year in which the pore pressure (P_p) measurement was taken. There seems to be more of a spatial trend than a temporal trend. The darker areas ($P_{obs}/P_{hyd} < 1$) are defined not only by data points from 1999 but also from 2004, whereas the lighter ($P_{obs}/P_{hyd} \geq 1$) areas are not only defined by data points from 2004, but also from 1998 to 2002. This may indicate that P_p not only depends on time (when dewatering began) but also on the area (there may be interaction with other formations).

Figure 29a shows elevation with respect to delta pressure for Big George coal. In general, if a fluid level remains at constant elevation while the topography increases, the pore pressure at the depth of the water table will be more subhydrostatic at the location of highest elevation, compared to the pore pressure at depth in the location of lower topography. This means that if elevation increases, delta pressure should also increase, i.e. the pore pressure should become more subhydrostatic. The data presented in this figure do not show this trend when considered as a whole. However, according to the trends observed in **Figure 29a**, it is possible to establish four different groups of these data (**Figure 29b**). For Group 1 there seems to exist a correlation between elevation and pore pressure since pore pressure tends to become more subhydrostatic with the increase in elevation. However, for Groups 2, 3, and 4, pore pressure becomes more subhydrostatic at constant elevation. In **Figure 29c**, fluid elevation is plotted against delta pressure and what can be seen here is that for Group 1 fluid elevation remains constant while delta pressure increases (i.e., pore pressure becomes more subhydrostatic).

For Groups 2, 3, and 4 fluid elevation decreases at the same time that pore pressure becomes more subhydrostatic. These findings are summarized in **Figure 30a**, where the brown line corresponds to elevation and the blue line corresponds to the fluid elevation. By determining the location of these wells in the basin we were able to identify that the wells belonging to Group 1 are all located on slopes of hills, the wells from Group 2 are located on a plateau, the ones from Group 3 are in the Powder River valley and the wells from Group 4 are located on a ridge (**Figure 30b**). In summary, wells located on the slopes become more subhydrostatic with elevation because the fluid level remains constant. In addition, wells located in plateaus, river valleys and ridges become more subhydrostatic at constant elevation because the fluid level decreases. Usually, the water table reflects the topography in a more subdued way. However, these data allow one to real-

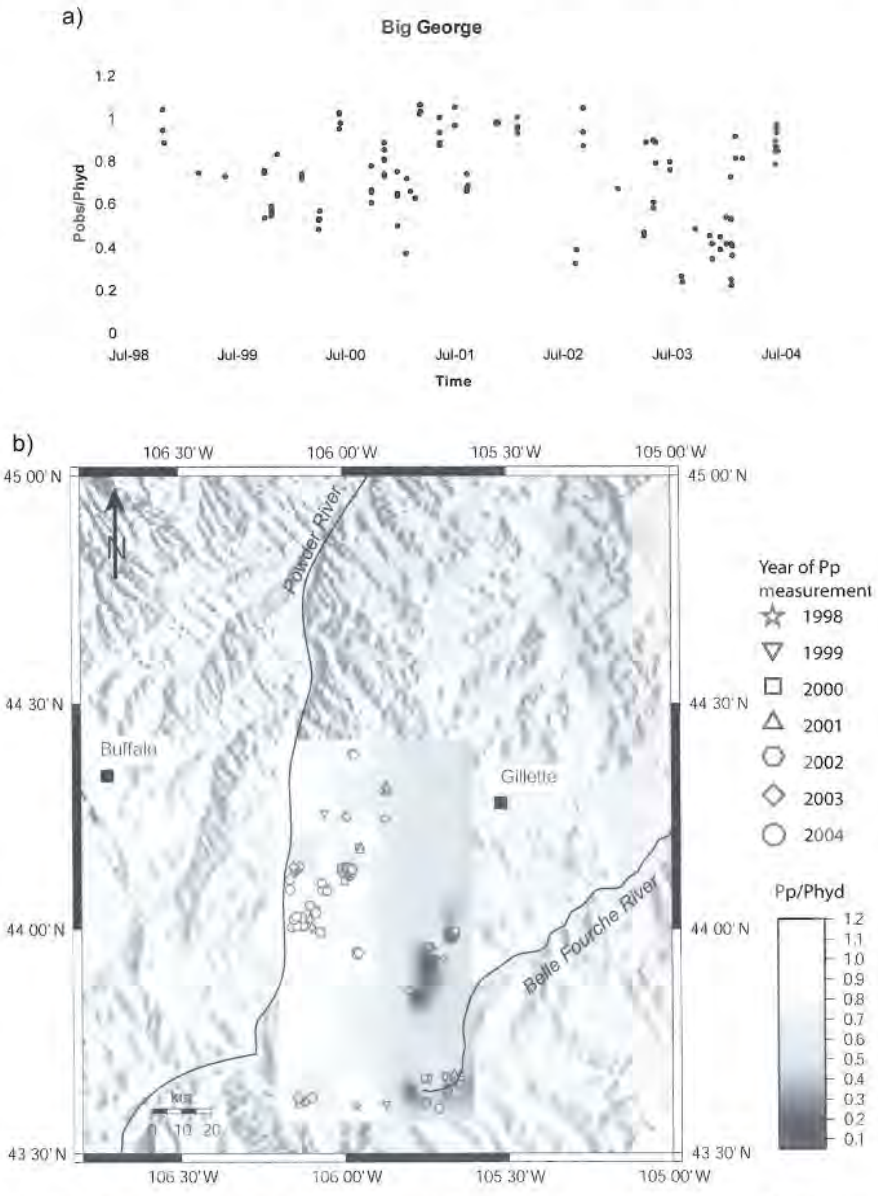


Figure 28. (a) Cross-plot of P_{obs}/P_{hyd} versus time. (b) Map of P_{obs}/P_{hyd} for Big George coal; symbols represent the year at which the pore pressure measurement was done.

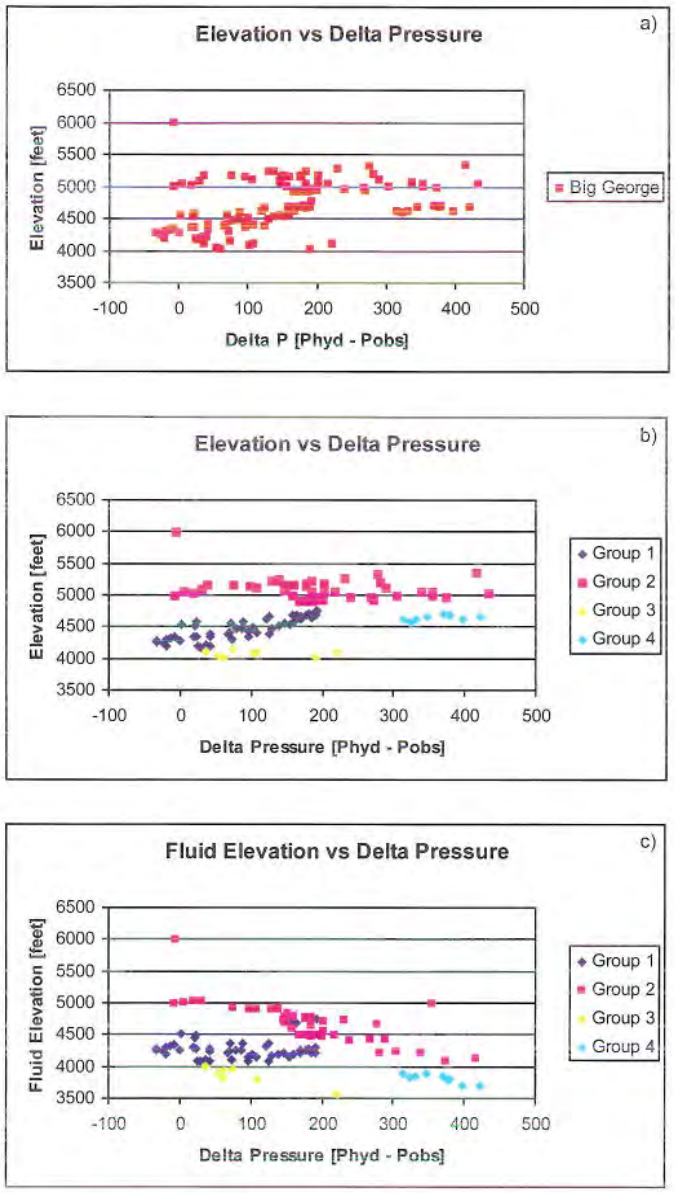


Figure 29. Elevation versus delta pressure for Big George coal. (a) Ungrouped data. (b) Same data grouped in four different groups. (c) Fluid level versus delta pressure for the four groups.

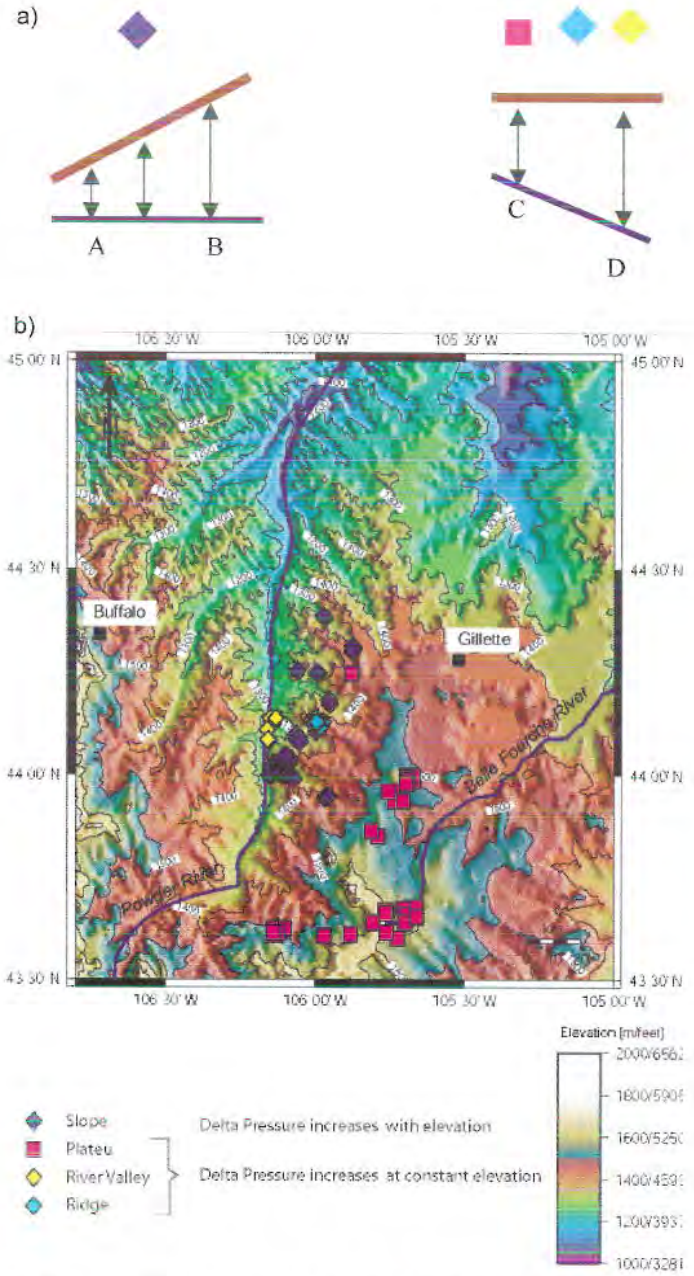


Figure 30. (a) Variations of fluid elevation and topography for Group 1 (on the left) and Groups 2, 3, and 4 (on the right). For Group 1 the pore pressure at point B is more subhydrostatic than at point A; for Groups 2, 3, and 4 the pore pressure at point D is more subhydrostatic than at point C. (b) Location of the wells that conform the different groups. The elevation contours are in meters.

ize that the water table does not follow the topography in the studied region, which might be indicating the impact of anthropogenic activities (e.g. domestic water wells, mining, CBNG operations) in the groundwater system.

With the limited amount of P_p data obtained, it has not been possible to find a clear correlation between P_p and depth, thickness or elevation. A possible explanation for this lack in trend in pore pressure is that the coal may not be a hydraulically isolated formation. The coals may be in communication with other formations resulting in a masked magnitude of the "coal" pore pressure. Since there may be a hydraulic connection between the coals and adjacent formations, the pore pressure magnitude obtained in the coal may be the pore pressure that results from the hydraulic interplay of all the formations hydraulically connected at a certain location in the basin.

Figure 31 shows an example in which the delta pressure has varied by 150 psi even though production has not started. This well is located in T46N, R74W (in Area D). An important observation about this well is that gas production starts before water production, which may originate from desorbed gas due to depressurization. The average water

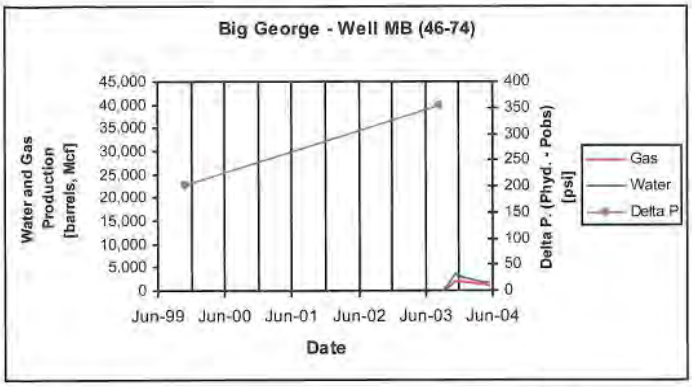


Figure 31. Logically, changes of pressure occur after dewatering starts. However, in this well the pore pressure changes before production starts.

production is 2082 barrels per month and the average gas production is 1416 MCF per month. S_3 data are not available for this specific well but the S_3 data from wells in this same field and in the same section (and adjacent sections) indicate that $S_3 = S_{hmin}$, corresponding to vertical fracture propagation. Thus, this well reinforces what has been observed before, that is, wells with vertical fractures that produce low water volumes produce gas immediately.

However, the reason why the pore pressure varies before the dewatering phase starts is unknown and deserves attention. Production-induced pore pressure changes may perhaps affect the magnitude of S_3 as well. However, further analysis is needed to understand how the reservoir works, its connection and correlation with adjacent formations and how the drawdown from one well affects the pore pressure in other wells and whether this inflicts a change in S_3.

Recommendations to achieve best well completion practices

In this study, we have demonstrated that water-enhancement activities during wellbore completion result in hydraulic fracturing of the coal. All of the wells with exceptionally high water production are associated with vertical fracture propagation. In these same wells, there are very significant delays in gas production, apparently due to inefficient depressurization of the coals. Approximately half of the wells characterized by vertical hydraulic fracturing are also characterized by excessive water production.

In areas of known vertical fracture propagation it is necessary to limit the injection during the water enhancement tests in order to prevent propagation of induced fractures into the overlying water-bearing formations. In areas of unknown least principal stress an alternative to the "standard" wellbore completion methods is suggested to limit the number of wells characterized by excessive water production and delayed gas. Water-enhancement procedures should be done in two steps. In the first step, a minifrac (about 2 bpm for about 2 min) should be done to determine the magnitude of the least principal stress and thus whether fracture propagation would be vertical or horizontal. If the least horizontal stress corresponds to the overburden (approximately 1 psi per foot), it is safe to assume that horizontal fracture propagation will occur and the water enhancement activities can proceed at whatever rate and duration the operator chooses. Because many wells with horizontal fractures tend to be poor gas producers, such wells could be hydraulically fractured (and propped) to enhance gas production without risk of significantly affecting the rate of water production. If the shut-in pressure is significantly less than the overburden (about 0.6 to 0.9 psi per foot), vertical hydraulic fracture growth is implied and significantly reduced pumping is advised. This would be beneficial from the perspective of minimizing produced waters and decreasing the time for initial gas production.

Mapping the thickness of a coal seam could also be used to predict the direction in which a fracture will propagate. As was shown in **Figures 11** and **12**, hydraulic fractures propagate in the vertical plane in coals as thick or thicker than 60 feet. Therefore, if the thickness of the coal is greater than 60 feet, the water enhancement test should be done with a reduced amount of water to prevent vertical hydraulic fracture propagation.

Summary and conclusions

Through analysis of water-enhancement tests performed in CBNG wells of the PRB, it is clear that the water-enhancement activities result in hydraulic fracturing of the coal and possibly the adjacent strata, resulting in perhaps both excess CBNG water production and inefficient depressurization of coals.

The magnitude of the least principal stress has been compiled for 372 wells, and this has demonstrated that both vertical and horizontal hydraulic fracture propagation occurs within the basin. Where the least principal stress is vertical, hydraulic fracture growth is horizontal and water production is minimal. Where the least principal stress is horizontal, fracture growth is vertical and water production is significantly greater for some wells. It is important to note that all of the wells with exceptionally high water production are always associated with vertical fracture growth. In these same wells, there are significant delays in gas production, perhaps due to inefficient depressurization of the coals. However, wells with vertical fractures that produce low water volumes are excellent gas producers (they produce more than 3000 MCF per month) and are better gas producers

than wells with horizontal fractures. Since wells with vertical fractures are, in general, excellent gas producers, it is inferred that the face cleats in the coals must be efficiently connected by the induced vertical fracture.

It has been identified that horizontal hydraulic fracturing is typical toward the Sheridan area. This may be a significant finding, as water injection wells are perhaps needed in the near future in this region because the water has a high content of sodium and will need to be properly disposed. Thus, knowing that there is no vertical connection between the coal seam that is being produced and the sand layers where the water may be injected is particularly important for the operators of the area if water injection activities are undertaken here.

While the reason for the variation in the magnitude of S_3 has not been determined it does appear that coal thickness affects the S_3 magnitudes. In general, in areas where a coal seam has a thickness greater than 60 feet S_3 is equivalent to the minimum horizontal stress, and therefore fractures propagate in the vertical direction. By knowing the areas where a coal seam is thicker than 60 feet, propagation of a vertical fracture into adjacent formations could be avoided by scaling down the water-enhancement procedure.

In order to minimize produced CBNG waters, recommendations for better well completion practices have been outlined. In areas of known vertical fracture propagation it is necessary to limit the injection during the water enhancement tests in order to prevent propagation of induced fractures into the overlying water-bearing formations. In areas of unknown least principal stress an alternative to the "standard" wellbore completion methods has been suggested to limit the number of wells characterized by excessive water production and delayed gas. A minifrac should be done to determine the magnitude of the least principal stress and thus whether fracture propagation would be vertical or horizontal. If the least horizontal stress corresponds to the overburden, horizontal fracture propagation will occur and the water enhancement activities can proceed at whatever rate and duration the operator chooses. As many wells with horizontal fractures tend to be poor gas producers, it is also suggested that such wells are hydraulically fractured (and propped) to enhance gas production. If the shut-in pressure is significantly less than the overburden, vertical hydraulic fracture growth is implied and significantly reduced pumping is advised. This would be beneficial from the perspective of minimizing produced waters and decreasing the time for initial gas production.

Acknowledgements

Thanks to Conoco-Phillips, Marathon Oil–Pennaco Energy, Williams, and Wolverine Energy for kindly providing the data used in this study. Thanks especially to Chris Hogle and Gabriel D'Arthenay for their kindness and interest in this work. Apache Corporation, Conoco-Phillips, and Marathon (sponsors of the Western Resources Project Foundation), supported this study.

References cited

Averitt, P., 1975, Coal Resources of the United States, January 1, 1974: U.S. Geological Survey Bulletin 1412, 131 p.

Ayers, W.B., Jr., 1986, Coal resources of the Tongue River Member, Fort Union Formation, Powder River Basin, Wyoming: Wyoming State Geological Survey Report of Investigations No. 35, 21 p.

Ayers, W.B., Jr., 2002, Coalbed gas systems, resources, and production and a review of contrasting cases from the San Juan and Powder River basins: AAPG Bulletin No. 86, p. 1853-1890.

De Bruin, R.H., and Lyman, R.M., 1999, Coalbed natural gas in Wyoming *in* Miller, W.R., editor, Coalbed methane and the Tertiary geology of the Powder River Basin, Wyoming and Montana: Wyoming Geological Association 50th Annual Field Conference Guidebook, p. 61-72.

De Bruin, R.H., Lyman, R.H., Jones, R.W., and Cook, L.W., 2000, Coalbed methane in Wyoming: Wyoming State Geological Survey Information Pamphlet 7, 15 p.

Flores, R.M., and Bader, L.R., 1999, Fort Union coal in the Powder River Basin, Wyoming and Montana: A Synthesis, *in* 1999 Resource Assessment of Selected Tertiary Coal Beds and Zones in the Northern Rocky Mountains and Great Plains Region: U.S. Geological Survey Professional Paper 1625-A, Part I: Powder River Basin, Chapter PS, 75 p.

Glass, G.B., 1980, Coal resources of the Powder River Coal Basin *in* Glass, G.B., editor, Guidebook to the coal geology of the Powder River Basin, Wyoming: Wyoming State Geological Survey Public Information Circular 14, p. 97-131.

Jones, N.R., 2005, Overview of an interactive online Internet-based map server (IMS) of Wyoming's northern Powder River Basin *in* Stine, J.R., editor, Coalbed Natural Gas Conference: 1—Research, monitoring, and

applications: Wyoming State Geological Survey Public Information Circular No. 43, p. 97-98.

Meyer, J., 1999, General draw-down map—Wyodak/Anderson coal bed, 1980 to 1998 *in* Miller, W.R., editor, Coalbed methane and the Tertiary geology of the Powder River Basin, Wyoming and Montana: Wyoming Geological Association 50th Annual Field Conference Guidebook, p. 87-88.

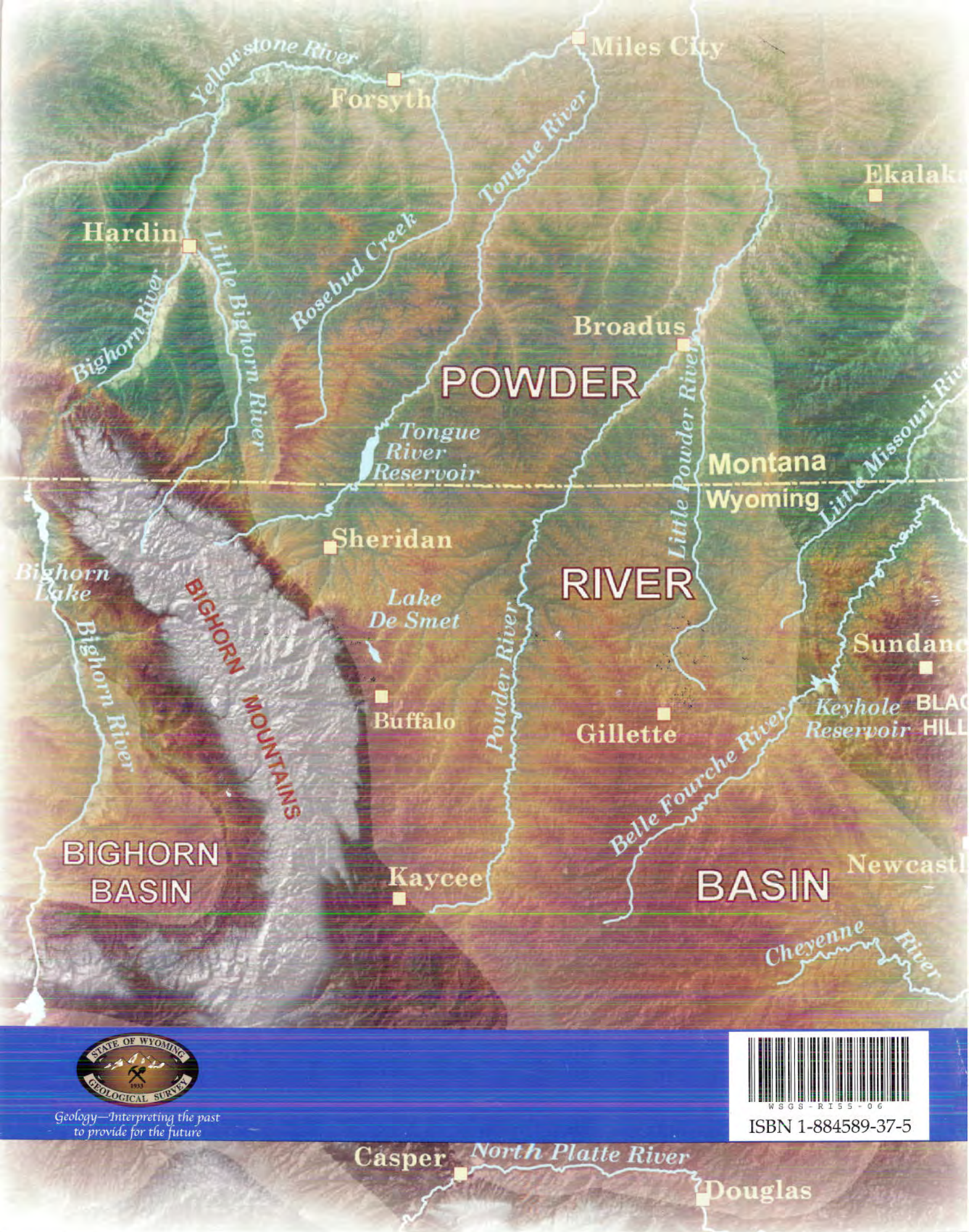
Montgomery, S.L., 1999, Powder River basin, Wyoming; an expanding coalbed methane (CBM) play: American Association of Petroleum Geologists Bulletin, v. 83, no. 8, p.1207-1222.

U.S. Environmental Protection Agency, 2002, DRAFT—Evaluation of impacts to underground sources of drinking water by hydraulic fracturing of coalbed methane reservoirs (EPA 816-D-02-006) <http://www.epa.gov/safewater/uic/CBNGstudy/docs.html>, accessed April 2003.

Wessel, P., and Smith, W.H.F., 1995, New version of the generic mapping tools released, EOS Transactions of the American Geophysical Union, vol. 76, p. 329.

Wyoming Oil and Gas Conservation Commission, 2004, <http://wogcc.state.wy.us≥, accessed August 2004.

Zoback, M.D., Barton, C.A., Brudy, M., Castillo, D.A., Finkbeiner, T., Grollimund, B., Moos, D.B., Peska, Pl, Ward, C.D., and Wiprut, D.J., 2003, Determination of stress orientation and magnitude in deep wells: International Journal of Rock Mechanics and Mining Sciences, v. 40, p. 1049-1076.



STATE OF WYOMING GEOLOGICAL SURVEY 1933

Geology—Interpreting the past to provide for the future

WSGS-RI55-06

ISBN 1-884589-37-5